# Factors Affecting Mitochondria Number and Distribution in *C.elegans* Touch Receptor Neurons and its Correlation with Neuronal Behavior

**THESIS**

Submitted in partial fulfillment
of the requirements for the degree of
**DOCTOR OF PHILOSOPHY**
by

**ANJALI AWASTHI**

Under the Supervision of

**Dr Sandhya P Koushika**

**(Department of Biological Science, TIFR, Mumbai)**


**BIRLA INSTITUTE OF TECHNOLOGY AND SCIENCE**

**PILANI (RAJASTHAN) INDIA**

**2014**

**BIRLA INSTITUTE OF TECHNOLOGY AND SCIENCE**

**PILANI (RAJASTHAN)**

# CERTIFICATE

This is to certify that the thesis entitled "**Factors Affecting Mitochondria Number and Distribution in *C.elegans* Touch Receptor Neurons and its Correlation with Neuronal Behavior"** and submitted by **Ms Anjali Awasthi** ID No. **2007PHXF434P** for award of Ph.D. of the Institute, embodies original work done by her under my supervision.

Signature in full of the Supervisor: ----------

Name in capital letters: **Dr SANDHYA P KOUSHIKA**

Designation: **Associate Professor**

Date:

## Acknowledgements

First of all I would like to thank my guide Dr. Sandhya P. Koushika for allowing me to pursue research in her laboratory. I would also like to thank her for her valuable guidance, constant support, advice, help, encouragement and involvement in my research work. I would also like to thank Dr K Vijay Raghavan (DBT) former Director NCBS and Dr Satyajit Mayor (NCBS) for allowing me to pursue research at NCBS, Bangalore. I would like to thank Prof. Bijendra Nath Jain (BITS-Pilani), Prof G Sundar (BITS-Pilani), Prof. Niranjan Swain (BITS-Pilani) and Prof. S. Gurunarayanan (BITS-Pilani) for motivating and cooperating in all aspects for pursuing my research work. I would like to thank Prof S. K Verma and Prof Hemant Jadhav for regularly keeping track of my progress, motivating and helping me in all possible ways. I would like to thank all the other members of Academic Research Division, BITS-Pilani for regular updates regarding semester requirements and deadlines. I would like to thank Dr. Krishanu Ray (DBS, TIFR) for allowing me to learn EM in his laboratory as well as for his valuable comments and advice for my research work. I would like thank Ms. Seema (TIFR, Mumbai), Mr. Hari (CCMB, Hyderabad), and Ms Bhavya (NCBS) for all help and support for pursuing EM work. I would also like to thank Dr Yamuna Krishnan for allowing me to use TEM, Facility NCBS. I would like to thank Dr Uma (NCBS), Dr Jagadish (ATREE, Bangalore) and Prof Gautam (IMSC, Chennai) for their valuable help and suggestions regarding statistical analysis.

I would like to thank Guru for introducing me to this project, teaching me genetics, imaging and analysis. I would also like to thank current members of the “Mito team” Nikhil and Jyoti; and former members Swathi and Eva Romero for all help, discussion and valuable suggestions. I would also like to thank Dr Sudip Mondal for doing simulations and initiating use of micro fluidic device in the laboratory. I would like to thank Dr Jitendra and Sunaina for help regarding molecular biology work. I would like to thank Bikash for discussion regarding unc-16 project. I would like to thank Selva for being like my elder sister and helping and motivating me at all times. I would like to thank Sucheta and Shikha who have been a great colleagues as well as wonderful friends. Professional as well as personal discussion with them has always been very stimulating. I would also like to thank former lab members Seema, Aparna, Kausalya, Jaffar, Ayush and Shalini for making my stay memorable. I would also like to thank my BITS-Pilani

colleagues Ms Rita, Ms Pushpanjali and all other Bangalore faculties for all their support, help and motivation.

My warm regards towards Ranjith, Gautam, Ashok Rao, Vishalakshi, and Shantha for administrative help during stay at NCBS. I would also like to thank the Kitchen Staff especially Krishna, Satish and Thirumala for making plates for us and helping in worm freezing. I would also like to thank Security Staff of NCBS for issuing lab key during odd hours. I would also like to thank instrumentation, lab support, civil and computer section at NCBS for their quick all time support.

I would also like to thank my family members without their support this work would not have been possible. First of all I would like to thank my parents for their constant motivation and physical support provided by taking care of my infant daughter and household chores so that I can concentrate and devote maximum time in my work. I would also like to thank my sisters Padma and Deepa for always being at my side and helping me in every possible way so that I can always be on track. I would also like to thank my daughter Nitya and my husband Chethan for their support, motivation and cooperation throughout in every possible way. I would also like to thank my brother in law Mr. Suresh and my sister in law Dr Anju for all the help and support provided by them in editing and reviewing my thesis. Last I would like to thank almighty for providing me this opportunity.

## Abstract

Mitochondria are vital organelles responsible for ATP generation, regulating calcium homeostasis, apoptosis and cell signaling. They are extremely dynamic organelle which adjusts its morphology, number, position and distribution depending on the metabolic and physiological needs of the cell. In neuronal cells distribution of mitochondria is very important and their dysfunction has been associated with many neurodegenerative diseases. Major aim of this thesis is to understand whether number and distribution of mitochondria maintains a set pattern in a neuron and is that pattern signature for the neuronal function attributed to it. To answer this query we used ***C.elegans*** six touch receptor neurons as a model. These neurons could be triggered externally by gentle touch and functioning of it produces visual output which can be scored and used as an index for the neuronal function.

We analyzed the pattern of mitochondria number and distribution in the sequential stages of ***C.elegans*** development. Our results show that, in control conditions increase in mitochondria number is proportionate to axonal growth. Increase in mitochondria number in proportion to axonal growth ensures maintenance of constant mitochondrial density in the axonal process throughout the development. Moreover, these mitochondria were not randomly arranged in the axon and were maintaining an optimum distance from each other. Different axonal segments depending on their proximity to other regions such as synapses or cell body also showed their own subset of distribution pattern which was observed consistently in all the developmental stages. Mitochondrial distribution was found to be sensitive to different stresses as well as chemical agents like anesthetics and subjecting animal to these agents perturbed the number or distribution or both.

Next we analyzed all the probable factors which could control mitochondrial number and distribution which included motor proteins, cytoskeletal links, mitochondrial dynamics, touch cell and mitochondrial function. Results showed that motor proteins regulated mitochondrial number but didn't show any effect on distribution. Whereas, rest all the factors effected both mitochondria number and distribution but to a varying degree of severity. Of all the factors listed, altered cytoskeleton structure showed the most severe effect in which axonal

mitochondrial density and distribution was significantly altered. Similar, trends to a milder extent were observed in mutants for touch receptor complex.

We checked whether mitochondrial number and distribution correlates to neuronal behavior by doing behavioral assays. Wild type and mutants with altered mitochondria number and distribution were scored for their gentle touch behavioral response. Results of the assay showed that wild type mitochondrial number and distribution was prerequisite for elucidating wild type touch response. Response elucidated by the animal for the behavioral assay was found inversely proportional to the degree of alteration in mitochondria number and distribution. Results of the assay thus confirmed that mitochondria number and distribution correlated to neuronal behavior.

# Table of Contents

Table of Contents

# Table of Contents

# Table of Contents

# List of Figures

# List of Tables

# List of Abbreviations

| | |
|---|---|
| **AAA** | ATPases Associated with diverse cellular Activities |
| **AD** | Alzheimer Disease |
| **ALM** | Anterior Lateral Microtubule cells |
| **ALS** | Amyotrophic Lateral Sclerosis |
| **ASC** | Amiloride-Sensitive Channels |
| **Aß** | Amyloid ß peptide |
| **ATP** | Adenosine triphosphate |
| **AVM** | Anterior Ventral Microtubule cell |
| **BDNF** | Brain Derived Neurotrophic Factor |
| **BMP** | Bone Morphogenetic Protein |
| **CGC** | Caenorhabditis Genetics Center |
| **CLASP** | Cytoplasmic Linker Associating Proteins |
| **CMT** | Charcot-Marie-Tooth |
| **CNS** | Central Nervous System |
| **DEG** | Degenerin |
| **DHC** | Dynein Heavy Chain |
| **Dpy** | Dumpy |
| **DRG** | Dorsal Root Ganglion |
| **DRP** | Dynamin Related Protein |
| **EBP** | End Binding Protein |
| **EGL** | Egg Laying Defective |
| **EM** | Electron Microscopy |

| | |
|---|---|
| **EMAP** | Echinoderm Microtubule Associated Protein |
| **ENaC** | Epithelial Sodium Channel |
| **GED** | GTP Effector Domain |
| **GFP** | Green Fluorescent Protein |
| **$H_0$** | Null Hypothesis |
| **$H_A$** | Alternative Hypothesis |
| **HPF** | High Pressure Freezing |
| **IMM** | Inner Mitochondrial Membrane |
| **ISI** | Inter Stimulus Interval |
| **JIP** | JNK-Interacting Protein |
| **JNK** | Jun Amino-terminal Kinases |
| **KHC** | Kinesin Heavy Chain |
| **KLC** | Kinesin Light Chain |
| **K-S test** | Kolmogorov-Smirnov test |
| **Lon** | Long |
| **MAPs** | Microtubule Associated Proteins |
| **MEC** | Mechanosensory |
| **MF** | Microfilaments |
| **MOM** | Mitochondrial Outer Membrane |
| **MPT** | Mitochondrial Permeability Transition |
| **MRC** | Mechano Receptor Current |
| **MRN** | Mechano Receptor Neurons |
| **MS** | Multiple Sclerosis |

| | |
|---|---|
| **MT** | Microtubules |
| **MTS** | Mitochondrial Targeting Sequence |
| **NGF** | Nerve Growth Factor |
| **NGM** | Nematode Growth Medium |
| **OMM** | Outer Mitochondrial Membrane |
| **PCR** | Polymerase Chain Reaction |
| **PD** | Parkinson Disease |
| **PF** | Protofilament |
| **PLM** | Posterior Lateral Microtubule cell |
| **PNP** | Paranode-Node-Paranode |
| **PNS** | Peripheral Nervous System |
| **PTL** | Protein with Tau-like repeats |
| **PTP** | Post Tetanic Potentiation |
| **PVM** | Posterior Ventral Microtubule cell |
| **RCD** | Respiratory Chain Deficiency |
| **RFP** | Red Fluorescent Protein |
| **ROS** | Reactive Oxygen Species |
| **SEM** | Standard Error of Mean |
| **SNB** | Synaptobrevin |
| **SOD** | Super Oxide Dismutase |
| **SVP** | Synaptic Vesicle Proteins |
| **+TIPs** | Microtubule Plus End Tracking Proteins |
| **TRN** | Touch Receptor Neurons |

| | |
|---|---|
| **TS** | Temperature Sensitive |
| **UNC** | Uncoordinated |
| **VDAC** | Voltage Dependent Anion Channel |
| **VGCC** | Voltage Gated Calcium Channel |
| **YFP** | Yellow Fluorescent Protein |

# Chapter 1

## Introduction

# 1. Introduction

Neurons are highly polarized cells which have differentiated processes both morphologically and functionally. Neuronal cells can be divided broadly into three processes: cell body (soma), axons and dendrites. As these processes are highly elongated, they are dependent on axonal transport for transport of wide variety of cargoes which include golgi derived vesicles, endocytic vesicles, lysosomes, autophagosomes, mitochondria, cytosolic proteins, cytoskeletal polymers etc. All these transport events are coordinated and regulated quite precisely which take care of the local as well as global needs of the cells so the concerned functions could take place. Thus disruption of this transport is responsible for causing many neurodegenerative diseases.

Mitochondrion is one of the important class of axonally transported organelle. Neurons are dependent on mitochondria for taking care of their ATP needs and it is reported that 90% of neuronal ATP requirement is taken care by mitochondria. Some of the energy intensive neuronal processes are ion transport during synaptic transmission, packaging and transport of neurotransmitters, firing of action potential, cytoskeleton assembly. As the landscape of the neuronal process is too long, efficient transport and placement of these organelles is a necessary prerequisite.

Like other class of neuronal cargoes, mitochondria also undergo bidirectional transport where the movement event is mixed with frequent pauses and reversals. Only half of the mitochondria present in the axons are reported to be moving, rest half are anchored and stationary. As neuronal function including synaptic activity are dependent on mitochondria, efficient mechanism for its transport and docking are very important. Disruption of this transport and coordination mechanism results in disrupted distribution and has been reported to be linked with several neurodegenerative diseases.

## 1.1. *Caenorhabditis elegans*: as a Model to Study Axonal Transport

### 1.1.1. Life Cycle of *C. elegans*

Use of nematode *Caenorhabditis elegans* as model organism was initiated by SydneyBrenner in 1960's (Brenner S, 1974). It is a small free living soil nematode which is found globally, it has two sexes, hermaphrodites and males both of which are approximately one millimeter long. Under laboratory conditions it is grown on NGM (Nematode growth medium) plates spotted with *E.Coli* (*OP50*) bacteria as food source. It has temperature dependent life cycle, comprising of four larval stages L1, L2, L3, L4 and egg laying adult (Fig 1.1). Life cycle from egg to egg laying parent takes 5.5 days when grown at 16$^{o}$C, 3.5 days at 20$^{o}$C and 2.5 days at 25$^{o}$C. Under well fed conditions both males and hermaphrodites live for 17 days. Under food deprivation conditions it undergoes alternative larval stage known as dauer. Dauer stage helps the worms to survive the adversity and these dauers can live for 3 months.

### 1.1.2. Nervous System of *C. elegans*

***C. elegans*** body is made of 959 somatic cells out of which 302 cells are neurons and 56 are glial cells (Sulston et al 1977, Sulston et al. 1983). ***C. elegans*** nervous system is divided broadly into pharyngeal nervous system made of 20 neurons and present in the pharyngeal region and rest 282 neurons comprise the somatic nervous system present in the head, tail, ventral nerve cord and dorsal nerve cord. Males have additional neurons which are specialized for mating behavior (Sulston et al. 1981). The somatic nervous system has presence of 6400 chemical synapses, 900 gap junctions and 1400 neuromuscular junctions (Varshney et al. 2011). Nervous system of ***C. elegans*** develops in three broad phases: first phase is during proliferation stage in embryogenesis, other two neuronal developments takes place during L1 and L2 larval stages (Sulston et al. 1983).

***C. elegans*** neurons are broadly classified into motor neurons, sensory neurons, interneurons and polymodal neurons depending upon their functional specialization (Altun et al 2011). Locomotory behavior such as swimming, thrashing and crawling are controlled by motor neurons. Out of 302 neurons 113 are classified as motor neurons. Some distinct classes of motor neurons are A and B type motor neurons which include VA, VB, DA, DB and AS neurons; all these neurons release acetylcholine neurotransmitter and have stimulatory action. Another class

is D-type motor neurons which include VD and DD neurons which secrete γ-aminobutyric acid and are inhibitory in action (Altun et al 2011).

Sensory neurons are responsible for sensing environmental signals like temperature, mechanical stimuli, pH, osmotic shock, odor, oxygen concentration, light sensation etc. Interneurons act as connecting link between two or more class of neurons. These neurons direct signals from one class of neuron to the other neuron (Altun et al 2011). Neural circuit which links mechanosensation with locomotion has involvement of mechanosensory neurons, interneurons and motor neurons (Goodman 2006) (Fig 1.4 C). Mechanosensory neurons ALM, PLM and AVM receive the mechanical stimuli. These neurons are connected to interneurons AVB, AVC, AVA and AVD by chemical synapse and gap junction (Goodman 2006). Mechanical stimulus transmitted to interneurons are directed to motor neurons DB, VB, DA and VA by the gap junction between the two which in turn is converted into forward and backward locomotory movement (Goodman 2006).

### 1.1.3. Benefits of *Caenorhabditis elegans* as a Model System

There are several benefits of using ***C. elegans*** as a model system to address various biological problems:

1) It is small in size, has short generation time and can be cultivated at ease under laboratory conditions.
2) It has presence of two sexes male and hermaphrodite. Majorly it propagates by self-fertilization, so the progenies are genetically identical. When, genetic manipulation needs to be done genetic crosses could be carried out with ease using males.
3) Has transparent skin and egg cell thus providing ease to visualize biological events in the live organism.
4) Has presence of 959 somatic cells (Sulston et al.1983) out of which 302 are neurons, lineage and circuitry of which is well established (White et al 1986).
5) Genome is mapped and shares 40% similarity to humans (***C. elegans*** Sequencing Consortium).

6) It has a powerful well established genetic system. The ways to manipulate genome using mutagens, molecular manipulations using microinjections or using genetic crosses/chromosome balancers is well established (Fay 2006, Edgley 2006).
7) Other experimental techniques like laser ablation of cells, protocols for biochemistry experiments using ***C. elegans*** are well documented.

## 1.2. Mitochondria Structure and Function

Most predominant theory for the origin of mitochondria is the endosymbiotic theory which states that mitochondria were free living prokaryotic cells and started living inside another host cell as endosymbiont (Margulis 1981). Genomic studies have shown the similarity of mitochondrial DNA to eubacterial genome and specifically to alpha proteobacteria (Gray et al 1994, Yang et al 1985). Size and shape of mitochondria varies from small spherical to long tubular structures depending upon the physiological state of the cell but approximately 0.5-1.0μm diameter in dimension. Most of the mitochondrial proteins are encoded by nuclear genome and transported to mitochondria but it also has its small circular DNA which encodes for thirty seven genes, thirteen of which are responsible for encoding proteins subunits of respiratory chain complex I, III, IV and V (Dimauro et al 2005).

Mitochondria are made up of inner and outer membrane. Both the membranes are made up of phospholipid bilayer which demarcates the mitochondria into five distinct compartments: inner membrane, inter membrane space, outer membrane, inner membrane matrix and cristae respectively. Mitochondrial ultra-structure also undergoes frequent remodeling depending upon the tissue type as well as physiological state of the cell.

Outer mitochondrial membrane (OMM) has equal ratio of protein to phospholipid. OMM has presence of proteins termed as porins which has approximate radius of $1.3–2\times10^{-9}$ m (Colombini et al 1987) which makes this membrane permeable to molecules up to 5 kDa (Colombini et al 1987, Mannella et al. 1992). Porins are also named as Voltage dependent anion channels (VDACs), and have been reported to be structurally conserved (Linden et al 1984, Sampson et al 1997, Young et al 2007). Voltage-dependent anion channel (VDAC) of the OMM along with adenine nucleotide translocase present in IMM and cyclophilin-D (CyP-D) present in matrix forms the mitochondrial permeability transition (MPT) pore complex (Crompton et al 1998,

Vyssokikh et al 2001). MPT has been reported to be involved in programmed cell death (Crompton 1999, Tsujimoto et al 2007). OMM thus acts as a membrane barrier between cytosolic space and mitochondria. It is the mediator for exchange of metabolites and ions for maintaining the structure and function of mitochondria.

Inner mitochondrial membrane has 80:20 ratio of protein to lipid. In contrast to outer mitochondrial membrane which is permeable to diverse metabolites and ions, IMM is very less permeable thus results in creating compartmentalization (Krauss 2001, Osman et al 2009). One of the signature lipid found in IMM is cardiolipin, it has a dimeric structure and it has been reported to be involved in stabilization of enzymes and respiratory chain complexes (Chen et al 2008). IMM has presence of machinery for oxidative phosphorylation as well has presence of specialized mechanism for transport of metabolites and ions (Krauss 2001, Osman et al 2009). Machinery present for oxidative phosphorylation is electron transport system and ATP synthase. Electron transport system is organized into four complexes known as Complex I, II, III and IV respectively. Some of the proteins involved in transport across IMM are adenine nucleotide translocase, $Na^+/Ca^+$ exchangers, calcium uniporter.

## 1.3. Factors Influencing Transport and Distribution of Mitochondria in Axon

### 1.3.1. Molecular Motors

Slow and fast axonal transport on cytoskeleton track takes place with the help of molecular motors. These motors are ATP dependent and convert chemical energy released by ATP hydrolysis into mechanical work in the form of movement of organelles (Liu et al 2003). These motors are specific for cytoskeleton structure on which they drive organelle movement. Fast axonal transport of mitochondria on microtubule tracks takes place with the help of anterograde motor kinesin (Tanaka et al 1998, Glater et al 2006, Pilling et al. 2006) and retrograde motor dynein (Pilling et al. 2006). Whereas, slow axonal transport on actin cytoskeleton is reported to be myosin motor mediated (Pathak et al 2010).

Kinesin-I is the first member of kinesin family identified to be involved in organelle transport in axons including mitochondria (Hirokawa et al 1991). Kinesin-I is known to have a heterotetrameric structure comprising of dimers of kinesin heavy chain (KHC) which binds to two kinesin light chains (KLC) (Fig 1.2) (Hirokawa et al 1989, Miki et al 2005). Kinesin heavy

chain has a globular head region at the N-terminal which is also known as motor domain of Kinesin. The head has sites for two important functions which are ATP hydrolysis and microtubule binding (Hirokawa et al 1989; Vale 2003). Head region is connected to a small neck region which in turn is connected to a long stalk made up of two coil-coil domain which dimerizes to make the dimeric structure. Last is the C-terminal tail region which binds with light chains as well as associates with the neuronal cargo (Fig 1.2). Isoforms of KHC are known as Kif5A, Kif5B and Kif5C in mammals (Vale 2003). Kif5 is reported as the prime motor for mitochondrial transport in mammals and disruption of these motors has been reported to result in abnormal mitochondrial clustering (Tanaka et al 1998, MacAskill et al 2010). In Drosophila mutation of Khc has reported to show similar effect resulting in impaired mitochondrial movement and disturbed distribution (Hurd et al 1996; Pilling et al 2006). In ***C. elegans*** *unc-116* encodes for kinesin heavy chain and mutants of *unc-116* have been reported to result in disrupting of mitochondrial transport thus no mitochondria were found in axonal processes and were localized only in cell body (Yan et al 2013). Apart from kinesin-I members of kinesin3 have also been reported to interact with mitochondria in mammals (Kif5B) (Tanaka et al 1998, MacAskill et al 2010) and fungi Neurospora (Nkin2) (Fuchs et al 2005).

Cytoplasmic Dynein is the primary retrograde motor responsible for bringing the organelles back to cell body from the axonal tract. Dynein motor has a complex structure comprising of Dynein heavy chain (DHC), dynein light chains (DLC), intermediate chains (IC) and light intermediate chains (LIC) (Fig 1.2) (Susalka et al 2000, Carter et al 2011). Dynein heavy chain also has a complex structure which is divided into the motor domain and the tail subunit, motor domain is responsible for ATPase activity and microtubule binding; whereas tail domain connects heavy chain to light and intermediate chain which binds to the cargo (Mocz et al 2001, Carter et al 2011). Motor domain has a ring structure made up of six AAA (ATPases Associated with diverse cellular Activities) domains; N-terminal region which form the linker sits on the top of the ring and its position changes based on presence or absence of ATP and drives the movement. C-terminal region is also aligned on the top of AAA ring. Coiled stalk with microtubule binding tip arises between the AAA4 and AAA5 domain (Fig 1.2) (Mocz et al 2001, Carter et al 2011). Dynactin has been reported as a large complex reported to be associated with dynein motor and responsible for enhancing motor processivity (King et al 2000). Mutation in both dynein (Pilling

et al 2006) and dynactin complex (Levy et al 2006) has been reported to effect mitochondrial transport and distribution.

Short distance slow axonal transport on actin filaments takes place with the help of myosin motors. Myosin mediated transport is prevalent in specific regions of axons like presynaptic terminals, dendritic spines and growth cones which are actin rich (Peters et al 1991, Bridgman 2004). Structure of myosin motor is quite similar to kinesin motor but myosin motor domain is considerably bigger in size compared to kinesin motor domain (Fig 1.2) (Rayment 1996, Holmes 2008). The motor domain of myosin is responsible for ATP hydrolysis and actin binding. In some of the myosin proteins, light chain is known to bind to motor domain to increase the strength of power stroke. Myosin V and VI has been reported to be involved in actin mediated mitochondrial transport in Drosophila neurons (Pathak et al 2010). Myosin V ortholog Myo2p has also been reported to be involved in mitochondrial transport in yeast (Boldogh et al 2004).

Motors connect to their cargoes either directly or linkage routed through some linkers or adaptor molecules (Goldstein et al 2000). Some of the adaptors are quite well known for their association with kinesin, dynein and myosin motors and being involved in mitochondrial transport. Some of the linkers well characterized for associating with kinesin motor and mitochondrial transport are syntabulin, milton and miro. Syntabulin co-localizes with mitochondria and knockdown of syntabulin expression disrupts mitochondrial distribution. This has been reported in cultured hippocampal neurons (Cai et al 2005). Milton and miro are another group of adaptors well documented for their involvement in mitochondrial transport in Drosophila and mammals (Cai et al 2009, Guo et al 2005, Glater et al 2006, Górska-Andrzejak et al 2003). In mammals two isoforms of miro: miro I and miro II are present (Fransson et al 2006); mammalian orthologue of milton are known as Trak 1 and 2 (trafficking kinesin-binding protein 1 and 2) (Brickley et al 2011). Miro is a $Ca^{2+}$ binding rho like GTPase present on the outer mitochondrial membrane which connects milton to KIF5 kinesin heavy chain (Glater et al 2006). Mutation in milton as well as miro has been reported to effect anterograde transport of mitochondria (Cai and Sheng 2009, Guo et al 2005, Glater et al 2006, Górska-Andrzejak et al 2003). Miro is a GTPase having two GTP binding domains and EF hands motifs which bind with $Ca^{2+}$; GTP hydrolysis or binding of $Ca^{2+}$ to the EF motifs has been reported as the possible mechanism for detaching mitochondria from the motors and hence resulting in halting of mitochondria (Cai et al 2009).

Similarly, dynactin complex is reported as adaptor for dynein which enhances the processivity of the dynein motor (Kardon et al 2009). Mmr1p has been reported as an adapter for Myo2p (yeast ortholog of myosin V) (Itoh et al 2004).

### 1.3.2. Cytoskeletal Links

Motor mediated mitochondrial movement takes place on the cytoskeletal tracks. Apart from controlling mitochondrial movement(Hollenbeck et al 2005), cytoskeleton framework has been reported to control mitochondrial morphology (Rappaport et al 1998), mitochondrial function (Rostovtseva et al 2008) as well as its positioning (Milner et al 2000). Axonal transport of organelles including mitochondria was considered predominantly microtubule based for a long time (Grafstein et al 1980, Allen et al 1985, Hirokawa et al 1986). Studies showing microtubule independent actin based transport (Kuznetsov et al 1992) and occurrence of bidirectional transport when MT tracks were disrupted using drug treatment (Morris et al 1995) gave strong lines of evidence for the presence of actin based transport. In the neurons presynaptic terminals, dendritic spines, growth cones have been reported to be actin rich (Peters et al 1991) and myosin motor has been reported for mediating slow axonal transport on actin cytoskeleton (Langford 1995, Baas et al 2004). Axonal mitochondria thus move both on microtubules and actin filaments but with different characteristic profiles. MT based mitochondrial transport is reported to be comparatively much faster compared to actin microfilaments MF (Morris et al 1995) based transport. Duty cycle was reported to be higher for MF compared to MT, whereas net direction of transport was retrograde for MF (Morris et al 1995). As the speed of actin mediated axonal transport is very low and net transport direction is retrograde, actin microfilament based mitochondrial transport is considered as less predominant mode and back-up means of transport during localized needs.

#### 1.3.2.1.Microtubules

Axonal microtubules have polar arrangement with plus end directed towards axonal terminals and minus ends towards the cell soma whereas in dendrites the polarity is mixed (Hirokawa et al 2004). Microtubule mediated organelle transport takes place with the help of molecular motors. Kinesin motors are plus-end directed and mediate anterograde transport whereas dynein mediate retrograde transport towards minus ends of microtubule.

#### 1.3.2.1.1. Structure of Microtubules

Microtubules are cytoskeleton structure found in all eukaryotic cells. They do various vital functions such as providing polarity and structural framework to the cell, play role in cell division, intracellular trafficking etc. They are heterodimers formed by polymerization of two globular proteins alpha and beta tubulin (Fig 1.3) (Desai et al 1997). Height of the dimer formed is 8nm. Alpha and beta tubulins have 50% amino acid similarity and have molecular weight of 55 kDa (Burns 1991). Both alpha and beta tubulin sub-units have GTP binding sites, alpha tubulin has non hydrolysable GTP binding site whereas, beta tubulin has hydrolysable GTP which can be exchanged by GDP (David-Pfeuty et al 1977, Spiegelman et al 1977). Alpha and beta tubulin heterodimers assemble head to tail into linear protofilaments. This head to tail arrangement gives polarity to the microtubule (Nogales 1999). Linear protofilaments assemble side by side to form microtubule which is a hollow cylinder of approximately 25 nm diameters (Desai et al 1997). Usual number of protofilament present in microtubules is 13. Head to tail arrangement of tubulins leads microtubule to have one end having only beta tubulin also known as plus end or faster growing end whereas the other end has all alpha tubulins termed as minus end or slow growing end (Allen et al 1974).

Microtubules show dynamic instability which is a phenomenon in which microtubules are continuously in phase of polymerization and depolymerization (Fig 1.3). Polymerization phase is known as rescue whereas depolymerization is known as catastrophe (Mitchison et al 1984 a, b). Proteins known as MAP's (Microtubule associated proteins) have been known to be associated with microtubules to provide them stability and help in assembly (Hirokawa N 1994). Plus end tracking proteins (+TIPs) are MAPs associated with microtubule growing end (Akhnamova et al 2008). +TIPs have been known to play role in controlling microtubule dynamics (Lansbergen et al 2006). Some of the members of +TIPs are cytoplasmic linker protein (CLIP)-170, CLIP-associating proteins (CLASPs), adenomatous polyposis coli (APC) tumor suppressor, and end-binding 1(EB-1) (Mimori et al 2003, Schuler and Pellman 2001). EB-1 has been known as one of the key members of +TIPs and has been known to play a vital role in regulating microtubule dynamicity (Vitre et al 2008, Rogers et al 2002).

#### 1.3.2.1.2. Microtubules and MAP's in *C. elegans*

In ***C. elegans*** 11, 13 and 15-protofilament microtubules are present (Chalfie et al 1982). 11 protofilament microtubule is the most predominant microtubule found in most of the neurons as well in muscles, hypodermis and intestine, whereas only mechanosensory neurons of our study have specialized 15-protofilament microtubules (Chalfie 1982, Chalfie et al 982). Average outer diameter of 11 protofilament microtubules in ***C. elegans*** is reported to be 24 nm whereas that of 15-protofilament is 30nm (Chalfie 1982). Sensory cilia have been reported to be having a varying arrangement of microtubules. They have outer doublet of microtubule arranged in a ring like fashion which encircles the inner microtubule arranged in singlets. Inner singlets comprise of 11 protofilament microtubules whereas outer doublet has one with 13 protofilaments (named as A-subfibers) and other with 11 protofilaments (named as B-subfibers) (Chalfie et al 1982).

Some of the MAP's which are found in ***C. elegans*** are ELP-1, PTL-1 and CLASPs. ELP-1 is a member of Echinoderm Microtubule-Associated Protein (EMAP). Expression of ELP-1 has been reported to be in embryos, larvae as well as adults. In embryo it is present in hypodermis, whereas in larvae and adults it is expressed in body wall muscles, spermatheca, and vulval muscles as well as in touch receptor neurons (Hueston et al 2008). ELP-1 was reported to associate specifically with touch receptor neuron and has been reported to contribute to mechanosensation (Hueston et al 2008). Association of ELP-1 with microtubule has been reported both in-situ as well as in-vivo (Hueston et al 2008).

PTL-1(Protein with Tau-like repeats-1) is another MAP present in ***C. elegans.*** It is a single member of MAP-2/Tau family in ***C. elegans*** (Gordon et al 2008). Using in-vitro experiments PTL-1 has been reported to bind to microtubules and promote its assembly in ***C. elegans*** (Goedert et al. 1996). PTL-1 is expressed in embryo, larvae as well as in adult ***C. elegans***. In embryos it is expressed in epidermal cells whereas in larvae and adults it is expressed in specialized five (ALML, ALMR, PLML, PLMR and AVM) mechanosensory neurons (Goedert et al. 1996). PTL-1 has been reported to be responsible for contributing to touch insensitivity and in mechanosensory defective mutants both *mec-7* and *mec-12* it enhances the mutant effect (Gordon et al 2008). CLASP is another group of MAP's for which there are three homologs known in ***C. elegans*** which are CLS-1, CLS-2 and CLS-3 all of which are involved in embryonic development (Espiritu et al 2012).

#### 1.3.2.1.3. 15-Protofilament Microtubule in *C. elegans*

Microtubules impart specialized functions to the neurons; same is the case of 15-Protofilament microtubules in ***C. elegans*** which are present only in six mechanosensory neurons. Six touch receptor (TRN's) neurons ALML, ALMR, AVM, PLML, PLMR and PVM respectively are responsible for sensing gentle touch (Fig 1.4 A). These touch neurons are encapsulated by mantle and embedded in hypodermis which is in-turn is in touch, with animal's cuticle (Chalfie et al 1981) (Fig 1.4 B). Each of these individual TRN's spans almost half of the animal's body length. These processes are in close proximity with animal's skin; covers almost the entire length and sense any external forces applied along the worm body.

Large diameter 15-protofilament microtubules as explained earlier are essential for gentle touch sensation and absence of them in touch neurons lead to touch insensitive phenotype. These specialized 15-protofilament microtubules are comprised of MEC-7 (β-tubulin) and MEC-12(α-tubulin) tubulins (Fukushige et al., 1999; Savage et al., 1989). Mec-7(β-tubulin) and mec-12(α-tubulin) genes forming the specialized protofilaments along with 10 other genes are known to be responsible for mechanosensation and failure to produce them leads to mec (mechanosensation deficient) phenotypes (Chalfie and Sulston, 1981). Most of the touch insensitive *mec-7* and *mec-12* mutants have been reported to have 11-protofilaments instead of normal 15-protofilament (Savage et al 1989). Structural integrity of the microtubule cell is thus important for elucidating normal touch response and alteration in it either by mutation in *mec-7/mec-12* genes or depolymerizing it using chemical treatment like colchicine shows similar effects (Chalfie and Thomson 1982). Disruption of 15-protofilament in *mec-7* and *mec-12* mutants have been reported to result in decrease in expression levels of many TRN proteins like MEC-2 and MEC-3 (Bounoutas at al 2011).

#### 1.3.2.1.4. Effect of Microtubule Stability on Mitochondrial Distribution and Morphology

Role of microtubules have been implicated in movement and distribution of many organelles like mitochondria (Summerhayes et al 1983), golgi apparatus (Thyberg et al 1985), endoplasmic reticulum (Terasaki et al, 1994) and lysosomes (Collot et al. 1984). Stability and integrity of microtubules has been reported as controlling factor to control movement and distribution of these organelles including mitochondria. Studies have also reported that mitochondria and

microtubules are co-distributed and some chemical link may exist between them (Heggeness et al 1978). Structural integrity of microtubules is important to control mitochondria distribution, thus depolymerization of microtubules by chemical agents has been reported to result in altered mitochondrial distribution (Heggeness et al 1978, Minin et al 2006). A similar result of regulation of mitochondrial distribution by microtubules has also been reported in Yeast (*Schizosaccharomyces pombe*) using temperature sensitive (TS) alpha and beta tubulin mutants. These TS mutants when were subjected to non-permissive temperature, it resulted in aggregated and asymmetric mitochondrial distribution (Yaffe et al 1996). Microtubules have also been reported to be involved in regulating mitochondrial biogenesis in mammalian cells and their depolymerization have been reported to impact mitochondrial volume and mass (Karbowski et al 2000).

### 1.3.3. Mitochondrial Dynamics

Mitochondrial fission and fusion are important events for quality control of mitochondria enabling them to maintain their structural and functional dynamics. Mitochondrial fission and fusion are known to play several vital roles like:

1) Maintenance and repair of mtDNA (Parone et al 2008),
2) Control of mitochondrial morphology (Santel et al 2001, Serasinghe et al 2008, Chen et al 2005, Nakamura 2006),
3) Maintaining normal respiration rate (Chen et al 2003, Chen et al 2005),
4) Equal distribution of proteins (Chen et al 2009),
5) Removal of damaged mitochondria by mitophagy (Twig et al 2008, Gomes et al., 2011) and
6) Promote apoptosis when mitochondria are severely damaged (Lee et al 2004).

#### 1.3.3.1.Mitochondrial Fusion

Mitochondrial fusion events require fusion of both outer and inner mitochondrial membrane. Proteins involved in both inner and outer mitochondrial membrane fusion are GTPases. Genes involved in outer membrane fusion are *Fzo*, *Mfn1* and *Mfn2*. Drosophila and Yeast fusion genes *Fzo*(fuzzy onions) and *yFzoIp* respectively were first set of fusion genes to be identified (Hales

et al 1997, Hermann et al. 1998). Homologues for the same in mammals are Mitofusins I and II (*Mfn1* and *Mfn2*) (Chen et al 2003, Eura 2003, Song et al 2009). All these proteins are GTPase which are present in N- terminal region (Legros et al 2002, Rojo et al 2002, Olichon et al 2002). They have a bipartite trans-membrane domain near the C- terminal region. This is flanked on both sides by heptad repeat region (HR1 and HR2) which is hydrophobic in nature (Fritz et al 2001, Rojo et al 2002). MFN1 and MFN2 show 80% homology to each other (Legros et al 2002, Rojo et al 2002). Another outer membrane fusion protein known in yeast is UGO1 (Sesaki and Jensen 2001).

Role of *Fzo* gene in Drosophila was known by *Fzo* mutant in which mitochondria failed to fuse during a specific stage in spermatogenesis. This gene is associated only with male specific germ line and is responsible for male sterility in Drosophila (Hales et al 1997). Another *Mfn* homologue found in Drosophila is known as *Marf* (Mitochondrial assembly regulatory factor), expressed in both germ-line and somatic cells (Hwa et al 2002, Dorn et al 2011). *FzoI* deletion in yeast resulted in highly fragmented mitochondria and eventually loss of mitochondrial DNA pool was observed in these mutants (Hermann et al 1998). *Mfn-1* and *Mfn-2* has been found to be associated with embryonic lethality in mouse and null mutants of these genes results in severely fragmented mitochondria in embryonic fibroblast in mouse (Chen et al 2003, Chen et al 2005). Mutations in *Mfn2* gene has been known to be associated with Charcot-Marie-Tooth type 2A (CMT2A) neuropathy (Zuchner et al 2004).

Fusion of mitochondria requires expression of Mitofusins/*Fzo* genes on both the mitochondria involved in fusion process (Koshiba et al 2004, Meeusen et al 2004, Hoppins et al 2009). Fusion first takes place between the outer mitochondrial membranes. Presence of GTPase domain is also necessary for the complete fusion to take place, absence of the same results in mitochondria to be close together to each other with a distance comparable to one of the heptad repeat domain(HR2) (Koshiba et al 2004). During fusion events FZO-I form homo-oligomer complex, whereas MFN1/MFN2 form both hetero as well as homo-oligomer complex (Eura et al 2003, Griffin et al 2006).

Inner mitochondrial membrane fusion proteins known in yeast is MGM1 (Sesaki at al 2003, Wong et al 2003). Ortholog for same present in mammals and drosophila are OPA-1, dOPA-1

respectively, both of which are known to be associated in causing optic atrophies (Alavi et al 2007, Davies et al 2007). These proteins are confined to inter-membrane space and are closely coupled to inner membrane (Olichon et al 2002). Structure of MGM-1/OPA-1 is that it has N terminal region which has a mitochondrial targeting sequence (MTS). MTS is responsible for mitochondrial import. Next is the trans-membrane region (TM) which is instrumental in anchoring protein to the inner mitochondrial membrane. Other domains present are GTPase domain, middle domain and GTP effector domain (GED) at C-terminal region (Olichon et al 2003). Out of the five characteristic domain of dynamin family, three domains (GTPase, Middle and GED) are present whereas PH domain and proline rich domain area are absent. Both MGM1 and OPA-1 are known to undergo post-translational modifications through proteolysis. In yeast proteolytic cleavage results in formation of long and short isoforms l-MGM1 and s-MGM1 (Delettre et al 2001, Herlan 2004).

Role of MGM1 in inner membrane fusion in yeast was reported by using temperature sensitive strain of yeast which could undergo outer membrane fusion but not inner membrane fusion (Meeusen et al 2006). These temperature sensitive mutants also displayed deformities in cristae development (Meeusen et al 2006). Depletion of OPA-1 results in mitochondrial fragmentation and has been reported by using siRNA against OPA-1 in cultured mammalian cell (Johnson et al 2010). Using mice heterozygous and *Drosophila melanogaster* homozygous mutants of *Opa-1*, it has been reported that it leads to increased mitochondrial fragmentation (Davies et al 2007, Yarosh et al 2008). Besides fusion, *Opa-1* has also been associated with various other functions like cristae remodeling (Frezza et al 2006), ATP production (Lodi et al 2004), apoptosis and cytochrome-c release (Amoult et al 2005). *Opa-1* gene has been reported to be the most predominant gene responsible for causing Autosomal Dominant Optic Atrophy (DOA) (Alexander et al 2000, Pesch et al 2001, Davies et al 2007). DOA is neuropathy in which there is degeneration of retinal root ganglion resulting in vision impairment (Kjer et al 1983, Davies et al 2007).

#### 1.3.3.2.Mitochondrial Fission

Fission process is controlled by *Dnm-1* in Yeast and *Drp-1* in flies and mammals (Bleazard et al 1999, Smirnova et al 2001, Aldridge et al 2007). DNM-1 and DRP-1 are dynamin related proteins having all the three core domains of the dynamin family which are GTPase, middle and

GED domain respectively (Van der Bliek 1999). In between middle and GED domain is B-insert region which anchors it to mitochondrial adaptor proteins which in turn is responsible for recruiting DRP to fission site (Romero et al 2009). Unlike fusion proteins which have separate proteins for inner and outer membrane fusion, fission doesn't have separate proteins. DRP-1 is predominantly cytosolic protein.

Apart from DNM-1/DRP-1, fission process requires involvement of many other receptor/adaptor proteins to form the fission complex. One such protein is FIS1 which is present in yeast as well as in mammals (Suzuki et al 2003). It is present on the mitochondrial outer membrane (MOM) and has a highly conserved TRP-region domain (tetra trico peptide repeat) in the cytosolic region (Suzuki et al 2003). Another cytosolic protein MDV1 has been reported in yeast which is required to form the fission complex (Tieu et al 2002). MDV1 has $NH_2$-terminal region which is reported to bind to TRP region of FIS-1, next is the central coiled-coil domain, and then is C-terminal domain which has at its end WD40 repeat (stretch of 40 amino acids with tryptophan (W) and aspartic acid (D)) which binds to DNM-1 to form the fission complex (Karren et al 2005). MDV1 has been reported to be found only in fungi, another paralogue of MDV1 known as CAF4 is also present in yeast this adaptor protein also has WD40 repeats (Griffin et al 2005). Steps for fission in yeast are 1) interface between Fis1 present on MOM with adapter molecules MDV1 (or CAF4) which are present as dimers. 2) FIS1/MDV1 form base and recruits DNM1 to MOM 3) DNM1 forms spirals around the fission site by oligomerization 4) DNM1 spirals leads to constriction and finally leads to fission at the site by GTP hydrolysis.

No homologues of *Mdv1/Caf4* are present in mammals. *Fis-1* though known to be present in mammals, its role has remained quite ambiguous and debatable. Some groups have reported that it is involved in mitochondrial fission as its down regulation results in elongated mitochondria (Yoon et al. 2003, Lee et al. 2004, Yu et al. 2005). But another study using RNAi mediated *hFis1* gene silencing in Hela cell lines reported no observable effect of the same on mitochondrial morphology and distribution (Otera et al., 2010). Another protein named as mitochondrial fission factor (MFF) present on MOM has been reported to be involved in fission (Gandre-Babbe et al 2008). It has also been reported that MFF and not hFIS1 is an essential factor for DRP-1 mediated fission (Otera et al., 2010). Other factors like MiD49, MiD51/MIEF

have also been reported to be involved in promoting DRP-1 dependent fission (Loson et al. 2013).

#### 1.3.3.3.Fission Fusion Genes in *C. elegans*

*Fzo-1* and *eat-3* are the outer and inner membrane fusion genes present in ***C. elegans***, these are homologues of *Fzo1/Mfn1, 2* and *Mgm1/Opa1* respectively (Kanazawa et al. 2008, Ichishita et al. 2008). DRP-1 is the fission protein present in ***C. elegans*** (Labrousse et al 1999, Jagasia et al 2005). *Fis1* and *Fis2* are the *Fis1* homologues present in ***C. elegans***, but no homologues for *Mdv1/Caf4* are reported (Breckenridge et al 2008). ***C. elegans*** mutants for *fzo-1*, *eat-3* and *drp-1* have been reported to result in altered mitochondrial morphology, reduced brood size and increased rate of embryonic lethality (Breckenridge et al 2008). In contrast *fis-1* and *2* mutants have been reported to show normal mitochondrial morphology and wild type characteristics.

CED-9 which is a anti apoptotic member of *Bcl-2* family and localized to MOM has been implicated to play role in ***C. elegans*** fission, fusion as well as apoptosis (Conradt et al 1998, del Peso et al 2000, Delivani et al 2006, Rolland et al 2009). ***C. elegans*** embryos, over expressing *ced-9* showed presence of globular mitochondria (Stephane et al 2009). CED-9 has been reported to show physical interaction with FZO-1 protein and its activity is *fzo-1* and *eat-3* dependent (Stephane et al 2009). Similar results have been reported by expressing of ***C. elegans*** CED-9 in cultured mammalian cells (Delivani et al. 2006). CED-9 has also been reported to show physical interaction with DRP-1 and for promoting this interaction EGL-1 another member of *Bcl-2* family (pro apoptotic BH3-only) has been involved (Lu et al 2011). Another group (Breckenridge et al 2009) has reported that CED-9 and EGL-1 has no role to play in mitochondrial fission/fusion process.

### 1.3.4. Neuronal Function

Neuronal activity has also been reported to effect mitochondrial transport and distribution (Li et al. 2004, Chang et al. 2006). Mitochondrial movement and distribution has been reported to be dependent on the growth state of the axon. By experiments done using cultured neurons, it has been reported that mitochondria accumulate in the vicinity of the growth cones and when axonal growth was blocked mitochondria were redistributed (Morris et al 1993). Even the presence of nerve growth factor (NGF) has been reported to influence mitochondrial distribution (Chada et al

2004). Similar observations were reported in the growing neurons in Drosophila larvae where mitochondrial transport has been reported to show anterograde bias (Pilling et al. 2006, O'Toole et al. 2008).

Neuronal activity mediated, in response to altered $Ca^{2+}$ levels or neurotransmitter release has also been reported to influence mitochondrial transport and distribution (Yi et al. 2004). $Ca^{2+}$ levels in the neurons are mediated by various events in neurons including neurotransmitter release (Zhang et al 2004) as well as action potentials (Zhang et al 2006). $Ca^{2+}$ has been reported to be controlling mitochondrial motility in multiple ways. EF hands of Rho like GTPase Miro bind to $Ca^{2+}$ which releases motor from the mitochondrial surface and thus results in halting of mitochondria (MacAskill et al 2009, Wang et al 2011). Experiments done in frog myelinated PNS axons have reported that firing of action potential reduces the percentage of mobile mitochondria significantly and this decrease in number of mobile mitochondria was $Ca^{2+}$dependent (Zhang 2010). Similar results were seen in myelinated CNS axons where firing of action potential was blocked using tetrodotoxin (TTX) application (Ohno et al 2011).

It has been reported that neuromodulator serotonin (5-HT) increases mitochondrial movement in hippocampal neurons (Chen et al 2007). 5-HT receptors activate AKT/Protein kinase B pathway and inhibition of *Akt* has also been reported to block mitochondrial movement. In contrast decreasing glycogen synthase kinase (GSK3beta) activity has been reported to enhance mitochondrial movement (Chen et al 2007). Dopamine has been reported to show the inhibitory effect on mitochondrial movement through the same AKT-GSK3beta signaling pathway (Chen et al 2008). Structural changes in the neurons like myelination and demyelination have also been reported to effect mitochondrial number, activity, velocity as well as size (Andrews H et al 2006, Dutta et al 2006, Kiryu-Seo et al 2010).

### 1.3.5. Mitochondrial Function

ATP production is one of the major functions of mitochondria. Mitochondrial membrane potential is one of the key determinant of the proton motive force which in turn drives all the mitochondrial functions like ATP production (Dimroth et al 2000), $Ca^{2+}$uptake (Komary et al 2010) free radical generation (Suskit et al 2012) and apoptosis (Gautier et al 2000). Along with mitochondrial membrane potential which is the major contributor for proton motive force in

mitochondria; trans-membrane proton gradient is another addition to proton motive force which finally drives ATP formation from ADP using ATP synthase (Dimroth et al 2000). Membrane potential of individual mitochondria has also been reported to drive the direction of their movement in axon. Mitochondria with high membrane potential have been reported to move in anterograde direction towards growth cone whereas low membrane potential mitochondria have been reported to travel retrogradely towards cell body (Miller et al 2004).

Local depletion of ATP in proximity with synapse and accumulation of ADP has been reported as another factor responsible for halting of mitochondria and localization in these regions (Mironov 2007). Calcium has been reported to play role in controlling mitochondrial movement and distribution (Yi et al 2004). It has also been reported that increase in level of cytosolic calcium levels during synaptic activity also results in uptake of $Ca^{2+}$ by mitochondria resulting in increase in mitochondria $Ca^{2+}$ concentration (Pitter et al 2002). It has also been reported that post synaptic activity and membrane depolarization, mitochondrial movement was inhibited which correlated with increase in mitochondria $Ca^{2+}$ concentration (Mironov 2006). Reactive oxygen species (ROS) are the most harmful bi-product produced during mitochondrial respiration (Dugan et al 1995, Murphy 2009). Superoxide dismutase (SOD) is the enzyme which neutralizes these radicals. These enzymes are present in cytoplasm as well as in mitochondria (Fridovich 1975, Sturtz et al 2001). Mutation in these enzymes has been reported to result in damaged mitochondria and blockage of mitochondrial anterograde transport (Sturtz et al 2001, De Vos et al 2007).

### 1.4. Mitochondria Transport and Neuronal Function

Mitochondria play a very vital role in functioning of neurons and its dysfunction has been reported to be associated with many neuronal disorders. Role of mitochondria in neuron starts from the stage when neurons are developing and until they become fully functional entities. During neuronal differentiation it has been reported that mitochondrial biomass increases and mitochondria movement velocity decreases (Vayssie` et al.1992, Chang et al 2006). Signaling molecules like nitric oxide and brain-derived neurotrophic factor (BDNF) which promote mitochondrial biogenesis have also been reported to influence neural progenitor cells differentiation and proliferation in mammalian brain (Cheng et al. 2003, Barsoum et al. 2006). During axogenesis it has been reported that mitochondria shows selective preference towards

neurite which forms axon and its density increases in these regions as compared to dendrites (Mattson et al 1999, Ruthel et al 2003). It has also been reported that mitochondria play role in establishing neuronal polarity (Mattson et al 1999) as well as in programmed cell death (PCD) in newly developed neurons (Kirkland et al 2003).

Mitochondria have also been reported to play role in synaptic plasticity. Mutations in proteins like DRP-1 and OPA1 which control mitochondrial dynamics and reduce dendritic mitochondrial content have been reported to result in loss of synapses and dendritic spines. Increasing dendritic mitochondrial content or mitochondrial activity has been reported to be associated with enhancing the number and plasticity of spines and synapses (Li et al 2004). In Drosophila *Drp-1* mutants, it has been reported that synapses were deprived of mitochondria resulting in elevated $Ca^{2+}$ levels in neuromuscular junctions (Verstreken et al. 2005). Mitochondrial $Ca^{2+}$ uptake and release has also been reported to be involved in Post-tetanic potentiation (PTP) and inhibiting it has been reported to block PTP (Tang et al 1997, Lee et al 2007). Sequestering of $Ca^{2+}$ by presynaptic mitochondria is important for maintenance of synaptic transmission (Billups et al 2002).

Mitochondrial distribution and functioning is extremely important for neuronal activity and its dysfunction and abnormal dynamics has been reported to be associated with many neurodegenerative diseases. In Alzheimer's disease (AD), mitochondrial dysfunction i.e. decreased ATP production, increased oxidative stress, increased $Ca^{2+}$ uptake, resulting in increased mitochondrial autophagy has been reported to be involved (Maurer et al 2000, Hirai et al 2001). Amyloid ß peptide (Aß) plaque (Goedert and Spillantini 2006) which is one of the hallmarks of AD has been reported to be responsible for causing mitochondrial dysfunction (Manczak et al. 2006). Similarly, in Parkinson's disease (PD), decreased activity of mitochondrial complex I has been reported to be responsible which in turn results in decreased ATP production, increased oxidative stress, increased $Ca^{2+}$ uptake and mitopathy (Swerdlow et al. 1996, Keeney et al. 2006). Moreover most of the genes like α-synuclein (Devi et al. 2008), Parkin (Greene et al. 2003), DJ-1 (Zhang et al. 2005) and PINK1 (Yang et al. 2006) which have been reported to be associated with PD has been reported to be linked to mitochondria directly or indirectly. In amyotropic lateral sclerosis (ALS) motor neurons showing neuromuscular

dysfunction tend to show increased free radical accumulation (Pedersen et al. 1998), decreased ATP production (von Lewinski et al 2005) and disturbed $Ca^{2+}$ buffering (Kruman et al. 1999).

## 1.5. *C. elegans* Touch Receptor Neurons as a Model to Study Mitochondrial Transport

Mitochondrial transport is vital for functioning of neuron and its alteration has been reported to impact neuronal development as well as it's functioning. We wanted to check whether altering mitochondrial distribution would affect signature function of a particular neuron. We aimed at quantifying and correlating the effect which mitochondrial distribution had on neuronal function, if it exists. In order to answer these questions we needed a neuronal system with the following properties:

1) Simple in organization made up of few neurons.
2) Landscape of individual neurons should be such that individual neurons can be independently traced down from cell body to axon tip. This will facilitate study of mitochondrial distribution.
3) Functioning of the neuron could be checked by triggering the axon externally and it produces some visual output which can be scored as an index for the neuronal function. To answer these questions, we choose ***C. elegans*** touch receptor neurons also known as mechanosensory neurons as the model system.

### 1.5.1. Mechanosensation in *C. elegans*

All living organisms from bacteria to human beings are subjected to a wide variety of mechanical stimuli due to contact with the external environment or mechanical stimuli generated due to its own movement. To convert these mechanical stimuli into neuronal signal (electrical or chemical synapses), these organisms are equipped with specialized cell known as mechanoreceptor neurons (MRNs) and this phenomenon is known as mechanotransduction (French 1992). In mechanoreceptor neurons, mechanical stimuli generate electrical signals which are transmitted to subsequent neurons mediated by electrical or chemical synapses. Mechanosensation has been known to be responsible in perception of many physiologically vital functions like touch, sound, balance, proprioception (position sense) etc. (Kellenberger S et al 2002).

***C. elegans*** is a free living soil nematode and is exposed to wide variety of mechanical stimuli in the environment due to rubbing to the soil particle or being in contact with other organisms. To respond to these stimuli, it has 30 mechanoreceptor neurons in hermaphrodite and 52 additional mechanoreceptor neurons specifically present in males (Goodman 2006). ***C. elegans*** has both ciliated and non-ciliated MRN's which have been reported to evoke response to mechanical stimuli in the form of locomotion, egg laying, defecation, feeding as well as mating (Thomas et al. 1990, Liu 1995). Six touch neurons of our study belong to the class of non-ciliated MRN's.

Ciliated MRN's present in ***C. elegans*** are ASH, FLP, OLQ, IL1, CEP, ADE, PDE and Male-specific MRNs (Kaplan et al 1993). ASH, FLP, OLQ and IL1 neurons are responsible for nose touch response (Kaplan et al 1993). All the above sets of neurons respond to nose touch by showing escape response or reversal movement (Kaplan et al 1993). Apart from mechanosensory response, ASH neuron has been reported to mediate other responses like odor sensory, osmosensory (high osmolarity), nociceptive (response to noxious stimuli such as toxic chemicals, acidic pH etc.) (Kaplan et al 1993, Bargmann et al 1990). Six touch receptor neurons (TRN's) present in ***C. elegans*** are non-ciliated TRN's. Structural organization of TRN's and touch receptor complex is described in the following sections.

#### 1.5.1.1.Structural and Functional Organization of *Touch Receptor Neurons (TRN's)*

Six touch receptor neurons (TRN's) present in ***C. elegans*** are non-ciliated TRN's. Four of these cells anterior lateral microtubule cells (ALMLeft and ALMRight) and posterior lateral microtubule cell (PLMLeft and PLMRight) are present on the lateral side and present at the time of hatching. Whereas, other two anterior ventral microtubule cell (AVM) and posterior ventral microtubule cell (PVM) are present in the ventral region and are developed post embryonically. These touch processes run longitudinally and cover almost the complete length of the organism (Fig 1.4 A). They are lined closely near the worm cuticle and are present in hypodermis; it is further surrounded by extra cellular matrix also known as mantle which is reported to be having varying thickness in different regions (Fig 1.4 B) (Chalfie and Sulston 1981). These cells have specialized large diameter (30nm) 15-protofilament microtubules which are specific only to these cells (Chalfie et al 1979).

Using laser ablation studies it was reported that these cells are responsible for gentle touch response. PLML and PLMR are responsible for gentle touch on posterior region which evokes a forward movement whereas ALMR and ALML are responsible for response to anterior touch which evokes a backward movement. AVM also shows weak response to head touch whereas PVM has been reported not to be involved in gentle touch response (Chalfie et al 1981). These neurons are also reported to be involved in plate tap response (Wicks et al. 1996). Forces for gentle touch which these worms can recognize and respond range from 10-20μN (Garcia-Anoveros 1997, Goodman et al 2003**)**, gentle touch insensitive worms can respond to harsh touch with forces greater than 100μN (Goodman et al 2003**)**.

ALM and AVM branches into nerve ring whereas; PLM and PVM branch into ventral nerve cord. These touch sensory neurons form gap junctions and synapses with different neurons to control this locomotory circuit (Chalfie et al. 1985). They have been reported to have a reciprocatory circuit: that is they form gap junction with opposite set of interneurons and synapses with the same set of interneurons. Anterior set ALM and AVM form gap junctions with AVD interneuron which is responsible for backward movement, similarly PLMR forms gap junction with PVC interneuron which is responsible for forward movement (Fig 1.4 C). ALM and AVM form synapses with AVB and PVC interneuron whereas PLMR forms synapses with AVA and AVD interneuron.

#### 1.5.1.2.Other Components of Gentle Touch Receptor Channel Complex

Apart from *mec-7*(β-tubulin) and *mec-12*(α-tubulin) genes which are needed for formation of specialized 15-protofilament microtubules, many other genes vital for gentle touch sensation has been identified using genetic screens (Chalfie et al 1981; Chalfie et al 1989). These screenings resulted in finding 16 such genes most of which were involved in sensing gentle touch and together with microtubule cell it formed the touch receptor channel complex or mechanotransduction complex (Fig 1.4 D) (Chalfie et al 1989).

Two genes *mec-4* and *mec-10* have been reported to form pore forming subunit of mechanotransduction complex. These are also known as the DEG/ENaC channels or amiloride sensitive channel as dominant gain of function mutation of these results in cell swelling and degeneration so known as degenerins (DEG) (Chalfie et al 1990, Driscoll et al 1991), they are

also referred as ENaC for epithelial (E) sodium (Na) channel (C) or amiloride-sensitive channels (ASC's) as diuretic amiloride results in blocking of these channels (Canessa 1994).

DEG/ENaC channels are found both in vertebrates and invertebrates and are responsible for doing a wide variety of mechanotransduction functions (Kellenberger et al 2002). Apart from *mec-4* and *mec-10*, few other genes which are member of DEG/ENaC family are present in ***C. elegans*** and are reported to play role in locomotion, muscle function, fluoride resistance etc (Mano et al 1999). It has been reported that DEG/ENaC proteins are evolutionary quite conserved and share quite a lot structural similarity across species (Bianchi et al 2002). ***C. elegans*** DEG/ENaC has been reported to show 20-30% homology with vertebrate DEG/ENaC.

MEC-4 is localized to only six touch receptor neurons whereas along with touch neurons, MEC-10 is expressed in FLP's and PVD neurons as well (Huang et al 1994). MEC-4 and MEC-10 are 768 and 730 amino acid long proteins respectively. Both the proteins have structural similarity and show around 50% homology. These proteins have intracellular and extracellular domains; both C and N terminus of the proteins are present in the intracellular domain. Two membranes spanning domain (MSD1 and MSD2) are present in between these two intracellular and extracellular domains. Extracellular domain has three cysteine rich domain (CSDI, CSDII and CSDIII), one extracellular regulatory domain (ERD) and one neurotoxin like domain (NTD) which overlaps with CSDIII domain (Tavernarakis et al 2001, 2000). MSD, CSD, ERD and NTD domains are all evolutionary conserved and are characteristic of DEG/ENaC channels.

MEC-4 and MEC-10 have been reported to have both physical and genetic interaction (Huang et al 1994; Gu et al 1996). It has been proposed that both MEC-4 and MEC-10 form a heterotetrameric complex (Huang M et al 1994; Gu et al 1996). Structure and function of these two proteins is studied using mutants which have been isolated using touch insensitive screen, much fewer mutants of *mec-10* have been isolated as compared to *mec-4* (Chalfie et al 1981; Chalfie et al 1989). Function of *mec-10* has been reported to be regulatory in the channel complex. Gain of function in *mec-4* results in *mec-4(d)* which causes touch cell degeneration. *Mec-4(d)* showed much weaker effect on *mec-10(d),* moreover weaker effect showed by *mec-10* was found to be dependent on *mec-4* (Huang et al 1994). Response for gentle touch is milder for *mec-10* as compared to *mec-4*; this has been supported by doing gene silencing by RNAi based approach and deletion mutants for *mec-10*(*tm1552* and *ok1104* alleles) and *mec-4(u253). Mec-10*

mutant showed better gentle touch response as compared to *mec-4* (Arnadóttir et al 2011). Moreover null mutant of *mec-4* having normal *mec-10* expression has been reported to show no mechanoreceptor current (MRC) (O'Hagan et al. 2005), whereas missense alleles of both *mec-4* and *mec-10* results in MRC's with decreased amplitude compared with wild type (Arnadóttir et al 2011).

Another two proteins MEC-2 and MEC-6 have been reported to physically interact with MEC-4 and MEC-10. They enhance gating/functioning of these channels and both are required for normal touch sensitivity (Chelur et al 2002, Goodman et al 2002). MEC-2 belongs to the family of stomatin like protein, named so due to its similarity to membrane-associated protein stomatin which is found in red blood cells (Huang M et al 1995). Size of MEC-2 protein is 481 amino acids and apart from touch neurons it is expressed in some other neurons near the pharyngeal region (Du et al 2001, Huang et al 1995). MEC-2 is a cytosolic protein which links DEG/ENaC channel to microtubule cytoskeleton. NH2 terminus of MEC-2 is linked to microtubule, next to NH2 domain is stomatin like domain which has a hydrophobic domain which links to the membrane and another proline rich-SH3 which links to DEG/ENaC channel (Goodman et al 2002, Huang et al 1995).

There are both genetic and biochemical evidences which prove the interaction of MEC-2 with microtubule cytoskeleton (MEC-7/MEC-12) and DEG/ENaC channel (MEC-4/MEC-10). Using Mec-2::LacZ fusion constructs; it was reported that MEC-2 was distributed in the six touch receptor axon and that N-terminus of MEC-2 was sufficient for MEC-2 distribution to the axon (Huang et al 1995). MEC-2 localization to six touch receptor neurons was also reported using MEC-2 specific antibodies (Zhang et al 2004). It was also reported that presence of 15-protofilament microtubules was important for MEC-2 distribution using *mec-7* null and *mec-12* loss of function mutants (Huang et al 1995). However, missense mutant alleles of *mec-12* showed strong effect on MEC-2 distribution in the similar experiments (Huang et al 1995).

Interaction between MEC-2 and MEC-4 has been proposed based on puncta co-localization observed between MEC-2 and MEC-4 YFP (Zhang et al 2004) as well as co-immunoprecipitation observed between MEC-2 and MEC-4 in Xenopus oocyte and CHO cell (Goodman et al 2002). GST pool down assay using GST-MEC-4 resulted in pooling down of MEC-2 as well as MEC-2 stomatin like region specifically; this gave a very strong evidence

regarding interaction between MEC-2 and MEC-4 and this interaction was through stomatin like region (Zhang et al 2004). Mutant form of *Mec-2* when expressed with *mec-4(d)/mec-10(d)* in Xenopus oocytes resulted in suppression of degenerin phenotype (Goodman et al 2002). Recordings of current amplitude have reported to show increase when MEC-2 was co-expressed with MEC-4 and MEC-10 in Xenopus oocytes (Goodman et al 2002). Along with MEC-4 and MEC-10; MEC-6 protein is also required for MEC-2 puncta distribution in the touch neurons (Zhang et al 2004).

Similar to *mec-4*, *mec-10* and *mec-2*, mutation in *mec-6* also results in touch insensitivity but all these components which together form the channel complex don't affect touch cell formation (Chelur et al 2002). MEC-6 is 377 amino acid long trans-membrane protein and shares 45% similarity with vertebrate paraxonase protein (Chelur et al 2002). Along with six touch receptor neurons, it is also expressed in several other neurons like HSN, PVD, PVC, in muscles, excretory canals etc. MEC-6 has been reported to assist in functioning of many other degenerin channels apart from MEC-4/MEC-10 in ***C. elegans*** (Chelur DS et al 2002). Similar to MEC-*2* co-expression of MEC-6 in MEC-4(d)/MEC-10(d) mutant resulted in suppression of degenerin phenotype and increased current amplitude (Chelur et al 2002). It has also been reported that effect of *mec-2* and *mec-6* on functioning of *mec-4/mec-10* degenerin channel is synergistic (Chelur et al 2002, Austin et al 2008).

## 1.6. Thesis Aim

Importance of mitochondria in functioning of neuron has been studied extensively using various model systems, but how mitochondria are distributed and positioned in the neuronal regions is poorly understood. One study using medial segmental nerves of Drosophila larvae have determined the density of mitochondria in 1st, 2nd and 3rd instar larval stages (Toole et al 2008). The neurons under study were nerve bundles, thus individual neurons could not be traced down. Moreover, as single nerve could not be traced independently, density was estimated by counting the number of mitochondria visible in 100μm bin for the entire axon bundle. Mitochondrial positioning with reference to the other mitochondria also could not be estimated. Due to large landscape of neuronal cells, no study has been done so far to understand the distribution of mitochondria in a single axon with the developmental stage of the animal. The effect of factors regulating mitochondrial distribution in reference to a single neuron has also not been studied. Moreover, proper functioning and positioning of mitochondria has been reported to be vital for neuronal function; and alteration in it has been reported to result in neurodegenerative diseases. But, no quantifiable relation between neuronal function and mitochondria has been reported till date. This thesis aims to answer all these questions.

Chapter 2 of this thesis describes the experimental methodology adopted during the course of all the experiments.

Chapter 3 of this thesis aims to study the number and distribution of mitochondria during the course of development in ***C. elegans*** touch receptor neuron. It analyzes the trend in mitochondrial density during the course of development. Mitochondrial distribution pattern in entire axon in totality and different axonal segments during the course of development is analyzed in depth. Pattern of mitochondrial distribution observed was explored using simulations and statistical approaches.

Chapter 4 of this thesis aims to explore all the possible factors which would have been instrumental in contributing to the pattern of mitochondrial distribution observed. Probable factors which may be contributing to mitochondrial distribution were classified into five broad classes:

1) Factors effecting entry and exit of mitochondria

2) Anchoring factors
3) Dynamics of mitochondria
4) Touch cell function
5) Mitochondrial function.

Mutated alleles for all these factors were closely analyzed and scored for the extent of effect they showed in disrupting mitochondrial transport and hence their number and distribution.

Chapter 5 of this thesis aims to explore whether mitochondrial number and distribution correlates to the neuronal function. All the mutants effecting mitochondrial distribution in varying degrees were scored for the behavioral response given by them in response to gentle touch. Extent of mitochondrial distribution defect and mechanosensation response was correlated using statistical tests.

Chapter 6 of thesis aims to explore the effect of growth and imaging conditions on mitochondria number and distribution. For all the experiments done in the previous three chapters animals were always grown in a well fed condition. Temperature and pH were constantly maintained and monitored. All the imaging experiments were done using 50mM sodium azide anesthetic. If the above conditions are not monitored closely worms are very frequently subjected to starvation and occasionally subjected to temperature and pH fluctuations. In this chapter we attempted to study the effect of some of the factors namely starvation, temperature, oxidative stress and anesthetic used (for worm immobilization) on mitochondria number and distribution.

Chapter 7 of this thesis aims to confirm the identity of tong tubular vesicular compartments observed in *unc-16* mutant by EM (Electron Microscopy Imaging). This was an independent work carried out to confirm some set of observations seen in our laboratory in *unc-16* mutant, and was not related to the question answered in earlier sections. Chapter 8 of this thesis summarizes the work completed and future course of direction.

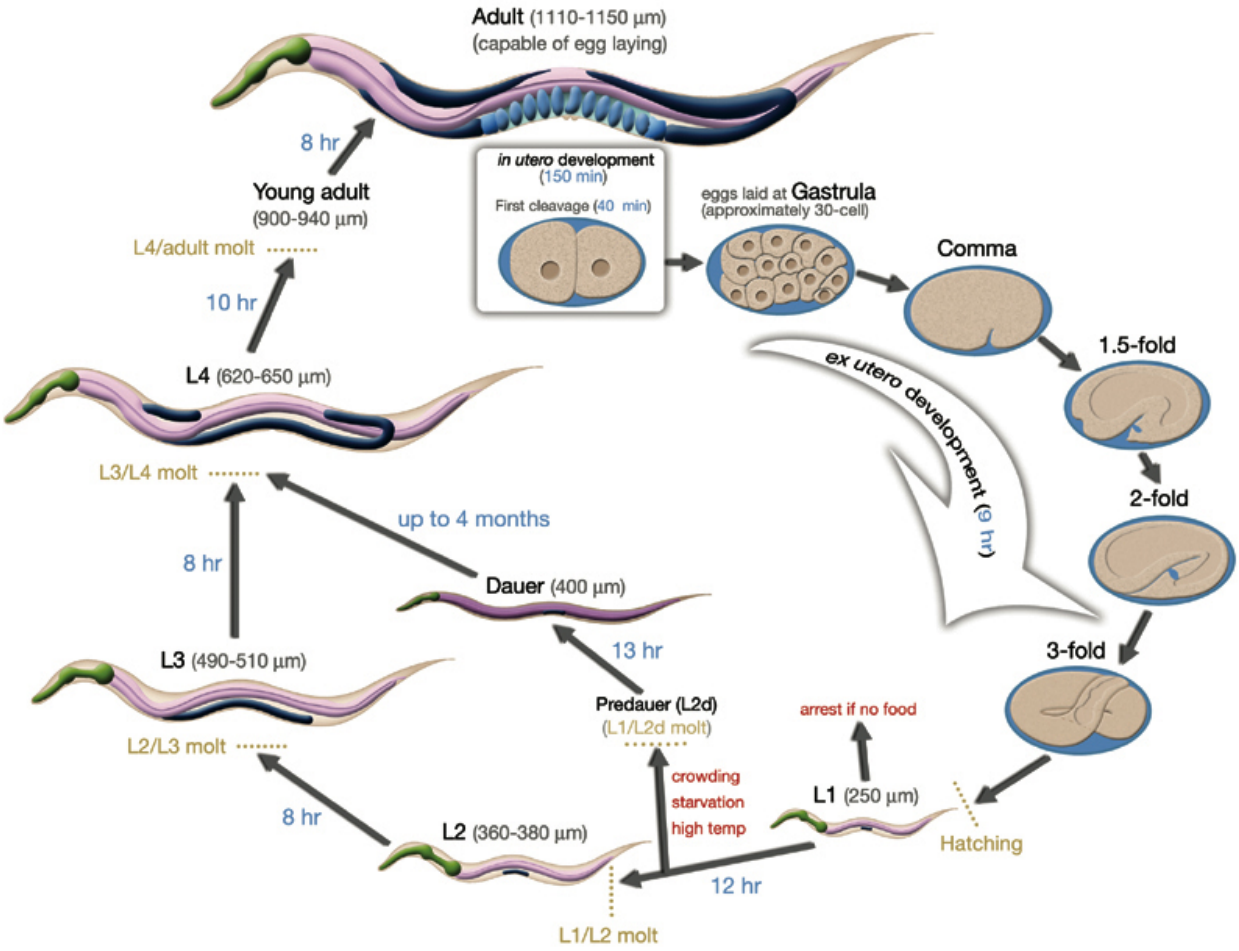


**Figure 1.1: Life Cycle of *C. elegans* at 22°C**

(Figure adapted from Altun, Z.F. and Hall, D.H. 2009. Introduction: In *WormAtlas*)

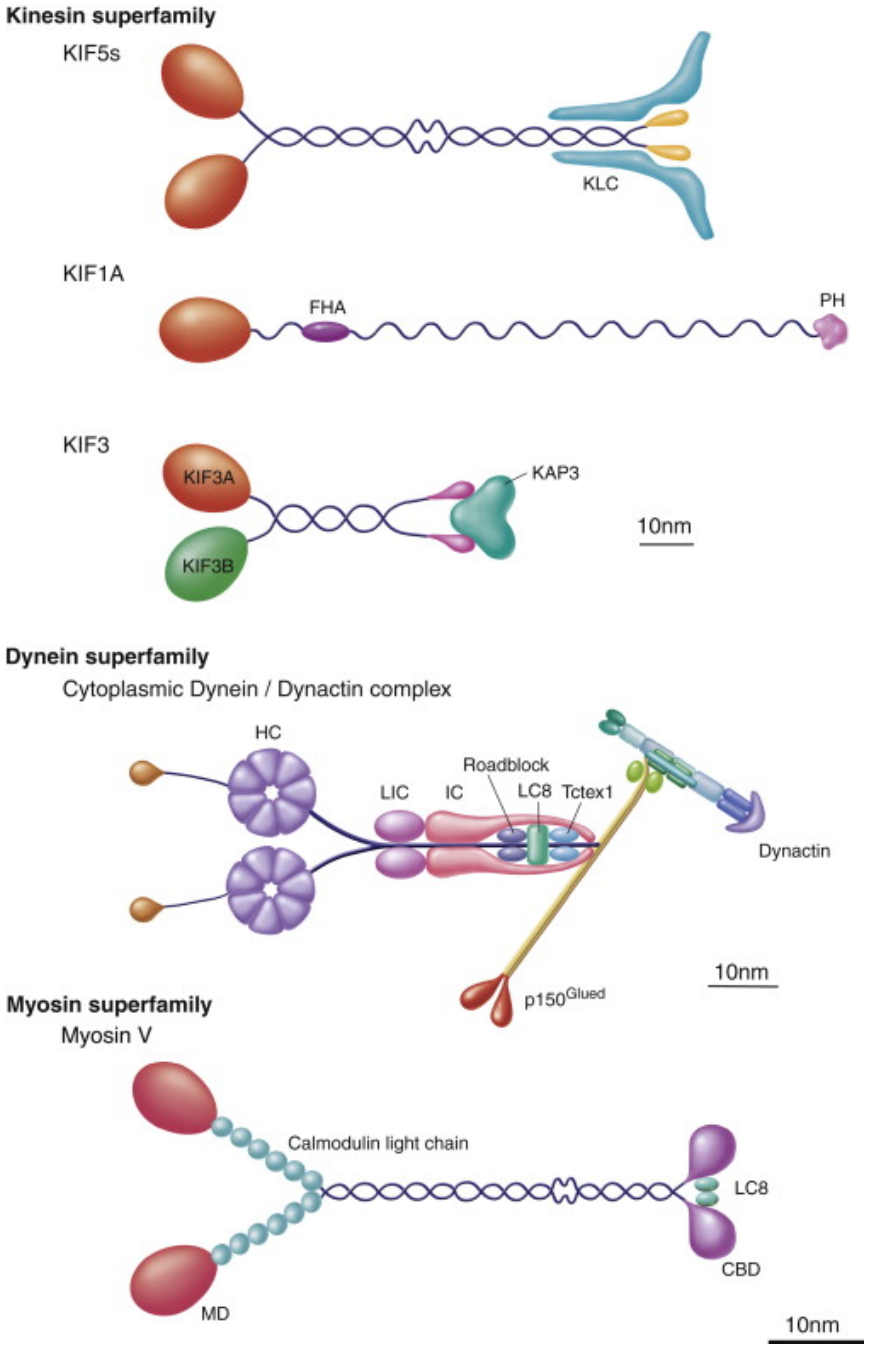


**Figure 1.2: Structural organization of Kinesin, Dynein and Myosin motors**

Abbreviations used HC: Heavy Chain; LIC: Light Intermediate chain; IC: Intermediate Chain; LC: Light Chain, CBD: Cargo binding domain. (Figure adapted from Hirokawa et. al, 2010. Neuron *68*(4): 610-638.)

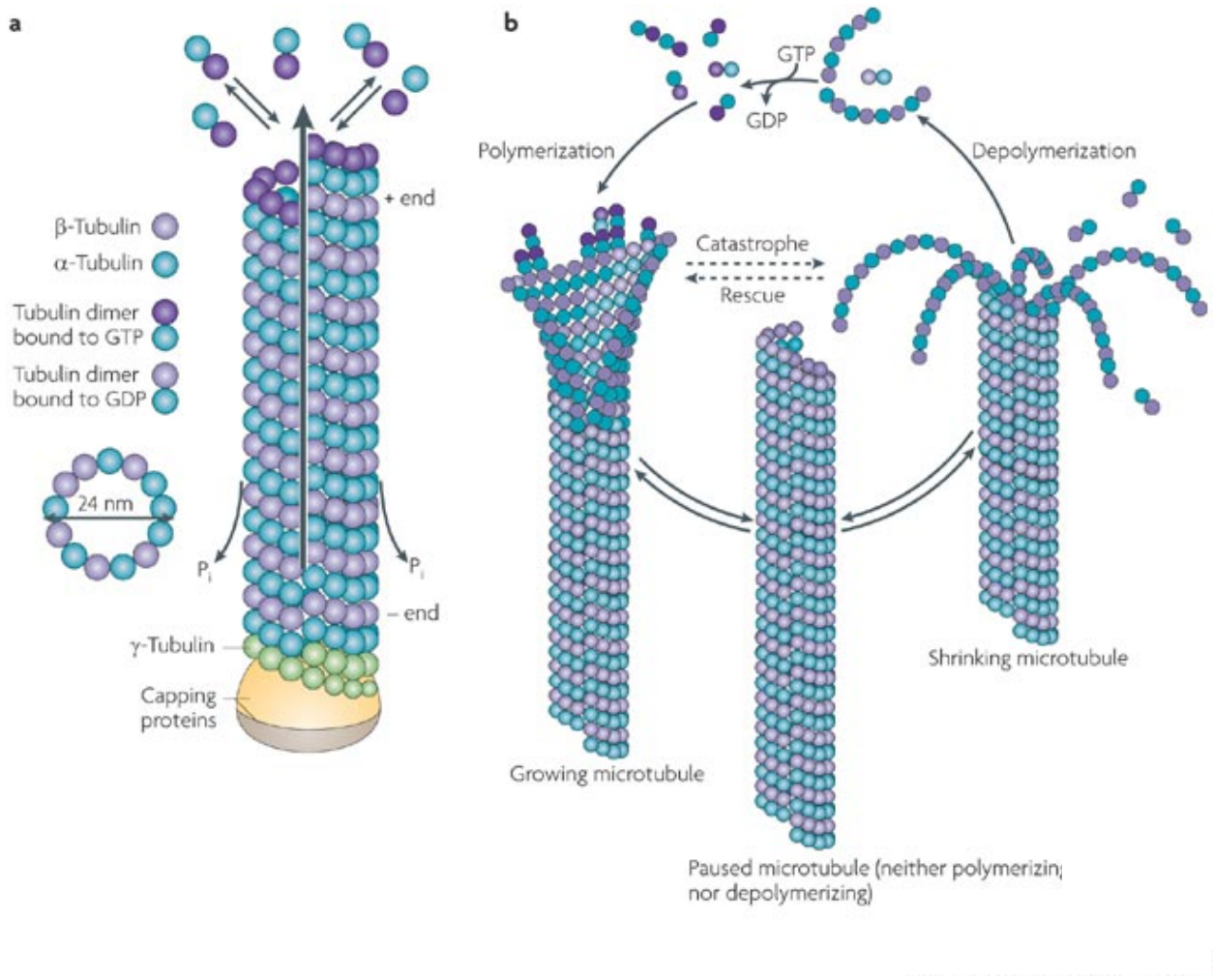


**Figure 1.3: (A-B) Structural organization of microtubules and its dynamic instability**

(Figure adapted from Cecilia Conde & Alfredo Cáceres, 2009. Nature Reviews Neuroscience 10: 319-332)

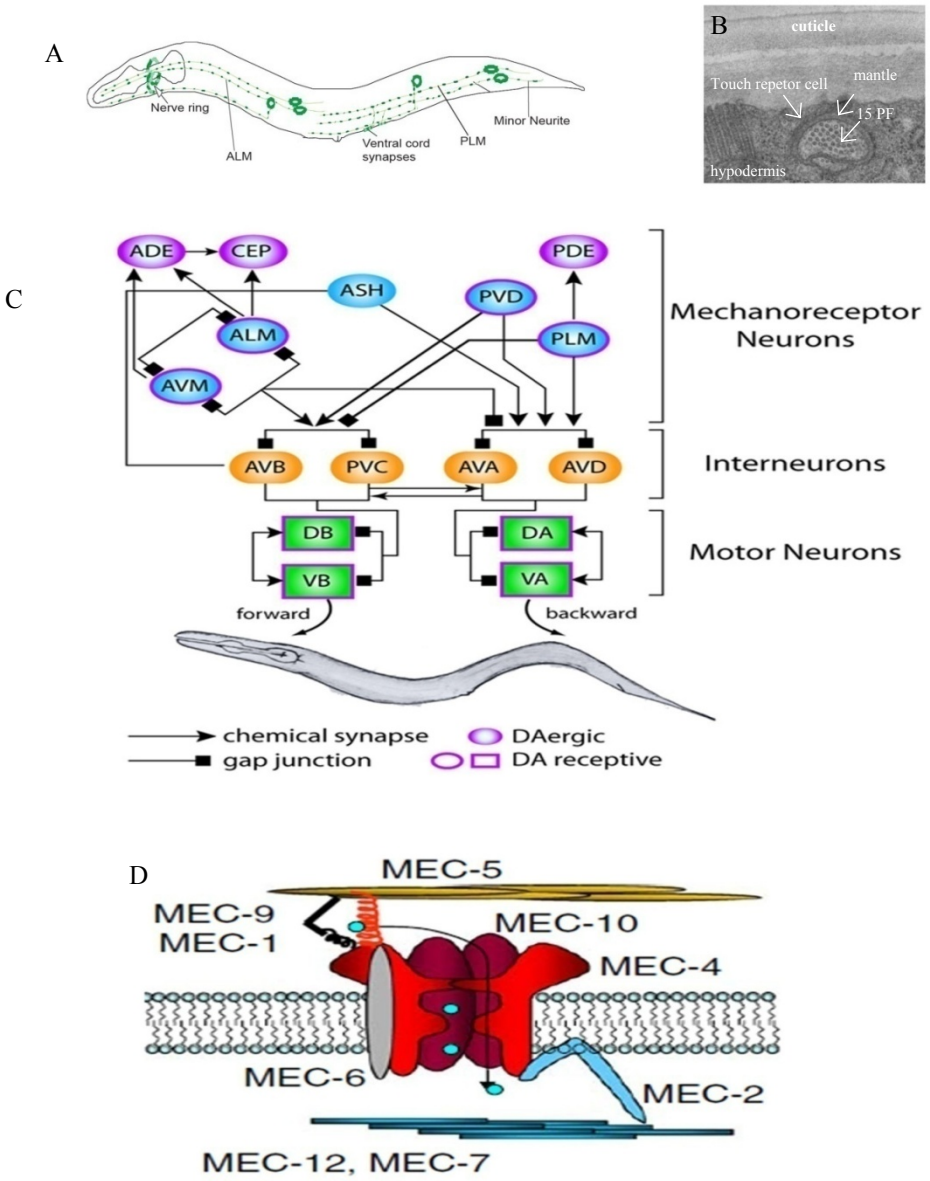


**Figure 1.4: (A-D) Represents structure and position of TRN, Neuronal circuit linking mechanosensation with locomotion and structure of touch receptor complex**

(A) Represents position of six touch receptor neurons in *C. elegans*
(B) EM micrograph of TRN (sample for EM imaging provided by David Halls Lab)
(C) Neuronal circuit linking mechanosensation with locomotion (adapted from Goodman, 2006. Mechanosensation, WormBook)
(D) Structural organization of touch transducing complex (adapted from Bianchi, 2007. Mol Neurobiology 36:254–271

# Chapter 2

## Material & Methods

# 2. Material and Methods

## 2.1. *C. elegans* Strains and Maintenance

Worm stocks were obtained from the Caenorhabditis Genetics Center (CGC is supported by National Institutes of Health - Office of Research Infrastructure Programs). They were grown at 22$^{o}$C on NGM agar media (composition in Appendix) seeded with *E.coli* strain *OP50* (details in Appendix) under standard laboratory conditions (Brenner 1974). Occasional contamination which was observed was removed by treatment with bleach, as eggs are resistant to bleach. For long term storage strains were maintained in liquid nitrogen using freezing media (composition in Appendix). The strains which were used in this study were *N2 (Wild type), jsIs609, unc-116(e2310), klc-2(km11), dhc-1(js319), dhc-1(or195), mec-7(e1343), mec-7(u443), mec-12(e1607), mec-12(e1605), eat-3(ad426), drp-1(tm1108), mec-4(u253), mec-2(e75), mec-10(zb2551), egl-19(ad1006), egl-19(ad695), egl-19(n2368) and ebp-1(mec-7P; CFPebp-1).*

Transgenic strain *jsIs609* was made by (Dr Sandhya, TIFR-Mumbai) by injecting plasmid containing $_{p}$mec-7::mitoGFP along with lin-15 marker into the wild type N2 worms. The extragenic line was exposed to γ–radiation for obtaining the integrated transgenic lines. Following strains : *unc-116(e2310), klc-2(km11), dhc-1(js319), dhc-1(or195), mec-7(e1343), mec-7(u443), mec-12(e1607), mec-12(e1605), eat-3(ad426), drp-1(tm1108), mec-4(u253), mec-2(e75), mec-10(zb2551), egl-19(ad1006), egl-19(ad695) and egl-19(n2368)* were obtained from CGC(Caenorhabditis Genetics Centre). *Ebp-1*(*mec-7P; CFPebp-1*) was obtained as an extragenic line from Dr Yishi Jin's laboratory (University of California, San Diego) and was integrated later using the protocol described later in this section.

## 2.2. Genetic Crossing Scheme

All the strains used in this study were crossed with transgenic strain *jsIs609* to enable visualization of mitochondria in six touch receptor neurons. Simple genetic crossing strategy was used to make mutants in *jsIs609* background. Mutant strains were crossed with *jsIs609* males. F1 progeny obtained was placed in isolated plates for selfing. F2 progeny showing mutant phenotype are selected and left in isolated plates for selfing. Plates throwing all mutant phenotypes were checked for the presence of GFP marker, which was than homozygosed.

Genotype of strains built was confirmed by using PCR. Strains which didn't have any visible phenotype were made either using some visible marker or exclusively by PCR based assays.

### 2.3. Isolation of Genomic DNA

Worms were grown on *OP50* plates until food was depleted. Worms were washed from the plates using M9 buffer (composition in Appendix) and transferred to a 15 ml conical glass tubes. Worms were successively (3-4 times) washed using M9 buffer by gently pelleting them using low spin, throwing the supernatant and resuspending the worm pellet in fresh M9 buffer. Washing with M9 buffer facilitated complete removal of bacteria. Worms were then suspended in 1 ml M9 buffer and transferred to 1.5 ml eppendorf tube.

After centrifugation at 13000 rpm the worm pellet was suspended in 500 µl of worm lysis solution (100mM tris pH 8.5, 100mM NaCl, 50mM EDTA, 1% SDS, and proteinase K 100µg/ml). Worms suspended in lysis solution were incubated at 60$^{o}$C for 90 minutes. RNaseA (20µg/ml) was then added and the tube was incubated at 37$^{o}$C for 30 minutes. The tube was spinned in a microfuge and the supernatant transferred to new tube and an equal volume of Phenol/CHCl3 was added. It was gently mixed which was followed by centrifugation at 13000 rpm for 3 minutes. The aqueous phase obtained was extracted. To this extract 2.5 volumes of absolute ethanol was added. Whole mixture was spinned at 13000 rpm for 10 minutes. The Pellet was washed with 70% ethanol to remove salt. The pellet was then re-suspended in 100µl TE buffer (composition in Appendix) and was stored at -20$^{o}$C. All the chemicals used in the genomic DNA extraction were from Sigma-Aldirich.

### 2.4. PCR Reaction Condition

The PCR with primer specific for the mutant to be screened was carried out. Primers were procured from Sigma-Aldirich. PCR reaction was set using chemicals from Sigma-Aldirich PCR kit. 50 µl of PCR reaction mix was prepared using 5 µl of 10X PCR buffer, 1 µl of dNTPs (10mM stock), 2.5 µl of each primer from (10µM stock), template concentration 200ng/ µl and Taq polymerase (1.25 units/50 µl PCR), rest of the volume was adjusted using nuclease free water. The PCR was performed under the following conditions: Step I 95 $^{o}$ C – 5 minutes (initial denaturation) Step II 95$^{o}$ C – 30 sec (denaturation) Step III Temperature set according to primer

annealing temperature – 45 sec (primer annealing) Step IV 70$^{o}$ C – 5 min (extension) Step V go to step 2 and repeat 20 times Step VI 70$^{o}$ C – 5 min (final extension) Step VII 10$^{o}$ C – hold.

### 2.5. Image Acquisition and Analysis

For all the light microscopy imaging (except when effect of different anesthetics was checked) animals were immobilized using 50mM sodium azide (Sigma-Aldrich) prepared in M9 media. Worms were mounted by application of anesthetic under cover slips on a 2% agarose pad. To check the effect of anesthetics 10 mM levamisole (Sigma-Aldrich) and 10mM Muscimol (Sigma-Aldrich) in M9 media were also used, worms were mounted in the similar ways as described above. All the images were acquired at 60X objective on Nikon 800E microscope. Microscope was installed with QEi camera (Media cybernetics). Images were acquired using Qcapture pro software. Five to six animals were mounted on a single slide and images were acquired within 30 minutes of anesthetics application. Worms were always aligned with pharyngeal region at the left and tail at the right orientation while taking the snapshots.

For time lapse imaging animals were anaesthetized by 3mM Levamisole on a 2% agarose pad. Image J micromanager plugin was used to acquire the time lapse movies. For EM imaging young adults of *unc-16(tb109)* and *N2* strains were fixed by high pressure freezing (HPF) technique. Fixation was carried out in Prof David Hall's laboratory (Albert Einstein College of Medicine, NY). 30 to 40 serial ultrathin (50-60nm) sections of mid body region were obtained using Leica Ultramicrotome (Leica EM UC6). Nerve cord region of sections was imaged using Tecnai G$^{2}$ 12 TWIN / BioTWIN TEM microscope. Images were acquired at operating voltage of 60kV.

All the image analysis was done using NIH Image J software (version 1.47, NIH). Intermitochondrial distance was measured by drawing segmented lines between the two mitochondria and distance between the two was measured using "measure" option under Analyze tool bar in Image J. To measure distance in actual units (μm) scale bar was set using camera pixel aspect ratio. Mitochondrial area was measured by adjusting the threshold to cover precisely the pixels covered by the mitochondria and then measuring the pixels covered using measure option. Size of the vesicles was determined by encircling the vesicle and measuring its length.

## 2.6. Gentle Touch Assay

Mechanosensation assay was performed on young adult worms. Worms used for mechanosenastion were grown always in controlled condition of 22$^{o}$C and were transferred every alternate day to avoid starvation. 20-30 L4 worms were picked on fresh plates from non starved, non crowded plates a day before and were assayed the subsequent day (within 12-15 hours post transfer). Gentle touch was given to the animal by touching them with an eyelash at the pharyngeal and tail regions respectively. Animals were given alternate ten anterior and ten posterior touches respectively and response elucidated by the worm for all the twenty touches was recorded sequentially in the form of positive and negative response. Response was considered positive when animal responded to the stimuli by moving away from it i.e. when animal was touched in anterior end it moves backwards whereas, when it was touched in tail region it moves forward. Effect of interstimulus interval on mechanosensation was assayed by giving 10 second spacing between first and second touch.

At least three independent trials each with 20-30 worm set were assayed. Percentage response of individual worm for the ten anterior and ten posterior touches was quantified for each set of trials Results of all the ten trials were averaged out to represent percentage response for anterior and posterior touch delivered by different genotypes.

## 2.7. Statistical Analysis

Statistical tests for normal distribution (Kolmogorov-Smirnov test, Anderson-Darling and Chi-Square test) and curve fitting for analysing type of mitochondrial distribution was carried out using Easy Fit 5.5 Professional Software. Rest all statistical tests, analysis and statistical graphs were done using MS-Excel.

## 2.8. Integration Protocol for Extragenic Strains

Approximately 100 (5 worms/plate) young adults were irradiated using UV Stratalinker set at 300µjoules (X100). Half of the worms were incubated at 25°C and other half at 20°C for 2- 3 weeks respectively. Worms were incubated at different temperatures to ease the screening process so that it can be done at different intervals. 1.5cm x 1.5cm chunks from starved plates were transferred to fresh plate. 10-15 animals from each master plate were picked onto individual plates, on the next day. A total of 200-300 such transgenic animals were picked.

Worms were allowed to self for two generations and then individual plates were screened to isolate the integrant.

# Chapter 3

## Mitochondrial Density Remains Constant during Development and Their Distribution is Regulated

# 3. Mitochondrial Density Remains Constant during Development and Their Distribution is Regulated

## 3.1. Introduction

All eukaryotic cells are dependent on mitochondria for their survival. Mitochondria are responsible for carrying out several vital functions like ATP generation, $Ca^{2+}$ homeostasis, generation of free radicals, apoptosis etc. In neuronal cells, positioning and distribution of mitochondria is even more important as these cells have complex morphology, are functionally heterogeneous and have high metabolic rate. As neuronal cells are longer, mitochondria needs to be transported to quite distant regions in axons. Along with this, neuronal regions are also functionally differentiated, some of which have higher energy needs as compared to other. Some of the energy intensive processes happening in neurons are firing of action potential, synthesis, packaging and transport of neurotransmitters, assembly of cytoskeleton elements etc. Apart from energy generation mitochondria are also involved in neuronal development, maintenance of synaptic plasticity by producing sufficient ATP and sequestering $Ca^{2+}$ generated during synaptic transmission, and also neuronal cell death.

As mitochondrial distribution and functioning is extremely important in neuronal cells, therefore its dysfunction and abnormal dynamics has been reported to be associated with many neurodegenerative diseases such as Alzheimer, Parkinson, Amyotropic lateral sclerosis etc. Alzheimer's disease (AD) has been associated with decreased ATP production, increased oxidative stress, increased $Ca^{2+}$ uptake, increased mitochondrial autophagy (Maurer et al 2000, Hirai et al 2001, Hashimoto et al., 2003, Mosconi et al 2008). Amyloid ß peptide (Aß) plaques (Goedert et al 2006) which is one of the hallmark of AD and has been reported to be responsible for causing mitochondrial dysfunction (Keller et al.1997, Manczak et al. 2006). Similarly, in Parkinson's disease (PD) decreased activity of mitochondrial complex I has been reported, decreased complex I activity results in decreased ATP production, increased oxidative stress, increased $Ca^{2+}$ uptake and mitopathy (Swerdlow et al. 1996, Keeney et al. 2006). Moreover most of the genes like α-synuclein (Devi et al. 2008), Parkin (Greene et al. 2003), DJ-1(Zhang et al. 2005), PINK1 (Yang et al. 2008), which have been reported to be associated with PD are reported to be linked to mitochondria directly or indirectly. Increased free radical accumulation

(Pedersen et al. 1998), decreased ATP production (von Lewinski et al 2005), disturbed $Ca^{2+}$ buffering (Kruman et al. 1999) has also been reported to be associated with Amyotropic lateral sclerosis (ALS). Thus the above citations clearly illustrate that disturbed mitochondrial dynamics is associated with many neurodegenerative diseases.

Mitochondrial biogenesis is known to take place both in the cell body as well as axon (Amiri et al 2008). Mitochondria are highly dynamic organelle and they are transported from their site of biogenesis to site of their requirement by motor mediated fast and slow axonal transport. Motor mediated fast mitochondrial transport on microtubules tracks mainly show two characteristics that are saltatory and bidirectional movement (Morris et al 1993). In addition only half of the mitochondria in the axon move with a velocity ranging from 0.3-2.0 μm $second^{-1}$ while the other half are stationary during the time imaged (Allen et al 1982, Hollenbeck 1996, Ligon et al 2000, Pilling et al 2006). Moreover, mitochondria can distribute themselves depending on the needs of the cell. ATP though is a freely diffusible molecule but, both non neuronal (Mechler et al 1981) and neuronal cells (Gotow et al. 1991, Morris et al 1993) are known to concentrate mitochondria in regions of high energy needs. Mitochondria are thus found to be more accumulated in the regions of the axons which have high energy demands like synapses, growth cones, nodes of Ranvier etc. (Gotow et al. 1991, Morris et al 1993, Li et al 2004).

Mitochondria localization and factors affecting it has been studied using different approaches. Effect of myelination and demyelination on mitochondrial localization has also been studied using both in-vitro and in-vivo approaches. Axons of both central nervous system (CNS) and peripheral nervous system (PNS) are encapsulated by myelin sheath (Hartline et al. 2007). Myelin is mainly composed of lipids (Gesine et al 2005) and acts as an insulator, thus helping in increasing the speed of impulse conduction (Hartline 2008). Myelinated axons are organized into distinct sub domains which are nodes, paranodes, juxtaparanodes and internodes; each of these distinct regions has its own structural and functional differences (James et al 2008). Mitochondria localization in these distinct regions has been studied extensively using different approaches. Histological experiments done using optic nerves of human, rabbit and pig has demonstrated more mitochondrial activity in unmyelinated regions compared to myelinated regions (Bristow et al 2002). Using EM imaging studies done on cat ventral and lateral spinal cord segments it is reported that paranode-node-paranode (PNP) region had high concentration

of mitochondria whereas highest concentration was observed in nodes of ranvier (Fabricius et al 1993). Another study done by a group using mice small diameter CNS axons (optic nerves and spinal cord) observed no preferential localization of mitochondria in PNP region (Edgar et al 2008).

Effect of dysmyelination and demyelination on mitochondrial localization has been studied using different approaches. One such approach was using Shiverer mouse model where CNS axons were hypomyelinated, it was reported that there was higher mitochondria number and two fold higher mitochondrial activity in the dysmyelinated axon (Andrews et al 2006). Effect of demyelination was studied using mice model overexpressing *Plp-1*(proteolipid protein gene 1). It was reported that there was higher mitochondria number as well as activity in the demyelinated optic nerve axons (Hogan et al 2009). Demyelination has also been reported as a cause for some of the neurological disorders like Multiple Sclerosis (Bjartmar et al 2003). Histology and biochemical studies done using demyelinated active MS lesions revealed the presence of enhanced mitochondrial activity as well as increased mitochondrial count in these regions (Dutta et al 2006, Witte et al 2009). Effect of demyelination and remyelination on mitochondrial velocity and size was also studied using rat dorsal root ganglion (DRG) culture (Kiryu-Seo et al 2010). It was reported that demyelination, increased the size of axonal stationary mitochondrial sites by 2.2-fold it also resulted in increased velocity of moving mitochondria which returned to control levels on remyelination (Kiryu et al 2010).

Apart from structural features like presence or absence of myelin sheath, other aspects like developmental stage of axon, ATP, cytosolic calcium levels, mitochondrial membrane potential, presence or absence of neurotransmitters have been reported to effect mitochondria transport and localization. Studies done using chick embryo neuronal culture have reported that high concentration of mitochondria was found near the growth cone and when axonal growth was halted mitochondria got redistributed (Morris et al 1993). Effect of nerve growth factor (NGF) signaling in mitochondria localization has also been reported. It states that mitochondria tend to accumulate in vicinity of NGF coated beads (Chada et al 2003, 2004).

Physiological state of mitochondria i.e. its membrane potential has also been reported to govern mitochondrial movement and distribution. Mitochondrial membrane potential is the thrust for all

the mitochondrial functions like ATP production (Dimroth et al 2000), $Ca^{2+}$uptake (Komary et al 2010) free radical generation (Suskit et al 2012) and apoptosis (Gautier et al 2000). Apart from mitochondrial density which is reported to be higher in the growing regions of axon it has also been reported that these regions have significantly higher membrane potential compared to the adjacent axonal stretch (Morris et al 1993, Miller et al 2004). Blocking of the axonal growth using drug treatment has been reported to restore uniform membrane potential in the axonal stretch (Morris et al 1993). ATP depletion and accumulation of ADP has also been reported as another factor responsible for halting of mitochondrial and its localization in the ATP depleted regions (Mironov 2007).

Based on the above discussion, ground state of mitochondria distribution at a particular time point is a signature of physiological state of a cell. Dynamic balance of fission and fusion has been reported to regulate mitochondria morphology, length and in turn its distribution and function (Chan 2006). Fission and fusion events are vital steps for controlling quality and quantity of mitochondria. Fission helps in segregating mitochondrial contents in the daughter cells, apart from that it also facilitates removal of damaged mitochondria (mitopathy) and also leads to apoptosis under extreme circumstances (Chen et al 2009). Similarly, fusion helps in intermixing of mitochondrial contents like mitochondrial matrix, proteins lipids and mitochondrial DNA (Westermann 2002).

Very few studies have been done so far to study mitochondrial distribution in axons and how density of mitochondria changes with axonal elongation. One such study using axonal culture using chick embryos has demonstrated that mitochondria have a uniform distribution in axons (Miller et al 2004). They have used individual frames of time lapse movies to locate the position of mitochondria and uniformity of distribution was reported by carrying out chi-square test.

Another paper by the same group (Toole et al 2008) has also looked at the effect of axonal elongation on density profile of mitochondria. For the same they have measured axon length of the medial segmental nerves of Drosophila $1^{st}$, $2^{nd}$ and $3^{rd}$ instar larval stages. They have also determined the mitochondrial density in these nerves. Drosophila larval medial segmental nerves are nerve bundles; proximal terminal and cell body of these nerves is located in the brain region whereas rest of the axon runs through the larval body and it terminates in the body length. Their

results reported increase in axon length as well as mitochondrial density with developmental stages. Trends reported for axon length/mitochondrial density were 468±124µm (0.34±0.06 mito/µm), 631±262 µm (0.37±0.05mito/µm) and 963±163µm (0.58±0.08mito/µm) for 1st, 2nd and 3rd instar larval stages respectively.

Another group has also analyzed mitochondrial distribution in growing and halted axons using chick embryo culture (sympathetic chain ganglion) (Morris et al 1993). They have termed distribution as uniform based on three statistical tests: linear regression with analysis of variance, Chi-square and Kolmogorov-Smirnov tests for grouped data. They have termed the distribution as uniform when it doesn't show significant difference from uniform distribution by any two tests at significance level of $P < 0.05$. As reported earlier they have reported mitochondrial distribution was skewed in the growing axon with high mitochondrial density in proximity to the growth cone. Mitochondrial distribution tends to become uniform once the axonal growth was halted by using chemical inhibitors.

In an attempt to understand how mitochondrion are distributed and is the distribution developmentally regulated, we have examined the positions of mitochondria in ***C. elegans*** touch neurons. These six neurons are specialized neurons which mediate response to gentle touch and have larger diameter microtubules (15-Protofilament) (Chalfie et al 1979). We have looked at mitochondrial distribution in these mechanosensory neurons using the transgenic strain *jsIs609.* We have looked at mitochondria number, density and distribution in these mechanosensory neurons across all developmental stages of ***C. elegans***. Our results show that mitochondria density and distribution are regulated and maintained throughout development.

## 3.2. Results

### 3.2.1. Mitochondria are visualized in the Six Mechanosensory Neurons by Matrix Targeted GFP in Transgenic Strain *jsIs609*

In order to visualize mitochondria in mechanosensory neurons, GFP was targeted to the mitochondrial matrix using the *mec-7* touch neuron specific promoter. Transgenic strain *jsIs609* (Fig 3.1) was identical to *N2* in morphology, viability and behavior such as locomotion and egg laying.

In *jsIs609* mitochondria were visible as distinct fluorescent puncta along the neuronal process and in synaptic regions (arrows) (Fig 3.1C-D & F-G). In addition some soluble GFP was also present along the neuronal process allowing us to visualize it. A mitochondrial network was also seen in the cell body of both anterior and posterior touch neurons (Fig 3.1E-H)

To establish that the *jsIs609* marked nearly all mitochondria in the neuron, we examined two other transgenic strains. *jsIs608*, another independent integrant of the same construct showed identical numbers, morphology and distribution of mitochondria. Further, a touch neuron specific transgene expressing matrix targeted mRFP showed the identical pattern. A strain harboring both *jsIs609* and *jsIs1073* (from Nonet lab, Washington University, St Louis) showed that identical structures were marked by both strains (Fig 3.1 I-N). *jsIs609* marks nearly all mitochondria was also confirmed by labeling mitochondria with mitotracker orange in primary ***C. elegans*** embryonic neuronal culture (this work was done by Eva Romero, a former post-doctoral fellow in the lab).

### 3.2.2. Mitochondrial Density is Regulated throughout the Development

To visualize, how the number of mitochondria varies during development, we quantified the number of mitochondria present corresponding to all the developmental stages from L1 to 1 day adult. We also measured respective axon lengths for all the development stages using Image J. A population of twenty five worms was assayed per developmental stage for both ALM and PLM processes.

Approximately around 3-4 fold increase in number of mitochondria was seen from L1 to 1 day adult in both ALM and PLM (Table 3.1 and Fig 3.2). Axon length also showed a 4-5 fold increase with development (Table 3.1 and Fig 3.2). We also quantified the number of mitochondria present per 100µm of axon length in all the developmental stages from L1 to 1 day adult. We found that mitochondrial density always maintained a number close to 5 mitochondria per 100µm of axon length with standard error (S.E.) < 0.5 in both ALM and PLM for all the developmental stages (Table 3.1 and Fig 3.2).

We also looked at the ratio of increase in number of mitochondria and increase in axon length from one developmental stage to another. We found that the increase in mitochondrial number as well as axon length always maintained a constant proportion throughout the development.

Results implied that increase in number of mitochondria was proportionate to axonal growth (Table 3.2).

### 3.2.3. Distribution is Initiated in Early Developmental Stages and Maintained in the Later Stages

To study whether a correlation exists between axon length and mitochondria number, we plotted correlation graph. Axon length was represented on X-axis whereas, position of the mitochondria on the axon starting from first mitochondria (nearest to the cell body) to the last were represented on the Y-axis. Correlation graphs were plotted for all the developmental stages. Invariably, the graphs for all the developmental stages showed positive and linear correlation (y=a + bx; where "y" is the dependent variable, "x" is independent variable, "a" is the intercept and "b" is the slope) between axon length and mitochondria number and position. Values of the coefficient of determination ($R^2$) showed the values ranging from approximately 0.7 for L1 to 0.94 for 1 day adult. L2 showed value of 0.85 whereas L3 and L4 stages showed the value close to 0.9 (Fig 3.3A-E). Values of $R^2$ depicted that in the earlier larval stages (L1 and L2) distribution is being set-up thus lower value of value of correlation between mitochondria position and axon length. Whereas, in later stages L3 and above mitochondria distribution has been set-up and is tightly regulated and maintained. Thus the above results indicate that a constant mitochondrial density is maintained in the axon throughout the development. This density may be regulated by physiological and cellular signals such as alteration in calcium concentration or release of neurotransmitters (Yi et al. 2004), growth factors such as NGF (Chada et al 2003, 2004), hypoxic stress (Li et al. 2009) etc.

Mitochondrial density appears tightly regulated and showed linear correlation with axon length. In an effort to understand mitochondrial distribution more closely we measured and looked at inter-mitochondrial distance between two consecutive mitochondria. Histograms were plotted for inter-mitochondrial distance versus frequency fraction of mitochondria for the given ranges for all the developmental stages. Mitochondria were more closely spaced in early development stages. Very larger inter-mitochondrial distances were also seen in early developmental stages but with a lower frequency (Fig 3.4 A-E). Histogram of early developmental stages showed more spread in the distribution. For a particular mitochondrial position, range of distance where the

mitochondria was present in the experimental set observed was more wide in early stages compared to the later ones (Fig 3.3 A –E).

### 3.2.4. Distribution of Mitochondria is Non-random

To check whether mitochondria are distributed evenly throughout the axon length, we divided the axon into three equal regions proximal (near cell body), middle region and distal region. We calculated approximate percentage of mitochondria distributed in all the three regions for different developmental stages. We observed that approximately 25% of the mitochondrial population was present in the proximal region in all the developmental stages (L1 to 1 day adult) while rest 75% was equally divided in middle and distal region (observed in L3, L4 and 1 day adult). The early developmental stages (L1 and L2) showed most (approx. 45%) accumulation of mitochondria in the middle region (Table 3.3). Distribution of mitochondria more in middle and distal region may be attributed to the more energy needs in these regions due to close proximity of these regions to nerve ring and synapses.

Previous studies done using cultured sympathetic chain ganglia dissected from chick embryo have reported presence of both skewed and uniform distribution of mitochondria in axons depending upon the growth state of axon (Morris et al 1993). In this study mitochondria were labeled with rhodamine 123 and distribution of mitochondria in 100µm vicinity of active growth cone was studied in the native state as well as when axonal elongation was halted by cytochalasin treatment. In the former case when axon was growing, distribution was reported to be skewed as most of the mitochondria were concentrated towards growth cone whereas in later case when axonal distribution was halted by 1 hour treatment with cytochalasin, distribution was uniform. To understand whether mitochondria distribution follows a uniform or normal distribution in our axon of interest we looked at the distribution graphically (by histograms) as well as through statistical tests. Uniform distribution in statistics, is a distribution in which every possible result is equally likely i.e. every one of $n$ values has equal probability$1/n$. Whereas, normal distributions also known as bell shaped distribution are symmetric around their mean. They have mean, median, and mode equal. Normal distributions are defined by the parameters, the mean (μ) and the standard deviation (σ). 68% of the area of a normal distribution is within one standard deviation of the mean. Approximately 95% of the area of a normal distribution is within two standard deviations of the mean (Zar 1999).

For histograms we plotted pooled inter-mitochondrial distance for all the developmental stages in Y axis against frequency of the respective distances on X-axis and did curve fitting for the same. Both the histograms for ALM and PLM had closer resemblance to normal distribution than uniform distribution (Fig 3.5 A-B). To confirm the normal distribution we carried out Chi-Square, Kolmogorov-Smirnov and Anderson-Darling statistical tests for normal distribution. All the three tests used were non parametrical. Null hypothesis ($H_0$) employed for all the three statistical tests was experimental data is not normally distributed and alternative hypothesis ($H_A$) was data is normally distributed. Null hypothesis was rejected and distribution was considered normal when p value obtained was $P < 0.05$. We termed the distribution as normal when null hypothesis was rejected by any two statistical tests at 95% confidence interval.

Chi-square test of goodness of fit is based on probability distribution function and this test calculates the difference between the observed (experimental) and expected distribution (Kvam et al 2007). Sum of squares of difference between experimental distribution data set and expected data was divided with expected frequency to obtain the Chi-square value. Kolmogorov-Smirnov (K-S) test uses the cumulative distribution function and compares the theoretical cumulative frequency data set with the experimental cumulative frequency data set (Kvam et al 2007). K-S test is reported as more powerful than Chi-square test and sample size is not a limiting factor for K-S test. Anderson Darling test is a modification of K-S test and gives more value to the tails and hence is considered better than K-S test (Kvam et al 2007).

When all the inter-mitochondrial distances were used to carry out statistical tests, it failed in all the above three tests both for ALM and PLM. This suggested that the distribution was not normal (Table 3.4 A and B). ALM and PLM in totality showed best fit for Generalized Gamma distribution (4P) and generalized extreme value distribution respectively. Statistical tests were also performed for proximal, distal and middle regions separately for pooled data set for all developmental stages for both ALM and PLM processes. When the individual regions were taken separately, most of the tests accepted alternate hypothesis and rejected the null hypothesis (Table 3.4 A&B) at $P<0.05$, thus implying individual regions in both ALM and PLM fits a normal distribution.

As per the above results each individual regions of the axons (proximal, middle and distal) have their own set of distribution pattern which complied with normal distribution and distribution in no case was random. To confirm that the above set of distribution has not appeared by chance, we carried out simulations for the data set which was done with the help of a post-doctoral fellow (Dr Sudip Mondal) in the laboratory. The simulation took a 400µm neuronal process length in which 20 mitochondria were placed randomly after which inter mitochondrial intervals were plotted. All the simulation graphs show an exponential decay in inter-mitochondrial intervals (Fig 3.6 A-B). Compared to experimental data which had only 2-3% of mitochondria less than 3µm inter-mitochondrial distance apart, simulation graphs had a value of 14% and above. This suggests that a regulatory process reduces the probability of two mitochondria from being placed close to each other *in vivo.* All the simulated histograms were different from our experimental graph, thus confirming that distribution of mitochondria in *jsIs609* is non-random.

To determine whether it is the size as opposed to the number of mitochondria that co-relate with the length of the neuronal process, we measured the pixels covered by each mitochondrion for the different developmental stages (Fig 3.7). We found that average area of the mitochondria was least in L1 stage (0.32µm$^2$) and most in L2 (0.61µm$^2$). L3, L4 and 1 day adult animals showed progressive increase in mitochondrial area with values corresponding to 0.48, 0.54 and 0.57µm$^2$ respectively for the ALM processes (Table 3.5). When we looked at average area of the mitochondria in proximal, middle and distal regions of the axon we found that proximal region has the smallest mitochondria (Table 3.6). Above result are in conformance with the live imaging data from our lab where higher flux was observed in the proximal region compared to distal region (work done by Jyoti Dubey) as well as reported results which states that stationary mitochondria shows higher area as compared to the moving mitochondria which were found to be smaller (Miller et al 2004). We tried correlating the area occupied by mitochondria with axon length. Similar to mitochondria number which showed a constant number per 100 µm of axon length in different developmental stages area covered by mitochondria per 100 µm of axon length also maintained a value in a specific range. It showed a value of 2.5 to 3 µm$^2$ for ALM processes and 2 to 2.5 µm$^2$ for PLM processes (Table 3.5). Above results thus imply that mitochondria density, distribution as well as size is tightly regulated in the axon to take care of the axonal functions.

### 3.2.5. Growth in Length of Neuronal Process and Mitochondria Distribution is Proportionate to Body Length of the Organism

Our findings show that numbers of mitochondria present are proportionate to the length of the neuronal process. To confirm the above findings, we used mutants which alter the length of the animal presuming it will alter length of the neuron as well. We wanted to analyze whether body length of organism will show proportionate effect on mitochondria number and axon length as well. To check this we analyzed two different mutant strains of ***C. elegans*** which had mutation in the set of genes which affects body length of the worm making them long (abbreviated as lon) or making them shorter than wild type/dumpy (abbreviated as dpy).

We looked at *lon-2(e678)* animals; *lon-2* activity is required in regulation of the DBL-1/BMP signaling pathway which regulates body length (Gumienny et al 2007). For the shorter/dumpy allele we looked at *dpy-6(e14)* strain. *Dpy-6* encodes a novel protein which is required for normal body morphology (Simmer et al 2003). Both *lon-2(e678)* and *dpy-6(e14)* animals had significantly different length from wild type (Fig 3.8 and Table 3.7). ALM axon length of 1 day adult for both *lon-2(e678)* and *dpy-6(e14)* were significantly different from wild type with values respectively 484.12±16.3(*lon-2*), 236.29±8.80 (*dpy-6*) and 406.11±5.88 (*jsIs609*) (Table 3.7). PLM also showed the similar trend. Numbers of mitochondria observed in ALM and PLM processes of both the strains were proportionate to their respective axon lengths. Number of mitochondria observed per 100µm of axon length was similar to *jsIs609* with value approx. around 5 mitochondria/100µm of axon (Table 3.8).

To check whether increase in axon length and mitochondria number with development in these strains was comparable to wild type, we quantified L4 larval stage for number and axon length and compared it with the adult data set. We found that in both *lon-2* and *dpy-6* strains, growth in axon length and increase in mitochondria number with development was comparable to wild type (Table 3.9).

## 3.3. Discussion

As per the above observations, using three different approaches it is confirmed that our reporter strain *jsIs609* labels all the mitochondria and is ideal to study mitochondrial dynamics in touch neurons. Mitochondria number per unit length remains conserved throughout the development.

Distribution of mitochondria in different developmental stages signified that distribution is initiated in the early developmental stages and is regulated and maintained in the later stages.

Maintenance of constant number of mitochondria per unit axon length throughout the development implies a complex array of molecular, cellular and physiological signals must be interplaying role in regulating this distribution. Positioning of mitochondria in the axonal segment should be such that it is able to support local ATP needs, $Ca^{2+}$ buffering, scavenge free radicals, apoptosis etc. Apart from maintaining the constant density in the neuronal process mitochondrial distribution was also observed to be very well organized, thus depicting regulatory mechanism must be in hold which prevented two mitochondria from being placed in too close proximity nor too distally. Maintenance of constant density and regulated distribution signifies that this constant pool per unit axon length was sufficient to take care of all the mitochondrial functions like ATP production, $Ca^{2+}$ buffering etc in the localized region.

Furthermore, average area of the mitochondria as well as area occupied by mitochondria per unit axon length was also found to be constantly maintained throughout the development. Results implied that signaling process is in hold throughout development which is maintaining distribution, moreover not only position, size is also well regulated and maintained. This implied that only properly sized mitochondria are transported from the neuronal cell body and in the axon the properly sized mitochondria are maintained by interplay of fission/fusion events.

Moreover different regions of the axon i.e. proximal, middle and distal regions also tend to show their own subset of distinctive distribution patterns. Out of the three regions, proximal region tend to show the lowest percentage (25%) of mitochondria whereas rest of the mitochondria were found to be uniformly distributed between middle and distal regions. Higher percentage of mitochondria in middle and distal regions may be presumed due to close proximity of these regions with synaptic areas. To meet the sudden need of mitochondria in these regions, mitochondria are stationed in the vicinity so that they can be quickly transported when required. Thus to overcome time delay in the event of sudden need, may be, more mitochondria's are recruited in these regions. Moreover average mitochondrial area was lowest in proximal region as compared to middle and distal regions. It has been reported that moving mitochondria are smaller as compared to the stationary mitochondria. So, the presence of smaller mitochondria in

proximal region may be due to the presence of larger pool of mobile mitochondria which are being transported both in anterograde and retrograde directions.

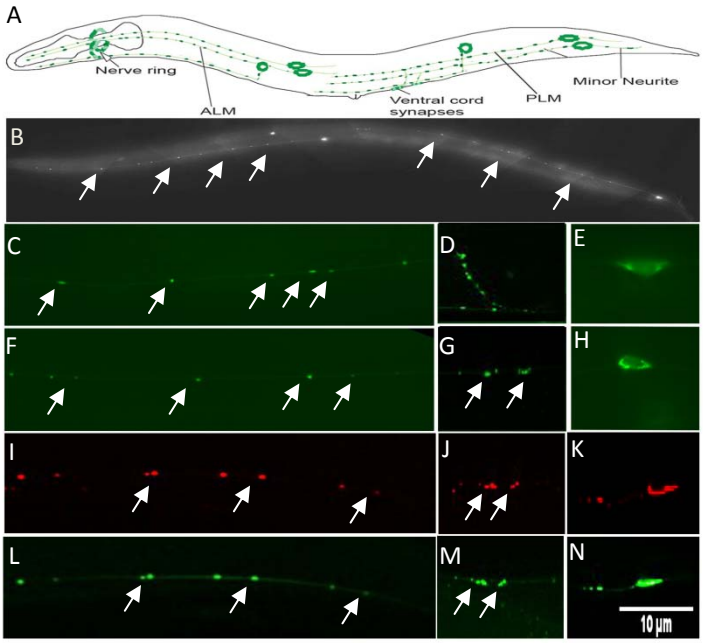


**Figure 3.1: GFP labels all the mitochondria in *jsIs609* mechanosensory neurons**

(A) Representative diagram showing six mechanosensory neurons. Green dots represent mitochondria.
(B) Reconstructed image of young adult worm representing ALM and PLM processes.
C), D) and E) Represents axon, nerve ring and cell body respectively of ALM.
F), G) and H) Represents axon, ventral synapse and cell body respectively of PLM
I), J), K), L), M) and N) Represents co-localization between GFP and mRFP targeted mitochondria.
I) and L) Represents co-localization in axonal region
J) and M) Represents co-localization in ventral synapse
K) and N) Represents co-localization in cell body region. Arrow heads represent mitochondria. Scale bar 10µm.

Table 3.1

| Larval Stages | Av. No. of mitochondria in ALM | Av. Axon length of ALM(µm) | Av. Mito. No./100µm of ALM Axon length | Av. No. of mitochondria in PLM | Av. Axon length of PLM(µm) | Av. Mito. No./100µm of PLM Axon length |
|---|---|---|---|---|---|---|
| L1 | 6.3±0.3 | 117.4±1.6 | 5.4±0.3 | 5.9±0.3 | 104.8±2.0 | 5.6±0.3 |
| L2 | 9.1±0.5 | 179.6±2.7 | 5.0±0.2 | 9.3±0.4 | 184.9±3.3 | 5.0±0.2 |
| L3 | 12.9±0.4 | 252.1±4.2 | 5.1±0.1 | 14.0±0.4 | 285.5±4.7 | 4.9±0.2 |
| L4 | 14.6±0.4 | 297.9±3.4 | 4.9±0.1 | 16.9±0.6 | 361.4±4.6 | 4.7±0.1 |
| 1 day adult | 19.1±0.5 | 406.1±5.9 | 4.7±0.1 | 25.3±1.0 | 507.2±8.1 | 5.0±0.1 |

**Table 3.1 Quantitation of average number of mitochondria and axon length with development.**
Data is represented as mean±SEM. ALM and PLM processes of 25-30 animals were used for analysis.

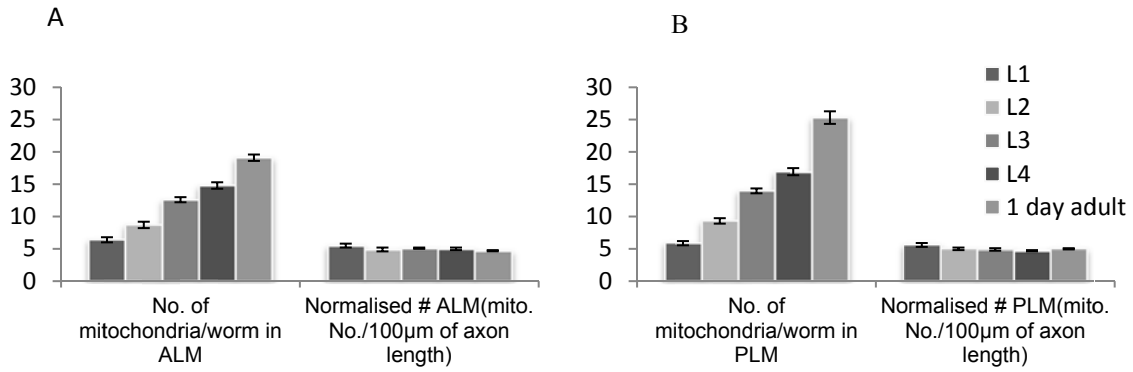


**Figure 3.2 (A-B) Graph showing increase in mitochondria number with development in ALM and PLM processes**
Normalised number of mitochondria per 100µm of axon length is also represented. Data is represented as mean±SEM. ALM and PLM processes of 25-30 animals were used for analysis.

Table 3.2

| Larval Stages | Av. No. of mitochondria in ALM | Fold increase in ALM mitochondria no. with development | Av. Axon length of ALM(µm) | Fold increase in ALM axon length with development | Av. No. of mitochondria in PLM | Fold increase in PLM mitochondria no. with development | Av. Axon length of PLM(µm) | Fold increase in PLM axon length with development |
|---|---|---|---|---|---|---|---|---|
| L1 | 6.3±0.3 | NA | 117.4±1.6 | NA | 5.9±0.3 | NA | 104.8±2.0 | NA |
| L2 | 9.1±0.5 | 1.4 | 179.6±2.7 | 1.5 | 9.3±0.4 | 1.6 | 184.9±3.3 | 1.8 |
| L3 | 12.9±0.4 | 1.4 | 252.1±4.2 | 1.4 | 14.0±0.4 | 1.5 | 285.5±4.7 | 1.5 |
| L4 | 14.6±0.4 | 1.2 | 297.9±3.4 | 1.2 | 16.9±0.6 | 1.2 | 361.4±4.6 | 1.3 |
| 1 DA | 19.1±0.5 | 1.3 | 406.1±5.9 | 1.4 | 25.3±1.0 | 1.5 | 507.2±8.1 | 1.4 |

**Table 3.2 Fold change in mitochondria number and axon length with development.**
Data is represented as mean±SEM. ALM and PLM processes of 25-30 animals were used for analysis.

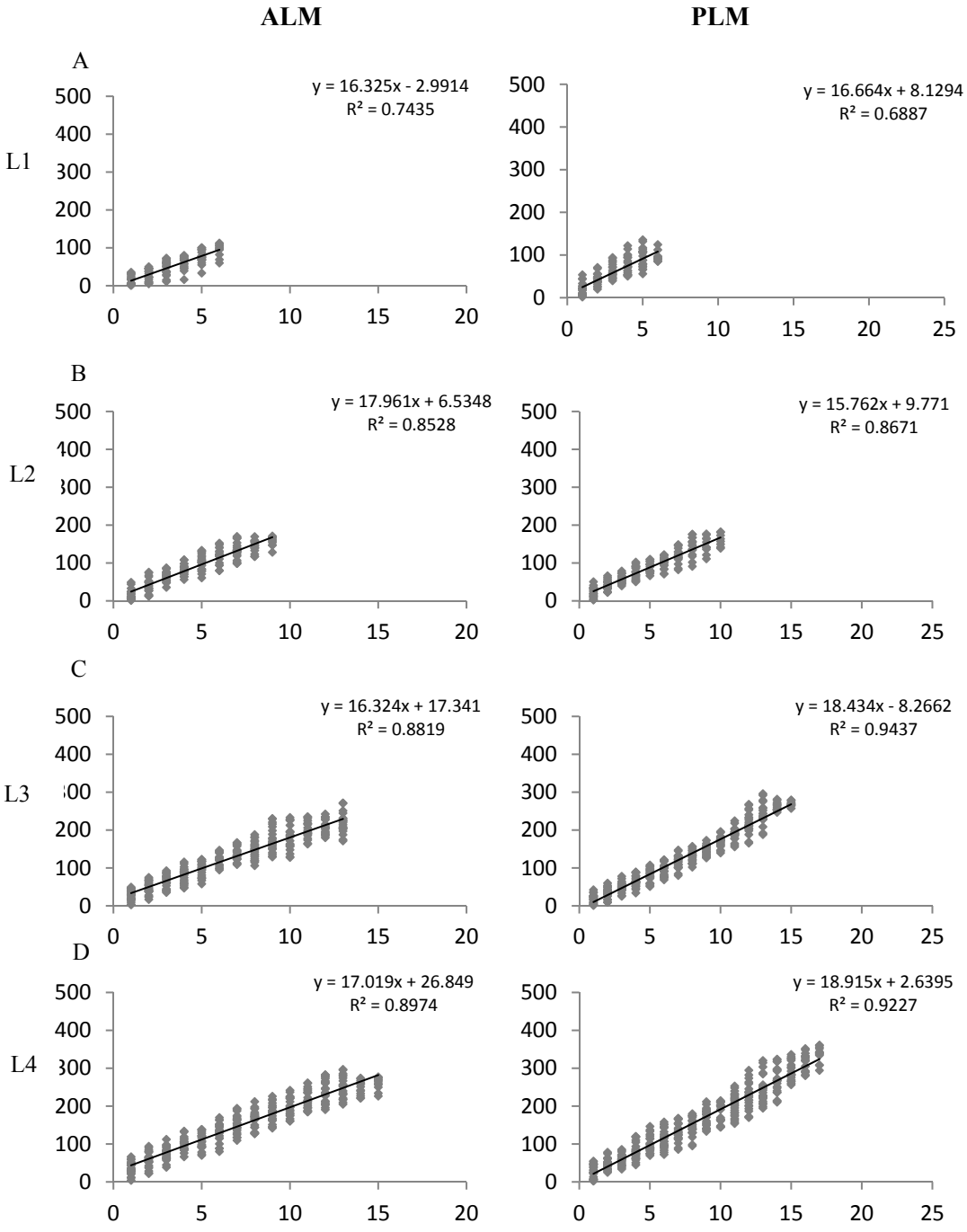
ALM
PLM
A
L1
y = 16.325x - 2.9914
R² = 0.7435
y = 16.664x + 8.1294
R² = 0.6887
B
L2
y = 17.961x + 6.5348
R² = 0.8528
y = 15.762x + 9.771
R² = 0.8671
C
L3
y = 16.324x + 17.341
R² = 0.8819
y = 18.434x - 8.2662
R² = 0.9437
D
L4
y = 17.019x + 26.849
R² = 0.8974
y = 18.915x + 2.6395
R² = 0.9227

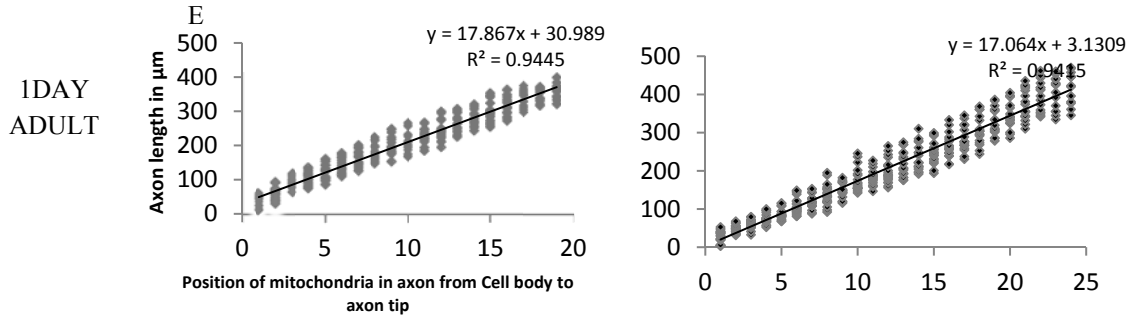


**Figure 3.3 (A-E) Regression graphs representing axon length versus mitochondrial position for all the developmental stages**

Y-axis represents axon length (µm); X-axis represents position of mitochondria in axon starting from first mitochondria near the cell body. Correlation equation "Y=a +bx" where "Y" is dependent variable, "x" is independent variable "a" is the intercept and "b" is the slope. Value of coefficient for correlation $R^2$ is also represented on the graph. Every position of mitochondria represented on the graph represents position points for 25 animals analyzed for every developmental stage.

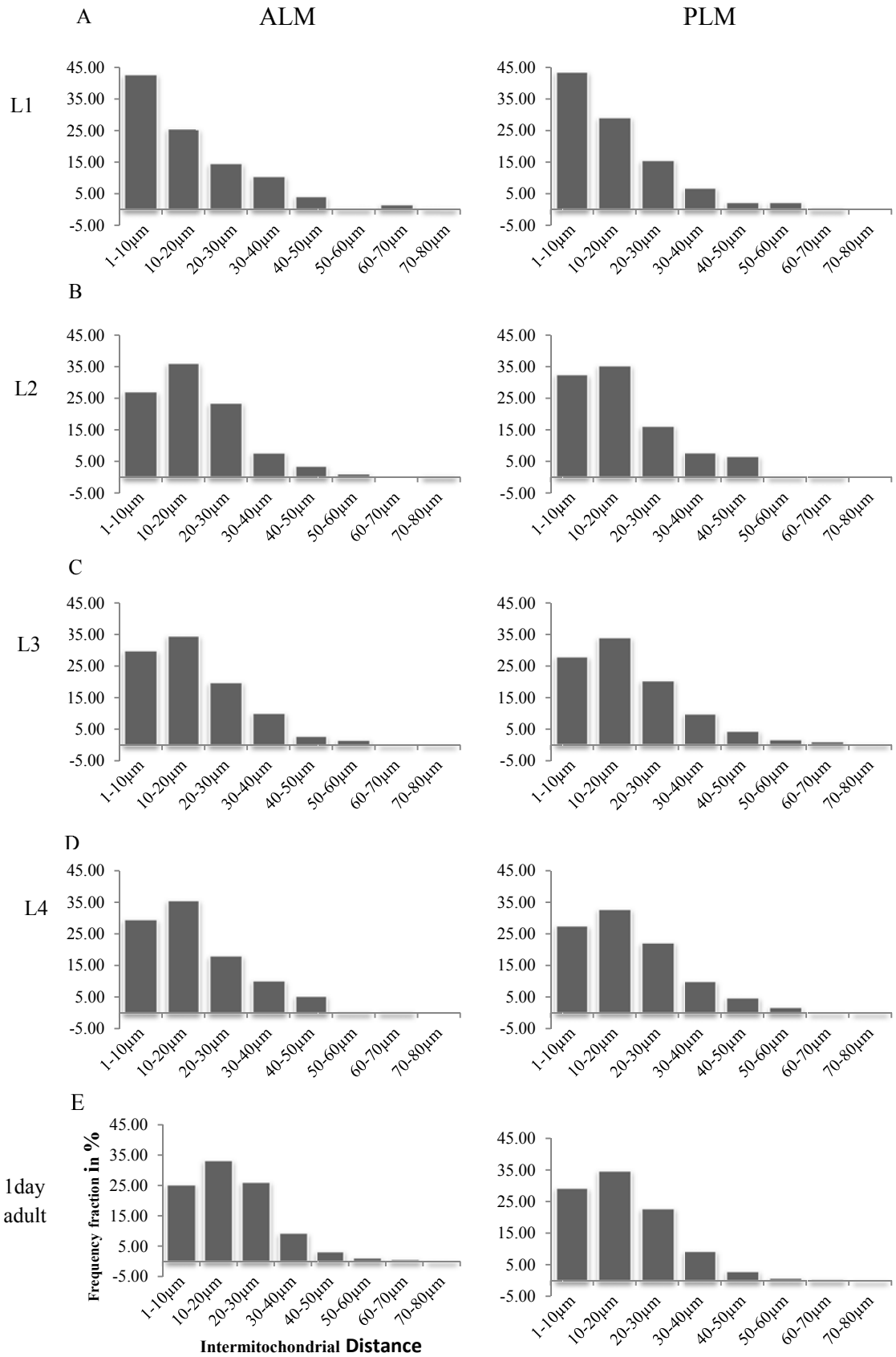
A
ALM
PLM
L1
B
L2
C
L3
D
L4
E
1day adult
45.00
35.00
25.00
15.00
5.00
-5.00
1-10µm
10-20µm
20-30µm
30-40µm
40-50µm
50-60µm
60-70µm
70-80µm
Frequency fraction in %
Intermitochondrial Distance

**Figure 3.4 (A-E) Represents range of intermitochondrial distances and percentage of mitochondria present in the corresponding range for ALM and PLM processes for all the developmental stages**

Percentage of mitochondria present in a particular range is represented as "Frequency fraction in %" in Y-axis. Range of intermitochondrial distance is represented on X-axis. Total of 25 animals were assayed for each developmental stage and all intermitochondrial distances for a set of 25 animals were used for making the plots.

Table 3.3

| | ALM mitochondrial density (%) | | | PLM mitochondrial density (%) | | |
|---|---|---|---|---|---|---|
| Larval Stages | Proximal region(near Cell body) | Middle region | Distal region | Proximal region(near Cell body) | Middle region | Distal region |
| L1 | 27.7±2.6 | 39.6±2.4 | 32.8±2.8 | 21.0±2.7 | 36.9±3.4 | 42.1±3.0 |
| L2 | 22.2±1.8 | 35.1±2.2 | 42.8±2.1 | 28.8±2.0 | 40.0±1.8 | 31.2±1.8 |
| L3 | 24.5±1.8 | 34.0±1.2 | 41.5±1.6 | 34.6±1.3 | 35.8±1.2 | 29.5±1.0 |
| L4 | 23.6±1.4 | 34.4±1.4 | 41.9±1.3 | 34.6±1.3 | 37.4±1.4 | 28.0±1.1 |
| 1 day adult | 24.6±1.0 | 34.7±1.1 | 40.7±0.9 | 36.3±1.1 | 34.1±1.1 | 29.6±1.2 |

**Table 3.3 Density of mitochondria in proximal, middle and distal region of axon in ALM and PLM processes for all the developmental stages**

Density is expressed as average percentage±SEM. Proximal, middle and distal regions are demarcated by dividing the axon into three equal parts according to the axon length. Proximal region is the region near cell body.

A

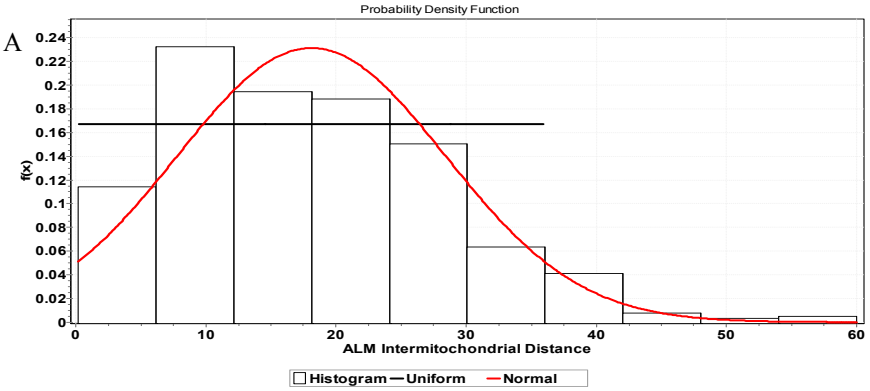

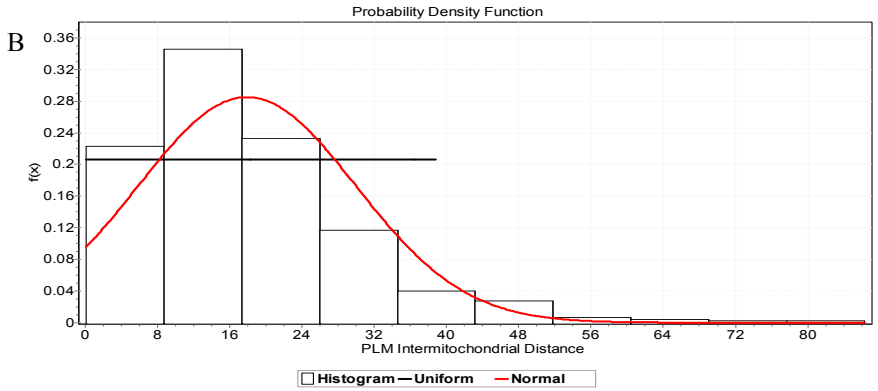


**Figure 3.5 (A-B) Histogram showing curve fitting for uniform and normal distribution for ALM (A) and PLM (B) processes**

Y-axis represents probability density; X-axis represents intermitochondrial distance range.

| | Kolmogorov-Smirnov test | | | Anderson-Darling test | | | Chi-Square test | | |
|---|---|---|---|---|---|---|---|---|---|
| Confidence Interval→ | 0.05 | 0.02 | 0.01 | 0.05 | 0.02 | 0.01 | 0.05 | 0.02 | 0.01 |
| All mitochondria | **Reject** | **Reject** | **Reject** | **Reject** | **Reject** | **Reject** | **Reject** | **Reject** | **Reject** |
| Only proximal mitochondria | **Reject** | Accept | Accept | Accept | Accept | Accept | Accept | Accept | Accept |
| Only middle mitochondria | Accept | Accept | Accept | Accept | Accept | Accept | Accept | Accept | Accept |
| Only distal mitochondria | **Reject** | Accept | Accept | Accept | Accept | Accept | **Reject** | Accept | Accept |

**Table 3.4 (A) Statistical tests for Normal distribution for ALM processes**

| | Kolmogorov-Smirnov test | | | Anderson-Darling test | | | Chi-Square test | | |
|---|---|---|---|---|---|---|---|---|---|
| Confidence Interval→ | 0.05 | 0.02 | 0.01 | 0.05 | 0.02 | 0.01 | 0.05 | 0.02 | 0.01 |
| All mitochondria | **Reject** | **Reject** | **Reject** | **Reject** | **Reject** | **Reject** | **Reject** | **Reject** | **Reject** |
| Only proximal mitochondria | **Reject** | Accept | Accept | **Reject** | Accept | Accept | Accept | Accept | Accept |
| Only middle mitochondria | Accept | Accept | Accept | **Reject** | **Reject** | Accept | Accept | Accept | Accept |
| Only distal mitochondria | Accept | Accept | Accept | **Reject** | Accept | Accept | Accept | Accept | Accept |

**Table 3.4 B Statistical tests for Normal distribution for PLM processes**

**Table 3.4 (A-B) Results of Kolmogorov-Smirnov, Anderson-Darling and Chi-Square test for intermitochondrial distance data**

Kolmogorov-Smirnov, Anderson-Darling and Chi-Square test were conducted on mitochondrial distribution data for the entire axon data set as well as proximal, middle and distal regions of the axon taken separately. Statistical tests were carried out for both ALM (Table 3.4 A) and PLM (Table 3.4 B) processes. Tests were carried out for 0.01, 0.02 and 0.05 confidence interval. Accept refers to when test complies with the alternate hypothesis tested. Alternate hypothesis is data set follows a normal distribution whereas; null hypothesis is the experimental data set follows a non normal distribution. "Accept" refers when alternate hypothesis is accepted and the test complies with normal distribution, "Reject" refers to vice-versa.

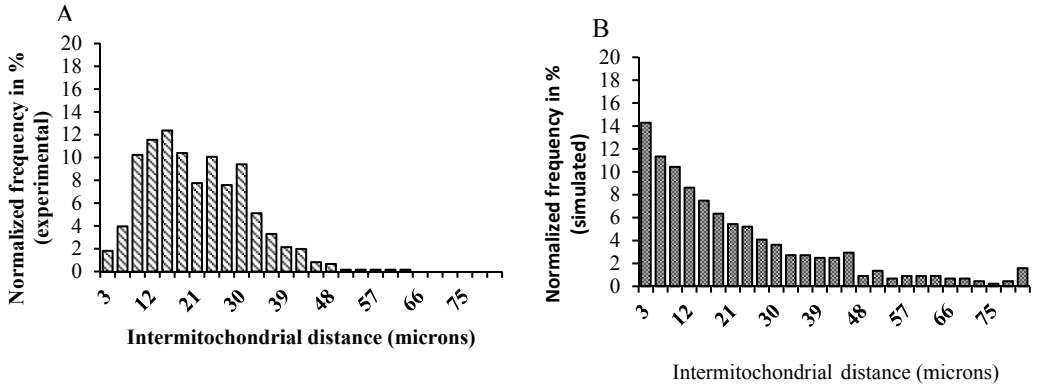


**Figure 3.6 (A-B) Represents experimental (A) and simulated (B) histograms for intermitochondrial distance data set**

Y-axis represents frequency fraction expressed in percentage for the data set while X-axis represents intermitochondrial distance range with 3µm interval range. For experimental histogram (3.5 A) intermitochondrial distance experimental data set of twenty five young adult animals was pooled together and histograms were plotted. Simulation histogram (3.5 B) was plotted by simulated axon using the experimental parameters of 400µm axon length and 20 mitochondria as the average number of mitochondria present in the axon. 25 axons were simulated using the above parameters where these 20 mitochondria were allowed to align randomly and the intermitochondrial distance obtained was measured.

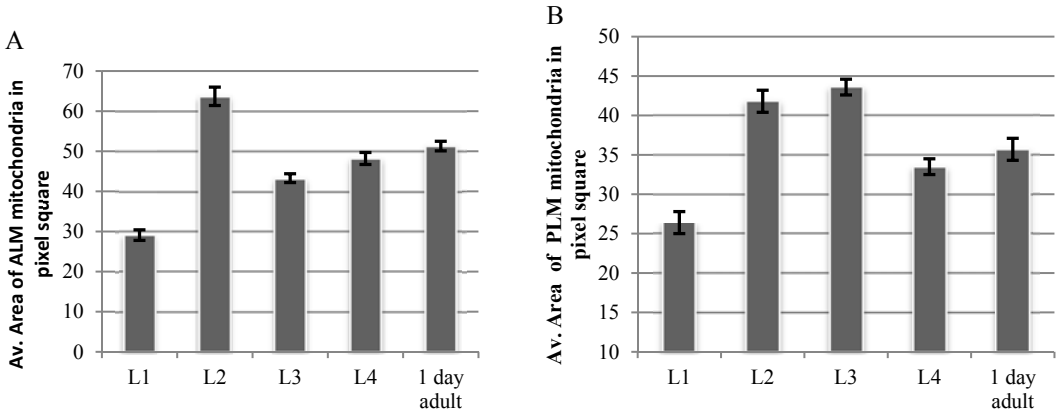


**Figure 3.7 (A-B) Represents average area occupied by mitochondria measured in square pixels in different developmental stages in ALM and PLM processes.**

Data is represented as mean±SEM. All the mitochondria present in 25-30 animals imaged were used for area calculation.

Table 3.5

| | ALM | | PLM | |
|---|---|---|---|---|
| Developmental Stages | Av. Area ($\mu m^2$) of mitochondria | Area ($\mu m^2$) occupied by mitochondria/100µm of axon length | Av. Area ($\mu m^2$) of mitochondria | Area ($\mu m^2$) occupied by mitochondria/100µm of axon length |
| L1 | 0.32±0.01 | 1.69±0.13 | 0.29±0.015 | 1.72±0.15 |
| L2 | 0.61±0.02 | 2.99±0.22 | 0.47±0.015 | 2.38±0.1 |
| L3 | 0.48±0.01 | 2.422±0.09 | 0.48±0.011 | 2.32±0.07 |
| L4 | 0.54±0.02 | 2.69±0.09 | 0.37±0.011 | 1.66±0.07 |
| 1 Day adult | 0.57±0.01 | 2.64±0.09 | 0.40±0.016 | 1.85±0.16 |

**Table 3.5 Analysis of average area ($\mu m^2$) of mitochondria for all the developmental stages for ALM and PLM processes.**

Data is represented as mean±SEM. Area occupied by mitochondria/100 µm of axon length is also tabulated.

Table 3.6

| | Average area of mitochondria in µm2 | | |
|---|---|---|---|
| | Proximal | Middle | Distal |
| L3 | 0.43±0.08 | 0.50±0.04 | 0.51±0.04 |
| L4 | 0.51±0.03 | 0.58±0.06 | 0.58±0.03 |
| 1 day adult | 0.46±0.03 | 0.64±0.05 | 0.69±0.09 |

**Table 3.6 Comparative analysis of average mitochondrial area in proximal, middle and distal regions of axons in L3, L4 and 1 day adult animals for ALM process.**

Area represented as mean±SEM.

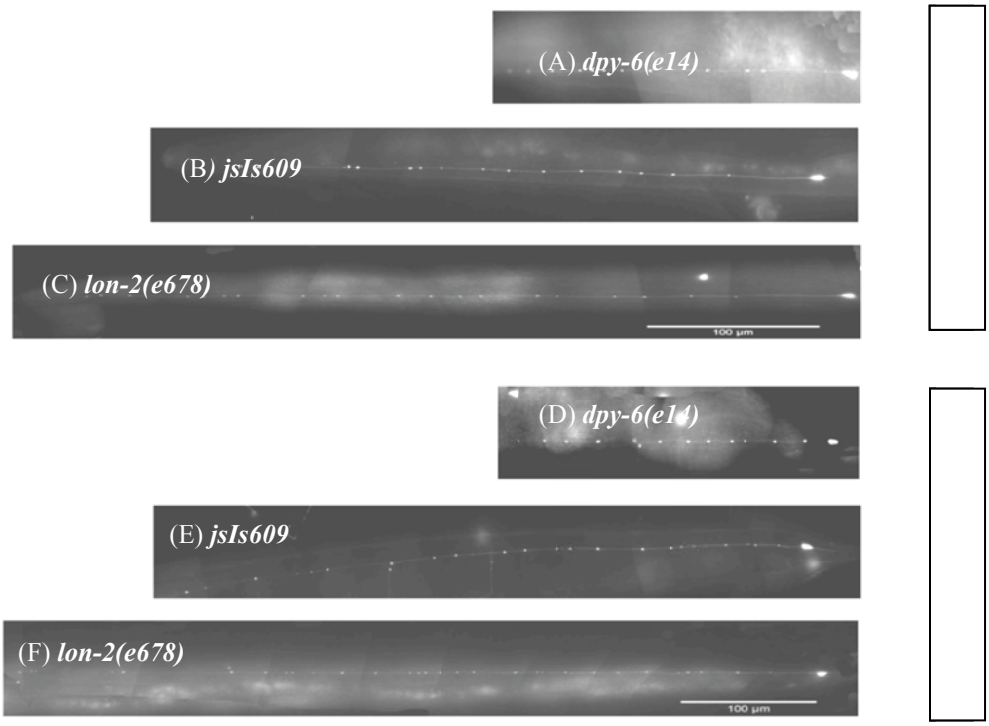


**Figure 3.8 (A-F) Represents reconstructed images of touch neurons of *jsIs609, lon-2(e678) and dpy-6(e14)* respectively**

A, B and C represents reconstructed ALM; D, E and F represents reconstructed PLM of *dpy-6(e14)*, *jsIs609* and *lon-2(e678)* respectively. Scale bar is 100µm. Images are constrained in proportion to their body length for representation.

Table 3.7

| Strains characterized (1 day adult) | Av. Axon length of ALM(µm) | Percentage change in ALM axon length compared to *jsIs609* | Av. Axon length of PLM(µm) | Percentage change in PLM axon length compared to *jsIs609* |
|---|---|---|---|---|
| *jsIs609* | 406.11±5.88 | NA | 507.22±8.09 | NA |
| *dpy-6(e14)* | 236.29±8.80 | 42% ↓ | 307.94±7.42 | 40% ↓ |
| *lon-2(e678)* | 484.12±16.31 | 19% ↑ | 606.55±15.7 | 20% ↑ |

**Table 3.7 Comparative table for axon length for *jsIs609, lon-2(e678) and dpy-6(e14)* strains.**

Data is represented as mean±SEM. Data set for 25-30 animals per strain was used for analysis.

Table 3.8

| Strains characterized (1 day adult) | Av. No. of mitochondria in ALM | Av. Axon length of ALM(µm) | Av. Mito. No./100µm of ALM Axon length | Av. No. of mitochondria in PLM | Av. Axon length of PLM(µm) | Av. Mito. No./100µm of PLM Axon length |
|---|---|---|---|---|---|---|
| *jsIs609* | 18.9±0.51 | 406.11±5.88 | 4.69±0.11 | 25.53±1.07 | 507.22±8.09 | 5.04±0.16 |
| *dpy-6(e14)* | 13.29±1.06 | 236.29±8.80 | 5.64±0.43 | 15.86±0.86 | 307.94±7.42 | 5.15±0.26 |
| *lon-2(e78)* | 25±1.01 | 484.12±16.31 | 5.25±0.34 | 30.4±2.06 | 606.55±15.7 | 5.01±0.30 |

**Table 3.8 Comparison of axon length and normalised data for *jsIs609, lon-2(e678) and dpy-6(e14).***

Data is represented as mean±SEM. Data set for 25-30 animals per strain was used for analysis.

Table 3.9 A

| Strains characterized | Av. No. of mitochondria in ALM (L4) | Av. No. of mitochondria in ALM (1 day adult) | Fold change in mitochondria no. from L4 to Adult | Av. Axon length of ALM(µm) in L4 | Av. Axon length of ALM(µm) 1 day adult | Fold change in axon length from L4 to adult |
|---|---|---|---|---|---|---|
| *jsIs609* | 15±0.45 | 18.9±0.51 | 1.26 | 295.28±3.46 | 406.11±5.88 | 1.38 |
| *dpy-6(e14)* | 10.73±0.30 | 13.29±1.06 | 1.24 | 187.69±2.91 | 236.29±8.80 | 1.26 |
| *lon-2(e78)* | 16.76±0.83 | 25±1.01 | 1.47 | 330.71±8.20 | 484.12±16.31 | 1.46 |

Table 3.9 B

| Strains | Av. No. of mitochondria in PLM (L4) | Av. No. of mitochondria in PLM ( 1 day adult) | Fold change in mitochondria no. from L4 to Adult | Av. Axon length of PLM(µm) in L4 | Av. Axon length of PLM(µm) 1 day adult | Fold change in axon length from L4 to adult |
|---|---|---|---|---|---|---|
| *jsIs609* | 17.44±0.57 | 25.53±1.07 | 1.46 | 362.69±3.98 | 507.22±8.09 | 1.4 |
| *dpy-6(e14)* | 12.91±0.49 | 15.86±0.86 | 1.23 | 221.40±4.65 | 307.94±7.42 | 1.4 |
| *lon-2(e78)* | 19.62±0.58 | 30.4±2.06 | 1.54 | 382.45±9.56 | 606.55±15.7 | 1.58 |

**Table 3.9 (A-B) Statistics of fold increase in mitochondria number and axon length with development in *jsIs609, lon-2(e678) and dpy-6(e14)* strains for ALM (A) and PLM (B) processes.**

Data is represented as mean±SEM. Data set for 25-30 animals per strain was used for analysis.

# Chapter 4

## Factors Effecting Number and Distribution of Mitochondria in *C.elegans* Touch Neurons

# 4. Factors Effecting Number and Distribution of Mitochondria in *C.elegans* Touch Neurons

## 4.1. Introduction

In the last chapter, we observed that mitochondrial distribution in the axons was non random and is maintained throughout the development. In an attempt to look at factors which would govern mitochondria distribution in these specialized touch neurons; we looked at all the probable factors which may directly or indirectly influence mitochondrial positioning in these neurons. The factors were broadly classified into five categories to evaluate their effect on mitochondrial number and distribution:

1) Factors effecting entry and exit of mitochondria
2) Anchoring factors
3) Dynamics of mitochondria
4) Touch cell function and
5) Mitochondrial function

Mitochondria are highly dynamic organelles and their biogenesis has been reported to take place both in the cell body as well as axon (Amiri et al 2008). Mitochondria undergo both fast and slow axonal transport. Long distance fast axonal transport of mitochondria on the microtubule tracks which have their plus end directed distally takes place with the aid of molecular motors. Kinesin-I is the anterograde motor and dynein is the retrograde motor. Mutants of Kinesin-I in Drosophila motor neurons as well as in non neuronal cells have resulted in altered mitochondrial transport and distribution (Pilling et al 2006, Tanaka et al 1998). In addition to Kinesin-I, a kinesin-3 family member has also been reported to interact with mitochondria (Tanaka et al 1998). Using similar approaches of motor inhibition using mutant study (Pilling et al 2006) and microinjection using anti-DIC (Dynein intermediate chain) antibody (Varadi et al 2004) dynein has been reported as the major retrograde motor (Varadi et al 2004, Pilling et al 2006). Both these anterograde and retrograde motors are vital components to control influx and efflux of mitochondria in the axon. We looked at effect of both of these motors on mitochondrial number and distribution in neurons of our study.

Axonal cytoskeleton is a very important factor which provides framework for transport and anchoring / docking of vital organelles. Microtubules and actin cytoskeleton both have been reported as the critical players for mitochondrial transport in axons (Yaffe et al 1996, Ligon et al 2000). It has been proposed that long range axonal transport takes place on the microtubule skeleton with the help of microtubule based motors whereas short distance transport takes place on actin cytoskeleton by myosin motor (Langford 1995).

Microtubules have been implicated to be involved in organelle movement and distribution from a long time (Bikle et al 1966, Smith et al 1975, Smith et al 1977). Apart from mitochondria, microtubules are known to regulate distribution of many other organelles like golgi apparatus (Thyberg et al 1985), endoplasmic reticulum (Terasaki et al 1994) and lysosomes (Collot et al 1984). Stability of microtubule has also been reported to effect organelle biogenesis as well as morphology. Different approaches like electron microscopy, labeling mitochondria with rhodamine and microtubule destabilizing drugs have been used to visualize the above effects.

Electron microscopic study using neuronal culture has shown the most important evidence for association of mitochondria with microtubules (Smith et al 1975, 1977). Initial experiments done by labeling mitochondria with rhodamine 123 in fibroma cells have shown correlation between mitochondria and microtubules or intermediate filament (Summerhayes et al 1983). Another study done using triple immunofluorescence in fibroblast culture has reported that mitochondria are associated with microtubules and not with intermediate filament (Ball et al 1982). They have also reported that many mitochondria are co-distributed with microtubules and there may be some chemical links between mitochondria and microtubule. It has also been reported that depolymerization of microtubules by chemical agents leads to altered mitochondrial distribution (Heggeness et al 1978).

Another study done using Yeast (*Schizosaccharomyces pombe*) temperature sensitive alpha and beta tubulin mutants has reported presence of aggregated and asymmetric mitochondrial distribution when grown in non permissive conditions (Yaffe et al 1996). It has also been reported in yeast that mitochondrial distribution and movement is solely microtubule dependent and motor doesn't play any role, this has been proved by using deletion of Kinesin (Klp3p) (Yaffe et al 1996, Brazer et al 2000). Mitochondria are anchored to microtubules and not molecular motors, this has been shown by use of electron microscopy/tomography, double

staining and incubating these cells with microtubule depolymerizing drugs such as nocodazole (Tanaka et al 1998, Yaffe et al 2003). Microtubule depolymerizing drugs have been reported to result in diffused and random spread of these mitochondria. Apart from regulating distribution and movement of mitochondria, microtubules have been reported to regulate mitochondrial biogenesis and chemical depolymerization of microtubules have been reported to effect mitochondrial volume / mass during cell cycle interphase (Karbowski et al 2000).

Six touch neurons of our study has specialized 15-protofilament microtubules which are necessary for responding to the gentle touch and absence of the same results in touch insensitivity (Chalfie 1982, Chalfie et al 1982). These specialized 15-protofilament microtubulues are comprised of MEC-7(β-tubulin) and MEC-12(α-tubulin) tubulins (Savage et al. 1989, Fukushige et al. 1999). Loss of function mutants of *mec-7* or *mec-12* genes resulted in replacement of 15-protofilament microtubules by 11-protofilaments (Savage et al 1989). Along with touch insensitivity these worms have been reported to exhibit axonal transport and synaptic defects (Bountas et al 2009). Depolymerizing microtubules using 1mM colchicines also results in touch insensitivity (Chalfie et al 1982).

Genetic screen for touch insensitivity has resulted in finding of mutants for both α and β-tubulin. α and β-tubulin mutants were touch insensitive and in them longer 15-protofilament microtubules were replaced by shorter 11-protofilaments (Chalfie et al 1982, Savage et al 1989). Mutants of both α and β-tubulins resulted in decrease in mechanoreceptor current (MRC) as well as its peak amplitude (Bountas et al 2009). MEC-12 has been reported as the only acetylated tubulin present in ***C. elegans***. In MEC-12, acetylated lysine is present at position 40; this lysine residue has been reported as vital in generating specialized 15-protofilament microtubule. Mutation in *mec-12* thus has been reported to results in touch insensitivity (Cueva et al 2012). We looked at mutants of both alpha and beta tubulin to see what effect they have on mitochondrial localization and distribution.

Mitochondrial fission and fusion are important events for quality control of mitochondria enabling them to maintain their structural and functional dynamics. Outer and inner membrane fusion genes present in ***C. elegans*** are *fzo-1* and *eat-3* which are homologues of *fzo1/mfn1, 2* and *mgm1/opa1* respectively (Kanazawa et al. 2008, Ichishita et al. 2008). Fission protein

present in ***C. elegans*** is DRP-1 (Labrousse et al 1999, Jagasia et al 2005). *Fis1* homologues present in ***C. elegans*** are *fis1* and *fis2*, but no homologues of *mdv1/caf4* is present (David et al 2008). Mutants of *fzo-1*, *eat-3* as well as *drp-1* have been reported to show defect in mitochondrial morphology, as well as reduced brood size and high rate of embryonic lethality (David et al 2008). Interplay of these fission and fusion process results in maintaining a pool of active mitochondria which could take care of vital activities for the cell. Inhibiting fusion-fission process thus should lead to disrupted mitochondrial dynamics thus disturbing mitochondrial distribution. We looked at the effect of both fusion and fission genes *eat-3* and *drp-1* on mitochondria distribution in six touch neurons of our study.

Touch receptor neuron (TRN's) channel of ***C. elegans*** is made up of pore-forming subunit and auxiliary subunits. Pore forming subunit is made up of two proteins MEC-4 and MEC-10 which are also known as DEG/ENaC. Two proteins MEC -2 and MEC -6 forms the auxiliary subunit which interacts with MEC -4 and MEC -10 and increase channel activity (O'Hagan et al. 2005). MEC -4 and MEC -10 have been reported to have both physical and genetic interaction (Huang et al 1994, Gu et al 1996). It has been proposed that both MEC -4 and MEC -10 form a heterotetrameric complex (Huang et al 1994, Gu et al 1996).

MEC -2 has been reported as a connecting link which connects microtubule cell with the channel complex. There are both genetic and biochemical evidences which prove the interaction of MEC-2 with microtubule cytoskeleton (MEC-7/MEC-12) and DEG/ENaC channel (MEC-4/MEC-10). Using MEC-2::LacZ fusion protein it was reported that MEC -2 was distributed in the six touch receptor neurons. The N-terminus of MEC -2 was sufficient for MEC -2 distributions in the axon (Huang et al 1995). It was also reported that presence of 15-protofilament microtubules was important for MEC-2 distribution (Huang et al 1995).

Interaction between MEC-2 and MEC-4 has been proposed based on puncta co-localization observed between MEC-2 and MEC-4 YFP (Shifang et al 2004) as well as co-immunoprecipitation observed between MEC-2 and MEC-4 in Xenopus oocyte and CHO cell (Goodman et al 2002). It has also been proposed that TRN channels interact with 15-pf microtubules and displacement of microtubules plays a role in channel opening (Huang et al 1994, Gu et al. 1996). As intact touch channel complex as well as cytoskeleton is essential for

elucidating normal touch response we reasoned that any effect, affecting functioning of touch receptor neuron may also contribute in mitochondrial distribution. We looked at mutants of *mec-4*, *mec-2* and *mec-10* to see their effects on number and distribution of mitochondria.

ATP production and calcium buffering are two main prime functions of mitochondria. Impairing these vital mitochondrial functions should ideally result in altering its positioning and distribution. It has also been reported that $Ca^{2+}$ levels play a vital role in movement, halting and positioning of mitochondria in axons and dendrites (Saotome et al 2008, Wang et al 2009). Miro which is a mitochondrial GTPase present on the outer mitochondrial membrane has been reported to be a calcium sensor through its EF hands. Binding of calcium to the EF hands is responsible for detaching of mitochondria from the motor complex and in turn results in halting of mitochondria (Saotome et al 2008, Wang et al 2009, Macaskill et al 2009). It has also been reported that in the touch neurons, gentle touch response results in MEC channel dependent rise in intracellular calcium (Bianchi 2007). As $Ca^{2+}$ has been reported to be involved in controlling mitochondrial positioning as well as in functioning of touch neurons of our study, we looked at how altering the calcium levels will effect mitochondrial number and distribution in theses touch neurons.

Microtubules show dynamic instability (Mitchison et al 1984 a, b) and this is controlled by many factors including MAP's (Microtubule associated proteins) (Hirokawa 1994). Plus end tracking proteins (+TIPs) are MAPs which are associated with microtubule growing end (Lansbergen et al 2006, Akhnamova et al 2008). EB-1 has been known as one of the key members of +TIPs and has been known to play a vital role in regulating microtubule dynamicity (Vitre et al 2008, Rogers et al 2002). As mitochondria are positioned on microtubule track, we also reasoned whether mitochondrial positioning has selectivity to certain regions of microtubules as compared to other. To study this we looked at the presence of mitochondria at the growing ends of microtubules.

In this chapter effect of all the probable factors which includes motors, cytoskeleton, mitochondrial dynamics, neuronal function and mitochondrial function has been studied to see their effect on mitochondrial number and distribution. Degree of overlap between the listed factors and probable reasons for the same has also been described. We also tried to answer whether mitochondria shows positional selectivity to certain regions of microtubules.

## 4.2. Results

### 4.2.1. Mitochondria Number in Axon is Altered in Motor Mutants but Distribution is not Effected

As kinesin-I and dynein are the primary motors responsible for mitochondrial transport on the microtubule cytoskeleton; we tried looking at the effect of mutation in kinesin-I and dynein components on mitochondrial number and distribution. Kinesin-I is made up of two heavy and two light chains, heavy chain control the motor activity whereas light chain is responsible for cargo binding (Alexander et al 2009). We looked at mutants of both Kinesin-I heavy and light chain. Kinesin-I heavy chain ortholog found in ***C. elegans*** is known as *unc-116*, whereas kinesin light chain is encoded by *klc-2*. We looked at hypomorphic alleles of Kinesin-I heavy chain and light chains which were respectively *unc-116(e2310)* and *klc-2(km11)*. Mutants of both kinesin heavy and light chains showed reduced number of mitochondria in ALM and PLM process as the anterograde transport was effected (Fig 4.1 and Table 4.1).

Cytoplasmic dynein motor has a complex structure comprising of two heavy chains, several intermediate chain, intermediate light chain and light chain (Milisav 1998, King 2000). Dynein is an ATP dependent motor and its heavy chain is responsible for propelling the motor (Asai et al 2001). Cytoplasmic dynein heavy chain homolog is encoded by *dhc-1* in ***C.elegans***; we looked at mutants of dynein heavy chain: *dhc-1(or195)* and *dhc-1(js319)* both of which has point mutation resulting in missense mutation and splice site generation respectively. Dynein mutant *dhc-1(js319)* and *dhc-1(or195)* both showed average mitochondria number closer to the wild type (approx 5mito/100µm of axon) both in ALM and PLM (Fig 4.1 and Table 4.1). As the retrograde transport is affected, the expected number of mitochondria should be more as compared to the control. It has been reported that axonal transport shows biasness towards anterograde direction (Pilling et al 2006). Biasness observed towards anterograde transport may be the probable reason accounting for the mitochondrial number similar to the wild type. It has been reported in Drosophila motor axons that 29% of mitochondria move anterograde, 14% retrograde and rest are stationary so the number of retrograde moving mitochondria would be too small to be detected as a significant difference in the number of mitochondria.

We also looked at how mitochondrion was distributed in these motor mutants. To analyze the same, we looked at how mitochondria was distributed in these mutants in different regions of the

axon and plotted the histogram for inter-mitochondrial distance. Distribution histograms of kinesin-I mutants *unc-116(e2310)* and *klc-2(km11)* were similar to wild type though frequency of mitochondria with larger inter-mitochondrial distance were more prevalent. This can be accounted due to lesser number of mitochondria in these strains (Fig 4.2). Dynein mutant's *js319* and *or195* both showed histogram quite similar to wild type where mitochondria were neither too closely placed nor too distantly located (Fig 4.2). Histogram of the motor mutants thus showed that distribution is regulated and mitochondria are evenly spaced.

Distribution of mitochondria in different regions of axons proximal, middle and distal region in both dynein and kinesin-I mutants was quite similar to wild type with larger percentage of mitochondria in the distal region of axon in ALM process and higher percentage in proximal region in PLM process (Table 4.2). Percentage of mitochondria which was too closely spaced or aggregated in these mutants (<3μm) was also found to be below 5% (Table 4.2). Both ALM and PLM showed similar trend in the results though the consistency in the effect was more prominent in ALM. As per the above results, altering of anterograde motor kinesin affected the number of mitochondria in the axons but mutation in motor didn't show the effect on the distribution of mitochondria (Table 4.2 and Fig 4.3)

### 4.2.2. Altering Cytoskeleton Structure Effects Both Number and Distribution

Motor based mitochondrial transport takes place on the microtubule cytoskeleton; any effect on this cytoskeleton must also affect mitochondrial transport. To investigate this effect we looked at microtubule mutants. We looked at alpha tubulin *(mec-12)* and beta tubulin *(mec-7)* mutants. We looked at the mitochondria number in partial loss of function alleles of *mec-7(u443)* and *mec-7(e1343)*. Mutation in *mec-7(u443) and mec-7(e1343)* resulted in replacement of 15-protofilament microtubule by 11 protofilament (Cathy et al 1994). We looked at mitochondria number per 100 μm of axon length in both *mec-7(u443)* and *mec-7(e1343)* which was approx 7 in ALM process and was significantly higher than the wild type (Fig 4.4, Table 4.3 and Fig 4.6). PLM processes didn't show any significant difference compared to the wild type (Fig 4.4, Table 4.3 and Fig 4.6).

MEC-12 alpha tubulin is also required for the formation of normal 15-protofilament microtubule and is also acetylated (Tentusari et al 1999). We looked at *mec-12(e1605)* and *mec-12(e1607)*

mutants, both the mutations resulted in touch insensitivity though the former *(e1605)* has presence of normal 15-protofilament microtubules whereas later *(e1607)* has 15-protofilament replaced by 11 protofilaments (Tentusari et al 1999). We looked at mitochondria number per 100 µm of axon length in both the *mec-12(e1605)* and *mec-12(e1607)* mutants, they showed mitochondrial density as 9 and 7 mitochondria per 100µm of axon length respectively in the ALM processes which was significantly higher than the wild type (Fig 4.4, Table 4.3 and Fig 4.6). Trend observed for PLM processes was not seen consistently in both the strains (Fig 4.4, Table 4.3 and Fig 4.6).

Mitochondrial distribution in different regions of axon was studied in these alpha and beta tubulin mutants. As the effect of mutation was more prominent in ALM processes, distribution histograms were plotted for ALM processes for both alpha and beta tubulin mutants. Both alpha (*mec-12*) and beta tubulin (*mec-7*) mutants showed histograms quite similar to our simulation graphs where shorter inter-mitochondrial distance were more prevalent as compared to the intermediate distance and graph showed an exponential decay (Fig 4.5). As the microtubule mutants had more number of mitochondria and smaller inter-mitochondrial distance were more prevalent, this appeared in the axon as clumps of mitochondria which was seen in all the regions of the axon.

We quantified these clumps which were prominently seen in these tubulin mutants as percentage of mitochondria less than 3µm apart, which are henceforth been quantified for all the mutants under study. ALM processes of all the tubulin mutants showed high percentage of closely spaced mitochondria (<3µm) ranging between 9 to 12% which was significantly higher than wild type (Fig 4.6). Similarly PLM also showed trend of closely spaced mitochondria (Table 4.4). We also looked at mitochondrial distribution in different regions of axon in beta tubulin mutants where mitochondria were found to be more aggregated towards the proximal region of axon in ALM process as compared to the wild type where distal region has more mitochondria in ALM (Table 4.4). Same trend similar to beta tubulin mutant was observed in *mec-12(e1607)* ALM mutant (where 15-protofilament microtubule is disrupted and replaced by 11 protofilament). Whereas, in *mec-12(e1605)* strain which has presence of normal microtubules, percentage of mitochondria allocated to different axonal segments was comparable to the wild type (Table 4.4).

Altered trend in mitochondrial density and distribution observed in the tubulin mutants was more prominent in ALM processes compared to PLM (Fig 4.6 and Table 4.3). As per the above results it implied that disrupting the organization of normal microtubules resulted in altered number and distribution of mitochondria in the axons and this effect is more prominent in ALM processes.

### 4.2.3. Altering Mitochondrial Dynamics Effects Both Number and Distribution

Mitochondrial fission-fusion dynamics is vital to maintain active pool of mitochondria. Mutation in many of the genes responsible for controlling mitochondrial dynamics has been reported to be associated with many neuronal diseases (Alexander et al 2000, Pesch et al 2001, Zuchner et al 2004). On the similar grounds, we reasoned that altering this dynamics must effect the mitochondrial distribution and in turn neuronal function as well. To look at the same we looked at ***C. elegans*** fission and fusion mutant's *drp-1* and *eat-3* respectively. We looked at *eat-3(ad426)* and *drp-1(tm1108)* alleles where the former had a point mutation resulting in strong reduction of function mutation (David et al 2010) whereas the later has 426 bp deletion followed by insertion of 18bp at the deletion site resulting in strong loss of function (David et al 2008).

As expected fission mutant *drp-1(tm1108)* resulted in lower mitochondrial density with value of 3 mitochondria/100µm of axon length. Similarly, *eat-3(ad426)* fusion mutant strain resulted in higher density of 6.3 mitochondria/100µm of axon length in the ALM processes (Fig 4.7 and Table 4.5). In fission mutant *drp-1(tm1108)* as fission process was affected it resulted in presence of longer and lesser mitochondrial number in the axon. Similarly, fusion mutant *eat-3(ad426)* resulted in smaller and more mitochondria number in the axon (Fig 4.7).

We looked at mitochondrial distribution in ALM processes of these fission-fusion mutants. Histograms of intermitochondrial distance in *eat-3(ad426)* mutant was quite skewed and showed the trend similar to the tubulin mutants whereas *drp-1(tm1108)* was similar to wild type but with more spread due to lesser number of mitochondria and hence larger intermitochondrial distance (Fig 4.8). Percentage of aggregated mitochondria (<3µm distance) observed was significantly higher than wild type in *eat-3(ad426)* with a value approx 12% whereas *drp-1(tm1108)* didn't show any significant difference from the wild type (Fig 4.9 and Table 4.6). Distribution of mitochondria in proximal, middle and distal regions of axon in ALM process was also found altered (Table 4.6). Similar, to other mutants studied fission/ fusion mutants also showed more

consistent trend in ALM as compared to PLM processes. As per the above results disrupting mitochondrial dynamics affected both mitochondria number and distribution though the effect observed was seen more prominent in fusion mutant.

### 4.2.4. DEG/ENaC Channel have very Mild Effect on Mitochondria Number and Distribution

As MEC-4 and MEC-10 form the pore forming subunit of DEG/ENaC channel and MEC-2 has been reported to show genetic interaction with MEC-7 ß tubulin (Gu et al., 1996), we looked at mutants of *mec-4*, *mec-2* and *mec-10* to see their effects on mitochondria number and distribution. We looked at *mec-4(u253)* which is a null allele (Hagan et al 2005), *mec-2(e75)* has a missense mutation (Zhang et al 2004) and *mec-10(tm1552)* has around 400 bp deletion (Chatzigeorgiou et al. 2010). All the above mutations has been reported to affect touch sensitivity, but *mec-4(u253)* which is a null allele has been reported to have most severe effect on touch sensitivity and thus has been reported to result in abolishing of mechanoreceptor current (MRC) (Hagan et al. 2005).

*mec-4(u253)* is a severe mutant whereas *mec-10(tm1552)* and *mec-2(e75)* were weaker mutants. Normalised number of mitochondria per 100µm of ALM axon length was found to be significantly different from wild type in *mec-4(u253)* with value corresponding to 6.3 and *mec-10(tm1552)* with value corresponding to 5.7(Fig 4.10, Table 4.7). *mec-2(e75)* didn't show any significant difference from wild type (Fig 4.10, Table 4.7). PLM showed values comparative to wild type for all the mutants (Fig 4.10, Table 4.7). Next we looked at mitochondria distribution histograms of ALM processes of these mutants. Only *mec-4(u253)* null mutant showed trends similar to the microtubule mutants in which small intermitochondrial distance were more prevalent whereas rest two showed trends quite similar to the wild type (Fig 4.11). Percentage of mitochondria showing aggregation was high in *mec-4(u253)* with value corresponding to 9% which was found to be significantly higher than wild type whereas in other two mutants no significant difference was observed compared to wild type (Fig 4.12 and Table 4.8). We also studied the distribution of mitochondria in different regions of axons in ALM and PLM process of these mutants, ALM showed mild effect on the same whereas PLM processes showed trends almost similar to the wild type. As per the trends observed *mec-4(u253)* which is a null mutant showed prominent effect on both number and distribution whereas other two mutant's *mec-*

*2(e75)* and *mec-10(tm1552)* didn't show any prominent effect on either. MEC-4(d) channel has been reported to be $Ca^{2+}$ permeable (Bianchi et al 2004) so the above effects seen in *mec-4(u253)* mutant might be due to combined effect to channel dysfunction as well as due to decrease in $Ca^{2+}$ permeability if the channel itself is involved in $Ca^{2+}$ conduction.

### 4.2.5. Cytosolic $Ca^{2+}$ Levels have Mild Effect on Mitochondria Number and Distribution

Calcium buffering is one of the key functions of mitochondria. Role of calcium has been reported in distribution of mitochondria, moreover its role has also been reported in the functioning of touch cells. As calcium is reported to be involved in multiple ways in the neuronal process of our study, we wanted to check how effecting the calcium will affect mitochondria number and distribution and in turn functioning of these processes. Voltage gated calcium channels (VGCC) are one of the key channels involved in regulating cytosolic calcium concentration and it has also been reported to be involved in $Ca^{2+}$ transient in touch cells (Suzuki et al., 2003). We looked at alpha-1 subunit of VGCC known as *egl-19* in ***C.elegans***. We looked at the gain of function mutants *egl-19(ad695)* and *egl-19(n2368)* respectively; these have been reported to result in increased calcium transient. We also looked at the loss of function allele, *egl-19(ad1006)* which has decreased calcium transient (Kerr et al., 2000).

Loss of function mutant *egl-19(ad1006)* didn't show any effect on mitochondrial density in both ALM and PLM processes and the density was same as wild type (Fig 4.13 and Table 4.9). Gain of function mutant *egl-19(ad695)* and *egl-19(n2368)* showed significant increase in mitochondrial density in the touch neuron processes (Fig 4.13 and Table 4.9). We looked at mitochondrial distribution histogram of ALM processes. Histograms of both gain and loss of function mutants of *egl-19* showed similarity to the wild type with regulated distribution and evenly spaced mitochondria (Fig 4.14). Though the distribution histogram was similar to wild type percentage of aggregated, mitochondria in ALM (<3um bin) was found to be significantly higher than the wild type (Fig 4.15 and Table 4.10). We then looked at mitochondrial distribution in proximal, middle and distal regions of ALM process. Gain of function mutants showed wild type like trends with higher mitochondrial percentage in the distal region and least in the proximal region (Table 4.10). In contrast loss of function mutant showed slightly skewed distribution with almost similar percentage of mitochondria present in all the regions. This trend in the distribution was quite similar to the one observed in *mec-4(u253)* and *drp-1(tm1108)*

mutants and was unlike tubulin mutant where the pattern was completely perturbed (Table 4.10). As per the above trend, gain of function mutants affected both number and distribution of mitochondria in the mutants studied. Whereas, loss of function mutants studied showed effect only on distribution. Results thus implied that cytosolic calcium levels have effect on both number and distribution of mitochondria.

### 4.2.6. Growing Ends of Microtubules are Co-localized with Mitochondria

Mitochondrial distribution was found to be most altered in microtubule mutants thus implying that integrity of microtubules is a prerequisite for proper distribution of mitochondria. So we questioned whether mitochondria have preference for certain regions of microtubules as compared to the other. In order to answer this query, we tried to observe if there is an occurrence of mitochondria at the growing ends of microtubules. In order to visualize the same, we built *ebp-1*(CFP line) with *jsIs1073* (mitochondrial RFP transgenic).

The built strain was imaged in both green and red filters and was analyzed to observe co-localization if any between ebp-1 puncta and the mitochondria. This point was quantified as well. Co-localization percentage between ebp-1 puncta and mitochondria was found to be 30% and 20% respectively in ALM and PLM processes (Fig 4.16 and Table 4.11). In both the cases, 25 animals were independently analyzed. Presence of mitochondria on the growing end of microtubule may be an additional mechanism which might be in operation for transport and distribution of mitochondria other than the motor driven transport. Thus the above experiment indicates that there is no preferential region and even the growing ends have significant proportion of mitochondria associated with them.

## 4.3. Discussion

All the possible factors which govern the mitochondrial number and distribution in touch neurons were studied. Any trend observed in the mitochondrial density or distribution was observed more consistently in the ALM processes as compared to the PLM. As per the above results, it implied that integrity of transport cytoskeleton is most vital in governing mitochondria number and distribution. Any mutation which altered either the structural organization of the microtubules or its function showed drastic effect on both number and distribution of mitochondria. It has been reported that in mec-7/ß tubulin mutant mislocalization of vesicles as

well as UNC-104/KIF1A motor was seen which were reported to be concentrated near the ALM cell body region as well as in ectopic processes beyond the cell body (Leonie et al 2002). May be similar processes is in hold in the tubulin mutants studied which is resulting in mislocalization of mitochondria in the axon.

Other factors which had modest effect on both number and distribution were factors contributing to mitochondrial dynamics (fission-fusion) as well as $Ca^{2+}$ levels. Altering mitochondrial fission-fusion dynamics resulted in altered number of mitochondria. Similarly, it also resulted in perturbed distribution of mitochondria in the axonal segments though the intensity of effect was varying depending on the type of mutation. Fusion mutants showed skewed distribution both in terms of higher prevalence of closely spaced mitochondria as well as completely altered mitochondrial distribution in axonal segments. Both the trends observed were found to be quite comparative to the tubulin mutants. Whereas, fission mutants showed mitochondrial distribution pattern comparable to the wild type.

Of all the DEG/ENaC channel mutants studied, only *mec-4(u253)* showed significant effect on both mitochondrial number and distribution. Mitochondrial distribution observed in *mec-4(u253)* axonal segments was similar to *egl-19(ad1006)* (lf) mutant as well as to *drp-1(tm1108)*. Similarity, in mitochondrial distribution pattern seen in all the three mutants may be attributed due to direct or indirect involvement of calcium in their functioning. For e.g. MEC-4(d) channel has been reported to be $Ca^{2+}$ permeable (Bianchi et al 2004) so the above effects seen in *mec-4(u253)* mutant might be due to decrease in $Ca^{2+}$ permeability if the channel itself is involved in $Ca^{2+}$ conduction. Similarly, role of VGCC dependent $Ca^{2+}$signaling has also been reported to be involved in phosporylating DRP-1 and hence controlling fission process (Han et al 2008). Thus presence of similar trends for mitochondrial distribution in these mutants may be due to direct or indirect deficit in their cellular $Ca^{2+}$ levels.

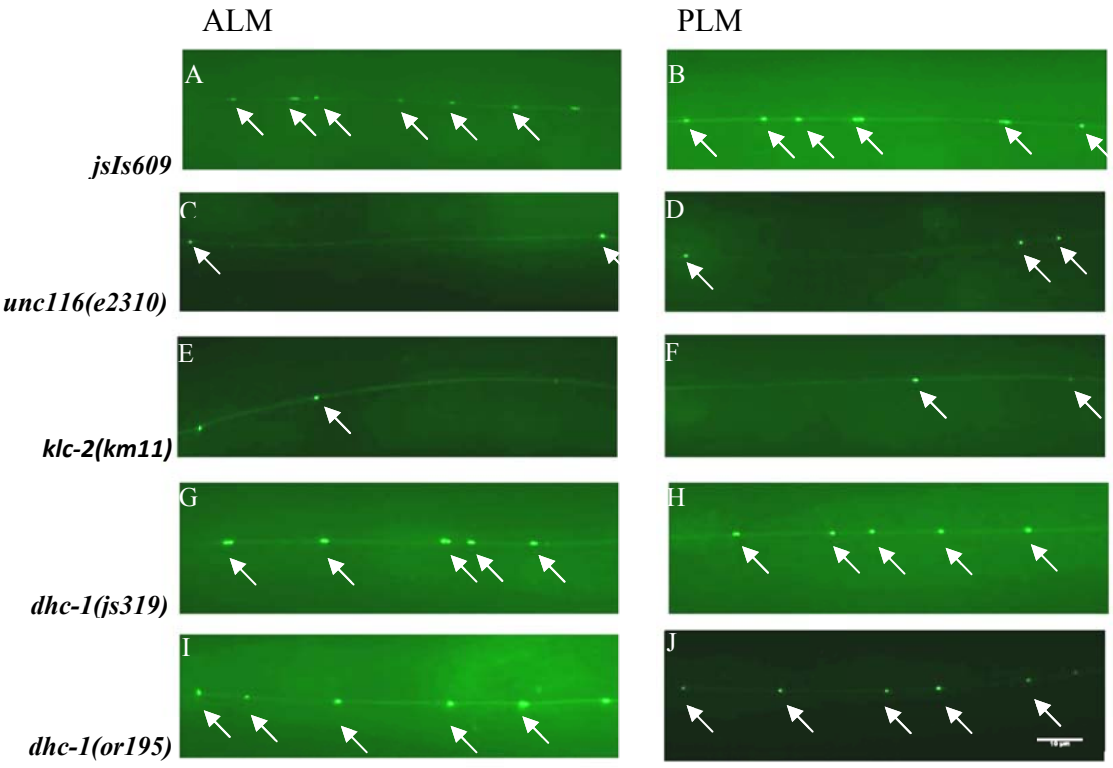


**Figure 4.1 Representative images showing mitochondrial distribution in ALM and PLM processes in WT (*jsIs609*) and motor mutants**

A-B) *jsIs609*; C-D) *unc-116(e2310),* E-F) *klc-2(km11)*; G-H) *dhc-1(js319),* I-J) *dhc-1(or195).* Position of mitochondria is marked by arrows. Scale bar is 10µm.

Table 4.1

| Strain | Av. No. of mitochondria in ALM | Av. Axon length of ALM(µm) | Av. Mito. No./100µm of ALM Axon length | Av. No. of mitochondria in PLM | Av. Axon length of PLM(µm) | Av. Mito. No./100µm of PLM Axon length |
|---|---|---|---|---|---|---|
| ***jsIs609*** | 19.1±0.5 | 406.1±5.9 | 4.7±0.1 | 25.3±1.0 | 507.2±8.1 | 5.0±0.1 |
| ***dhc-1(or195)*** | 18.6±0.5 | 408.2±5.11 | 4.6±0.12 | 24.1±0.7 | 493.2±10.4 | 4.9±0.1 |
| ***dhc-1(js319)*** | 21.5±0.6 | 409.4±6.03 | 5.25±0.14 | 31.8±0.7 | 547.0±7.2 | 5.8±0.1 |
| ***unc-116(e2310)*** | 7.25±0.6 | 287.1±4.25 | 2.55±0.2 | 8.5±0.7 | 329.3±5.6 | 2.6±0.2 |
| ***klc-2(km11)*** | 10.8±0.8 | 311.9±7.4 | 3.5±0.3 | 9.2±0.6 | 424.3±10.6 | 2.2±0.2 |

**Table 4.1 Average mitochondria number and axon length in motor mutants.**

Data is represented as mean±SEM. ALM and PLM processes of 25-30 animals were used for analysis.

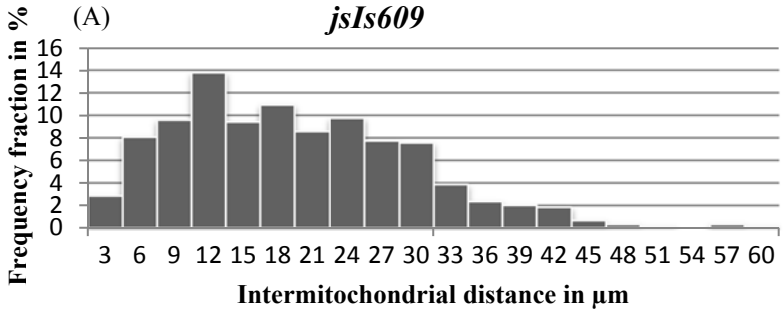


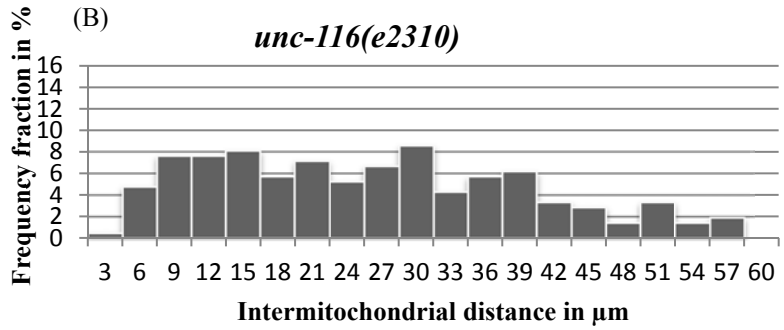

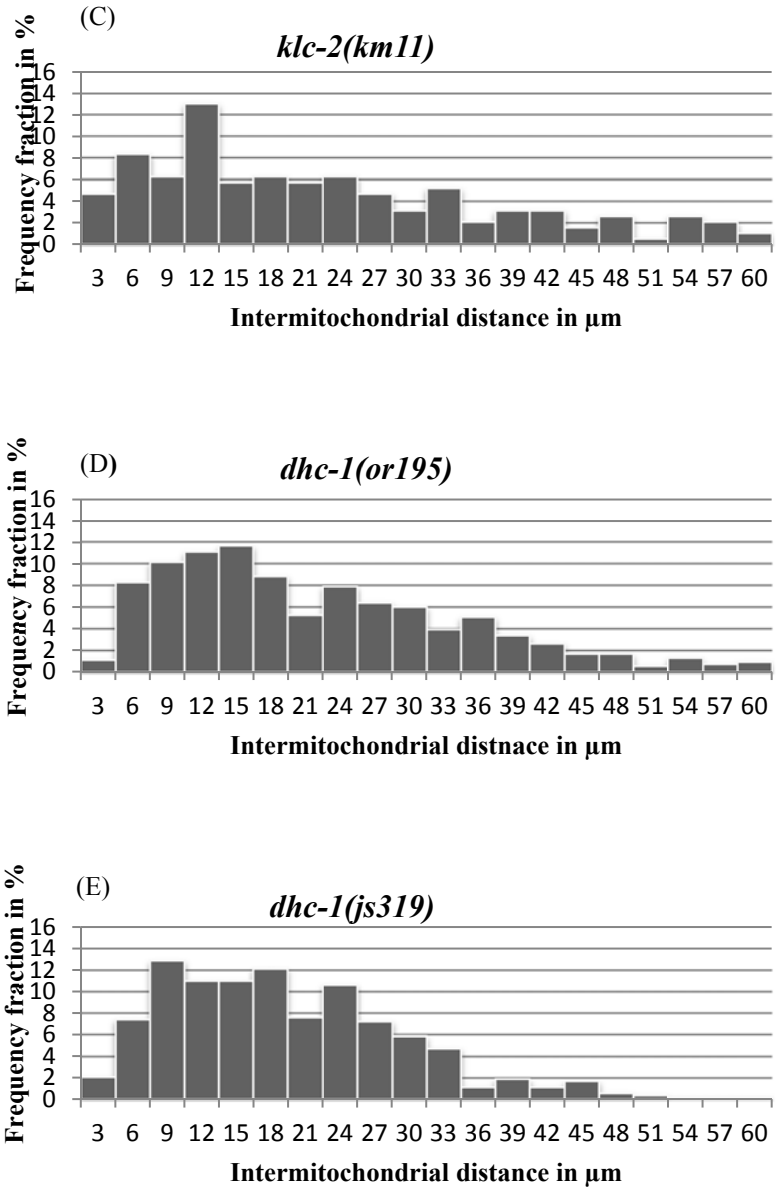


**Figure 4.2 Distribution histogram of intermitochondrial distance for motor mutants.**

X-axis represents intermitochondrial distance range expressed in µm; Y- axis represents percentage of mitochondria observed in particular range in the respective mutants studied (a*) jsIs609* (b) *unc-116(e2310)* (c) *klc-2(km11)* (d) *dhc-1(or195)* (e) *dhc-1(js319).*Intermitochondrial dataset of 25-30 animals imaged was used for analysis.

Table 4.2

| Strain | Mitochondrial density in ALM | | | | Mitochondrial density in PLM | | | |
|---|---|---|---|---|---|---|---|---|
| | Proximal region(near Cell body) | Middle region | Distal region | % of aggregated (<3µm) mitochondria | Proximal region(near Cell body) | Middle region | Distal region | % of aggregated (<3µm) mitochondria |
| ***jsIs609*** | 24.6±1.0 | 34.7±1.1 | 40.7±0.9 | 2.7 | 36.3±1.1 | 34.1±1.1 | 29.6±1.2 | 2.88 |
| ***dhc-1(or195)*** | 23.1±1.1 | 30.3±1.2 | 46.6±1.2 | 0.9 | 37.2±1.4 | 26.6±1.1 | 36.2±1.4 | 3.3 |
| ***dhc-1(js319)*** | 24.9±0.9 | 33.5±1.4 | 41.5±1.3 | 2.1 | 35.3±1.2 | 35.5±1.2 | 29.2±1.5 | 4.54 |
| ***unc-116(e2310)*** | 22.1±2.4 | 36.1±3.5 | 41.8±3.2 | 0.34 | 33.4±2.6 | 33.4±2.7 | 33.0±2.2 | 2.1 |
| ***klc-2(km11)*** | 29.7±2.9 | 29.5±2.5 | 40.8±2.3 | 3.5 | 22.9±2.4 | 32.8±2.6 | 44.3±3.0 | 3.1 |

**Table 4.2: Mitochondrial density in ALM and PLM axonal segments in motor mutants**

Motor mutants *unc-116(e2310)*, *klc-2(km11)*, *dhc-1(or195)* and *dhc-1(js319)* are compared with wild type *(jsIs609).* Mitochondrial density data is represented as mean±SEM. Distribution data set of 25-30 animals was used for analysis

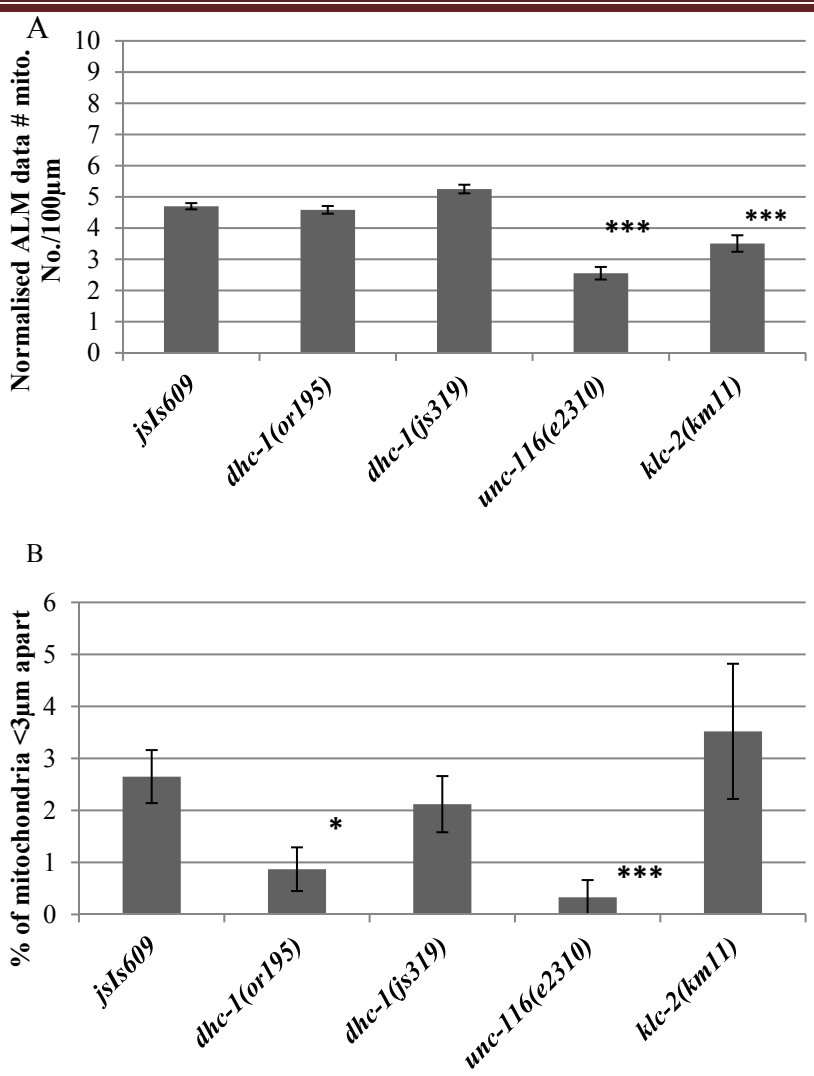


**Figure 4.3 (A-B) Graph showing normalised axonal mitochondrial density and percentage of closely spaced mitochondria (<3 µm) in motor mutants**

(A) Graph represents average number of mitochondria/100µm of axon length observed for different mutants.
(B) Data represents percentage of <3µm spaced mitochondria observed in different mutants. Data is represented as mean±S.E. Student t-test was carried out for all the mutants studied with respect to wild type, p value is illustrated as *. "*" refers to $p<0.05$ and "***" refers to $p< 0.001$.

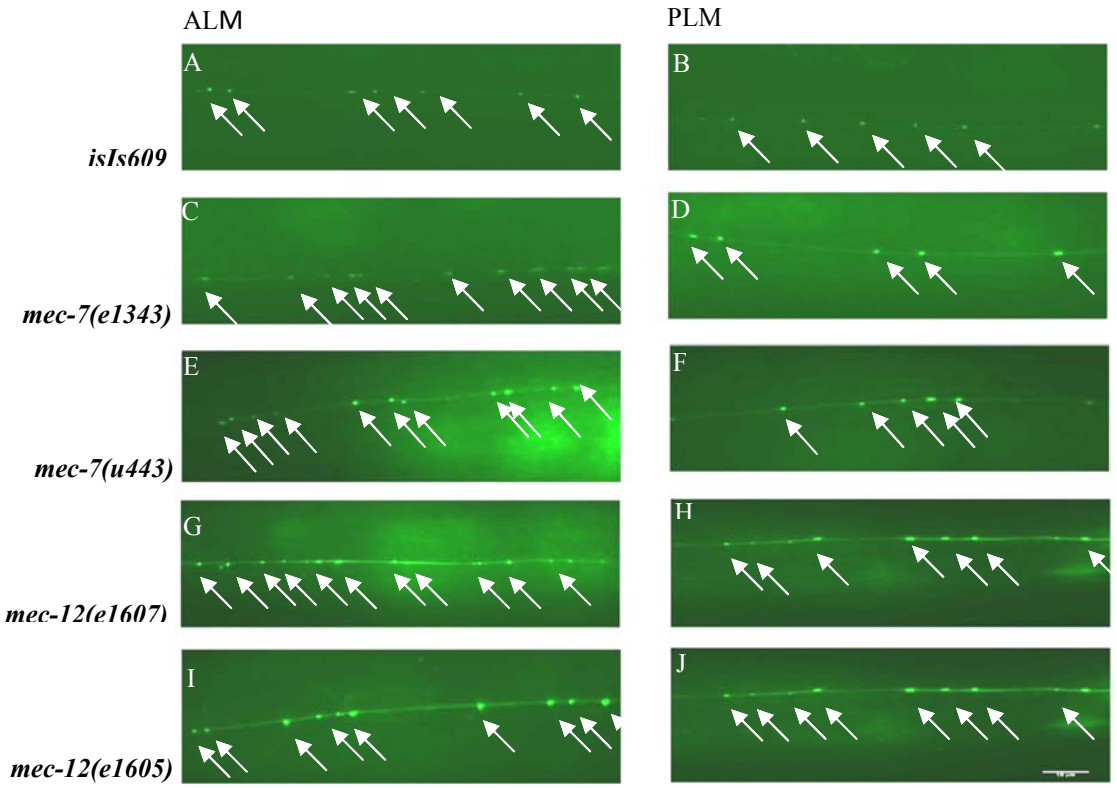


**Figure 4.4 Representative images showing mitochondrial distribution in ALM and PLM processes in WT (*jsIs609*) and tubulin mutants**

A-B) *jsIs609*; C-D) *mec-7(e1343),* E-F) *mec-7(u443)*; G-H) *mec-12(e1607),* I-J) *mec-12(e1605).* Position of mitochondria is marked by arrows. Scale bar is 10µm

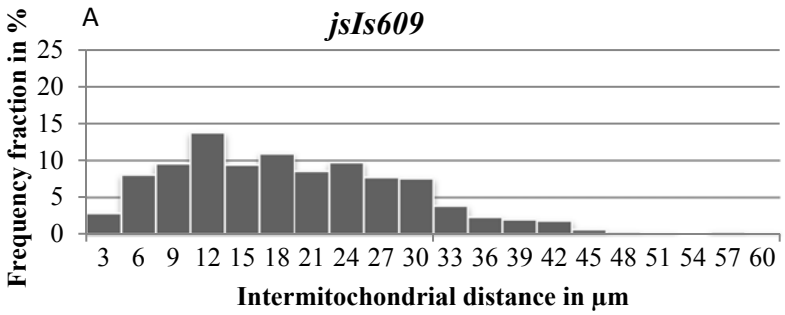
A
jsIs609
Frequency fraction in %
0
5
10
15
20
25
3 6 9 12 15 18 21 24 27 30 33 36 39 42 45 48 51 54 57 60
Intermitochondrial distance in µm

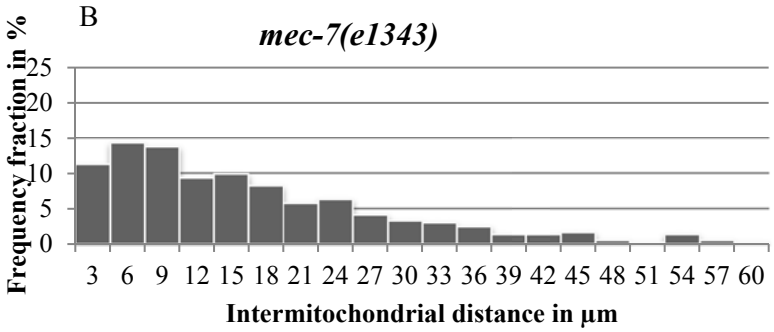
B
mec-7(e1343)
Frequency fraction in %
0
5
10
15
20
25
3 6 9 12 15 18 21 24 27 30 33 36 39 42 45 48 51 54 57 60
Intermitochondrial distance in µm

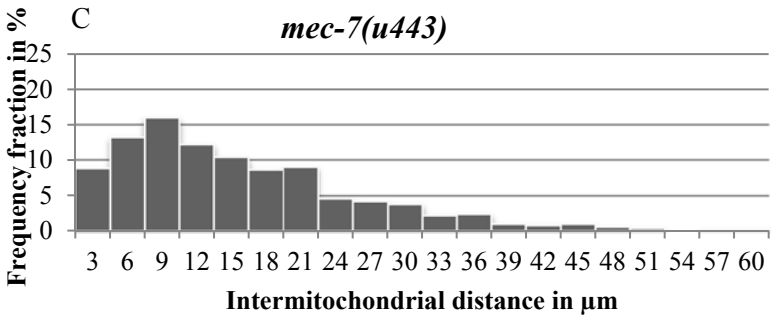
C
mec-7(u443)
Frequency fraction in %
0
5
10
15
20
25
3 6 9 12 15 18 21 24 27 30 33 36 39 42 45 48 51 54 57 60
Intermitochondrial distance in µm

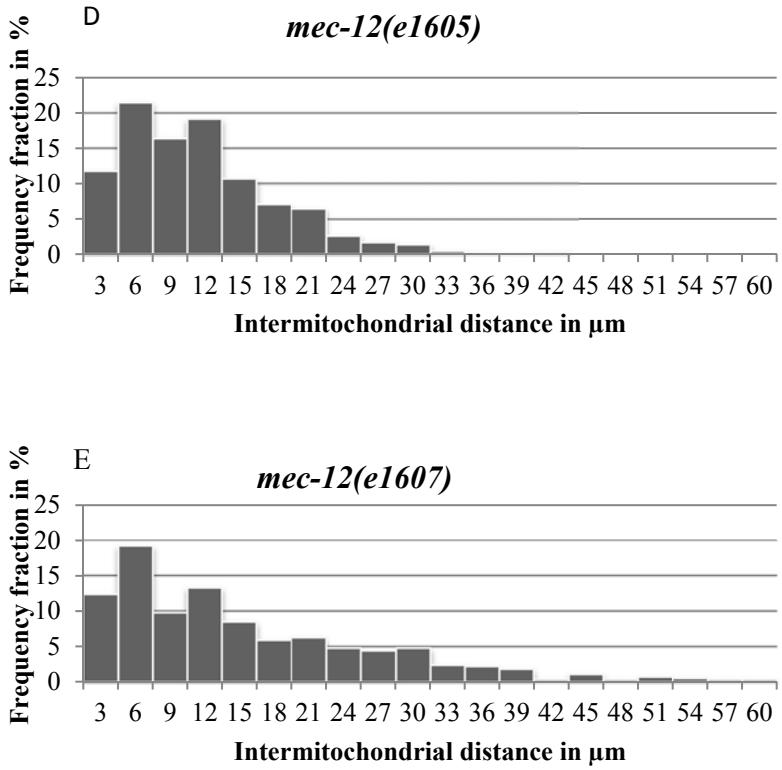


**Figure 4.5 Histogram for intermitochondrial distance in tubulin mutants.**

X- axis represents intermitochondrial distance range expressed in µm; Y- axis represents percentage of mitochondria observed in particular range in the respective mutants studied (a) *jsIs609* (b) *mec-7(e1343)* (c) *mec-7(u443)* (d) *mec-12(e1605)* (e) *mec-12(e1607).*Intermitochondrial dataset of 25-30 animals was used for analysis.

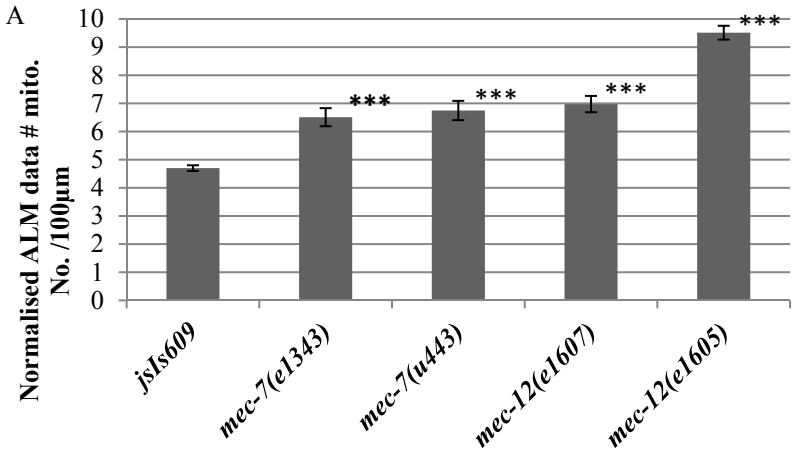

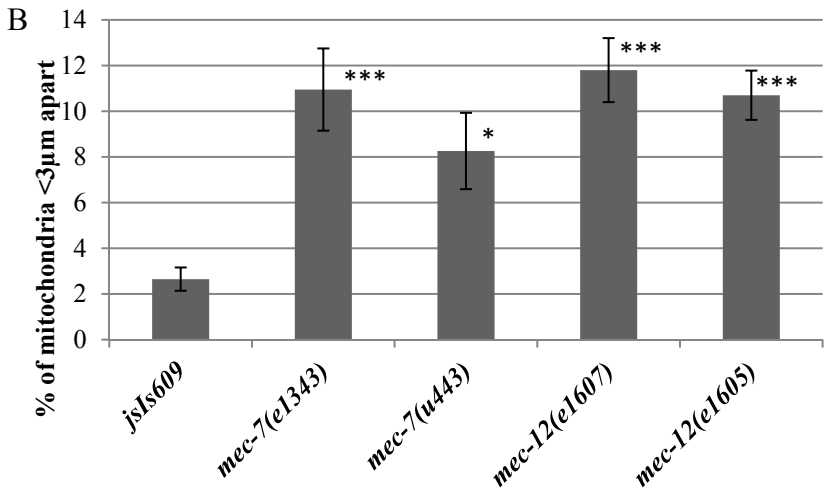


**Figure 4.6 (A-B) Graph showing normalised axonal mitochondrial density and percentage of closely spaced mitochondria (<3 µm) in tubulin mutants**

(A) Graph represents average number of mitochondria/100µm of axon length observed for different mutants.
(B) Data represents percentage of <3µm spaced mitochondria observed in different mutants. Data is represented as mean±S.E. Student t-test was carried out for all the mutants studied with respect to wild type, p value is illustrated as *. "*" refers to p<0.05 and "***" refers to p< 0.001. Dataset of 25-30 animals was used for analysis.

Table 4.3

| Strain | Av. No. of mitochondria in ALM | Av. Axon length of ALM(µm) | Av. Mito. No./100µm of ALM Axon length | Av. No. of mitochondria in PLM | Av. Axon length of PLM(µm) | Av. Mito. No./100µm of PLM Axon length |
|---|---|---|---|---|---|---|
| ***jsIs609*** | 19.1±0.5 | 406.1±5.9 | 4.7±0.1 | 25.3±1.0 | 507.2±8.1 | 5.0±0.1 |
| ***mec-7(e1343)*** | 20.9±1.1 | 322.9±9.2 | 6.5±0.3 | 13.5±0.8 | 319.2±10.3 | 4.3±0.3 |
| **mec-7(u443)** | 23.9±1.1 | 358.8±8.9 | 6.7±0.3 | 20.6±1.1 | 397.7±13.7 | 5.1±0.1 |
| ***mec-12(e1607)*** | 29.1±1.2 | 418.5±9.1 | 7.0±0.3 | 23.5±0.9 | 426.7±7.3 | 5.5±0.2 |
| ***mec-12(e1605)*** | 34.9±1.0 | 368.1±7.2 | 9.5±0.2 | 34.1±1.1 | 442.4±13.3 | 7.7±0.2 |

**Table 4.3 Mitochondria number and axon length in microtubule mutants**

Data is represented as mean±SEM. Dataset of 25-30 animals was used for analysis.

Table 4.4

| Strain | Mitochondrial density in ALM | | | | Mitochondrial density in PLM | | | |
|---|---|---|---|---|---|---|---|---|
| | Proximal region(near Cell body) | Middle region | Distal region | % of aggregated (<3µm) mitochondria | Proximal region(near Cell body) | Middle region | Distal region | % of aggregated (<3µm) mitochondria |
| ***jsIs609*** | 24.6±1.0 | 34.7±1.1 | 40.7±0.9 | 2.7 | 36.3±1.1 | 34.1±1.1 | 29.6±1.2 | 2.88 |
| ***mec-7(e1343)*** | 42.5±2.2 | 27.8±1.8 | 29.7±1.8 | 11 | 39.7±2.3 | 29.6±1.5 | 30.7±2.2 | 5.35 |
| ***mec-7(u443)*** | 37.8±1.9 | 32.7±1.8 | 29.5±2.3 | 8.3 | 34.9±3.0 | 36.5±2.6 | 28.6±3 | 5.11 |
| ***mec-12(e1607)*** | 37.6±1.9 | 30±1.8 | 32.4±2.0 | 11.8 | 30.4±1.8 | 37.3±1.4 | 32.2±1.6 | 8.96 |
| ***mec-12(e1605)*** | 26.1±1.0 | 33.8±1.2 | 40.2±0.9 | 10.7 | 37.7±1.6 | 32.9±1.2 | 29.4±1.8 | 7.85 |

**Table 4.4: Mitochondrial density in ALM and PLM axonal segments in microtubule mutants.**
Mitochondrial density data is represented as mean±SEM. Dataset of 25-30 animals was used for analysis.

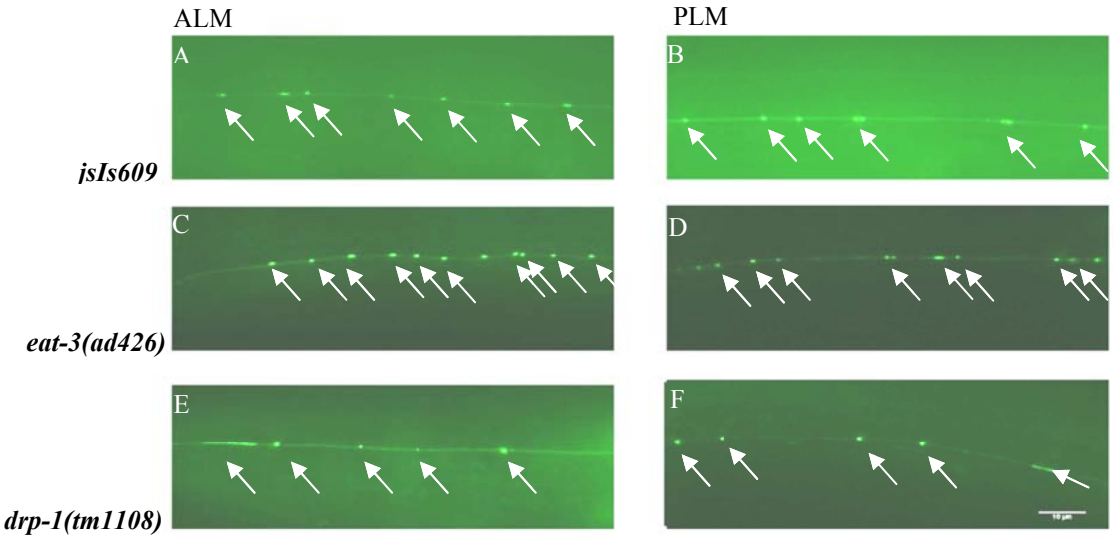


**Figure 4.7: Representative images showing mitochondrial distribution in ALM and PLM processes in WT (*jsIs609*) and fission-fusion mutants**

(A-B) *jsIs609*; (C-D) *eat-3(ad426),* (E-F) *drp-1(tm1108).* Position of mitochondria is marked by arrows. Scale bar is 10µm.

Table 4.5

| Strain | Av. No. of mitochondria in ALM | Av. Axon length of ALM(µm) | Av. Mito. No./100µm of ALM Axon length | Av. No. of mitochondria in PLM | Av. Axon length of PLM(µm) | Av. Mito. No./100µm of PLM Axon length |
|---|---|---|---|---|---|---|
| ***jsIs609*** | 19.1±0.5 | 406.1±5.9 | 4.7±0.1 | 25.3±1.0 | 507.2±8.1 | 5.0±0.1 |
| ***eat-3(ad426)*** | 21.0±0.8 | 332.4±6.2 | 6.3±0.3 | 22.4±1.1 | 430.7±8.3 | 5.2±0.3 |
| ***drp-1(tm1108)*** | 11.4±0.5 | 357.7±3.7 | 3.2±0.2 | 14.5±0.5 | 438.0±3.8 | 3.3±0.2 |

**Table 4.5 Average mitochondria number and axon length in mitochondrial fission-fusion mutants.**

Data is represented as mean±SEM. Dataset of 25-30 animals was used for analysis.

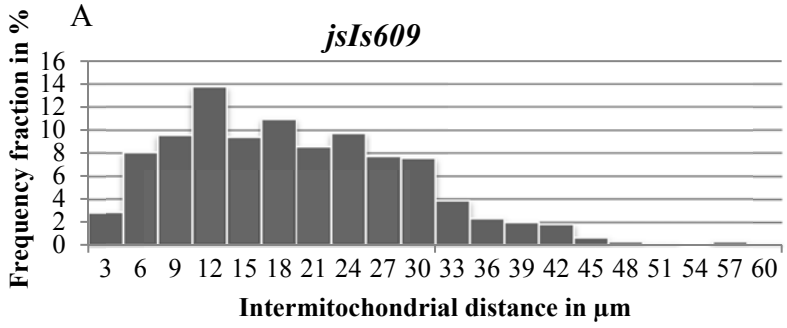


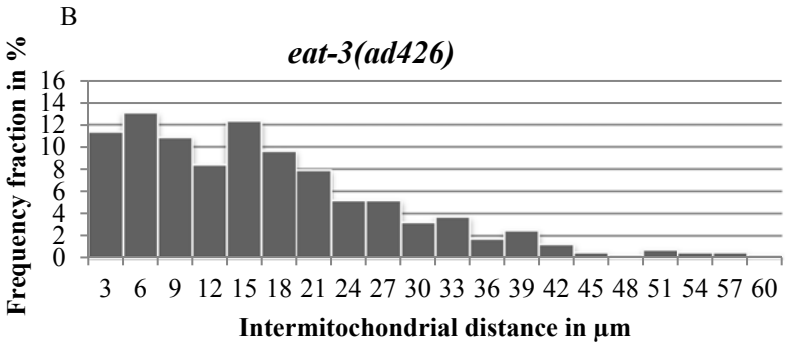

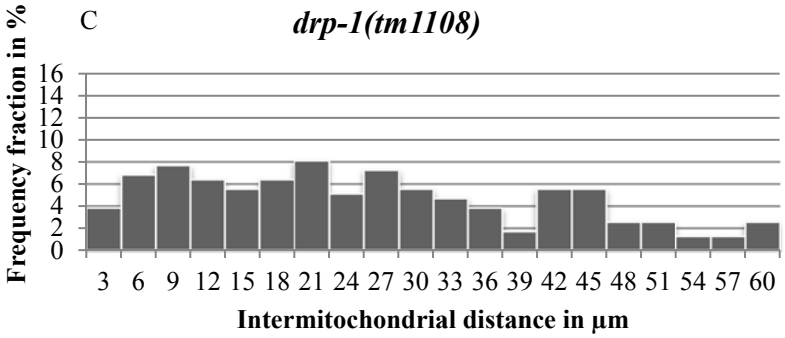


**Figure 4.8 Intermitochondrial distance histogram in mitochondrial fission and fusion mutants**

Horizontal axis represents intermitochondrial distance range expressed in µm vertical axis represents percentage of mitochondria observed in particular range in the respective mutants studied (A) *jsIs609* (B) *eat-3(ad426)* (C) *drp-1(tm1108).* Dataset of 25-30 animals was used for analysis.

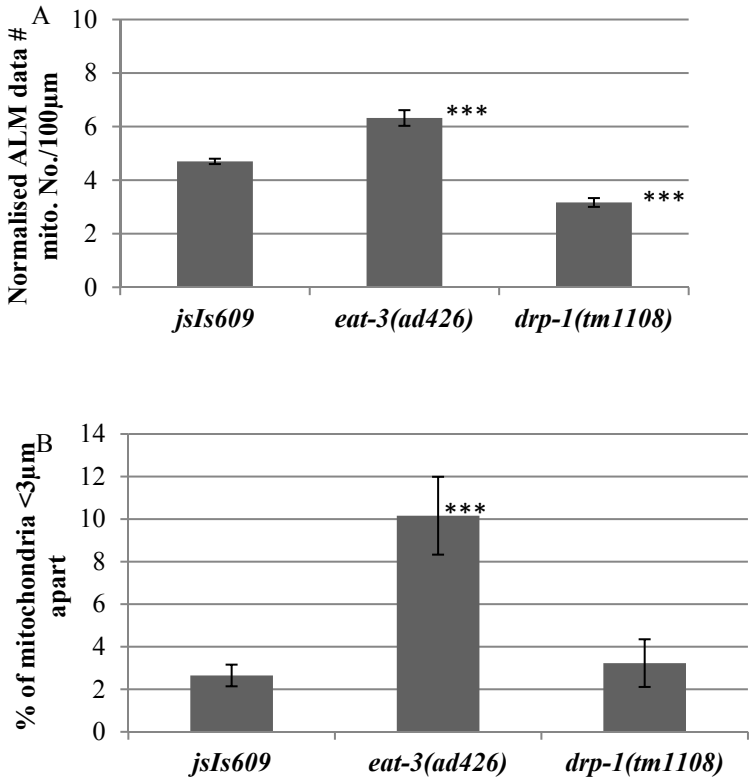


**Figure 4.9 (A-B) Graph showing normalised axonal mitochondrial density and percentage of closely spaced mitochondria (<3 µm) in fission-fusion mutants**

(A) Graph represents average number of mitochondria/100µm of axon length observed for different mutants.

(B) Data represents percentage of <3µm spaced mitochondria observed in different mutants. Data is represented as mean±S.E. Student t-test was carried out for all the mutants studied with respect to wild type, p value is illustrated as *. "*" refers to $p<0.05$ and "***" refers to $p< 0.001$. Dataset of 25-30 animals was used for analysis.

Table 4.6

| Strain | Mitochondrial density in ALM | | | | Mitochondrial density in PLM | | | |
|---|---|---|---|---|---|---|---|---|
| | Proximal region(near Cell body) | Middle region | Distal region | % of aggregated (<3µm) mitochondria | Proximal region(near Cell body) | Middle region | Distal region | % of aggregated (<3µm) mitochondria |
| ***jsIs609*** | 24.6±1.0 | 34.7±1.1 | 40.7±0.9 | 2.7 | 36.3±1.1 | 34.1±1.1 | 29.6±1.2 | 2.88 |
| ***eat-3(ad426)*** | 37.9±2.0 | 31.5±1.5 | 30.6±1.8 | 10.2 | 40.5±2.4 | 27.0±2.1 | 32.5±1.9 | 3.72 |
| ***drp-1(tm1108)*** | 33.5±2.4 | 32.3±3.0 | 34.2±2.8 | 3.2 | 30.9±3.0 | 34.5±2.3 | 34.5±2.6 | 5.8 |

**Table 4.6: Mitochondrial density in ALM and PLM axonal segments of fission-fusion mutants.**

Mitochondrial density data is represented as mean±SEM. Dataset of 25-30 animals was used for analysis.

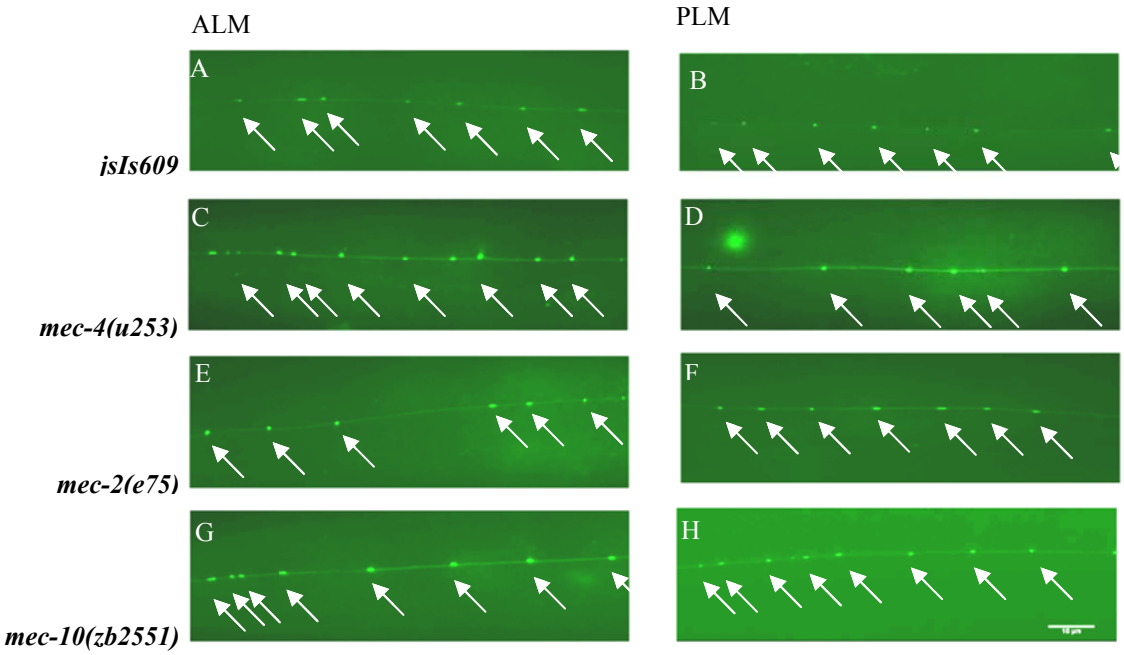


**Figure 4.10 Representative images showing mitochondrial distribution in ALM and PLM processes in WT (*jsIs609*) and DEG/ ENaC**

A-B) *jsIs609*; C-D) *mec-4(u253),* E-F) *mec-2(e75)*; G-H) *mec-10(zb2551).* Position of mitochondria is marked by arrows. Scale bar is 10µm.

Table 4.7

| Strain | Av. No. of mitochondria in ALM | Av. Axon length of ALM(µm) | Av. Mito. No./100µm of ALM Axon length | Av. No. of mitochondria in PLM | Av. Axon length of PLM(µm) | Av. Mito. No./100µm of PLM Axon length |
|---|---|---|---|---|---|---|
| ***jsIs609*** | 19.1±0.5 | 406.1±5.9 | 4.7±0.1 | 25.3±1.0 | 507.2±8.1 | 5.0±0.1 |
| ***mec-4(u253)*** | 26.1±0.9 | 415.0±7.9 | 6.3±0.2 | 22.8±0.8 | 475±8.2 | 4.8±0.2 |
| ***mec-2(e75)*** | 19.9±0.6 | 400.5±7.3 | 5.0±0.1 | 27.4±1.2 | 470.4±9.7 | 5.8±0.2 |
| ***mec-10(zb2551)*** | 22±0.8 | 386.3±7.5 | 5.7±0.2 | 27.8±1.7 | 554.2±10.8 | 5.0±0.3 |

**Table 4.7 Average mitochondria number and axon length in DEG/ENaC mutants.**

Data represented as mean±SEM. Dataset of 25-30 animals was used for analysis.

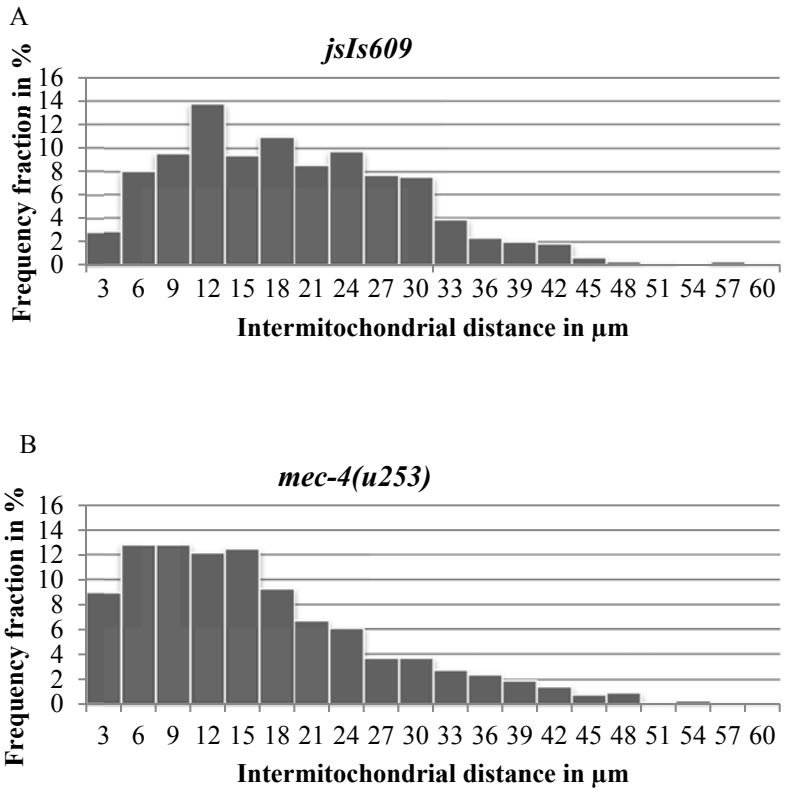

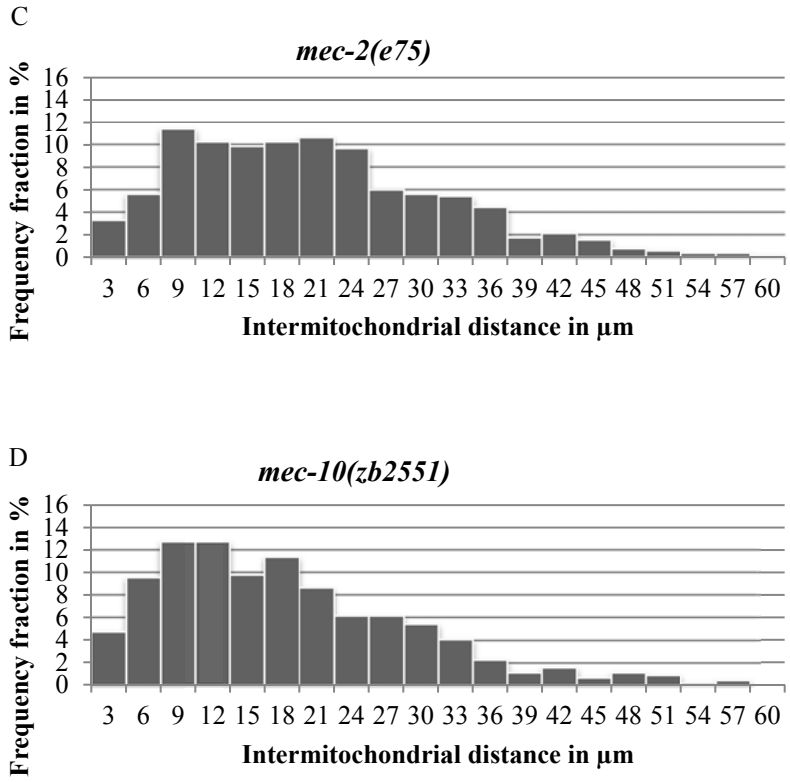


**Figure 4.11: Distribution histogram for intermitochondrial distance for DEG/ENaC channel mutants**

Horizontal axis represents intermitochondrial distance range expressed in µm, vertical axis represents percentage of mitochondria observed in a particular range in the respective mutants studied (A) *jsIs609* (B) *mec-4(u253)* (C) *mec-2(e75)* (D) *mec-10(zb2551)*. Intermitochondrial dataset of 25-30 animals was used for analysis.

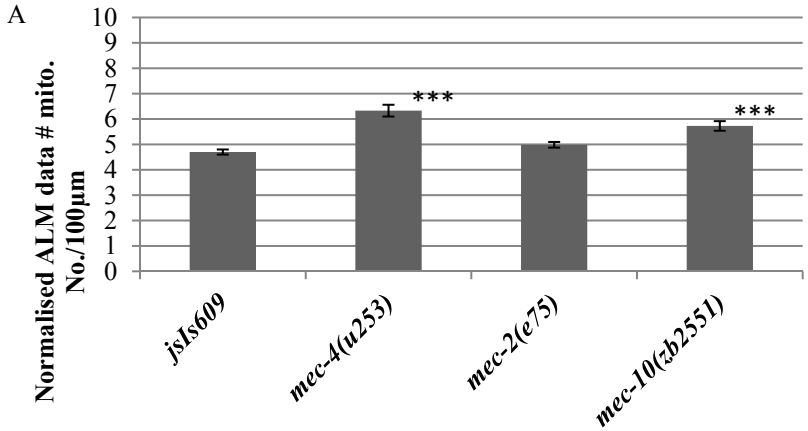

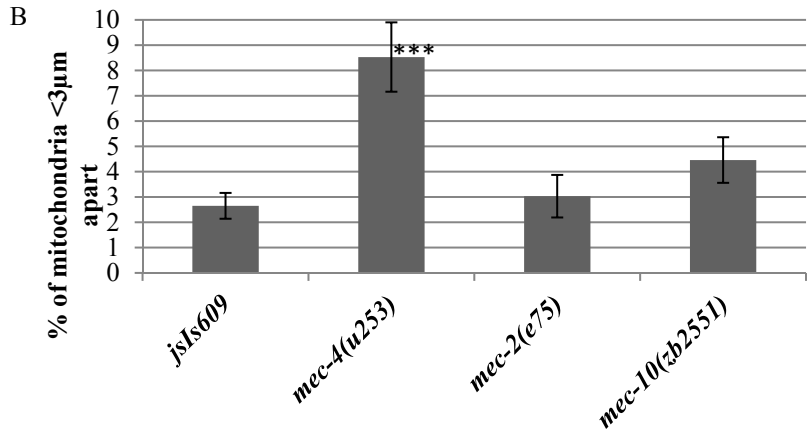


**Figure 4.12 (A-B): Graph showing normalised axonal mitochondrial density and percentage of closely spaced mitochondria (<3 µm) in DEG/ENaC channel mutants**

(A) Graph represents average number of mitochondria/100µm of axon length observed for different mutants.
(B) Data represents percentage of <3µm spaced mitochondria observed in different mutants. Data is represented as mean±S.E. Student t-test was carried out for all the mutants studied with respect to wild type, p value is illustrated as *. "*" refers to p<0.05 and "***" refers to p< 0.001. Dataset of 25-30 animals was used for analysis.

Table 4.8

| Strain | Mitochondrial density in ALM | | | | Mitochondrial density in PLM | | | |
|---|---|---|---|---|---|---|---|---|
| | Proximal region(near Cell body) | Middle region | Distal region | % of aggregated (<3µm) mitochondria | Proximal region(near Cell body) | Middle region | Distal region | % of aggregated (<3µm) mitochondria |
| ***jsIs609*** | 24.6±1.0 | 34.7±1.1 | 40.7±0.9 | 2.7 | 36.3±1.1 | 34.1±1.1 | 29.6±1.2 | 2.88 |
| ***mec-4(u253)*** | 32.2±1.6 | 34.4±1.2 | 33.3±1.8 | 8.5 | 37.5±1.7 | 32.1±1.6 | 30.3±1.4 | 5.94 |
| ***mec-2(e75)*** | 30.0±1.3 | 35.0±1.4 | 35.0±1.3 | 3 | 40.9±1.3 | 35.2±1.4 | 23.9±1.0 | 4.7 |
| ***mec-10(zb2551)*** | 30.1±1.3 | 34.8±1.5 | 35.1±1.5 | 4.5 | 42.2±2.5 | 33.0±1.8 | 24.8±1.9 | 5.24 |

**Table 4.8: Mitochondrial density in ALM and PLM axonal segments in DEG/ENaC mutants.**

Mitochondrial density data is represented as mean±SEM. Dataset of 25-30 animals was used for analysis.

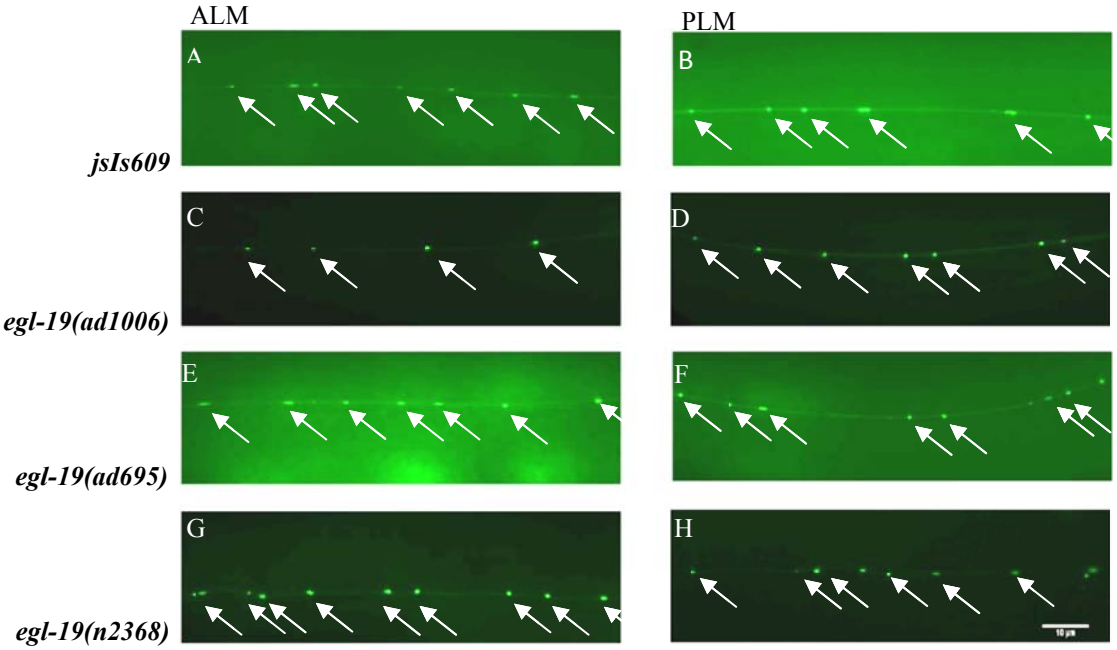


**Figure 4.13 Representative images showing mitochondrial distribution in ALM and PLM processes in WT (*jsIs609*) and VGCC mutants**

A-B) *jsIs609*; C-D) *egl-19(ad1006),* E-F) *egl-19(ad695)*; G-H) *egl-19(n2368).* Position of mitochondria is marked by arrows. Scale bar is 10µm.

Table 4.9

| Strain | Av. No. of mitochondria in ALM | Av. Axon length of ALM(µm) | Av. Mito. No./100µm of ALM Axon length | Av. No. of mitochondria in PLM | Av. Axon length of PLM(µm) | Av. Mito. No./100µm of PLM Axon length |
|---|---|---|---|---|---|---|
| ***jsIs609*** | 19.1±0.5 | 406.1±5.9 | 4.7±0.1 | 25.3±1.0 | 507.2±8.1 | 5.0±0.1 |
| ***egl-19(ad1006)*** | 22.1±0.8 | 436±6.8 | 5.0±0.2 | 27.3±1.0 | 550.0±10.6 | 5.0±0.1 |
| ***egl-19(ad695)*** | 23.4±1.1 | 376.4±8.5 | 6.2±0.3 | 27.9±1.0 | 463.6±11.8 | 6.0±0.2 |
| ***egl-19(n2368)*** | 18.5±0.5 | 265.1±7.2 | 7.1±0.3 | 23.3±1.0 | 399.6±9.9 | 5.8±0.2 |

**Table 4.9 Statistics of mitochondria number and axon length in VGCC channel mutants.**

Data is represented as mean±SEM. Dataset of 25-30 animals was used for analysis.

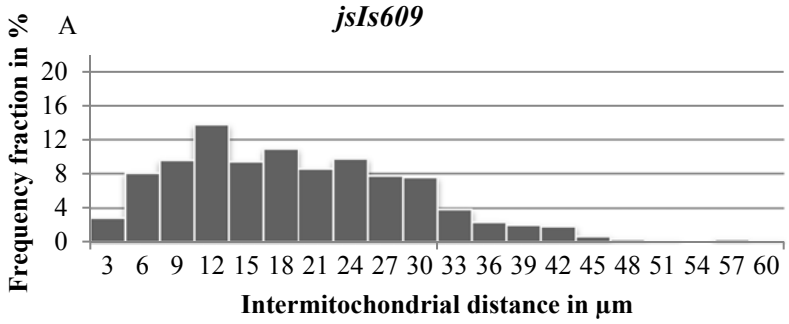


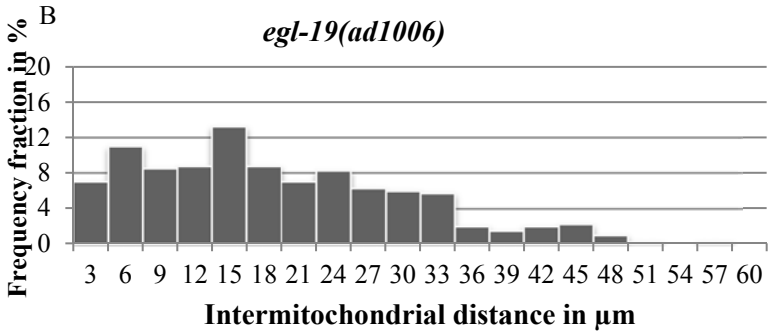

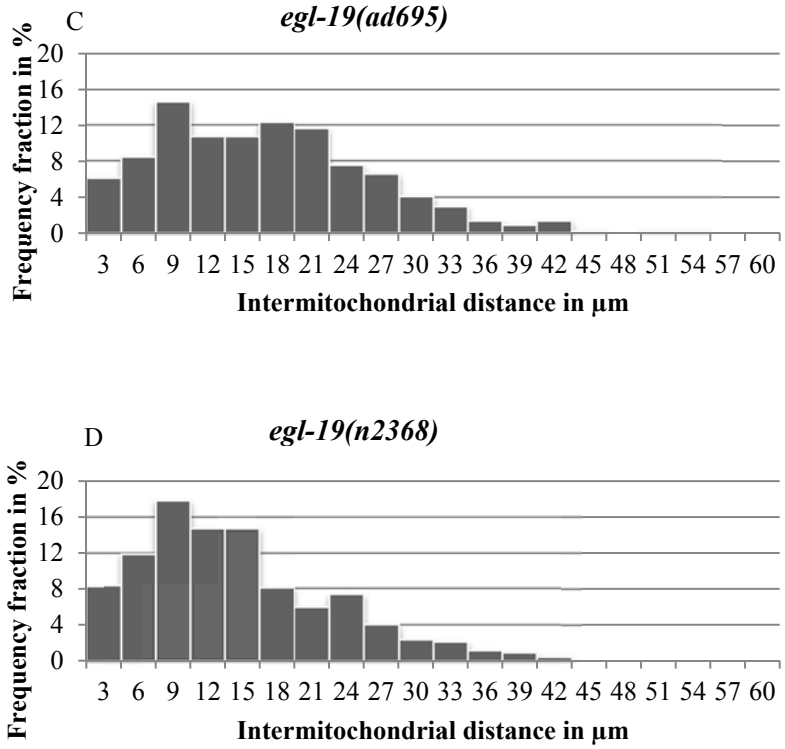


**Figure 4.14 Distribution histogram for intermitochondrial distance for Voltage gated calcium channel mutants.**

X- axis represents intermitochondrial distance range expressed in µm; Y-axis represents percentage of mitochondria observed in particular range in the respective mutants studied (A) *jsIs609* (B) *egl-19(ad1006)* (C) *egl-19(ad695)* (D) *egl-19(n2368).* Intermitochondrial dataset of 25-30 animals was used for analysis.

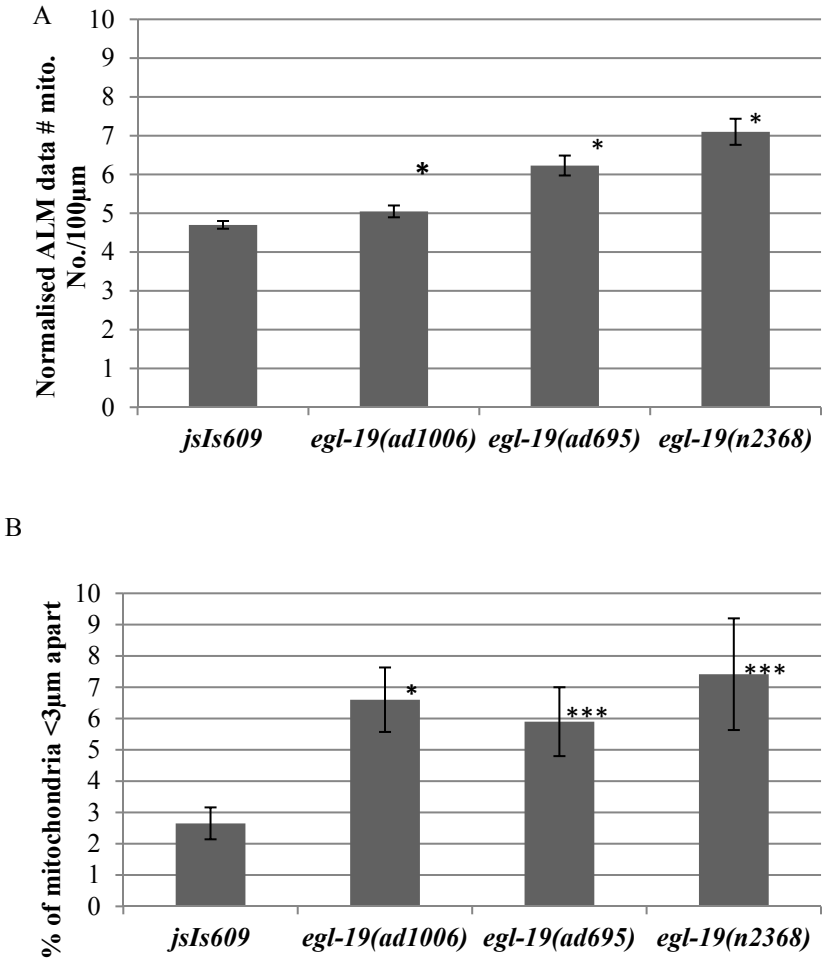


**Figure 4.15 (A-B) Graph showing normalised axonal mitochondrial density and percentage of closely spaced mitochondria (<3 µm) in VGCC mutants**

(A) Graph represents average number of mitochondria/100µm of axon length observed for different mutants.
(B) Data represents percentage of <3µm spaced mitochondria observed in different mutants. Data is represented as mean±S.E. Student t-test was carried out for all the mutants studied with respect to wild type, p value is illustrated as *. "*" refers to $p<0.05$ and "***" refers to $p< 0.001$. Dataset of 25-30 animals was used for analysis.

Table 4.10

| Strain | Mitochondrial density in ALM | | | | Mitochondrial density in PLM | | | |
|---|---|---|---|---|---|---|---|---|
| | Proximal region(near Cell body) | Middle region | Distal region | % of aggregated (<3µm) mitochondria | Proximal region(near Cell body) | Middle region | Distal region | % of aggregated (<3µm) mitochondria |
| ***jsIs609*** | 24.6±1.0 | 34.7±1.1 | 40.7±0.9 | 2.7 | 36.3±1.1 | 34.1±1.1 | 29.6±1.2 | 2.88 |
| ***egl-19(ad1006)*** | 33.7±2.1 | 34.5±2.2 | 31.7±1.2 | 6.6 | 41.5±1.3 | 32.6±1.2 | 25.8±1.3 | 6.23 |
| ***egl-19(ad695)*** | 30.5±1.3 | 34.0±1.3 | 35.5±1.2 | 5.9 | 39.2±1.9 | 31.8±1.0 | 28.9±1.9 | 3.59 |
| ***egl-19(n2368)*** | 22.2±1.1 | 32.7±1.4 | 45.1±1.2 | 7.4 | 31.7±1.6 | 32.6±1.5 | 35.7±1.6 | 5.14 |

**Table 4.10: Mitochondrial density in ALM and PLM axonal segments in VGCC channel mutants.**

Mitochondrial density data is represented as mean±SEM. Dataset of 25-30 animals was used for analysis.

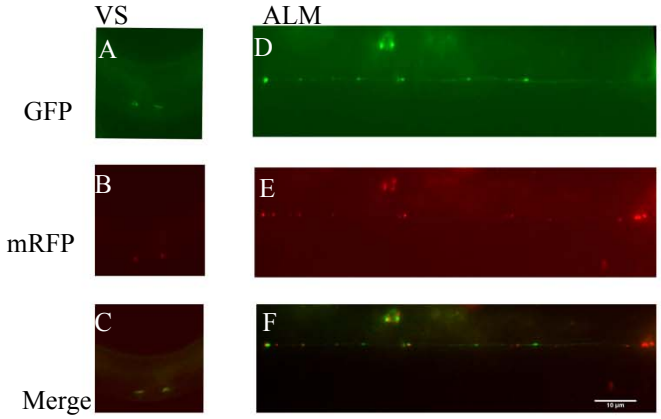


**Figure 4.16 (A-F) Represents co-localization between ebp-1 puncta (GFP) labeled and mitochondria (mRFP)**

(A-C) Represents co-localization observed in Ventral Synapse region (VS)
(A) Represents ebp-1 puncta (GFP labeled) in VS
(B) Mitochondria (mRFP) labeled
(C) Represents co-localization between the two.
(D-F) Represents co-localization observed in ALM axon
(D) Represents ebp-1 puncta (GFP labeled)
(E) Mitochondria (mRFP) labeled
(F) Represents co-localization between the two.
Scale bar is 10µm.

Table 4.11

| | Av. No. of ebp-1 punctas observed | Av. No. of mitochondria observed | Av. No. of ebp-1 punctas showing co-localization with mitochondria | % of ebp-1 showing co-localization with mitochondria |
|---|---|---|---|---|
| ALM | 6.13±0.71 | 10.8±0.44 | 1.96±0.27 | 31.9 |
| PLM | 9.26±1.43 | 14.5±0.93 | 1.95±0.42 | 21.02 |

**Table 4.11: Ebp-1 and mitochondria co-localization statistics.**

Data represented as mean±SEM. Dataset of 20-25 animals was used for analysis.

# Chapter 5

## Mitochondria Number and Distribution Correlates to Neuronal Function

# 5. Mitochondria Number and Distribution Correlates to Neuronal Function

## 5.1. Introduction

Mitochondrial function is essential for all cell types and is even more critical for neuronal cells due to their high energy needs. Apart from energy production, mitochondria are involved in many other vital functions like calcium buffering, regulating apoptosis, free radicals generation and synthesis of steroids. As mitochondria are involved in ATP production and many other vital functions their dysfunction has been reported to be associated with aging, degenerative diseases, as well as with cancer (Wallace 2005, Kujoth et al 2005, Knott et al 2008).

Perturbation of mitochondrial dynamics and $Ca^{2+}$ regulation has been reported to be associated with many neurodegenerative diseases. Mutated fusion genes have been known to be associated with many neurodegenerative diseases like Mutations in *Mfn 2* cause Charcot-Marie-tooth (CMT) subtype 2A (CMT2A), similarly mutations in *OPA1* causes optic atrophy(Kijima K et al 2005, Zuchner et al 2004, Carelli et al 2004, Amati-Bonneau et al 2008). Similarly, mitochondrial fission genes are known to be responsible in causing CMT subtype 4A disease (Kabzinska et al 2006). Role of $Ca^{2+}$ dysregulation and mitochondrial dysfunction has also been implicated in many other neurodegenerative diseases like Alzheimer's disease (Khachaturian 1994, Hirai et al 2001, Wang et al 2009), Parkinson's disease (Danzer et al 2007, Furukawa et al 2006), Huntington's disease (Lim et al 2008) and Amyotrophic lateral sclerosis (Grosskreutz et al 2010).

Changes in cytosolic calcium levels are associated with neuronal activity. These changes result in an increase in mitochondrial calcium transients, while its membrane potential results in neuronal behavior (Kann et al 2003, Kovacs et al 2005). Thus mitochondrial functioning is reported to be directly or indirectly involved in neuronal behavior. In the last chapter, we looked at different factors which are contributing for mitochondrial density and distribution in touch neurons. As per our results we found that various factors were contributing for normal number and distribution and each of these factors had different degree of severity. Out of all the factors studied, tubulin and channel mutant (*mec-4(u253)*) were found to be affecting the density and

distribution most. As the above mentioned mutants are proven set of genes responsible for mechanosensation defect, we then reasoned whether this altered number and distribution is instrumental in their mechanosensation defective phenotype. To resolve this query, we carried out gentle touch mechanosensation assay using an eyelash for all the mutants to check whether mitochondria number and distribution correlates to neuronal function.

Gradual decrease in response to repeated stimuli is known as habituation (Thompson et al 1966). In ***C. elegans*** habituation has been observed when worms are exposed to repeated gentle touch or tap response (Rankin et al. 1990). Gentle touch or tap response elicit avoidance behavior in the form of forward and backward movements which is governed by mechanosensory neurons (Rankin et al 1990). It has been reported that for tap response habituation was faster in case of shorter inter-stimulus interval as compared to longer inter-stimulus interval (Broster et al 1994). We also reasoned about the effect of increasing inter-stimulus interval in the mechanosensory defective strain while giving gentle touches. In an effort to observe this point, instead of giving consecutive alternate touches which were approximately 1.5 seconds apart (inter-stimulus interval between first anterior and subsequent posterior touch), we increased the gap to 10 seconds and quantified the behavioral response.

In this study we reported that mitochondrial density (Mitochondria number /100µm of axon length) and distribution (<3µm bin) is correlated to behavioral response. Both the factors show statistically significant negative relationship with behavioral response with wild type levels as the cut-off. Increase of any of the two variables (density and <3µm bin) beyond the wild type threshold showed negative impact on behavioral response. Though the effects seen above were diminished when the inter-stimulus interval (ISI) was increased and in such cases irrespective of the genotypes, all the strains showed very high positive behavioral response to gentle touch stimulus.

## 5.2. Results

### 5.2.1. Mutants with High Normalised Number and Higher Clumping Showed Poor Behavior

We did gentle touch behavioral assay for the mutants and scored them for the responses exhibited for a series of ten alternate anterior and posterior touches respectively. Our control strain *jsIs609* showed positive response to 85% of ALM touches which was comparable to *N2* (control strain) which showed response to 90% touches. All the mechanosensation defective strains were assayed and scored for behavioral responses. All the *mec-7* and *mec-12* strains which showed very high altered number and distribution showed very poor behavioral response (approx 30-45% positive response for ALM touches). Similar, responses were shown by *mec-4(u253)* which had the similar trend for number and distribution (Table 5.1).

*Mec-2* and *mec-10* strains which had the mitochondrial density close to the wild type and mild clumping responded to 60-65% touches. Looking at this trend, we assayed some other strains which did not belong to the proven set of mechanosensation defective genes. *Eat-3* which also had high density and high clumping showed positive response to only 45% touches. All the strains with higher mitochondrial density in axon and high clumping compared to wild type showed poor behavioral response. We then questioned the effect of lower density (compared to control) on behavior and assayed the strains which showed these trends. All the strains *unc-116(e2310)*, *klc-2(km11)* and *drp-1(tm1108)* which had mitochondrial density below wild type and mitochondrial aggregation compared to or below wild type showed poor response (60-70%) as compared to wild type (Table 5.1 and Fig 5.1).

All the strains which were analyzed for behavioral response had affected mitochondria number or distribution due to being involved in mitochondrial transport dynamics or function. In an effort to look whether we could find some other strain which affects number and distribution but without being involved in any such pathway we looked for *unc-16* mutants. *Unc-16* is ***C. elegans*** homolog of mouse *JIP3* and Drosophila *Sunday Driver* (Verhey et al 2001, Bowman et al 2000). UNC-16 is known to interact with KLC-2 and KHC component of Kinesin-1 (Bowman et al 2000, Sun F 2011) and has also been reported to be responsible for regulating vesicle transport in ***C. elegans*** (Byrd D T et al 2001). While looking for its role in mitochondrial transport using

*unc-16* mutants it was reported that *unc-16* mutants showed increased number of mitochondria in axon and this effect was motor independent (work done by Guru Prasad Reddy). One of the mutant *unc-16(e109)* which is a reported strong allele of the same (Byrd et al 2001) was assayed for mitochondria number, distribution as well as behavior. *Unc-16(e109)* showed high normalised number of mitochondria in axon (12 mito/100µm of axon). Percentage of mitochondrial clumping (<3µm bin) observed was very high (17%) and the positive behavioral response observed was 43%. So, the behavioral trend observed in *unc-16(e109)* mutants showed a consistent trend and correlation between mitochondria number and distribution as was observed in other mutants (Table 5.1 and Fig 5.1).

All the mutants studied for mitochondrial density and distribution showed three characteristic trends (which we quantified and were different in the mutants and the wild type): 1) Mitochondrial density in axon 2) Clumping of mitochondria (<3µm bin) 3) Distribution of mitochondria in different axonal segments. As the trend in behavioral response implied correlation between number, distribution and behavior; we tried to scrutinize whether some relationship exists between these factors and behavior and to validate the findings, we plotted graph for these variables corresponding to the behavioral response (Fig 5.2).

Mitochondrial density in axon and percentage of clumped mitochondria (<3µm bin) showed a very prominent negative relationship with behavior with wild type as cutoff (Fig 5.2 A-B) Mutants with both higher and lower trends in mitochondrial density and clumping showed lower behavioral response compared to wild type. As distal region of axon showed higher density of mitochondria in wild type whereas other mutants showed disturbed ratio, we also checked whether it also correlates to neuronal behavior; but it showed abrupt trend (Fig 5.2 C). Trends in above results implied that mitochondrial density in axon and percentage of clumped mitochondria (<3µm bin) correlates with mechanosensation behavior.

### 5.2.2. Mitochondrial Density and Distribution Showed Statistically Significant Correlation with Behavior

The trend in results implied that mitochondria density and distribution is correlated. To confirm the same statistical tests were carried out. We first checked whether linear correlation exists between the dependent variable behavior and independent variables mitochondrial density and

clumping of mitochondria (<3µm bin). We also calculated the correlation coefficient (r) using MS Excel (Fig 5.3 A-B). The correlation coefficient has a value between -1 and 1 which is used to determine whether two paired sets of data are related. Values between 0.5-1.0 denote strong positive linear correlation and the one ranging from -0.5 to -1 denotes strong negative linear correlation. Both mitochondrial density and clumping of mitochondria (< 3µm bin) showed negative linear correlation with value respectively -0.52 (p=0.02) and -0.77 (p=0.0002) which showed significantly high correlation. Higher values of correlation coefficient for both normalised mitochondria number in axon and <3µm bin indicated poor behavioral response.

As both the variables showed significant correlation with behavior, we also carried out multiple regression analysis. Multiple linear regression analysis is used to model the relationship between two or more explanatory variables and a response variable by fitting a linear equation to observed data. Every value of the independent variable *x* is associated with a value of the dependent variable *y*. Multiple linear regression model was carried out using dependent variable "Y" which is average response to anterior touches (expressed in %) and the independent variables (X's) *Av. Mito. No. /100µm of ALM* and *% of aggregated (<3µm) mitochondria*. The model aimed to determine whether average response to anterior touches (behavioral response) could be predicted using the variables *Av. Mito. No. /100µm of ALM* (Norm ALM) and *% of aggregated (<3µm) mitochondria*.

Results of multiple linear regressions are summarized in Fig 5.4 and Table 5.3. Value of coefficient of determination ($R^2$) obtained is 0.70 with $p<0.01$ which denotes that 70% of variation in behavioral response can be explained by mitochondria density and aggregation percentage (Fig 5.4). Value of intercept in the regression equation was 63.5 with $p<0.001$, regression coefficient or ß weights for Norm ALM is 6.15 with $p<0.05$ and for <3µm is -5.83 with $p< 0.001$ which was found to be statistically significant (Table 5.3). As the value of $R^2$ was high and all other variables were found to be statistically significant, results of the regression analysis denotes that behavioral response could be predicted using the variables *normalised ALM* and *<3 µm bin*.

To confirm the regression model, we also did residual analysis and developed residual plots. Residual is the value obtained by the difference between observed and predicted values of

dependent variables. Values of the residual were calculated using MS Excel and residual plot was developed. Scatter plot was made by plotting Residuals on Y-axis and the values of dependent variables (*Norm ALM* and *<3µm bin)* on X-axis. The residual plot depicted a random pattern highlighting the fact that trends in the data showed a decent fit for the linear regression model (Fig 5.5 A-B).

### 5.2.3. Altering Mitochondria Number and Distribution Alters Behavior

The results above show mitochondria number and distribution shows statistically significant correlation with behavior. To justify this point, we also tried altering mitochondrial number by diluting the effect of a particular mutant gene by replacing one copy of the gene by wild type using genetic crosses. We used similar approach for *unc-116(e2310)* and *unc-16(e109)* both of which had extreme variations in mitochondria number and distribution and none of them belong to the known set of mechanosensory defective genes.

Mutants of both *unc-116(e2310)/+* and *unc-16(e109)/+* which had one wild type copy of gene were characterized for mitochondrial density, distribution and assayed for behavior. *unc-116(e2310)/+* mutant resulted in normalised number of 5.2 mitochondria/100µm which was comparative to wild type but high as compared to *unc-116(e2310)* which had normalised number of 2.5/100µm. Percentage of aggregated mitochondria (<3µm) for *unc-116(e2310)* and *unc-116(e2310)/+* was 0.4% and 3.6% respectively. Behavioral response of *unc-116(e2310)/+* mutant was compared to wild type and it showed 89% response compared to *unc-116(e2310)* which responded positively to only 62.33% touches (Table 5.4).

Similar to above, *unc-16(e109)/+* with one wild type copy of gene showed decrease in mitochondrial density in axon with the value of 5.1 mitochondria/100µm compared to *unc-16(e109)* which had value of 11.5/100µm. Percentage of mitochondria showing clumping was also significantly reduced with value corresponding to 3.7% compared to *unc-16(e109)* which had 17% clumping. As expected, the behavioral response showed by *unc-16(e109)/+* was improved drastically to 91% positive response for anterior touches and was comparable to wild type. Results of this experiment confirmed that mitochondria number and distribution were the contributing factors for behavioral response and altering one affected the other (Table 5.4).

### 5.2.4. Inter-stimulus Interval (ISI) Governs the Behavioral Response

In the above set of experiments, alternate gentle touch stimulus was given without any spacing between the stimuli. The duration of stimuli between alternate touches was approximately 1.5 second. All the strains irrespective of their genotype assayed showed positive response to the first gentle touch administered to them. Frequency of positive response to subsequent touches showed decline thereafter depending on the genotype. As all the strains showed positive response to first touch it implied that they are capable of detecting the stimulus and show positive response for the same. Thus the slowing down of behavioral response to second and subsequent touches is due to habituation and some mutants habituate faster than the others. The same has been reported for tap withdrawal assay (Broster et al 1994) but its effect on gentle touch assay with respect to mechanosensory defective mutants has never been assayed and characterized.

To look at the effect of inter-stimulus interval (ISI) on gentle touch behavioral response, we increased the time duration between the alternate touches to 10 seconds and assayed a set of mutants. Tubulin mutants *mec-7(e1343), mec-12(e1607)* and *mec-12(e1605)* showed very poor (30-45%) behavioral response to consecutive touches (ISI 1.5 sec). When, the ISI was increased to 10 second behavioral response increased for all the tubulin mutants to approximately 80% and above (Table 5.5). Control strain as well as all other mutants assayed showed increased percentage of positive response when ISI was 10 second compared to ISI of 1.5 second (Table 5.5). Results of the above experiment thus indicated that if the inter-stimulus interval was sufficiently placed, all genotypes irrespective of the mutation responded to majority of the touches (Fig 5.6).

## 5.3. Discussion

Involvement of mitochondrial dysfunction has been reported in the etiology of many neurodegenerative diseases like Alzheimer's, Parkinson's and Huntington's. In Alzheimer's etiology, overproduction of amyloid ß-peptide is the cause which results in events like oxidative stress leading to perturbed mitochondrial function like $Ca^{2+}$ homeostasis, ATP production and finally damage to mitochondrial membrane due to toxic metabolites produced during the course of events initiated (Khachaturian 1994, Hirai et al 2001, Wang et al 2009). Similarly, mitochondrial dysfunction attributed due to reduced activity of mitochondrial complex I has been

reported to be associated with the etiology of Parkinson's disease (Swerdlow et al. 1996). Involvement of mitochondrial dysfunction has also been reported in psychiatric disorders like bipolar disorder and schizophrenia (Shao et al 2008). In-vitro experiments modeling epileptiform activity have reported changes in mitochondrial membrane potential and mitochondrial calcium concentration during the activity episode (Kovacs et al 2001).

All the above references cite direct or indirect involvement of mitochondria in neuronal function and activity but any quantifiable correlation between the two has never been reported. Six touch neurons of our study are specialized for sensing gentle touch stimuli and respond to the same by showing locomotion in reverse direction of the stimuli. Mitochondria number and distribution is found to be highly regulated and several factors were found to be influencing it. In the tubulin mutants, organization of specialized 15-protofilament microtubule was disrupted which resulted in highly perturbed number and distribution. Identical pattern of disturbed distribution and number of mitochondria was observed in one of the channel mutants. Behavioral response to gentle touches in these mutants was very poor, similar results were seen in other mutants like *eat-3* and *unc-16* which showed similar trend in density and distribution of mitochondria. Strains which had mild effect on either number or distribution showed behavioral trends between wild type and severely mechanosensory defective mutants. Strains which had the above factors towards the lower side also resulted in behavior deficit but not as severe as was observed in tubulin mutants. Trends in the results showed correlation between mitochondrial number and distribution. Correlation between mitochondrial number and distribution was proved to be showing statistically significant correlation with neuronal behavior.

Moreover, all the mutants responded to the first touch given to them. When we played with the inter-stimulus interval and increased it to a certain extent (10 seconds), in such cases all the mutants responded to the touches quite robustly. Result of the experiment thus indicates that mutants showing poor response results in rapid desensitization in the mechanosensory circuit which may be a reason for their poor mechanosensory response. Thus, when inter-stimulus interval is increased allowing the worm to recover from earlier stimulus, worms tends to respond to majority of the stimulus. Results of our experiments thus indicate that a strong correlation exists between mitochondria number/distribution versus behavior.

Table 5.1

| Strain | Av. Mito. No./100µm of ALM Axon length | % of aggregated (<3µm) mitochondria | Mitochondrial density in distal region of ALM axon in % | Average Response to anterior touches (in %) |
|---|---|---|---|---|
| ***dhc-1(js319)*** | 5.3 | 2.1 | 42 | 94.2 |
| ***dhc-1(or195)*** | 4.6 | 0.9 | 47 | 87.5 |
| ***jsIs609*** | 4.7 | 2.7 | 41 | 85.7 |
| ***egl-19(ad695)*** | 6.2 | 5.9 | 36 | 85.6 |
| ***egl-19(ad1006)*** | 5.0 | 6.6 | 32 | 71.9 |
| ***klc-2(km11)*** | 3.5 | 3.5 | 41 | 69.7 |
| ***mec-2(e75)*** | 5.0 | 3.0 | 35 | 65.4 |
| ***drp-1(tm1108)*** | 3.2 | 3.2 | 34 | 64.8 |
| ***mec-10(zb2551)*** | 5.7 | 4.5 | 35 | 64.7 |
| ***unc-116(e2310)*** | 2.6 | 0.3 | 42 | 62.3 |
| ***mec-12(e1605)*** | 9.5 | 10.7 | 40 | 45.3 |
| ***eat-3(ad426)*** | 6.3 | 10.2 | 31 | 44.8 |
| ***unc-16(e109)*** | 11.5 | 17.0 | 43 | 42 |
| ***mec-12(e1607)*** | 7.0 | 11.8 | 32 | 40.8 |
| ***mec-4(u253)*** | 6.3 | 8.5 | 33 | 39.1 |
| ***mec-7(e1343)*** | 6.5 | 11.0 | 29 | 30.5 |

**Table 5.1 Gentle touch behavioral response for anterior touches shown by different strains**

A series of consecutive twenty gentle touches (alternate anterior and posterior touches) were given by eyelash. Percentage of positive response to anterior touches elucidated by each mutant is tabulated. Results of atleast three independent trials with 20-30 worms per trial were averaged to obtain the final value. This table also represents the number and distribution statistics for the ALM processes for the mutants analyzed.

Table 5.2

| Strain | Av. Mito. No./100µm of PLM Axon length | % of aggregated (<3µm) mitochondria | Mitochondrial density in distal region of PLM axon in % | Average Response to posterior touches (in %) |
|---|---|---|---|---|
| ***unc-116(e2310)*** | 2.6 | 2.1 | 33 | 60.8 |
| ***jsIs609*** | 5.0 | 2.9 | 36 | 82.0 |
| ***klc-2(km11)*** | 2.2 | 3.1 | 44 | 67.7 |
| ***dhc-1(or195)*** | 4.9 | 3.3 | 37 | 77.3 |
| ***egl-19(ad695)*** | 6.0 | 3.6 | 39 | 82.5 |
| ***eat-3(ad426)*** | 5.2 | 3.7 | 41 | 37.8 |
| ***dhc-1(js319)*** | 5.8 | 4.5 | 35 | 88.6 |
| ***mec-2(e75)*** | 5.8 | 4.7 | 41 | 57.7 |
| ***mec-10(zb2551)*** | 5.0 | 5.2 | 42 | 51.6 |
| ***mec-7(e1343)*** | 4.3 | 5.4 | 40 | 14.4 |
| ***drp-1(tm1108)*** | 3.3 | 5.8 | 31 | 62.9 |
| ***mec-4(u253)*** | 4.8 | 5.9 | 38 | 19.9 |
| ***egl-19(ad1006)*** | 5.0 | 6.2 | 42 | 66.2 |
| ***unc-16(e109)*** | 8.0 | 7.6 | 35 | 25.2 |
| ***mec-12(e1605)*** | 7.7 | 7.9 | 38 | 25.6 |
| ***mec-12(e1607)*** | 5.6 | 9.0 | 30 | 18.4 |

**Table 5.2 Gentle touch behavioral responses for posterior touches shown by different strains**

A series of consecutive twenty gentle touches (alternate anterior and posterior touches) were given by eyelash. Percentage of positive response to posterior touches elucidated by each mutant is tabulated. Results of atleast three independent trials with 20-30 worms per trial were averaged to obtain the final value. This table also represents the number and distribution statistics for the PLM processes for the mutants analyze

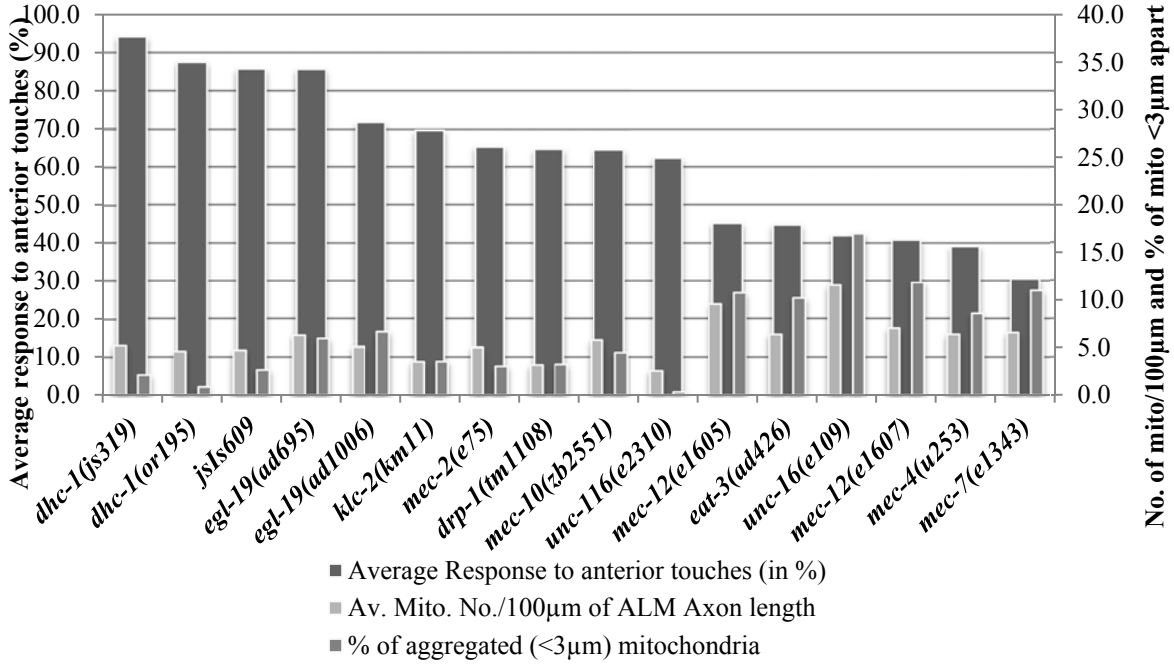


**Figure 5.1 Graph showing relationship between average responses to anterior touches versus Normalised ALM (number of mitochondria/100µm) and <3µm bin (percentage of mitochondria with intermitochondrial distance less than <3µm)**

Y-axis represents average response to anterior touches whereas secondary Y-axis represents normalised ALM and <3µm bin.

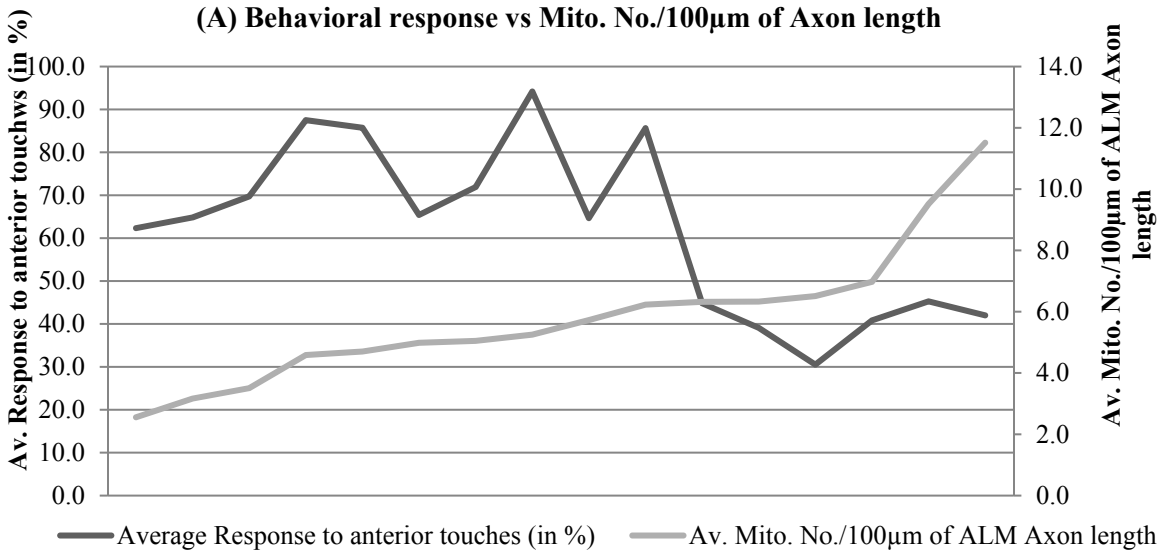

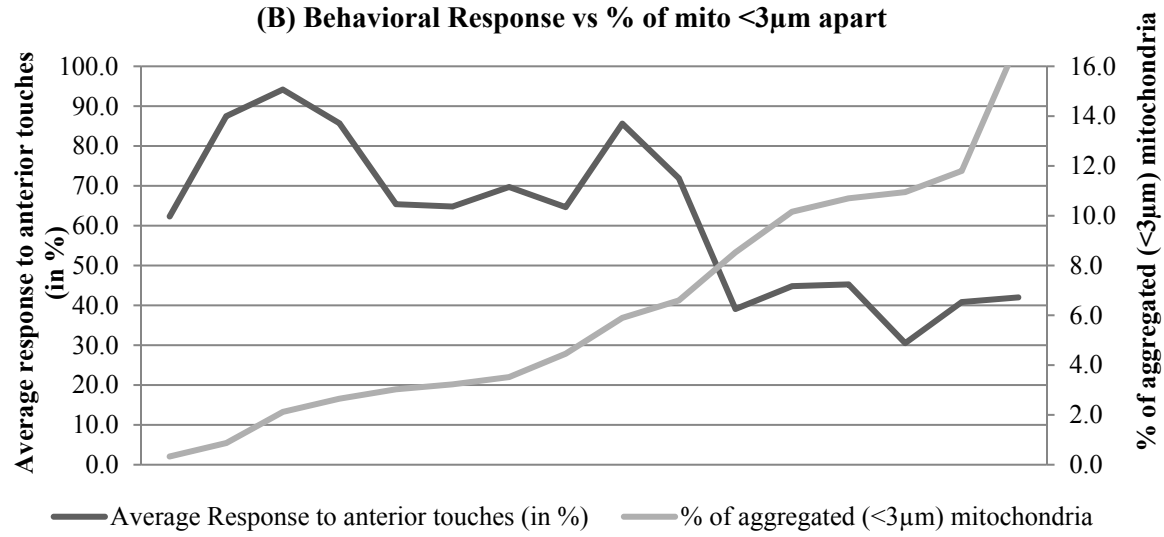


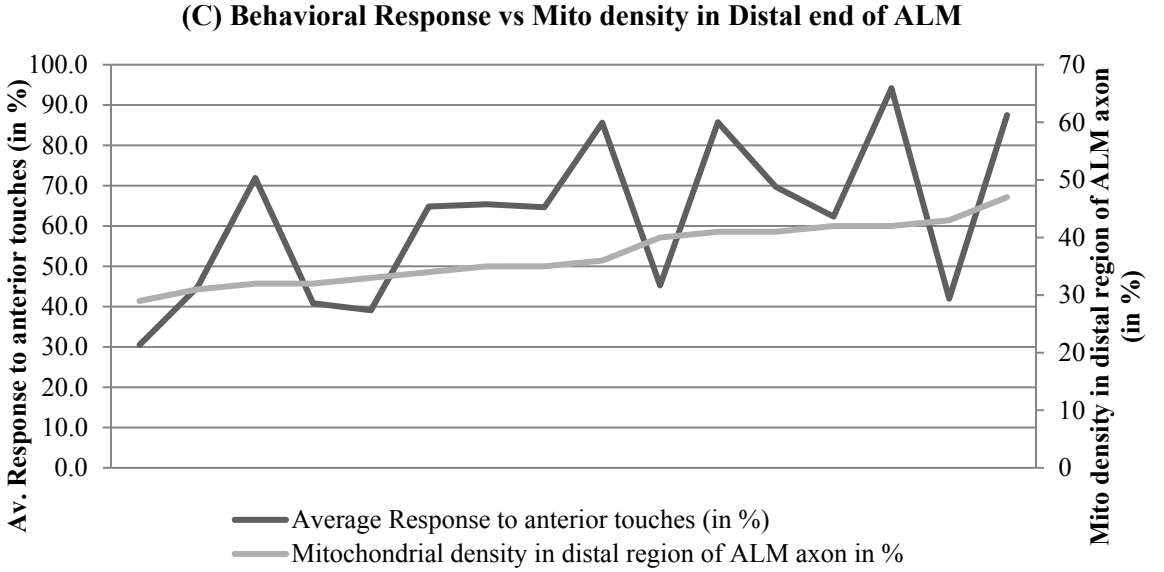


**Figure 5.2 (A-C) Graph showing relationship between the behavioral response and mitochondria number and distribution variables**

(A)Graph showing relationship between behavioral response and normalised ALM (mitochondria number /100µm of axon length).

(B) Graph showing relationship between behavioral response and <3µm bin (% of mitochondria with intermitochondrial distance less <3µm).

(C) Graph showing relationship between behavioral response and percentage of mitochondria in the distal region of ALM.

For all the graphs average response to anterior touches is plotted in Y-axis and secondary Y-axis represents the variables.

A

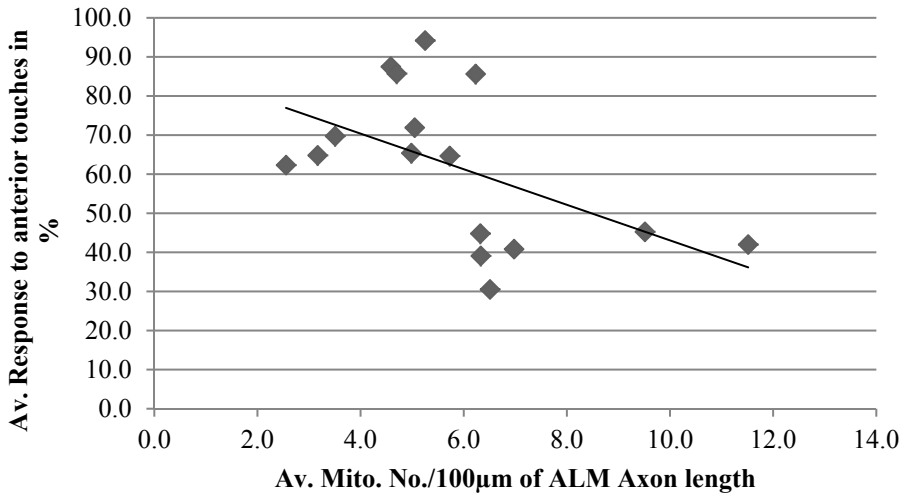


Correlation coefficient (r) = -0.51. Negative linear relationship

B

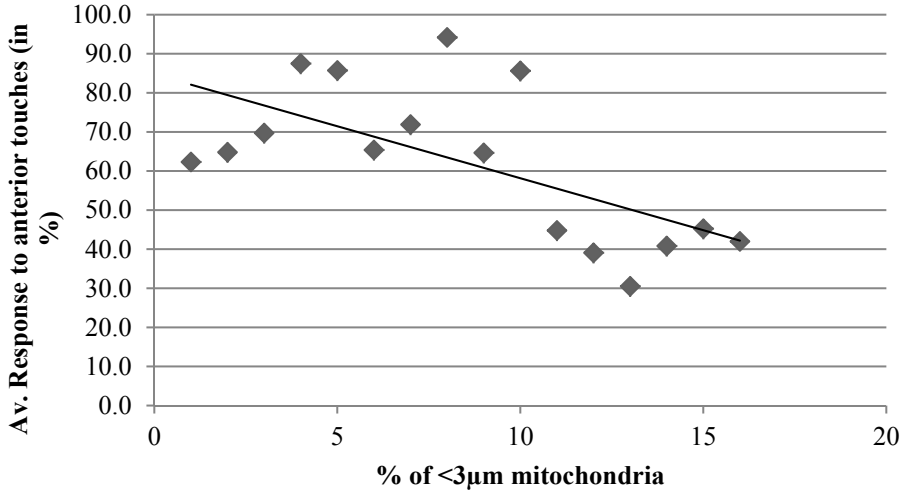


Correlation coefficient (r) = -0.77. Negative linear relationship

**Figure 5.3 (A-B) Scatter plot showing linear relationship between average response to anterior touches versus Normalised ALM (A) and <3 µm bin (B)**

(A) Average response to anterior touches is plotted on Y-axis versus normalised ALM (mitochondria number /100µm of axon length) X-axis. Value of r = -0.51 representing negative linear relationship.
(B) Average response to anterior touches plotted on Y-axis versus <3µm bin (% of mitochondria with intermitochondrial distance less <3µm) plotted in X-axis. Value of r = -0.77 representing negative linear relationship.

$$Y = 63.53 + 6.15*X1 - 5.83*X2$$

**Figure 5.4 Multiple linear regression equation**

Model predicts overall function score, Y, for behavioral response to anterior touches, X1: Normalised ALM (mitochondria number /100µm of axon length), X2: <3µm bin (% of mitochondria with intermitochondrial distance less <3µm). 63.53 is the Y intercept point whereas 6.15 and -5.83 are values of regression coefficients for X1 and X2 variables. Final model had a coefficient of determination $R^2$ as 0.70, indicating that the two variables in the model explain 70% of the variation in the response variable.

**Table 5.3**

| Variables | Coefficients(ß) | SE | 95% CI | *t Stat* | *P-value* |
|---|---|---|---|---|---|
| Intercept | 63.53 | 10.026 | 41.87 to 85.19 | 6.337 | <0.001 |
| Normalised ALM | 6.15 | 2.773 | 0.16 to 12.14 | 2.220 | <0.05 |
| <3µm Bin | -5.83 | 1.325 | -8.69 to -2.97 | -4.401 | <0.001 |

**Table 5.3 Regression parameter estimates, P values and confidence intervals for the variables normalised ALM and <3µm bin**

Normalised ALM represents mitochondria number /100µm of axon length and <3µm bin denotes % of mitochondria with intermitochondrial distance <3µm.

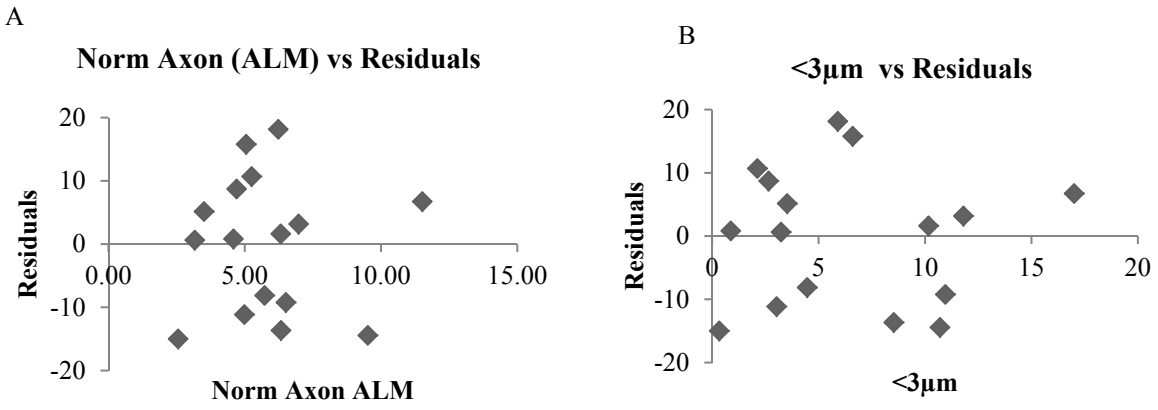


**Figure 5.5 (A-B) Graph showing plot between residuals and Normalised ALM and <3µm bin**

(A) Residuals are represented on Y-Axis and normalised ALM (mitochondria number /100µm of axon length) is represented on X-axis. Plot depicts a random pattern.
(B) Graph showing plot between residuals Y-axis and values of <3µm bin (% of mitochondria with intermitochondrial distance less <3µm) represented on X-axis. Plot depicts a random pattern.

Table 5.4

| Strain | Av. Mito. No./100µm of ALM Axon length | % of aggregated (<3µm) mitochondria | Average Response to anterior touches (in %) |
|---|---|---|---|
| ***jsIs609*** | 4.7 | 2.7 | 85.7 |
| ***unc-116(e2310)*** | 2.6 | 0.3 | 62.3 |
| ***unc-16(e109)*** | 11.5 | 17.0 | 42.0 |
| ***unc-116(e2310)/+*** | 5.18 | 3.6 | 88.9 |
| ***unc-16(e109)/+*** | 5.1 | 3.7 | 91.3 |

**Table 5-4: Mitochondria number, distribution and behavioral response for mutant/+ genotype is tabulated**

A copy of mutant gene was replaced by wild type using genetic crosses. Percentage of positive response to anterior touches elucidated by each mutant is tabulated. Results of atleast three independent trials with 20-30 worms per trial were averaged to obtain the final value. This table also represents the number and distribution statistics for the ALM processes for the mutants analyzed.

Table 5.5

| Strain | Av. Mito. No./100µm of ALM Axon length | % of aggregated (<3µm) mitochondria | Average Response to anterior touches (in %) ISI 1.5 seconds | Average response to anterior touches (in %) ISI 10 seconds |
|---|---|---|---|---|
| ***jsIs609*** | 4.7 | 2.7 | 85.7 | 99.0 |
| ***dhc-1(js319)*** | 5.3 | 2.1 | 94.2 | 99.0 |
| ***dhc-1(or195)*** | 4.6 | 0.9 | 87.5 | 98.8 |
| ***unc-116(e2310)*** | 2.6 | 0.3 | 62.3 | 87.8 |
| ***mec-7(e1343)*** | 6.5 | 11.0 | 30.5 | 80.4 |
| ***mec-12(e1607)*** | 7.0 | 11.8 | 40.8 | 76.8 |
| ***mec-12(e1605)*** | 9.5 | 10.7 | 45.3 | 92.2 |
| ***mec-4(u253)*** | 6.3 | 8.5 | 39.1 | 84.7 |
| ***mec-2(e75)*** | 5.0 | 3.0 | 65.4 | 96.4 |
| ***mec-10(zb2551)*** | 5.7 | 4.5 | 64.7 | 96.2 |
| ***eat-3(ad426)*** | 6.3 | 10.2 | 44.8 | 95.8 |

**Table 5.5: Anterior touch behavioral response for different strains at 1.5 and 10 seconds inter-stimulus interval (ISI)**

1.5 seconds ISI interval is when consecutive alternate anterior and posterior touches were given. For 10 second ISI: after first anterior touch posterior touch was given after 10 seconds. Table also represents the number and distribution statistics for the ALM processes for the mutants analyzed. Percentage of positive response to anterior touches elucidated by each mutant is tabulated. Results of atleast three independent trials with 20-30 worms per trial were averaged to obtain the final value. This table also represents the number and distribution statistics for the ALM processes for the mutants analyzed.

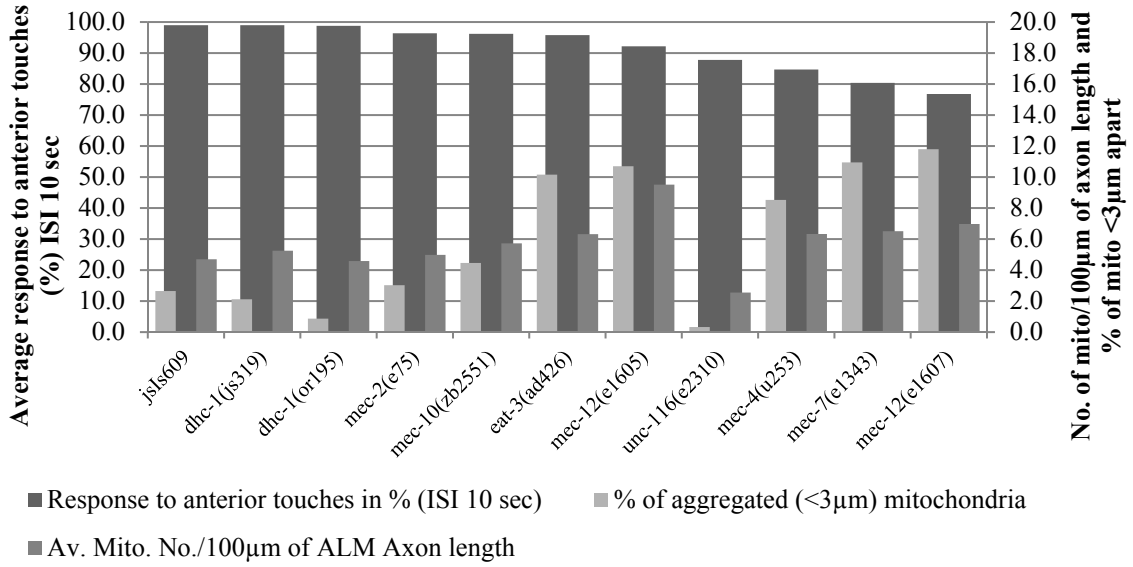


**Figure 5.6 Graph showing relationship between average responses to anterior touches at 10second inter-stimulus interval**

Average behavioral response to anterior touches is plotted in Y-axis. Values of normalised ALM (number of mitochondria/100µm) and <3µm bin (percentage of mitochondria with intermitochondrial distance <3µm) are represented in secondary Y-axis.

# Chapter 6

## Effect of Growth and Imaging Conditions on Mitochondria Number and Distribution

# 6. Effect of Growth and Imaging Conditions on Mitochondria Number and Distribution

## 6.1. Introduction

***C. elegans*** strains used to study mitochondria number and distribution were all grown in controlled conditions of temperature (22$^{o}$C) and pH. All the animals used were regularly transferred to fresh food source before they start crowding up, thus the animals used were all well fed. L1 to L4 developmental stages used for analysis were picked from non starved un-crowded plates, whereas for 1 day adult analysis L4 worms were picked from non starved non crowded plates a day before and imaged on the next day. For imaging animals were placed on 2% agarose pads made on glass slides, 50mM Sodium Azide was the anesthetic used to immobilize the worms. During normal growth during laboratory conditions as well in the environment, worms are subjected to diverse kinds of stress. Worms are subjected to food deprivation, temperature, oxidative, osmotic and pH stress. We tried looking at effect of some of these stress on mitochondria number and distribution. We also looked at effect of anesthetics used for worm immobilization on mitochondria number and distribution.

Mitochondria are the prime source for reactive oxygen species (ROS) generation during oxidative phosphorylation (Hermann et al 2008, Kowaltowski et al 2009). Respiratory complexes I and III have been reported as the prime sites responsible for generating free radicals due to incomplete reduction of oxygen (Chandel et al 2000, Lambert et al 2004). Moderate concentration of reactive oxygen species (ROS) has been reported as vital for mediating cellular signaling and thus proper cellular function (Dröge 2002, Kowaltowski et al 2009). But, at concentrations beyond threshold ROS are extremely toxic and results in damaging the molecular machinery and may result in cell death (Balaban et al 2005, Valko et al 2004). Mitochondria are the most vulnerable targets of ROS and ROS mediated mitochondrial damage has been reported as a cause for many neurodegenerative diseases and aging (Balaban et al 2005).

Various factors which results in cellular stress has been reported to result in ROS generation by mitochondria (Kuznetsov et al 2011). It has also been reported that ROS generation has profound effect on mitochondrial dynamics especially fission (Barsoum et al 2006, Pletjushkina et al 2006,

Jendrach et al 2008). It has been reported that ROS mediated triggering of mitochondrial fission events elevates ROS production (Yu et al. 2008). It has been reported that stress results in activation of machinery for assembly of fission proteins like DRP-1 in the cytoplasm and the activated protein is then shipped to mitochondria which activates fission events (Park et al 2011, Giedt et al 2012). Blocking of these fission events has been reported to have protective effect in preventing the cellular and organ damage (Ong et al 2010, Grohm et al 2012).

Starvation stress results in ROS formation this has been reported by experiments done using cell culture (Scherz-Shouval et al 2007). It has also been reported that mitochondrial respiratory chain deficiency (RCD) induces mitochondrial stress response which mimics starvation conditions (Tyynismaa et al 2010) and RCD has been reported to be causative agent for various myopathies (Suomalainen et al 1992). Increase in NAD+/NADH and AMP/ATP ratios are reported to induce fasting response resulting in mitochondrial biogenesis and oxidative ATP production. Sirtuin-I (SIRT-1) and AMPK Signaling Pathway have been reported as sensors for NAD+/NADH and AMP/ATP ratios. During RCD, protective response for fasting including mitochondrial biogenesis is blocked (Suomalainen et al 2014). Moreover, supplement of nicotinamide riboside (NR), a vitamin B3-analogue has been reported to promote fasting induced responses like mitochondrial biogenesis, oxidative ATP production and prevent myopathy (Canto et al 2012, Khan et al 2014). Another study done to see the effect of starvation on neuronal cell cultures have reported change in mitochondrial morphology from tubular to small rounded form during starvation, they have also reported that during starvation mitochondrial dynamics switch towards fusion rather than fission due to this they observe reduction in expression of fission protein DRP-1 and see aberrant increase in MFN1 (Wappler et al 2013).

Temperature stress has been reported to result in oxidative stress in many marine animals (Abele et al 1998, Abele et al 2002). Studies done in marine invertebrates have also reported temperature dependence for mitochondrial activity which decreased when subjected to temperature beyond permissive range, whereas ROS formation was reported to show consistent increase with temperature rise (Abele et al 2002). Mild heat stress has been reported to increase mitochondrial biogenesis in muscles and this happens via activation of the AMPK/SIRT1/PGC-1α pathway (Liu et al 2012).

Mitochondria are the prime source of hydrogen peroxide ($H_2O_2$) production. $H_2O_2$ has been reported to act as intracellular messenger and regulate several physiological processes such as apoptosis (Pierce et al 1991), development (Pierce et al 1991), cell proliferation (Burdon 1995; Lennon et al 1991) etc. Levels of $H_2O_2$ are tightly regulated during normal physiological conditions and deregulation of this results in disruption of cellular signaling and oxidative damage. It has been reported that non permissive exposure of $H_2O_2$ to neuronal cells results in increase in mitochondrial membrane potential (Buckman et al 2001, Bajic et al 2013), increase in intracellular calcium levels (Kart et al 2005) and depletion of ATP (Yoo et al 2005; Bajic et al 2013).

Apart from environmental conditions use of chemical anesthetics also severely effect mitochondrial structure and function. Several studies have been done to study the effect of anesthetics on mitochondrial structure and function and all the studies invariably of when anesthetics were applied i.e. prior to tissue harvesting or added to isolated mitochondria have reported to drastically affect mitochondrial structure and function. Anesthetics have been reported to affect mitochondrial function by effecting ATPase activity (Lenaz et al 1978); inhibiting Calcium homeostasis (Brnaca et al 1988, Yang et al 2008); hampering oxidative phosphorylation (Rottenberg 1983, Tsyganii et al 1984), induce apoptosis (Loop et al 2005, Wei et al 2008, Liang et al 2008). Anesthetics have also been reported to alter mitochondrial ultra-structure (Hertsens et al 1984), including altering of mitochondrial membrane composition (Lenaz et al 1978, Dekutovich et al 1986).

Some of the commonly used anesthetics to immobilize ***C. elegans*** are sodium azide (Sulston et al 1988), levamisole (Lewis et al 1980) and muscimol (Ghosh et al 2008). It has been reported that sodium azide is inhibitor of cytochrome *c* oxidase (Duncan et al 1966) as well as ATP synthase (Van der Bend et al 1985). Moreover sodium azide is also reported to inhibit axonal transport (Fang et al 2012). Levamisole is reported as an acetylcholine agonist acting at nematode muscle receptors resulting in muscle paralysis (Lewis 1980, Robertson et al 1993). Similarly, muscimol is a GABA agonist (McIntire et al 1993). We checked effect of these three anesthetics sodium azide, levamisole and muscimol respectively on mitochondria density in the axon. We also

looked at effect of starvation, temperature and $H_2O_2$ mediated oxidative stress on mitochondria number and distribution.

## 6.2. Results

### 6.2.1. Choice of Anesthetic Effected Mitochondrial Density

We checked the effect of three anesthetics sodium azide (50mM), levamisole (10mM) and muscimol (10mM) respectively on mitochondria number and distribution in ALM and PLM processes of *jsIs609* strain of ***C. elegans***. For all the stress experiments fifteen to twenty animals were analyzed for every set. Sodium azide which is a cytochrome C inhibitor and inhibitor for axonal transport of mitochondria showed least mitochondrial density in ALM (4.7mito/100µm) and PLM (5.1mito/100µm) processes. Whereas, acetylcholine agonist levamisole and GABA agonist muscimol showed significantly higher densities compared to sodium azide in both ALM and PLM processes (Fig 6.1 and Table 6.1). ALM processes showed mitochondrial density value as 7.8 mitochondria/100µm and 6.4 mitochondria/100µm for levamisole and muscimol respectively. Similarly, mitochondrial density of 7.2 mitochondria/100µm of axon length was observed in PLM process for both levamisole and muscimol (Fig 6.1 and Table 6.1).

Above results suggested that the choice of anesthetic was having considerable effect on axonal mitochondrial density. Though, mitochondrial density vas varying in different anesthetics however no observable change was observed in mitochondrial morphology under different anesthetics. So, to answer which anesthetics will closely resemble the actual mitochondrial density we attempted to analyze mitochondrial density in anesthetic free condition by using micro-fluidic device (Mondal et al 2011). L4 animals imaged in device showed average number of mitochondria as 20.1±1.44 (mean±SEM) and mitochondrial density value as 5.9±0.38 mitochondria/100µm (mean±SEM) for PLM processes (work done by Jyoti Dubey). The data set obtained in anesthetics free condition showed closest resemblance to sodium azide anesthetic.

### 6.2.2. Starvation Results in Arrest in Growth of Axon

L4 animals were washed with M9 buffer and subjected to starvation stress by transferring them to unspotted plates. Worms were subjected to starvation for 72 hours and observations were made at $0^{th}$, $12^{th}$h, $24^{th}$h, $48^{th}$h and $72^{th}$h time points under both starved and control conditions.

We imaged and analyzed ALM processes of worms subjected to starvation. We observe that in time course of 72 hours no drastic change in axon length was observed (Table 6.2 and Fig 6.2). At $0^{th}$ hour axon length observed was 323.1±9.0 (mean±SEM) µm which increased to 352.8±7.5 (mean±SEM) µm only by the end of 72th hour during starvation, whereas in control conditions it increased to 481.1±10.8 (mean±SEM) µm. Under normal conditions axon length increased approximately by 160µm in the time span of 72 hours whereas under starvation there was only 30 µm increase in axon length in this time span.

We also analysed average number of mitochondria in the ALM process. We didn't observe any change in the average mitochondrial number which remained fairly constant with a value of approximately 15 mitochondria for the entire 72 hours time span whereas under control conditions it increased from a value of 15±0.5 (mean±SEM) at $0^{th}$ hour to 22±1.0 (mean±SEM) at the end of $72^{th}$ hour (Table 6.2 and Fig 6.2). However, under both the conditions starved versus non starved mitochondrial density in axonal processes was tightly maintained with an approximate value of 4.5 mitochondria/100µm of axon length for the entire 72 hour duration (Table 6.2). We also observed the mitochondrial morphology during starvation. We didn't observe any visual change in morphology of axonal mitochondria, though cell body at later stages ($72^{th}$ hour) started losing its usual network appearance in some animals and started appearing fragmented.

### 6.2.3. Heat and Peroxide Stress Affected Mitochondrial Morphology

We exposed *jsIs609* worms to heat stress (HS) by incubating L4 animals at $37^{o}$C for 3 hours. Exposing animals to $37^{o}$C for 3 hours effected worm's health drastically and the animals appeared severely sick. Mitochondria and cell body morphology appeared severely altered (Fig 6.3). Mitochondria had totally lost its tubular structure and all mitochondria were very small and round in appearance. Some of the mitochondria even appeared vacuolar and showed jiggling movement inside the vacuole. Cell body had lost its normal filamentous appearance and it became severely fragmented (Fig 6.3). We also analysed mitochondrial density in the ALM axonal processes which showed a significant ($p<0.005$) higher density (5.7±0.24 mito/100µm) compared to control (4.7±0.2 24 mito/100µm) (Table 6.3). As density was significantly altered we also looked at intermitochondrial distance in worms exposed to HS, we observed that there was

increase (6.3%) in percentage of mitochondria which were closely aggregated (<3µm apart) in heat stress condition compared to our control (3%).

We supposed that increased mitochondrial density due to heat stress may be the reason for mitochondrial clumping. Increased mitochondrial density during HS signified that mitochondrial dynamics was altered and fission process was initiated. To check whether the HS was responsible for activating fission machinery resulting in mitochondrial fragmentation we checked percentage of big mitochondria in *drp-1(tm1108)* worms in control and HS condition. If the fission process was activated percentage of big mitochondria in *drp-1(tm1108)* mutant should also show some change. Mitochondria were classified as big if length of the tubular mitochondrial were 2µm or above. As expected percentage of bigger mitochondria were reduced in HS *Drp-1* with value of 15% compared to control conditions where 34% of the total mitochondria were classified as big.

Worms were subjected to oxidative stress by transferring L4 worms for 1 hour in 20mM hydrogen peroxide solution made in M9 buffer. Worms subjected to oxidative stress using 20mM hydrogen peroxide showed change in mitochondrial morphology which was predominantly round and small. Network like morphology of cell body was also lost and they became fragmented in appearance (Fig 6.3). We characterized the mitochondrial density in ALM axonal processes which didn't show any significant change as compared to control (Table 6.3). Effect of 1 hour oxidative stress were seen more in the morphology but didn't showed any effect on mitochondrial number.

## 6.3. Discussion

Mitochondria are involved in a variety of cellular processes and hence they are the most promising target which is affected quite readily during diverse cellular stress. We examined effect of some of these stress; which our model organism was exposed to during experimental conditions. Our results show that any kind of stress, to which animal was exposed either directly or indirectly affected mitochondria in one or the other way.

Sodium azide which is a known cytochrome C inhibitor and inhibitor for axonal transport of mitochondria showed least mitochondrial density. Mitochondrial density in presence of sodium

azide was found to be even lower than the anesthetic free condition. As worms were exposed to sodium azide only while immobilizing this short exposure thus can't abrupt mitochondrial density moreover as it has been reported to act as axonal transport inhibitor it should ideally result in ceasing the cellular machinery in its native form. Other two anesthetics GABA agonist muscimol and acetylcholine agonist levamisole showed significantly higher mitochondrial density. GABA and acetylcholine receptors are present on ***C.elegans*** body walls muscle. Both these anesthetics are not reported to effect mitochondrial function nor are expected to affect axonal transport in touch neurons so the unexpected high mitochondrial density observed remains largely misunderstood. Both these anesthetics took considerably longer time approximately around 10-15 minutes to immobilize the worm, worms showed vigorous thrashing movements in both these anesthetics prior to get immobilized. Might be vigorous thrashing movements observed may be the possible reason for increased mitochondrial density. Moreover, imaging animals in an anesthetics free condition using micro-fluidic devices has its own set of limitations as worms were immobilized by applying pressure which also results in another kind of stress for the animal. Anesthetics which are used routinely during experimentation to immobilize animals were affecting mitochondria in distinct ways which needs to be explored further.

Starvation has been reported to effect mitochondria in multiple ways by affecting its morphology as well as increasing ROS formation. In our experiment L4 worms exposed to starvation for 72 hours duration didn't alter mitochondrial density however, changes in mitochondrial morphology especially in cell body was observed at extreme time points for starvation. We found that animal coped with starvation stress by growth arrest. In normal conditions, at every 12-18 hours growth period we used to see approximately 1.5 times growth in axon length and number of mitochondria also used to increase proportionately to maintain axonal mitochondrial density. Whereas, during starvation we found growth was halted and due to this axonal length didn't increase proportionately, however mitochondrial density was maintained precisely. Our observation of growth arrest due to starvation is in conformance with the similar observations which report dietary restriction reduces normal body size (Palgunow et al 2012).

Temperature stress to 37$^{o}$C affected worm health as well as mitochondria severely. Both mitochondrial density as well as morphology was found to be effected. Mitochondria were smaller and larger in number in the axonal process. Increase in mitochondrial density and loss of mitochondrial tubular structure implied that mitochondrial dynamics was altered and fission events prevailed. Exposure to oxidative stress using peroxide also resulted in alteration of mitochondrial morphology to small fragmented form. It has been reported that during stress fission events dominates and results in fragmenting of mitochondria (Youle et al 2012). Oxidative stress is reported to trigger fission events in many cells (Pletjushkina et al 2006). So, for both temperature and oxidative stress fragmentation of mitochondria might be due to fission events. Fission event has been reported to increase ROS formation which in turn activates pathways for autophagy. It has also been reported that mitochondria exposed to oxidative stress as well as damaged mitochondria have low membrane potential which are the most vulnerable targets for autophagy (Zhang et al 2009). Fragmented mitochondria observed in our experiments might be also having altered membrane potential and might be the entities prone to autophagy.

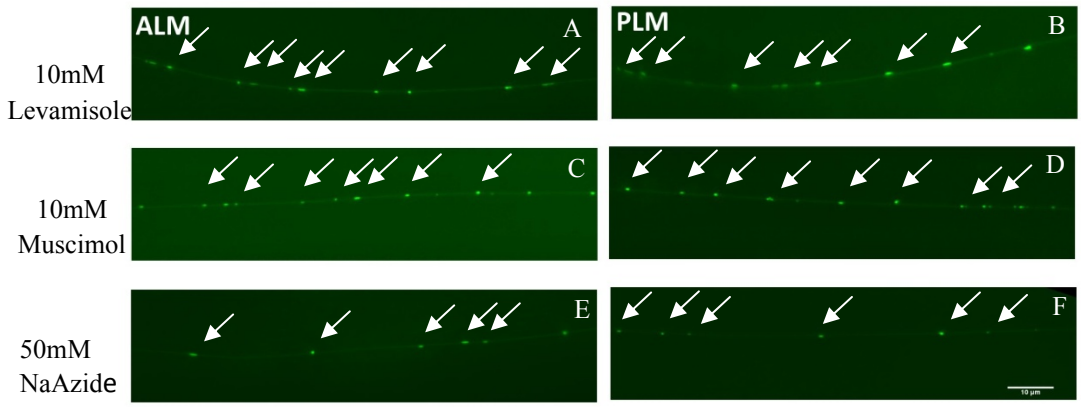


**Figure 6.1 Representative images showing variation in mitochondrial number observed under different anesthetics used for immobilizing the animal**

(A and B) Represent ALM and PLM processes imaged after use of 10mM Levamisole.
(C and D) Represent ALM and PLM processes imaged after use of 10mM Muscimol.
(E and F) Represent ALM and PLM processes imaged after use of 50mM Sodium Azide.
Mitochondria are marked by arrows. Scale bar is 10μm.15-20 animals were analyzed for each experimental set.

Table 6.1

| Anesthetic | Av. No. of mitochondria in ALM | Av. ALM Axon length (μm) | Av. Mito. No./100μm of ALM Axon length | Av. No. of mitochondria in PLM | Av. PLM Axon length (μm) | Av. Mito. No./100 μm of PLM Axon length |
|---|---|---|---|---|---|---|
| Na Azide (50mM) | 18.8±0.47 | 399.28±6.22 | 4.72±0.10 | 25.9±1.1 | 508.76±9.88 | 5.06±0.16 |
| Levamisole (10mM) | 30.67±2.52 | 393.86±6.53 | 7.82±0.71 | 37.12±1.59 | 518.94±11.81 | 7.19±0.37 |
| Muscimol (10mM) | 27.27±1.70 | 429.4±7.09 | 6.36±0.39 | 36.4±2.14 | 506.59±9.71 | 7.16±0.34 |

**Table 6.1 Mitochondrial number and density statistics in the ALM and PLM process during use of different anesthetics**

Data is represented as mean ±SEM. 15-20 animals were analyzed for each experimental set.

Table 6.2

| | Control | | | Starvation | | |
|---|---|---|---|---|---|---|
| Time Points | Av. No. of mitochondria in ALM | Av. Axon length of ALM(µm) | Av. Mito. No./100µm of ALM Axon length | Av. No. of mitochondria in ALM | Av. Axon length of ALM(µm) | Av. Mito. No./100µm of ALM Axon length |
| 0 h | 15±0.5 | 323.2±9 | 4.7±0.2 | | | |
| 12 h | 16.5±0.7 | 370.33±12.9 | 4.5±0.2 | 14±0.4 | 326.16±7.4 | 4.43±0.1 |
| 24h | 19±0.7 | 432.58±13 | 4.4±0.2 | 14.8±0.7 | 329.5±7 | 4.5±0.2 |
| 48 h | 21.14±1.0 | 470.75±12 | 4.5±0.2 | 15±0.6 | 345.1±16.8 | 4.5±0.2 |
| 72h | 22.22±1.0 | 481.11±10.8 | 4.6±0.2 | 15±0.6 | 352.8±7.5 | 4.3±0.2 |

**Table 6.2 Effect of starvation on axonal length and mitochondrial density**

L4 worms grown in control condition and under starvation were analyzed for average mitochondrial number and mitochondrial density in the neuronal process. Worms were imaged at 0$^{th}$ hour, 12$^{th}$ hour, 24$^{th}$ hour, 48$^{th}$ hour and 72$^{th}$ hour time points and results were tabulated. Result is represented as mean±SEM. 15-20 animals were analyzed for each time point.

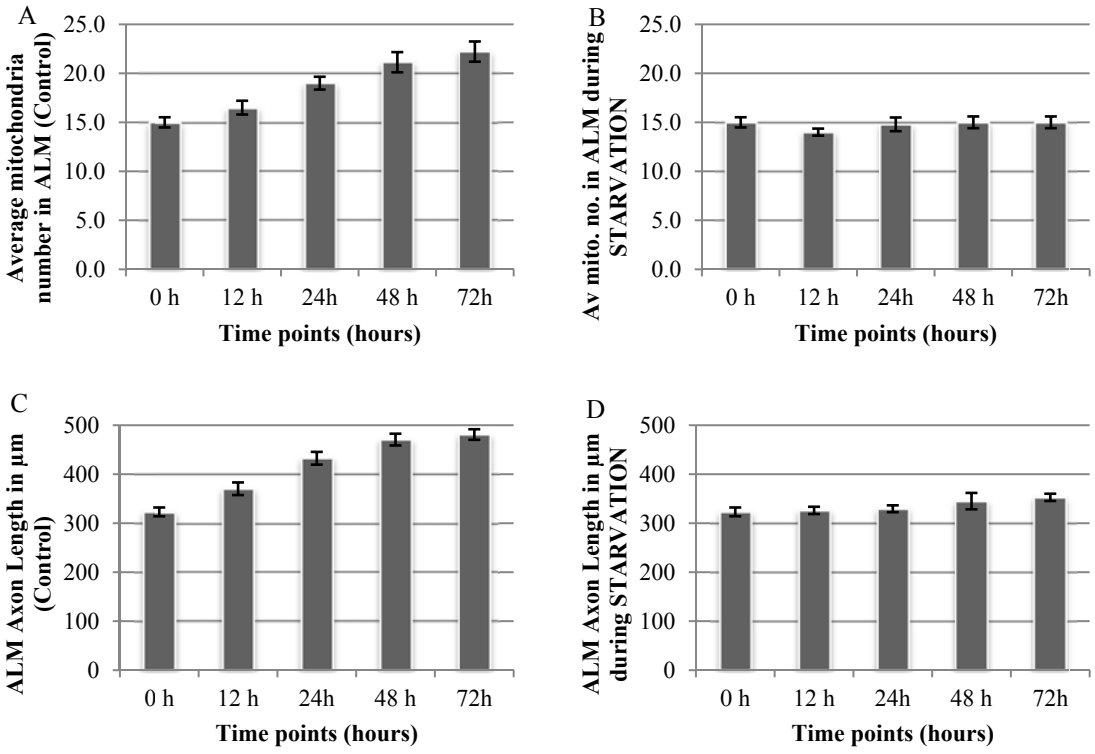


**Figure 6.2 (A-D) Represents effect of starvation on average number of mitochondria and axon length**

(A-B) Variation in average mitochondrial number observed in ALM processes imaged at 0th hour (L4 worms ), 12th hour, 24th hour, 48th hour and 72nd hour during control and starvation (food deprived) conditions.
(C –D) Represent Variation in axon length observed during similar conditions.
Data is represented as mean±SEM. 15-20 animals were analyzed for each experimental set.

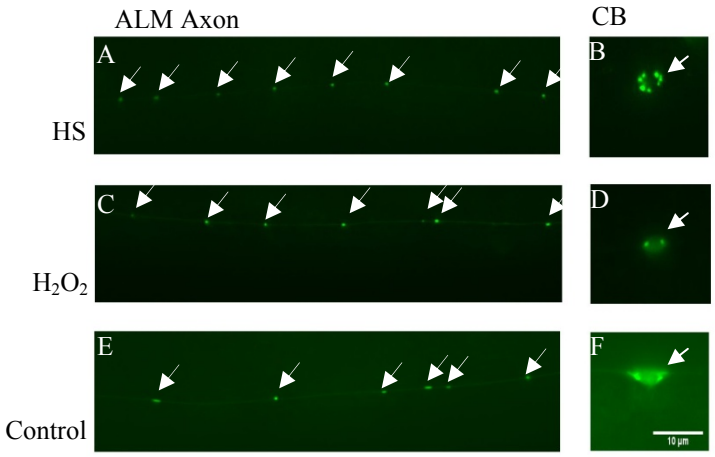


**Figure 6.3 Represents effect of heat stress (37°C /3hours) and oxidative stress (20mM $H_2O_2$/1hour) on cell body and mitochondrial morphology**

(A- B) Represents ALM axon and cell body (CB) subjected to heat stress (HS).
(C-D) represents axon and CB subjected to oxidative stress.
(E- F) Represents axon and CB morphology seen in control conditions.
Scale bar 10µm. 15-20 animals were analyzed for each experimental set.

Table 6.3

| | Av. No. of mitochondria in ALM | Av. Axon length of ALM(µm) | Av. Mito. No./100 µm of ALM Axon length |
|---|---|---|---|
| L4 (control) | 15±0.5 | 4.7±0.2 | 323.12 |
| L4 (37°C 3 hour) | 17.3±0.7 | 5.7±0.24 | 305.4±9.4 |
| L4 ($H_2O_2$ 1hour) | 15.3±0.9 | 4.9±0.21 | 315.5±9.7 |

**Table 6-3: Mitochondria number and density in response to heat and oxidative stress**

Average number of mitochondria and mitochondrial density in the ALM process for L4 worms grown in control conditions compared to those exposed to heat stress (37°C /3hours) and oxidative stress (20mM $H_2O_2$/1hour). 15-20 animals were analyzed for each experimental set. Data is represented as mean±SEM.

# Chapter 7

## UNC-16 Plays an Important Role in Determining Size of Vesicular Compartments

# 7. UNC-16 Plays an Important Role in Determining Size of Vesicular Compartments

## 7.1. Introduction

UNC-16/JIP-3 is a JNK-scaffolding protein which associates with kinases of JNK signaling pathway and promotes signaling activity. It is also known to be involved with neuronal transport machinery. Role of UNC-16 is well studied in terms of anterograde transport of cargoes in neurons (Byrd et al 2001, Brown et al 2009, Edwards et al 2013). One such major neuronal cargo whose localization gets affected in *unc-16* mutants is pre-synaptic vesicle proteins (Brown et al 2009). Transport of synaptic vesicle proteins (SVPs) is exclusively dependent on Kinesin-3 motors. UNC-104/kinesin-3 is one major motor in ***C.elegans***, which is known to transport SVPs from neuronal cell bodies (Hall et al 1991). Mutation in *unc-104* leads to accumulation of SVPs in neuronal cell body. However, *unc-16* was isolated as a suppressor of *unc-104* by Yishi Jin's group (Byrd et al 2001) as well as in our lab independently (Kumar et al 2010). We got *tb109* as one of the allele of *unc-16*, which has an early stop codon (work done by Jitendra Kumar and Bikash Choudhary).

*Unc-104;unc-16* animals showed partial restoration of SVPs transport in neuronal processes, unlike *unc-104*. We tried to understand the *unc-16* mediated suppression of *unc-104* phenotype. Work from our lab (work done by Bikash Choudhary) showed that SVPs formed in *unc-16* were of altered identity. These results were supported by behavioral, biochemical and light microscopy experiments. Through light microscopy live –imaging, we showed the presence of large structures carrying SVPs in neuronal processes of *unc-16* animals which were absent in wild type. These observations were also supported by static images, where large accumulations of SVPs tagged to GFP were observed in neuronal processes of *unc-16*. Moreover, data from our lab as well as other groups have reported presence of other vesicular bodies in neuronal processes unlike wild type. Therefore, I tried confirming the identity of these large structures observed in neuronal processes at ultra-structure level in *unc-16* by comparing them to wild type through EM imaging.

## 7.2. Results

### 7.2.1. EM Imaging Confirmed the Presence of Large Vesicular Compartments in *unc-16(tb109)*

Experiments done by Bikash Choudhary have reported that SNB-1::GFP or GFP::RAB-3 was frequently present as large sized puncta in *unc-16(tb109)* animals. These large sized puncta were found distributed throughout the neuronal processes. To confirm the identity of these large puncta I performed Electron microscopy analysis of the neuronal processes in the dorsal and ventral cord regions for both *unc-16(tb109)* and *N2* animals. Young adult animals of *unc-16(tb109)* and *N2* used for imaging and analysis were fixed by high pressure freezing (HPF) technique in Prof David Hall's laboratory (Albert Einstein College of Medicine, NY).

Nine worms were fixed and approximately ten to twenty serial sections per worms were imaged. Both dorsal and ventral cord regions were imaged and diameter of synaptic vesicles was measured using Image J. Average size of vesicles for both *unc-16(tb109)* and *N2* was quantified. Relative number of big vesicles (size > 40 nm) in both *unc-16(tb109)* and *N2* was estimated. We found that *unc-16(tb109)* animals showed significantly large vesicular profiles compared to *N2* animals (Fig 7.1 and Fig 7.2). Average diameter of vesicles was also comparatively high in *unc-16(tb109)* compared to *N2* (Fig 7.2). Results obtained by our EM analysis were found to be consistent with the recent studies from Edward et al (Edward et al 2013).

## 7.3. Discussion

EM Imaging and analysis confirmed the identity of the big punctas as SV's. Loss of function in *unc-16* has resulted in formation of aberrant SVP transport carriers which were independent of requirement of UNC-104. These SVP transport carriers are of altered size originating from neuronal cell bodies. Results thus suggest that sorting and packaging machineries involved at cell bodies might be disturbed in *unc-16* animals.

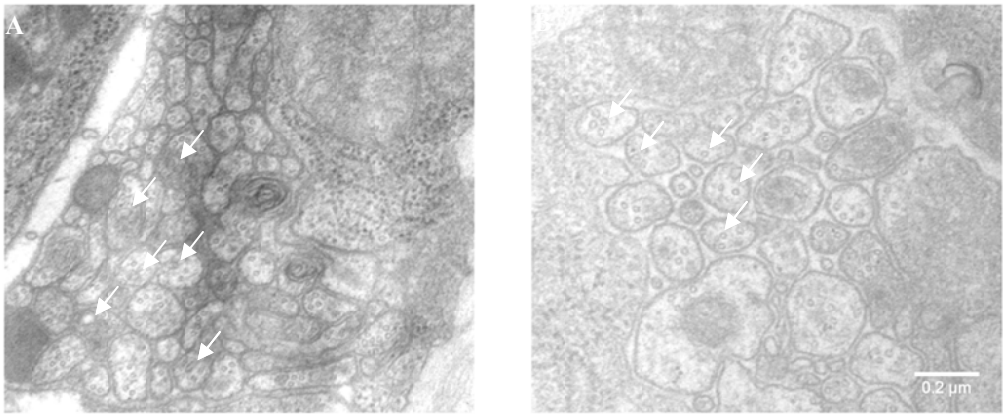


**Figure 7.1 (A-B) EM micrograph of *unc-16(tb109)* representing the presence of large vesicular compartments**

(A) Represents EM micrograph of *unc-16(tb109)* representing the presence of large vesicular compartments in neuronal cord region; vesicles are marked by arrowheads.
(B) Represents EM micrograph of *N2* showing the presence of normal vesicles which are marked by arrow heads. Scale bar is 0.2µm.

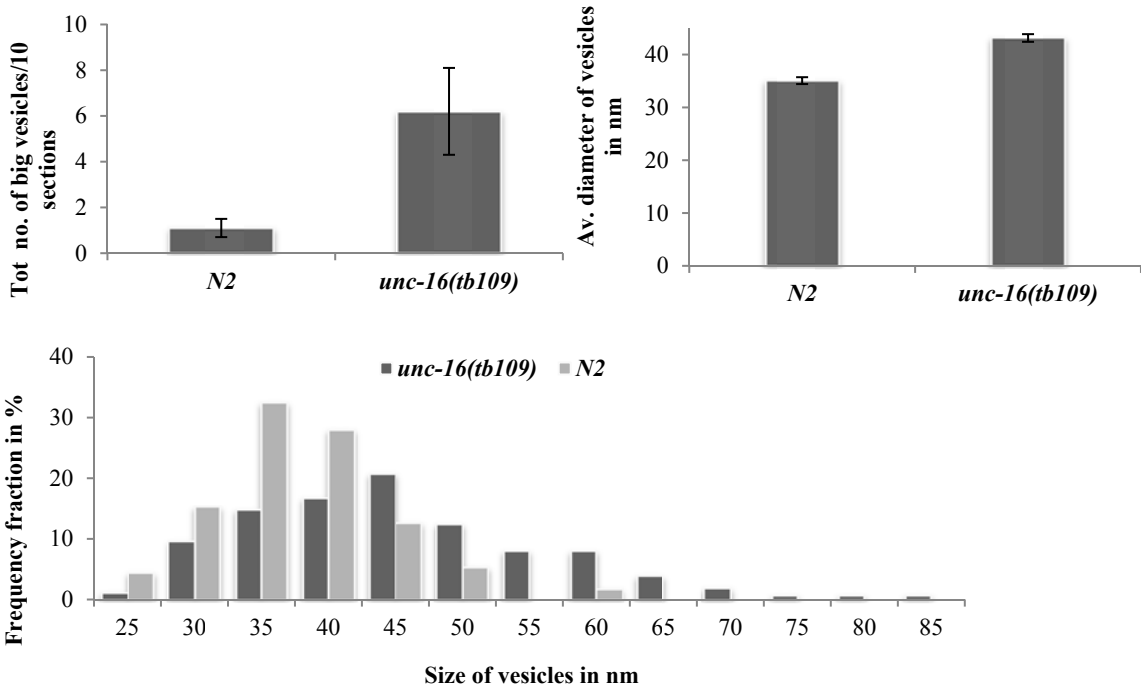


**Figure 7.2 (A-C) Graphs showing comparison of number and size of vesicles in *unc-16(tb109)* and *N2***

(A) Represents the comparison between numbers of big vesicles observed in *unc-16(tb109)* with Wild type (*N2*).
(B) Average diameter of vesicle observed in *unc-16(tb109)* was found to be higher compared to Wild type (*N2*).
(C) Frequency of larger diameter vesicles prevailed in *unc-16(tb109)* compared with Wild type

# Chapter 8

## Conclusion and Future Directions

# 8. Conclusion and Future Directions

Importance of mitochondria in neuronal cells has been studied extensively. It has also been implicated that mitochondria are required by neurons in every stage starting from axogenesis, neuronal growth, differentiation and later on for its proper functioning. Mitochondria has also been reported to take care of the localized needs in certain axonal regions and in order to do so they re-position themselves and accumulate in the vicinity of such regions. In the axon mitochondria have been reported to maintain always quality check by regulating their fission fusion dynamics.

Several studies have been done to study the mitochondrial distribution in a localized region in neurons and how this distribution varies during neuronal function. However, due to huge landscape of neurons and difficulty in tracking individual axons no single study has been done so far which studied how mitochondria are distributed in these axons. It has been proposed in several studies that mitochondrion contributes to neuronal function. But, no study has been done which directly correlates mitochondrial distribution with the function associated with a particular neuron. We aimed at studying how mitochondria were distributed in axon and whether they correlate with neuronal function.

As mitochondria are vital for neuronal function they must ideally maintain a uniform pattern so that they can take care of the neuronal needs in localized regions. First we aimed to study how mitochondria were distributed in axon at a particular time point. We also aimed to study how this distribution was regulated with axonal growth. Fast axonal transport of mitochondria on microtubule track takes place by the aid of molecular motors. Along with molecular motors and anchoring skeleton several other factors like $Ca^{2+}$ levels, mitochondrial dynamics, mitochondrial membrane potential and neuronal activity all have been associated to control mitochondrial distribution. Extent of effect of all these factors in terms of mitochondrial number, distribution and density has never been explored. We explored all these factors in terms of their effect on mitochondrial number and distribution. We also explored correlation between mitochondrial number and distribution with neuronal behavior.

We studied mitochondrial number and distribution using ***C. elegans*** six touch receptor neurons as the model. These six touch receptor neurons are specialized both anatomically as well as

functionally. These neurons have presence of specialized 15-protofilament microtubules which are instrumental in mechanosensory response for gentle touch. We used ***C. elegans*** transgenic strain *jsIs609* where GFP marks mitochondrial matrix which is expressed in six mechanosensory neurons. Mitochondria number and distribution was studied in *jsIs609* across the development. Results showed that mitochondrial density was developmentally regulated. Mitochondria had a unique non random distribution pattern which was initiated in the early developmental stages and was maintained later on. Within the axonal segments different regions also had their own set of distribution profile which was consistently maintained throughout the development.

A detailed study of all the possible factors governing mitochondrial number and distribution was undertaken. Results revealed that altering of the anterograde motor kinesin-I had a major effect on density which got reduced significantly, whereas it didn't had any significant effect on mitochondrial distribution. Retrograde motor didn't show any prominent effect on either. Effect of cytoskeleton integrity seemed to be vital for controlling both mitochondrial number and distribution. Mechanosensory mutants having mutation in either alpha or beta tubulin showed significantly higher mitochondrial density and severely altered distribution. Large percentage of mitochondria in these tubulin mutants were closely aggregated which was never observed in the control. Calcium channel mutants also showed similar but milder effects and resulted in both altered number and distribution. Mutant for mitochondrial fusion affected both number and distribution significantly whereas, fission mutant had significant effect only on density. Mutants for DEG/ENaC channels showed effect either on mitochondrial number or distribution or both. Mutants which showed altered mitochondrial density and distribution also showed altered mitochondrial distribution trends in the axonal segments.

Along with alpha and beta tubulin, there are several other genes reported to be involved in mechanosensation and mutants of them have been reported as mechanosensation defective. All the tubulin mutants had altered mitochondrial number and distribution whereas, DEG/ENaC channels mutants had altered mitochondrial number or distribution or both. Mitochondria have been reported to be vital for neuronal function. Altered number and distribution of mitochondria may be instrumental in their mechanosensation defective behavior. To confirm whether mitochondrial number and distribution correlated with neuronal behavior, behavioral assays were carried out. All the mutants showing different degree of altered number and distribution were

assayed. Results of the behavioral assay showed that percentage of behavioral response showed by the mutant was inversely proportional to the degree of its altered number and distribution. Mutants like alpha and beta tubulin which had severely altered number and distribution showed most poor behavioral response whereas mutants with mild effect showed behavior intermediate between tubulin mutants and wild type. We also analyzed the effect of inter-stimulus interval on behavioral response. Our results demonstrated that increasing inter-stimulus interval improved behavioral response in all the mutants. We also analyzed the effect of growth and imaging conditions on axonal mitochondrial morphology, number and distribution. Anesthetic chemicals used during imaging and exposure to various stress like starvation, temperature and oxidative stress during animal's growth showed different degree of effect on mitochondrial morphology, number and distribution.

Some of the specific contributions of research undertaken are as under:-

1) Mitochondria number and distribution in a single neuron throughout the development studied for the first time. Results reveal mitochondria number and distribution are regulated throughout the development.
2) All the possible factors in the context of single neurons which may contribute to mitochondrial number and distribution thoroughly examined. Results report that motor proteins contribute to mitochondrial density but did not affect mitochondrial distribution. Integrity of cytoskeleton structure had very prominent effect both on mitochondrial density as well as distribution. Other factors such as mitochondrial dynamics, mitochondrial and neuronal function affected either mitochondrial density or distribution or both.
3) Quantifiable relationship between mitochondria and neuronal behavior demonstrated. Mitochondrial density and distribution showed a statistically significant correlation with neuronal behavior.

Results of all these studies done implied that mitochondrial number and distribution was tightly regulated. Integrity of the transport machinery was most vital for regulating this distribution. Other factors like $Ca^{2+}$ levels, structure of the neuronal cell as well as the physiological conditions also showed effect on number and distribution. Number and distribution of

mitochondria was found as a signature for the neuronal behavior. In this study we analyzed only the physical presence or absence of mitochondria or its morphology, the functional state of the mitochondria was not put into account. Increase in mitochondrial density in some of the mutants might be the mechanism to overcome the compromised mitochondrial quality. This study can be further extended for the different mutants studied from mitochondrial functional angle. Functional state of mitochondria in the mutants studied can be assayed by electrophysiology based assay. Functional state of mitochondria in the axon will also give a better degree of correlation with the neuronal behavior. Some of the mutants studied such Mec-4(DEG/ENaC) channels are regulating some other processes like $Ca^{2+}$ conduction So, altering these will effect multiple pathways, which can be explored further to propose a model to link mitochondrial distribution with behavior. Factors affecting mitochondria number and its correlation with neuronal behavior have been studied in mechanosensory neurons only. The above set of results can be further validated by investigating it in other subset of neurons.

# Bibliography

Abele, D., Burlando, B., Viarengo, A., & Pörtner, H. O. (1998). Exposure to elevated temperatures and hydrogen peroxide elicits oxidative stress and antioxidant response in the Antarctic intertidal limpet Nacella concinna. *Comparative Biochemistry and Physiology Part B: Biochemistry and Molecular Biology*, *120*(2), 425-435.

Abele, D., Heise, K., Pörtner, H. O., & Puntarulo, S. (2002). Temperature-dependence of mitochondrial function and production of reactive oxygen species in the intertidal mud clam Mya arenaria. *Journal of Experimental Biology*, *205*(13), 1831-1841.

Akhmanova, A., & Steinmetz, M. O. (2008). Tracking the ends: a dynamic protein network controls the fate of microtubule tips. *Nature reviews Molecular cell biology, 9*(4), 309-322.

Alavi, M. V., Bette, S., Schimpf, S., Schuettauf, F., Schraermeyer, U., Wehrl, H. F., Ruttiger, L, Beck, S. C., Tonagel, F., Pichler, B. J., Knipper, M., Peters, T., Laufs, J & Wissinger, B. (2007). A splice site mutation in the murine Opa1 gene features pathology of autosomal dominant optic atrophy. *Brain*, *130*(4), 1029-1042.

Aldridge, A. C., Benson, L. P., Siegenthaler, M. M., Whigham, B. T., Stowers, R. S., & Hales, K. G. (2007). Roles for Drp1, a dynamin-related protein, and milton, a kinesin-associated protein, in mitochondrial segregation, unfurling and elongation during Drosophila spermatogenesis. *Fly (Austin)*, *1*(1), 38-46.

Alexander, C., Votruba, M., Pesch, U. E., Thiselton, D. L., Mayer, S., Moore, A., Rodriguez, M., Kellner, U., Leo-Kottler, B., Auburger, G., Bhattacharya, S. S. & Wissinger, B. (2000). OPA1, encoding a dynamin-related GTPase, is mutated in autosomal dominant optic atrophy linked to chromosome 3q28. *Nature genetics*, *26*(2), 211-215.

Allen, C., & Borisy, G. G. (1974). Structural polarity and directional growth of microtubules of Chlamydomonas flagella. *Journal of molecular biology, 90*(2), 381-402.

Allen, R. D., Metuzals, J., Tasaki, I, Brady, S.T. &Gilbert, S.P. (1982). Fast axonal transport in squid giant axon. *Science. 218*(4577), 1127-9.

Allen, R. D., Weiss, D. G., Hayden, J. H., Brown, D. T., Fujiwake, H., & Simpson, M. (1985). Gliding movement of and bidirectional transport along single native microtubules from squid

axoplasm: evidence for an active role of microtubules in cytoplasmic transport. *The Journal of cell biology, 100*(5), 1736-1752.

Altun, Z. F., & Hall, D. H. (2009). Introduction to *C. elegans* anatomy. *WormAtlas*.

Altun, Z.F. & Hall, D.H. (2011). Nervous system, general description. *WormAtlas*.

Amati-Bonneau, P., Valentino, M. L., Reynier, P., Gallardo, M. E., Bornstein, B., Boissière, A., Campos, Y., Rivera, H., de la Aleja, J. G., Carroccia, R., Iommarini, L., Labauge, P., Figarella-Branger, D., Marcorelles, P., Furby, A., Beauvais, K., Letournel, F., Liguori, R., La Morgia, C., Montagna, P., Liguori, M., Zanna, C., Rugolo, M., Cossarizza, A., Wissinger, B., Verny, C., Schwarzenbacher, R., Martín, M. A., Arenas, J., Ayuso, C., Garesse, R., Lenaers, G., Bonneau, D., & Carelli, V. (2008). OPA1 mutations induce mitochondrial DNA instability and optic atrophy 'plus' phenotypes. *Brain*, *131*(2), 338-351.

Amiri, M & Hollenbeck, P. J. (2008). Mitochondrial biogenesis in the axons of vertebrate peripheral neurons. *Developmental Neurobiology. 68*(11), 1348-61.

Andrews, H., White, K., Thomson, C., Edgar, J., Bates, D., Griffiths, I., Turnbull, D. & Nichols, P. (2006). Increased axonal mitochondrial activity as an adaptation to myelin deficiency in the Shiverer mouse. *Journal of neuroscience research*, *83*(8), 1533-1539.

Árnadóttir, J., O'Hagan, R., Chen, Y., Goodman, M. B., & Chalfie, M. (2011). The DEG/ENaC protein MEC-10 regulates the transduction channel complex in *Caenorhabditis elegans* touch receptor neurons. *The Journal of Neuroscience*, *31*(35), 12695-12704.

Arnoult, D., Grodet, A., Lee, Y. J., Estaquier, J., & Blackstone, C. (2005). Release of OPA1 during apoptosis participates in the rapid and complete release of cytochrome c and subsequent mitochondrial fragmentation. *Journal of Biological Chemistry*, *280*(42), 35742-35750.

Baas, P. W., & Buster, D. W. (2004). Slow axonal transport and the genesis of neuronal morphology. *Journal of neurobiology*, *58*(1), 3-17.

Bajic, A., Spasic, M., Andjus, P. R., Savic, D., & Parabucki, A. (2013). Fluctuating vs. Continuous Exposure to H2O2*:* The Effects on Mitochondrial Membrane. Potential, Intracellular Calcium, and NF-kB in Astroglia. *PLOS ONE*. *8*(10), e76383.

Balaban, R. S., Nemoto, S. & Finkel , T. (2005). Mitochondria, oxidants, and aging. *Cell. 120*(4), 483-95.

Ball, E. H., & Singer, S. J. (1982). Mitochondria are associated with microtubules and not with intermediate filaments in cultured fibroblasts. *Proceedings of the National Academy of Sciences, 79*(1), 123-126.

Bargmann, C. I., Thomas, J. H., & Horvitz, H. R. (1990). Chemosensory cell function in the behavior and development of *Caenorhabditis elegans*. In *Cold Spring Harbor symposia on quantitative biology 55*, 529-538.

Barsoum, M. J., Yuan, H., Gerencser, A. A., Liot, G., Kushnareva, Y., Gräber, S., Kovacs, I., Lee, W. D., Waggoner, J., Cui, J., White, A. D., Bossy, B., Martinou, J. C., Youle, R. J., Lipton, S. A., Ellisman, M. H., Perkins, G. A. & Bossy-Wetzel, E. (2006). Nitric oxide induced mitochondrial fission is regulated by dynamin related GTPases in neurons. *The EMBO journal*, *25*(16), 3900-3911.

Bianchi, L., & Driscoll, M. (2002). Protons at the gate: DEG/ENaC ion channels help us feel and remember. *Neuron*, *34*(3), 337-340.

Bianchi, L., Gerstbrein, B., Frøkjær-Jensen, C., Royal, D. C., Mukherjee, G., Royal, M. A., Xue, J., Schafer, W. R. & Driscoll, M. (2004). The neurotoxic MEC-4 (d) DEG/ENaC sodium channel conducts calcium: implications for necrosis initiation. *Nature neuroscience*, *7*(12), 1337-1344.

Bianchi, L. (2007). Mechanotransduction: touch and feel at the molecular level as modeled in Caenorhabditis elegans. *Molecular neurobiology, 36*(3), 254-271.

Bikle, D., Tilney, L. G., & Porter, K. R. (1966). Microtubules and pigment migration in the melanophores of Fundulus heteroclitus L. *Protoplasma, 61*(3-4*)*, 322-345.

Billups, B., & Forsythe, I. D. (2002). Presynaptic mitochondrial calcium sequestration influences transmission at mammalian central synapses. *The Journal of neuroscience*, *22*(14), 5840-5847.

Bjartmar, C, Wujek, J.R. & Trapp, B.D. (2003). Axonal loss in the pathology of MS: consequences for understanding the progressive phase of the disease. *Journal of the Neurological Sciences. 206(2)*, 165-171.

Bleazard, W., McCaffery, J. M., King, E. J., Bale, S., Mozdy, A., Tieu, Q., Nunnari, J. & Shaw, J. M. (1999). The dynamin-related GTPase Dnm1 regulates mitochondrial fission in yeast. *Nature cell biology*, *1*(5), 298-304.

Boldogh, I. R., Ramcharan, S. L., Yang, H. C., & Pon, L. A. (2004). A type V myosin (Myo2p) and a Rab-like G-protein (Ypt11p) are required for retention of newly inherited mitochondria in yeast cells during cell division. *Molecular biology of the cell, 15*(9), 3994-4002.

Bounoutas, A., Kratz, J., Emtage, L., Ma, C., Nguyen, K. C., & Chalfie, M. (2011). Microtubule depolymerization in *Caenorhabditis elegans* touch receptor neurons reduces gene expression through a p38 MAPK pathway. *Proceedings of the National Academy of Sciences, 108*(10), 3982-3987.

Bounoutas, A., O'Hagan, R., & Chalfie, M. (2009). The Multipurpose 15-Protofilament Microtubules in *C. elegans* Have Specific Roles in Mechanosensation. *Current Biology*, *19*(16), 1362-1367.

Bowman, A. B., Kamal, A., Ritchings, B. W., Philp, A. V., McGrail, M., Gindhart, J. G., & Goldstein, L. S. (2000). Kinesin-dependent axonal transport is mediated by the sunday driver (SYD) protein. *Cell*, *103*(4), 583-594.

Branca, D., Varotto, M. L, Vincenti, E. & Scutari, G (1988). The inhibition of calcium efflux from rat liver mitochondria by halogenated anesthetics. *Biochemical and Biophysical Research Communications*. *155*(2), 978-83

Brazer, S. C. W., Williams, H. P., Chappell, T. G. & Cande, W. Z. (2000). A fission yeast kinesin affects Golgi membrane recycling. *Yeast, 16*(2)*,* 149-166.

Breckenridge, D. G., Kang, B. H., Kokel, D., Mitani, S., Staehelin, L. A. & Xue, D. (2008). *Caenorhabditis elegans* drp-1 and fis-2 Regulate Distinct Cell-Death Execution Pathways Downstream of ced-3 and Independent of ced-9. *Molecular cell, 31*(4), 586-597

Breckenridge., D.G., Kang, B. H. & Xue. D. (2009). Bcl-2 proteins EGL-1 and CED-9 do not regulate mitochondrial fission or fusion in *Caenorhabditis elegans. Curr. Biol, 19* (9),768–773.

Brenner, S. (1974). The genetics of *Caenorhabditis elegans*. *Genetics, 77*(1), 71-94.

Brickley, K., & Stephenson, F. A. (2011). Trafficking kinesin protein (TRAK)-mediated transport of mitochondria in axons of hippocampal neurons. *Journal of Biological Chemistry, 286*(20), 18079-18092.

Bridgman, P. C. (2004). Myosin dependent transport in neurons. *Journal of neurobiology*, *58*(2), 164-174.

Bristow, E. A., Griffiths, P. G., Andrews, R. M., Johnson, M. A., & Turnbull, D. M. (2002). The distribution of mitochondrial activity in relation to optic nerve structure. *Archives of ophthalmology*, *120*(6), 791-796.

Broster, B. S., & Rankin, C. H. (1994). Effects of changing interstimulus interval during habituation in *Caenorhabditis elegans*. *Behavioral neuroscience*, *108*(6), 1019.

Brown, A. L., Liao, Z., & Goodman, M. B. (2008). MEC-2 and MEC-6 in the *Caenorhabditis elegans* sensory mechanotransduction complex: auxiliary subunits that enable channel activity. *The Journal of general physiology*, *131*(6), 605-616.

Brown, H. M., Van Epps, H. A., Goncharov, A., Grant, B. D., & Jin, Y. (2009). The JIP3 scaffold protein UNC-16 regulates RAB-5 dependent membrane trafficking at *C. elegans* synapses. *Developmental neurobiology*, *69*(2-3), 174-190.

Buckman, J. F., Hernández, H., Kress, G. J., Votyakova, T. V., Pal, S., & Reynolds, I. J. (2001). MitoTracker labeling in primary neuronal and astrocytic cultures: influence of mitochondrial membrane potential and oxidants. *Journal of neuroscience methods*, *104*(2), 165-176.

Burdon, R. H. (1995). Superoxide and hydrogen peroxide in relation to mammalian cell proliferation. *Free Radical Biology and Medicine*, *18*(4), 775-794.

Burns, R.G. (1991). Alpha-, beta-, and gamma tubulins: sequence comparisons and structural constraints. *Cell Motil. Cytoskeleton. 20 (3),* 181–89

Byrd, D. T., Kawasaki, M., Walcoff, M., Hisamoto, N., Matsumoto, K., & Jin, Y. (2001). UNC-16, a JNK-Signaling Scaffold Protein, Regulates Vesicle Transport in *C. elegans*. *Neuron*, *32*(5), 787-800.

Cai, Q., Gerwin, C., & Sheng, Z. H. (2005). Syntabulin-mediated anterograde transport of mitochondria along neuronal processes. *The Journal of cell biology*, *170*(6), 959-969.

Cai, Q., & Sheng, Z. H. (2009). Moving or stopping mitochondria: Miro as a traffic cop by sensing calcium. *Neuron, 61(4),* 493-496.

Canessa, C. M., Merillat, A. M., & Rossier, B. C. (1994). Membrane topology of the epithelial sodium channel in intact cells. *American Journal of Physiology-Cell Physiology*, *267*(6), C1682-C1690.

Cantó, C., Gerhart-Hines, Z., Feige, J. N., Lagouge, M., Noriega, L., Milne, J. C., Elliott, P. J., Puigserver, P., & Auwerx, J. (2009). AMPK regulates energy expenditure by modulating NAD+ metabolism and SIRT1 activity. *Nature*, *458*(7241), 1056-1060.

Canto, C., Houtkooper, R. H., Pirinen, E., Youn, D. Y., Oosterveer, M. H., Cen, Y., Fernandez-Marcos, P. J., Yamamoto, H., Andreux, P. A., Cettour-Rose, P., Gademann, K., Rinsch, C., Schoonjans, K., Sauve, A. A., & Auwerx, J. (2012). The NAD+ Precursor Nicotinamide Riboside Enhances Oxidative Metabolism and Protects against High-Fat Diet-Induced Obesity. *Cell metabolism*, *15*(6), 838-847.

Carelli, V., Ross-Cisneros, F. N., & Sadun, A. A. (2004). Mitochondrial dysfunction as a cause of optic neuropathies. *Progress in retinal and eye research*, *23(1),* 53-89.

Carter, A. P., Cho, C., Jin, L., & Vale, R. D. (2011). Crystal structure of the dynein motor domain. *Science*, *331*(6021), 1159-1165.

Chada, S. R., & Hollenbeck, P. J. (2003). Mitochondrial movement and positioning in axons: the role of growth factor signaling. *Journal of experimental biology*, *206*(12), 1985-1992.

Chada, S. R., & Hollenbeck, P. J. (2004). Nerve growth factor signaling regulates motility and docking of axonal mitochondria. *Current biology*, *14*(14), 1272-1276.

Chalfie, M. (1982). Micrutubule structure in *Caenorhabditis elegans*. *Cold Spring Harb Symp Quant Biol. 46*, 255-261

Chalfie, M., & Au, M. (1989). Genetic control of differentiation of the *Caenorhabditis elegans* touch receptor neurons. *Science*, *243*(4894), 1027-1033.

Chalfie, M., & Sulston, J. (1981). Developmental genetics of the mechanosensory neurons of *Caenorhabditis elegans*. *Developmental biology*, *82*(2), 358-370.

Chalfie, M., & Thomson, J. N. (1979). Organization of neuronal microtubules in the nematode *Caenorhabditis elegans*. *The Journal of cell biology*, *82*(1), 278-289.

Chalfie, M., & Thomson, J. N. (1982). Structural and functional diversity in the neuronal microtubules of *Caenorhabditis elegans*. *The Journal of cell biology*, *93*(1), 15-23.

Chalfie, M., & Wolinsky, E. (1990). The identification and suppression of inherited neurodegeneration in *Caenorhabditis elegans*. *1990*, 410-416.

Chalfie, M., Sulston, J. E., White, J. G., Southgate, E., Thomson, J. N., & Brenner, S. (1985). The neural circuit for touch sensitivity in *Caenorhabditis elegans. The Journal of neuroscience*, *5*(4), 956-964.

Chan, D. C. (2006). Mitochondria: dynamic organelles in disease, aging, and development. *Cell*, *125*(7), 1241-1252.

Chandel, N. S., McClintock, D.S., Feliciano, C. E., Wood, T. M., Melendez, J. A., & Schumacker, P. T. (2000). Reactive oxygen species generated at mitochondrial complex III stabilize hypoxia-inducible factor-1alpha during hypoxia: a mechanism of O2 sensing. *Journal of Biological Chemistry. 275*(33), 25130-8.

Chang, D. T. & Reynolds, I. J. (2006). Differences in mitochondrial movement and morphology in young and mature primary cortical neurons in culture. *Neuroscience*, *141*(2), 727-736.

Chang, D. T., Honick, A. S., & Reynolds, I. J. (2006). Mitochondrial trafficking to synapses in cultured primary cortical neurons. *The Journal of neuroscience*, *26*(26), 7035-7045.

Chatzigeorgiou, M., Grundy, L., Kindt, K. S., Lee, W. H., Driscoll, M., & Schafer, W. R. (2010). Spatial asymmetry in the mechanosensory phenotypes of the *C. elegans* DEG/ENaC gene mec-10. *Journal of neurophysiology, 104(6)*, 3334-3344.

Chelur, D. S., Ernstrom, G. G., Goodman, M. B., Yao, C. A., Chen, L., O'Hagan, R., & Chalfie, M. (2002). The mechanosensory protein MEC-6 is a subunit of the *C. elegans* touch-cell degenerin channel. *Nature*, *420*(6916), 669-673.

Chen, H., & Chan, D. C. (2005). Emerging functions of mammalian mitochondrial fusion and fission. *Human molecular genetics*, *14*(suppl 2), R283-R289

Chen, H & Chan, D.C. (2009). Mitochondrial dynamics–fusion, fission, movement, and mitophagy–in neurodegenerative diseases. *Human Molecular Genetics. 18*(2), R169–R176.

.Chen, H., Detmer, S. A., Ewald, A. J., Griffin, E. E., Fraser, S. E., & Chan, D. C. (2003). Mitofusins Mfn1 and Mfn2 coordinately regulate mitochondrial fusion and are essential for embryonic development. *The Journal of cell biology*, *160*(2), 189-200.

Chen, S., Owens, G. C., Crossin, K. L., & Edelman, D. B. (2007). Serotonin stimulates mitochondrial transport in hippocampal neurons. *Molecular and Cellular Neuroscience*, *36*(4), 472-483.

Chen, S., Owens, G. C., & Edelman, D. B. (2008). Dopamine inhibits mitochondrial motility in hippocampal neurons. *PLoS One*, *3*(7), e2804.

Chen, S., Tarsio, M., Kane, P. M., & Greenberg, M. L. (2008). Cardiolipin mediates cross-talk between mitochondria and the vacuole. *Molecular biology of the cell, 19(12),* 5047-5058.

Cheng, A., Wang, S., Cai, J., Rao, M. S., & Mattson, M. P. (2003). Nitric oxide acts in a positive feedback loop with BDNF to regulate neural progenitor cell proliferation and differentiation in the mammalian brain. *Developmental biology*, *258*(2), 319-333.

Collot, M., Louvard, D., & Singer, S. J. (1984). Lysosomes are associated with microtubules and not with intermediate filaments in cultured fibroblasts. *Proceedings of the National Academy of Sciences*, *81*(3), 788-792.

Colombini, M., Yeung, C. L., Tung, J., & König, T. (1987). The mitochondrial outer membrane channel, VDAC, is regulated by a synthetic polyanion. *Biochimica et Biophysica Acta (BBA)-Biomembranes, 905(2),* 279-286.

Conde, C., & Cáceres, A. (2009). Microtubule assembly, organization and dynamics in axons and dendrites. *Nature Reviews Neuroscience*, *10*(5), 319-332.

Conradt, B., & Horvitz, H. R. (1998). The *C. elegans* Protein EGL-1 Is Required for Programmed Cell Death and Interacts with the Bcl-2–like Protein CED-9. *Cell*, *93*(4), 519-529.

Crompton, M. (1999). The mitochondrial permeability transition pore and its role in cell death. *Biochem. Journal, 341*, 233-249.

Crompton, M., Virji, S., & Ward, J. M. (1998). Cyclophilin D binds strongly to complexes of the voltage dependent anion channel and the adenine nucleotide translocase to form the permeability transition pore. *European Journal of Biochemistry*, *258*(2), 729-735.

Cueva, J. G., Hsin, J., Huang, K. C., & Goodman, M. B. (2012). Posttranslational acetylation of α-tubulin constrains protofilament number in native microtubules. *Current Biology*, *22*(12), 1066-1074.

Danzer, K. M., Haasen, D., Karow, A. R., Moussaud, S., Habeck, M., Giese, A., Kretzschmar, H., Hengerer, B., & Kostka, M. (2007). Different species of α-synuclein oligomers induce calcium influx and seeding. *The Journal of Neuroscience*, *27*(34), 9220-9232.

David-Pfeuty, T., Erickson, H. P., & Pantaloni, D. (1977). Guanosinetriphosphatase activity of tubulin associated with microtubule assembly. *Proceedings of the National Academy of Sciences*, *74*(12), 5372-5376.

Davies, V. J., Hollins, A. J., Piechota, M. J., Yip, W., Davies, J. R., White, K. E., Nicols, P. P., Boulton, M. E., & Votruba, M. (2007). Opa1 deficiency in a mouse model of autosomal dominant optic atrophy impairs mitochondrial morphology, optic nerve structure and visual function. *Human Molecular Genetics*, *16*(11), 1307-1318.

De Vos, K. J., Chapman, A. L., Tennant, M. E., Manser, C., Tudor, E. L., Lau, K. F., Brownlees, J., Ackerley, S., Shaw, P. J., McLoughlin, D. M., Shaw, C. E., Leigh, P. N., Miller, C. C., &

Grierson, A. J. (2007). Familial amyotrophic lateral sclerosis-linked SOD1 mutants perturb fast axonal transport to reduce axonal mitochondria content. *Human molecular genetics*, *16*(22), 2720-2728.

Dekutovich, G. V., & Kargapolov, A. V. (1985). Characteristic effect of local anesthetics on the phospholipid composition of mitochondria. *Voprosy meditsinskoi khimii, 32(6),* 38-41.

del Peso, L., González, V. M., Inohara, N., Ellis, R. E., & Núñez, G. (2000). Disruption of the CED-9· CED-4 Complex by EGL-1 Is a Critical Step for Programmed Cell Death in *Caenorhabditis elegans*. *Journal of Biological Chemistry*, *275*(35), 27205-27211.

Delettre, C., Griffoin, J. M., Kaplan, J., Dollfus, H., Lorenz, B., Faivre, L., Lenaers, G., Belenguer, P., & Hamel, C. P. (2001). Mutation spectrum and splicing variants in the OPA1 gene. *Human genetics*, *109*(6), 584-591.

Delivani, P., Adrain, C., Taylor, R. C., Duriez, P. J., & Martin, S. J. (2006). Role for CED-9 and Egl-1 as regulators of mitochondrial fission and fusion dynamics. *Molecular cell*, *21*(6), 761-773.

Desai, A., & Mitchison, T. J. (1997). Microtubule polymerization dynamics. *Annual review of cell and developmental biology, 13*(1), 83-117.

Devi, L., Raghavendran, V., Prabhu, B. M., Avadhani, N. G., & Anandatheerthavarada, H. K. (2008). Mitochondrial import and accumulation of alphasynuclein impair complex I in human dopaminergic neuronal cultures and Parkinson disease brain. *Journal of. Biological. Chemistry*. *283*(14), 9089–9100.

DiMauro, S., & Davidzon, G. (2005). Mitochondrial DNA and disease. *Annals of medicine, 37*(3)*,* 222-232.

Dimroth, P., Kaim, G., & Matthey, U. (2000). Crucial role of the membrane potential for ATP synthesis by F (1) F (o) ATP synthases. *Journal of Experimental Biology*, *203*(1), 51-59.

Dorn, G. W., Clark, C. F., Eschenbacher, W. H., Kang, M. Y., Engelhard, J. T., Warner, S. J., Matkovich, S. J., & Jowdy, C. C. (2011). MARF and Opa1 control mitochondrial and cardiac function in Drosophila. *Circulation research*, *108*(1), 12-17.

Driscoll, M., & Chalfie, M. (1991). The mec-4 gene is a member of a family of *Caenorhabditis elegans* genes that can mutate to induce neuronal degeneration. *Nature. 349*(6310), 588-93.

Dröge, W. (2002) Free radicals in the physiological control of cell function. *Physiological Review. 82(1),* 47-95.

Du, H., & Chalfie, M. (2001). Genes regulating touch cell development in *Caenorhabditis elegans*. *Genetics*, *158*(1), 197-207.

Dugan, L. L., Sensi, S. L., Canzoniero, L. M., Handran, S. D., Rothman, S. M., Lin, T. S., Goldberg, M. P., & Choi, D. W. (1995). Mitochondrial production of reactive oxygen species in cortical neurons following exposure to N-methyl-D-aspartate. *The Journal of neuroscience*, *15*(10), 6377-6388.

Duncan, H. M., & Mackler, B. (1966). Electron Transport Systems of Yeast III: Preparation and properties of cytochrome oxidase. *Journal of Biological Chemistry*, *241*(8), 1694-1697.

Dutta, R., McDonough, J., Yin, X., Peterson, J., Chang, A., Torres, T., Gudz, T., Macklin, W. B., Lewis, D. A., Fox, R. J., Rudick, R., Mirnics, K., & Trapp, B. D. (2006). Mitochondrial dysfunction as a cause of axonal degeneration in multiple sclerosis patients. *Annals of neurology*, *59*(3), 478-489.

Edgar, J. M., McCulloch, M. C., Thomson, C. E., & Griffiths, I. R. (2008). Distribution of mitochondria along small□diameter myelinated central nervous system axons. *Journal of neuroscience research*, *86*(10), 2250-2257.

Edgley, M. L. et al. Genetic balancers (2006), WormBook, ed. The *C. elegans* Research Community, *WormBook*.

Edwards, S. L., Yu, S. C., Hoover, C. M., Phillips, B. C., Richmond, J. E., & Miller, K. G. (2013). An organelle gatekeeper function for *Caenorhabditis elegans* UNC-16 (JIP3) at the axon initial segment. *Genetics*, *194*(1), 143-161.

Espiritu, E.B., Krueger, L.E., Ye, A., & Rose L.S. (2012) CLASPs function redundantly to regulate astral microtubules in the *C. elegans* embryo. *Dev Biol, 368(2),* 242-54

Eura, Y., Ishihara, N., Yokota, S., & Mihara, K. (2003). Two mitofusin proteins, mammalian homologues of FZO, with distinct functions are both required for mitochondrial fusion. *Journal of Biochemistry*, *134*(3), 333-344.

Fabricius, C., Berthold, C. H., & Rydmark, M. (1993). Axoplasmic organelles at nodes of Ranvier. II. Occurrence and distribution in large myelinated spinal cord axons of the adult cat. *Journal of neurocytology*, *22*(11), 941-954.

Fang, C., Bourdette, D., & Banker, G. (2012). Oxidative stress inhibits axonal transport: implications for neurodegenerative diseases. *Molecular Neurodegeneration 7*(29), 1-13

Fay, D. Genetic mapping and manipulation: Chapter 1-Introduction and basics (2006), WormBook, ed. The *C. elegans* Research Community, *Wormbook.*

Figueroa-Romero, C., Iñiguez-Lluhí, J. A., Stadler, J., Chang, C. R., Arnoult, D., Keller, P. J., Hong, Y., Blackstone, C., & Feldman, E. L. (2009). SUMOylation of the mitochondrial fission protein Drp1 occurs at multiple nonconsensus sites within the B domain and is linked to its activity cycle. *The FASEB Journal*, *23*(11), 3917-3927.

Fransson, Å., Ruusala, A., & Aspenström, P. (2003). Atypical Rho GTPases have roles in mitochondrial homeostasis and apoptosis. *Journal of Biological Chemistry*, *278*(8), 6495-6502.

French, A.S. (1992). Mechanotransduction. *Annual Rev Physiology 54* 135-52

Frezza, C., Cipolat, S., Martins de Brito, O., Micaroni, M., Beznoussenko, G. V., Rudka, T., Bartoli, D., Polishuck, R. S., Danial, N. N., De Strooper, B , & Scorrano, L. (2006). OPA1 controls apoptotic cristae remodeling independently from mitochondrial fusion. *Cell*, *126*(1), 177-189.

Fridovich, I. (1975). Superoxide dismutases. *Annual review of biochemistry*, *44*(1), 147-159.

Fritz, S., Rapaport, D., Klanner, E., Neupert, W. &Westermann, B. (2001) Connection of the mitochondrial outer and inner membranes by Fzo1 is critical for organellar fusion. *Journal of Cell Biology. 152(4),* 683-92.

Fuchs, F., & Westermann, B. (2005). Role of Unc104/KIF1-related motor proteins in mitochondrial transport in *Neurospora crassa*. *Molecular biology of the cell, 16(1),* 153-161.

Fukushige, T., Siddiqui, Z. K., Chou, M., Culotti, J. G., Gogonea, C. B., Siddiqui, S. S., & Hamelin, M. (1999). MEC-12, an alpha-tubulin required for touch sensitivity in *C. elegans*. *Journal of cell science*, *112*(3), 395-403.

Furukawa, K., Matsuzaki-Kobayashi, M., Hasegawa, T., Kikuchi, A., Sugeno, N., Itoyama, Y., Wang, Y., Yao, P. J., Bushlin, I., & Takeda, A. (2006). Plasma membrane ion permeability induced by mutant alpha-synuclein contributes to the degeneration of neural cells. *Journal of Neurochemistry 97(4),* 1071–1077.

Gandre-Babbe, S., & van der Bliek, A. M. (2008). The novel tail-anchored membrane protein Mff controls mitochondrial and peroxisomal fission in mammalian cells. *Molecular biology of the cell*, *19*(6), 2402-2412.

García-Añoveros, J., & Corey, D. P. (1997). The molecules of mechanosensation. *Annual review of neuroscience*, *20*(1), 567-594.

Gautier, I., Geeraert, V., Coppey, J., Coppey-Moisan, M., & Durieux, C. (2000). A moderate but not total decrease of mitochondrial membrane potential triggers apoptosis in neuron-like cells. *Neuroreport*, *11*(13), 2953-2956.

Ghosh, R., & Emmons, S. W. (2008). Episodic swimming behavior in the nematode *C. elegans*. *Journal of Experimental Biology*, *211*(23), 3703-3711.

Giedt, R. J., Yang, C., Zweier, J. L., Matzavinos, A., & Alevriadou, B. R. (2012). Mitochondrial fission in endothelial cells after simulated ischemia/reperfusion: role of nitric oxide and reactive oxygen species. *Free Radical Biology and Medicine*, *52*(2), 348-356.

Glater, E. E., Megeath, L. J., Stowers, R. S., & Schwarz, T. L. (2006). Axonal transport of mitochondria requires milton to recruit kinesin heavy chain and is light chain independent. *The Journal of cell biology, 173*(4), 545-557.

Goedert, M., & Spillantini, M. G. (2006). A century of Alzheimer's disease. *Science*, *314*(5800), 777-781.

Goedert, M., Baur, C. P., Ahringer, J., Jakes, R., Hasegawa, M., Spillantini, M. G., Smith, M. J., & Hill, F. (1996). PTL-1, a microtubule-associated protein with tau-like repeats from the nematode *Caenorhabditis elegans*. *Journal of cell science*, *109*(11), 2661-2672.

Gomes, L. C., Di Benedetto, G., & Scorrano, L. (2011). During autophagy mitochondria elongate, are spared from degradation and sustain cell viability. *Nature cell biology*, *13*(5), 589-598.

Goodman, M. B., & Schwarz, E. M. (2003). Transducing touch in *Caenorhabditis elegans*. *Annual review of physiology*, *65*(1), 429-452.

Goodman, M. B., Ernstrom, G. G., Chelur, D. S., O'Hagan, R., Yao, C. A., & Chalfie, M. (2002). MEC-2 regulates *C. elegans* DEG/ENaC channels needed for mechanosensation. *Nature*, *415*(6875), 1039-1042.

Goodman, M.B. Mechanosensation (2006), WormBook, ed. The *C. elegans* Research Community, *WormBook*.

Gordon, P., Hingula, L., Krasny, M. L., Swienckowski, J. L., Pokrywka, N. J., & Raley-Susman, K. M. (2008). The invertebrate microtubule-associated protein PTL-1 functions in mechanosensation and development in *Caenorhabditis elegans*. *Development genes and evolution*, *218*(10), 541-551.

Górska Andrzejak, J., Stowers, R. S., Borycz, J., Kostyleva, R., Schwarz, T. L., & Meinertzhagen, I. A. (2003). Mitochondria are redistributed in Drosophila photoreceptors lacking Milton, a kinesin associated protein. *Journal of Comparative Neurology*, *463*(4), 372-388.

Gotow, T, Miyaguchi, K & Hashimoto, P. H. (1991). Cytoplasmic architecture of the axon terminal: filamentous strands specifically associated with synaptic vesicles. *Neuroscience. 40*(2), 587-98.

Grafstein, B., & D. S. Forman. (1980). Intracellular transport in neurons. *Physiol. Rev. 60* (4), 1167-1283.

Gray, M. W. (1992). The endosymbiont hypothesis revisited. *Int. Rev. Cytol, 141*(233-357).

Gray, M. W., & Doolittle, W. F. (1982). Has the endosymbiont hypothesis been proven? *Microbiological Reviews*, *46*(1), 1.

Greene, J. C., Whitworth, A. J., Kuo, I., Andrews, L. A., Feany, M. B., & Pallanck, L. J. (2003). Mitochondrial pathology and apoptotic muscle degeneration in Drosophila parkin mutants. *Proceedings of the National Academy of Sciences*, *100*(7), 4078-4083.

Griffin, E. E., & Chan, D. C. (2006). Domain interactions within Fzo1 oligomers are essential for mitochondrial fusion. *Journal of Biological Chemistry*, *281*(24), 16599-16606.

Griffin, E. E., Graumann, J., & Chan, D. C. (2005). The WD40 protein Caf4p is a component of the mitochondrial fission machinery and recruits Dnm1p to mitochondria. *The Journal of cell biology*, *170*(2), 237-248.

Grohm, J., Kim, S. W., Mamrak, U., Tobaben, S., Cassidy-Stone, A., Nunnari, J., Plesnila, N, & Culmsee, C. (2012). Inhibition of Drp1 provides neuroprotection in vitro and in vivo. *Cell Death & Differentiation*, *19*(9), 1446-1458.

Grosskreutz, J., Van Den Bosch, L., & Keller, B. U. (2010). Calcium dysregulation in amyotrophic lateral sclerosis. *Cell calcium*, *47*(2), 165-174.

Gu, G., Caldwell, G. A., & Chalfie, M. (1996). Genetic interactions affecting touch sensitivity in *Caenorhabditis elegans*. *Proceedings of the National Academy of Sciences*, *93*(13), 6577-6582.

Gumienny, T. L., MacNeil, L. T., Wang, H., de Bono, M., Wrana, J. L., & Padgett, R. W. (2007). Glypican LON-2 is a conserved negative regulator of BMP-like signaling in *Caenorhabditis elegans*. *Current Biology. 17(2),* 159-64.

Guo, X., Macleod, G. T., Wellington, A., Hu, F., Panchumarthi, S., Schoenfield, M., Marin, L., Charlton, M. P., Atwood, H. L., & Zinsmaier, K. E. (2005). The GTPase dMiro is Required for Axonal Transport of Mitochondria to Drosophila Synapses. *Neuron*, *47*(3), 379-393.

Hales, K. G., & Fuller, M. T. (1997). Developmentally regulated mitochondrial fusion mediated by a conserved, novel, predicted GTPase. *Cell*, *90*(1), 121-129.

Hall, D. H., & Hedgecock, E. M. (1991). Kinesin-related gene unc-104 is required for axonal transport of synaptic vesicles in *C. elegans*. *Cell*, *65*(5), 837-847.

Han, X. J., Lu, Y. F., Li, S. A., Kaitsuka, T., Sato, Y., Tomizawa, K., Nairn, A.C., Takei, K., Matsui, H., & Matsushita, M. (2008). CaM kinase Iα–induced phosphorylation of Drp1 regulates mitochondrial morphology. *The Journal of cell biology*, *182*(3), 573-585.

Hartline, D. K, & Colman, D. R. (2007). Rapid conduction and the evolution of giant axons and myelinated fibers. *Current Biology.17* (1), R29–35.

Hartline, D. K. (2008).What is myelin? *Neuron Glia Biology. 4*(2*),* 153-63.

Hashimoto, M., Rockenstein, E., Crews, L., & Masliah, E. (2003). Role of protein aggregation in mitochondrial dysfunction and neurodegeneration in Alzheimer's and Parkinson's diseases. *Neuromolecular medicine*, *4*(1-2), 21-35.

Heggeness, M. H., Simon, M., & Singer, S. J. (1978). Association of mitochondria with microtubules in cultured cells. *Proceedings of the National Academy of Sciences, 75(8),* 3863-3866.

Herlan, M., Bornhövd, C., Hell, K., Neupert, W., & Reichert, A. S. (2004). Alternative topogenesis of Mgm1 and mitochondrial morphology depend on ATP and a functional import motor. *The Journal of cell biology*, *165*(2), 167-173.

Hermann, G. J., Thatcher, J. W., Mills, J. P., Hales, K. G., Fuller, M. T., Nunnari, J., & Shaw, J. M. (1998). Mitochondrial fusion in yeast requires the transmembrane GTPase Fzo1p. *The Journal of cell biology*, *143*(2), 359-373.

Hermann, M., Kuznetsov, A., Maglione, M., Smigelskaite, J., Margreiter, R., & Troppmair, J. (2008). Cytoplasmic signaling in the control of mitochondrial uproar? *Cell Communication and Signaling*, *6*(1), 4.

Hertsens, R., Jacob, W., & Van Bogaert, A. (1984). Effect of hypnorm, chloralosane and pentobarbital on the ultrastructure of the inner membrane of rat heart mitochondria. *Biochimica et Biophysica Acta (BBA)-Biomembranes, 769(2),* 411-418.

Hirai, K., Aliev, G., Nunomura, A., Fujioka, H., Russell, R. L., Atwood, C. S., Johnson, A. B., Kress, Y., Vinters, H. V., Tabaton, M., Shimohama, S., Cash, A. D., Siedlak, S. L., Harris, P. L., Jones, P. K., Petersen, R. B., Perry, G., & Smith, M. A. (2001). Mitochondrial abnormalities in Alzheimer's disease. *The Journal of Neuroscience*, *21*(9), 3017-3023.

Hirokawa, N. (1994). Microtubule organization and dynamics dependent on microtubule-associated proteins. *Current opinion in cell biology*, *6*(1), 74-81.

Hirokawa, N., & Takemura, R. (2004). Kinesin superfamily proteins and their various functions and dynamics. *Experimental cell research*, *301*(1), 50-59.

Hirokawa, N., & Yorifuji, H. (1986). Cytoskeletal architecture of reactivated crayfish axons, with special reference to crossbridges among microtubules and between microtubules and membrane organelles. *Cell motility and the cytoskeleton, 6(5),* 458-468.

Hirokawa, N., Niwa, S., & Tanaka, Y. (2010). Molecular motors in neurons: transport mechanisms and roles in brain function, development, and disease. *Neuron*, *68*(4), 610-638.

Hirokawa, N., Pfister, K. K., Yorifuji, H., Wagner, M. C., Brady, S. T., & Bloom, G. S. (1989). Submolecular domains of bovine brain kinesin identified by electron microscopy and monoclonal antibody decoration. *Cell, 56(5),* 867-878.

Hirokawa, N., Sato-Yoshitake, R., Kobayashi, N., Pfister, K. K., Bloom, G. S., & Brady, S. T. (1991). Kinesin associates with anterogradely transported membranous organelles in vivo. *The Journal of cell biology, 114(2),* 295-302.

Hogan, V., White, K., Edgar, J., McGill, A., Karim, S., McLaughlin, M., Griffiths, I., Turnbull, D., & Nichols, P. (2009). Increase in mitochondrial density within axons and supporting cells in response to demyelination in the Plp1 mouse model. *Journal of neuroscience research*, *87*(2), 452-459.

Hollenbeck, P. J. (1996). The pattern and mechanism of mitochondrial transport in axons. *Front Biosci*, *1*, d91-d102.

Hollenbeck, P. J., & Saxton, W. M. (2005). The axonal transport of mitochondria. *Journal of cell science, 118(23)*, 5411-5419.

Holmes, K. C. (2008). Myosin structure. In *Myosins* 35-5. Springer Netherlands.

Hoppins, S., & Nunnari, J. (2009). The molecular mechanism of mitochondrial fusion. *Biochimica et Biophysica Acta (BBA)-Molecular Cell Research*, *1793*(1), 20-26.

Huang, M., & Chalfie, M. (1994). Gene interactions affecting mechanosensory transduction in *Caenorhabditis elegans*. *Nature*, *367*(6462), 467-470.

Huang, M., Gu, G., Ferguson, E. L., & Chalfie, M. (1995). A stomatin-like protein necessary for mechanosensation in *C. elegans*. *Nature*, *378*(6554), 292-295.

Hueston, J. L., Herren, G. P., Cueva, J. G., Buechner, M., Lundquist, E. A., Goodman, M. B., & Suprenant, K. A. (2008). The *C. elegans* EMAP-like protein, ELP-1 is required for touch sensation and associates with microtubules and adhesion complexes. *BMC developmental biology*, *8*(1), 110.

Hurd, D. D., & Saxton, W. M. (1996). Kinesin mutations cause motor neuron disease phenotypes by disrupting fast axonal transport in Drosophila. *Genetics*, 144(3), 1075-1085.

Hwa, J. J., Hiller, M. A., Fuller, M. T., & Santel, A. (2002). Differential expression of the Drosophila mitofusin genes fuzzy onions fzo and dmfn *Mechanisms of development*, *116*(1), 213-216.

Ichishita, R., Tanaka, K., Sugiura, Y., Sayano, T., Mihara, K., & Oka, T. (2008). An RNAi screen for mitochondrial proteins required to maintain the morphology of the organelle in *Caenorhabditis elegans*. *Journal of biochemistry*, *143*(4), 449-454.

Imai, S., Armstrong, C.M., Kaeberlein, M. & Guarente, L. (2000) Transcriptional silencing and longevity protein Sir2 is an NAD-dependent histone deacetylase. *Nature. 403 (6771),* 795 – 800

Itoh, T., Tohe, A., & Matsui, Y. (2004). Mmr1p is a mitochondrial factor for Myo2p dependent inheritance of mitochondria in the budding yeast. *The EMBO journal*, *23*(13), 2520-2530.

Jagasia, R., Grote, P., Westermann, B., & Conradt, B. (2005). DRP-1-mediated mitochondrial fragmentation during EGL-1-induced cell death in *C. elegans*. *Nature, 433(7027),* 754-760.

Johnson, D., & Nehrke, K. (2010). Mitochondrial fragmentation leads to intracellular acidification in *Caenorhabditis elegans* and mammalian cells. *Molecular biology of the cell*, *21*(13), 2191-2201.

Kabzinska, D., Drac, H., Rowinska-Marcinska, K., Fidzianska, A., Kochanski, A., & Hausmanowa-Petrusewicz, I. (2006). Early onset Charcot-Marie-Tooth disease caused by a homozygous Leu239Phe mutation in the GDAP1 gene. *Acta myologica. 25*(1), 34-37.

Kanazawa, T., Zappaterra, M. D., Hasegawa, A., Wright, A. P., Newman-Smith, E. D., Buttle, K. F., McDonald, K., Mannella, C. A., & van der Bliek, A. M. (2008). The *C. elegans* Opa1 homologue EAT-3 is essential for resistance to free radicals. *PLoS genetics*, 4(2), e1000022.

Kang, J. S., Tian, J. H., Pan, P. Y., Zald, P., Li, C., Deng, C., & Sheng, Z. H. (2008). Docking of axonal mitochondria by syntaphilin controls their mobility and affects short-term facilitation. *Cell, 132(1),* 137-148.

Kann, O., Kovács, R., & Heinemann, U. (2003). Metabotropic receptor-mediated $Ca^{2+}$ signaling elevates mitochondrial $Ca^{2+}$ and stimulates oxidative metabolism in hippocampal slice cultures. *Journal of neurophysiology*, *90*(2), 613-621.

Kaplan, J. M., & Horvitz, H. R. (1993). A dual mechanosensory and chemosensory neuron in *Caenorhabditis elegans*. *Proceedings of the National Academy of Sciences*, *90*(6), 2227-2231.

Karbowski, M., Spodnik, J. H., Teranishi, M. A., Wozniak, M., Nishizawa, Y., Usukura, J., & Wakabayashi, T. (2001). Opposite effects of microtubule-stabilizing and microtubule-destabilizing drugs on biogenesis of mitochondria in mammalian cells. *Journal of Cell Science*, *114*(2), 281-291.

Kardon, J. R., Reck-Peterson, S. L., & Vale, R. D. (2009). Regulation of the processivity and intracellular localization of *Saccharomyces cerevisiae* dynein by dynactin. *Proceedings of the National Academy of Sciences, 106*(14), 5669-5674.

Karren, M. A., Coonrod, E. M., Anderson, T. K., & Shaw, J. M. (2005). The role of Fis1p–Mdv1p interactions in mitochondrial fission complex assembly. *The Journal of cell biology*, *171*(2), 291-301.

Keeney, P. M., Xie, J., Capaldi, R. A., & Bennett, J. P. (2006). Parkinson's disease brain mitochondrial complex I has oxidatively damaged subunits and is functionally impaired and misassembled. *The Journal of neuroscience*, *26*(19), 5256-5264.

Kellenberger, S., & Schild, L. (2002). Epithelial sodium channel/degenerin family of ion channels: a variety of functions for a shared structure. *Physiological reviews*, *82*(3), 735-767.

Keller, J. N., Kindy, M. S., Holtsberg, F. W., Clair, D. K. S., Yen, H. C., Germeyer, A., Steiner, S. M., Bruce-Keller, A. J., Hutchins, J. B , & Mattson, M. P. (1998). Mitochondrial manganese superoxide dismutase prevents neural apoptosis and reduces ischemic brain injury: suppression of peroxynitrite production, lipid peroxidation, and mitochondrial dysfunction. *The Journal of neuroscience*, *18*(2), 687-697.

Kerr, R., Lev-Ram, V., Baird, G., Vincent, P., Tsien, R. Y., & Schafer, W. R. (2000). Optical Imaging of Calcium Transients in Neurons and Pharyngeal Muscle of *C. elegans Neuron, 26(3),* 583-594.

Khachaturian, Z. S. (1994). Calcium Hypothesis of Alzheimer's Disease and Brain Aginga. *Annals of the New York Academy of Sciences*, *747*(1), 1-11.

Khan, N. A., Auranen, M., Paetau, I., Pirinen, E., & Euro, L (2014). Effective treatment of mitochondrial myopathy by nicotinamide riboside, a vitamin B3. *EMBO Molecular Medicine 2014 (Epub)*

Kijima, K., Numakura, C., Izumino, H., Umetsu, K., Nezu, A., Shiiki, T., Ogawa, M., Ishizaki, Y., Kitamura, T., Shozawa, Y., & Hayasaka, K. (2005). Mitochondrial GTPase mitofusin 2 mutation in Charcot–Marie–Tooth neuropathy type 2A. *Human genetics*, *116*(1-2), 23-27.

King, S. J., & Schroer, T. A. (2000). Dynactin increases the processivity of the cytoplasmic dynein motor. *Nature Cell Biology, 2*(1), 20-24.

Kirkland, R. A., & Franklin, J. L. (2003). Bax, reactive oxygen, and cytochrome c release in neuronal apoptosis. *Antioxidants and Redox Signaling*, *5*(5), 589-596.

Kirszenblat, L., Neumann, B., Coakley, S., & Hilliard, M. A. (2013). A dominant mutation in mec-7/β-tubulin affects axon development and regeneration in *Caenorhabditis elegans* neurons. *Molecular biology of the cell*, *24*(3), 285-296.

Kiryu-Seo, S., Ohno, N., Kidd, G. J., Komuro, H., & Trapp, B. D. (2010). Demyelination increases axonal stationary mitochondrial size and the speed of axonal mitochondrial transport. *The Journal of Neuroscience*, *30*(19), 6658-6666.

Kjer, P., Jensen, O. A., & Klinken, L. (1983). Histopathology of eye, optic nerve and brain in a case of dominant optic atrophy. *Acta ophthalmologica*, *61*(2), 300-312.

Knott, A. B., Perkins, G., Schwarzenbacher, R., & Bossy-Wetzel, E. (2008). Mitochondrial fragmentation in neurodegeneration. *Nature Reviews Neuroscience*, *9*(7), 505-518.

Komary, Z., Tretter, L., & Adam-Vizi, V. (2010). Membrane potential-related effect of calcium on reactive oxygen species generation in isolated brain mitochondria. *Biochimica et Biophysica Acta (BBA)-Bioenergetics*, *1797*(6), 922-928.

Koshiba, T., Detmer, S. A., Kaiser, J. T., Chen, H., McCaffery, J. M., & Chan, D. C. (2004). Structural basis of mitochondrial tethering by mitofusin complexes. *Science*, *305*(5685), 858-862.

Kovács, R., Kardos, J., Heinemann, U., & Kann, O. (2005). Mitochondrial calcium ion and membrane potential transients follow the pattern of epileptiform discharges in hippocampal slice cultures. *The Journal of neuroscience*, *25*(17), 4260-4269.

Kovacs, R., Schuchmann, S., Gabriel, S., Kardos, J., & Heinemann, U. (2001). $Ca^{2+}$ signalling and changes of mitochondrial function during low $Mg^{2+}$ induced epileptiform activity in organotypic hippocampal slice cultures. *European Journal of Neuroscience*, *13*(7), 1311-1319.

Kowaltowski, A. J., de Souza-Pinto, N. C., Castilho, R. F. &Vercesi, A.E. (2009). Mitochondria and reactive oxygen species. *Free Radical Biology and Medicine. 15:47*(4), 333-43.

Kraft, R., Grimm, C., Grosse, K., Hoffmann, A., Sauerbruch, S., Kettenmann, H., Schultz, G., & Harteneck, C. (2004). Hydrogen peroxide and ADP-ribose induce TRPM2-mediated calcium

influx and cation currents in microglia. *American Journal of Physiology-Cell Physiology*, *286*(1), C129-C137.

Krauss, S. (2001). Mitochondria: Structure and role in respiration. *eLS*.

Kruman, I. I., Pedersen, W. A., Springer, J. E., & Mattson, M. P. (1999). ALS-linked Cu/Zn–SOD mutation increases vulnerability of motor neurons to excitotoxicity by a mechanism involving increased oxidative stress and perturbed calcium homeostasis. *Experimental neurology*, *160*(1), 28-39.

Kujoth, G. C., Hiona, A., Pugh, T. D., Someya, S., Panzer, K., Wohlgemuth, S. E., Hofer, T., Seo, A. Y., Sullivan, R., Jobling, W. A., Morrow, J. D., Van Remmen, H., Sedivy, J. M., Yamasoba, T., Tanokura, M., Weindruch, R., Leeuwenburgh, C., & Prolla, T. A. (2005). Mitochondrial DNA mutations, oxidative stress, and apoptosis in mammalian aging. *Science*, *309*(5733), 481-484.

Kumar, J., Choudhary, B. C., Metpally, R., Zheng, Q., Nonet, M. L., Ramanathan, S., Klopfenstein, D. R & Koushika, S. P. (2010). The *Caenorhabditis elegans* Kinesin-3 motor UNC-104/KIF1A is degraded upon loss of specific binding to cargo. *PLoS genetics*, *6*(11), e1001200.

Kuznetsov, A. V., Kehrer, I., Kozlov, A. V., Haller, M., Redl, H., Hermann, M., Grimm, M., & Troppmair, J. (2011). Mitochondrial ROS production under cellular stress: comparison of different detection methods. *Analytical and bioanalytical chemistry*, *400*(8), 2383-2390.

Kuznetsov, S. A., Langford, G. M., & Weiss, D. G. (1992). Actin-dependent organelle movement in squid axoplasm.

Kvam, P H, Brani Vidakovic, B (2007). Nonparametric Statistics with Applications to Science and Engineering. *John Wiley & Sons.*

Labrousse, A. M., Zappaterra, M. D., Rube, D. A., & van der Bliek, A. M. (1999). *C. elegans* Dynamin-Related Protein DRP-1 Controls Severing of the Mitochondrial Outer Membrane. *Molecular cell*, *4*(5), 815-826.

Lambert, A. J. & Brand, M. D. (2004). Superoxide production by NADH:ubiquinone oxidoreductase (complex I) depends on the pH gradient across the mitochondrial inner membrane. *Biochemical Journal. 382( 2)*, 511-7.

Langford, G. M. (1995). Actin-and microtubule-dependent organelle motors: interrelationships between the two motility systems. *Current opinion in cell biology*, *7*(1), 82-88.

Lansbergen, G., & Akhmanova, A. (2006). Microtubule plus end: a hub of cellular activities. *Traffic*, 7(5), 499-507.

Lee, D., Lee, K. H., Ho, W. K., & Lee, S. H. (2007). Target cell-specific involvement of presynaptic mitochondria in post-tetanic potentiation at hippocampal mossy fiber synapses. *The Journal of Neuroscience*, *27*(50), 13603-13613.

Lee, Y. J., Jeong, S. Y., Karbowski, M., Smith, C. L., & Youle, R. J. (2004). Roles of the mammalian mitochondrial fission and fusion mediators Fis1, Drp1, and Opa1 in apoptosis. *Molecular biology of the cell*, *15*(11), 5001-5011.

Legros, F., Lombès, A., Frachon, P., & Rojo, M. (2002). Mitochondrial fusion in human cells is efficient, requires the inner membrane potential, and is mediated by mitofusins. *Molecular biology of the cell*, *13*(12), 4343-4354.

Lenaz, G., Curatola, G., Mazzanti, L., Parenti-Castelli, G. & Bertoli, E. (1978). .Effects of general anesthetics on lipid protein interactions and ATPase activity in mitochondria. *Biochemical Pharmacology*. *27*(24):2835-44.

Lennon, S. V., Martin, S. J., & Cotter, T. G. (1991). Dose dependent induction of apoptosis in human tumour cell lines by widely diverging stimuli. *Cell proliferation*, *24*(2), 203-214.

Levy, J. R., Sumner, C. J., Caviston, J. P., Tokito, M. K., Ranganathan, S., Ligon, L. A., Wallace, K. E., LaMonte, B. H., Harmison, G. G., Puls, I., Fischbeck, K. H., & Holzbaur, E. L. (2006). A motor neuron disease–associated mutation in p150Glued perturbs dynactin function and induces protein aggregation. *The Journal of cell biology, 172(5),* 733-745.

Lewinski, F. V., & Keller, B. U. (2005). Ca2+ mitochondria and selective motoneuron vulnerability: implications for ALS. *Trends in neurosciences*, *28*(9), 494-500.

Lewis, J. A., Wu, C. H., Berg, H., & Levine, J. H. (1980). The genetics of levamisole resistance in the nematode *Caenorhabditis elegans*. *Genetics*, *95*(4), 905-928.

Li, Y, Lim, S, Hoffman, D, Aspenstrom, P, Federoff, H.J. & Rempe, D. A. (2009). HUMMR, a hypoxia- and HIF-1a-inducible protein, alters mitochondrial distribution and transport. *Journal of Cell Biology.185*(6), 1065–1081.

Li, Z., Okamoto, K. I., Hayashi, Y., & Sheng, M. (2004). The importance of dendritic mitochondria in the morphogenesis and plasticity of spines and synapses. *Cell*, *119*(6), 873-887.

Liang, G., Wang, Q., Li, Y., Kang, B., Eckenhoff, M. F., Eckenhoff, R. G., & Wei, H. (2008). A presenilin-1 mutation renders neurons vulnerable to isoflurane toxicity. *Anesthesia & Analgesia*, *106*(2), 492-500.

Ligon, L. A., & Steward, O. (2000). Role of microtubules and actin filaments in the movement of mitochondria in the axons and dendrites of cultured hippocampal neurons. *Journal of Comparative Neurology*, *427*(3), 351-361.

Lim, D., Fedrizzi, L., Tartari, M., Zuccato, C., Cattaneo, E., Brini, M., & Carafoli, E. (2008). Calcium homeostasis and mitochondrial dysfunction in striatal neurons of Huntington disease. *Journal of biological chemistry*, *283*(9), 5780-5789.

Lindén, M., Andersson, G., Gellerfors, P., & Nelson, B. D. (1984). Subcellular distribution of rat liver porin. *Biochimica et Biophysica Acta (BBA)-Biomembranes, 770(1),* 93-96.

Liu, C. T., & Brooks, G. A. (2012). Mild heat stress induces mitochondrial biogenesis in C2C12 myotubes. *Journal of Applied Physiology*, *112*(3), 354-361.

Liu, K. S., & Sternberg, P. W. (1995). Sensory regulation of male mating behavior in *Caenorhabditis elegans*. *Neuron*, *14*(1), 79-89.

Liu, M. S., Todd, B. D., & Sadus, R. J. (2003). Kinetics and chemomechanical properties of the F1-ATPase molecular motor. *The Journal of chemical physics, 118(21),* 9890-9898.

Lodi, R., Tonon, C., Valentino, M. L., Iotti, S., Clementi, V., Malucelli, E., Barboni, P., Longanesi, L., Schimpf, S., Wissinger, B., Baruzzi, A., Barbiroli, B., & Carelli, V. (2004).

Deficit of in vivo mitochondrial ATP production in OPA1 related dominant optic atrophy. *Annals of neurology*, *56*(5), 719-723.

López-Doménech, G., Serrat, R., Mirra, S., D'Aniello, S., Somorjai, I., Abad, A., Vitureira N, García-Arumí E, Alonso MT, Rodriguez-Prados M, Burgaya F, Andreu AL, García-Sancho J, Trullas R, Garcia-Fernàndez J, & Soriano, E. (2012). The Eutherian Armcx genes regulate mitochondrial trafficking in neurons and interact with Miro and Trak2. *Nature communications*, *3*, 814.

Losón, O. C., Song, Z., Chen, H., & Chan, D. C. (2013). Fis1, Mff, MiD49, and MiD51 mediate Drp1 recruitment in mitochondrial fission. *Molecular biology of the cell*, *24*(5), 659-667.

Lu, Y., Rolland, S. G., & Conradt, B. (2011). A molecular switch that governs mitochondrial fusion and fission mediated by the BCL2-like protein CED-9 of *Caenorhabditis elegans*. *Proceedings of the National Academy of Sciences*, *108*(41), E813-E822.

MacAskill, A. F., Rinholm, J. E., Twelvetrees, A. E., Arancibia-Carcamo, I. L., Muir, J., Fransson, A., Aspenstrom, P., Attwell, D., & Kittler, J. T. (2009). Miro1 is a calcium sensor for glutamate receptor-dependent localization of mitochondria at synapses. *Neuron*, *61*(4), 541-555.

MacAskill, A. F., & Kittler, J. T. (2010). Control of mitochondrial transport and localization in neurons. *Trends in cell biology*, *20*(2), 102-112.

Manczak, M., Anekonda, T. S., Henson, E., Park, B. S., Quinn, J., & Reddy, P. H. (2006). Mitochondria are a direct site of Aβ accumulation in Alzheimer's disease neurons: implications for free radical generation and oxidative damage in disease progression. *Human molecular genetics*, *15*(9), 1437-1449.

Mano, I., & Driscoll, M. (1999). DEG/ENaC channels: a touchy superfamily that watches its salt. *Bioessays*, *21*(7), 568-578.

Mannella, C. A., Forte, M., & Colombini, M. (1992). Toward the molecular structure of the mitochondrial channel, VDAC. *Journal of bioenergetics and biomembranes, 24(1),* 7-19.

Margulis L. (1981) Symbiosis in Cell Evolution. *Freeman, San Francisco, 1981*

Mattson, M. P., & Partin, J. (1999). Evidence for mitochondrial control of neuronal polarity. *Journal of neuroscience research*, *56*(1), 8-20.

Maurer, I., Zierz, S., & Möller, H. J. (2000). A selective defect of cytochrome c oxidase is present in brain of Alzheimer disease patients. *Neurobiology of aging*, *21*(3), 455-462.

Mclntire, S. L., Jorgensen, E., & Horvitz, H. R. (1993). Genes required for GABA function in *Caenorhabditis elegans*. *Nature. 364(6435),* 334–337.

Mechler, F, Fawcett, P. R, Mastaglia F. L., & Hudgson, P. (1981). Mitochondrial myopathy. *The Journal of Neuroscience. 50(2),* 191-200.

Meeusen, S., DeVay, R., Block, J., Cassidy-Stone, A., Wayson, S., McCaffery, J. M., & Nunnari, J. (2006). Mitochondrial inner-membrane fusion and crista maintenance requires the dynamin-related GTPase Mgm1. *Cell*, *127*(2), 383-395.

Meeusen, S., McCaffery, J. M., & Nunnari, J. (2004). Mitochondrial fusion intermediates revealed in vitro. *Science*, *305*(5691), 1747-1752.

Miki, H., Okada, Y., & Hirokawa, N. (2005). Analysis of the kinesin superfamily: insights into structure and function. *Trends in cell biology*, *15*(9), 467-476.

Miller, K. E., & Sheetz, M. P. (2004). Axonal mitochondrial transport and potential are correlated. *Journal of cell science*, *117*(13), 2791-2804.

Milner, D. J., Mavroidis, M., Weisleder, N., & Capetanaki, Y. (2000). Desmin cytoskeleton linked to muscle mitochondrial distribution and respiratory function. *The Journal of cell biology*, *150*(6), 1283-1298.

Mimori-Kiyosue, Y., & Tsukita, S. (2003). "Search-and-capture" of microtubules through plus-end-binding proteins (+ TIPs). *Journal of biochemistry*, 134(3), 321-326.

Minin, A. A., Kulik, A. V., Gyoeva, F. K., Li, Y., Goshima, G., & Gelfand, V. I. (2006). Regulation of mitochondria distribution by RhoA and formins. *Journal of cell science*, *119*(4), 659-670.

Mironov, S. L. (2006). Spontaneous and evoked neuronal activities regulate movements of single neuronal mitochondria. *Synapse*, *59*(7), 403-411.

Mironov, S. L. (2007). ADP regulates movements of mitochondria in neurons. *Biophysical journal*, *92*(8), 2944-2952.

Mitchison, T., & Kirschner, M. (1984a). Microtubule assembly nucleated by isolated centrosomes. *Nature*, *312(5991),* 232-237.

Mitchison, T., & Kirschner, M. (1984b). Dynamic instability of microtubule growth. *Nature*, *312(5991),* 237-242.

Mocz, G., & Gibbons, I. R. (2001). Model for the motor component of dynein heavy chain based on homology to the AAA family of oligomeric ATPases. *Structure*, 9(2), 93-103.

Mondal, S., Ahlawat, S., Rau, K., Venkataraman, V., & Koushika, S. P. (2011). Imaging in vivo neuronal transport in genetic model organisms using microfluidic devices. *Traffic, 12*(4), 372-385.

Moreira, P. I., Siedlak, S. L., Wang, X., Santos, M. S., Oliveira, C. R., Tabaton, M., Nunomura, A., Szweda, L. I., Aliev, G., Smith, M. A., Zhu, X., & Perry, G. (2007). Increased autophagic degradation of mitochondria in Alzheimer disease. *Autophagy*, *3*(6), 614.

Morris, R. L., & Hollenbeck, P. J. (1993). The regulation of bidirectional mitochondrial transport is coordinated with axonal outgrowth. *Journal of cell science*, *104*(3), 917-927.

Morris, R. L., & Hollenbeck, P. J. (1995). Axonal transport of mitochondria along microtubules and F-actin in living vertebrate neurons. *The Journal of cell biology*, *131*(5), 1315-1326.

Mosconi, L., De Santi, S., Li, J., Tsui, W. H., Li, Y., Boppana, M., Laska, E., Rusinek, H & de Leon, M. J. (2008). Hippocampal hypometabolism predicts cognitive decline from normal aging. *Neurobiology of aging*, *29*(5), 676-692.

Murphy, M. (2009). How mitochondria produce reactive oxygen species. *Biochem. J*, *417*, 1-13.

Nakamura, N., Kimura, Y., Tokuda, M., Honda, S., & Hirose, S. (2006). MARCH V is a novel mitofusin 2 and Drp1 binding protein able to change mitochondrial morphology. *EMBO reports*, *7*(10*),* 1019-1022.

Nogales, E. (1999). A structural view of microtubule dynamics. *Cellular and Molecular Life Sciences CMLS, 56(1-2),* 133-142.

O'Toole, M., Latham, R., Baqri, R. M., & Miller, K. E. (2008). Modeling mitochondrial dynamics during in vivo axonal elongation. *Journal of theoretical biology*, *255*(4), 369-377.

O'Hagan, R., Chalfie, M., & Goodman, M. B. (2005). The MEC-4 DEG/ENaC channel of *Caenorhabditis elegans* touch receptor neurons transduces mechanical signals. *Nature neuroscience*, *8*(1), 43-50.

Olichon, A., Baricault, L., Gas, N., Guillou, E., Valette, A., Belenguer, P., & Lenaers, G. (2003). Loss of OPA1 perturbates the mitochondrial inner membrane structure and integrity, leading to cytochrome c release and apoptosis. *Journal of Biological Chemistry*, *278*(10), 7743-7746.

Olichon, A., Emorine, L. J., Descoins, E., Pelloquin, L., Brichese, L., Gas, N., Guillou, E., Delettre, C., Valette, A., Hamel, C. P., Ducommun, B., Lenaers, G., & Belenguer, P. (2002). The human dynamin-related protein OPA1 is anchored to the mitochondrial inner membrane facing the inter-membrane space. *FEBS letters*, *523*(1), 171-176.

Ong, S. B., Subrayan, S., Lim, S. Y., Yellon, D. M., Davidson, S. M., & Hausenloy, D. J. (2010). Inhibiting mitochondrial fission protects the heart against ischemia/reperfusion injury. *Circulation*, *121*(18), 2012-2022.

Osman, C., Merkwirth, C., & Langer, T. (2009). Prohibitins and the functional compartmentalization of mitochondrial membranes. *Journal of cell science*, *122*(21), 3823-3830.

Otera, H., Wang, C., Cleland, M. M., Setoguchi, K., Yokota, S., Youle, R. J., & Mihara, K. (2010). Mff is an essential factor for mitochondrial recruitment of Drp1 during mitochondrial fission in mammalian cells. *The Journal of cell biology*, *191*(6), 1141-1158.

Palgunow, D., Klapper, M. &Döring, F. (2012). Dietary Restriction during Development Enlarges Intestinal and Hypodermal Lipid Droplets in *Caenorhabditis elegans*. *PloS one*7(11), e46198

Park, S. W., Kim, K. Y., Lindsey, J. D., Dai, Y., Heo, H., Nguyen, D. H., Ellisman, M. H., Weinreb, R. N., & Ju, W. K. (2011). A selective inhibitor of drp1, mdivi-1, increases retinal ganglion cell survival in acute ischemic mouse retina. *Investigative ophthalmology & visual science*, *52*(5), 2837-2843.

Parone, P. A., Da Cruz, S., Tondera, D., Mattenberger, Y., James, D. I., Maechler, P., Barja, F., & Martinou, J. C. (2008). Preventing mitochondrial fission impairs mitochondrial function and leads to loss of mitochondrial DNA. *PloS one*, *3*(9), e3257.

Pathak, D., Sepp, K. J., & Hollenbeck, P. J. (2010). Evidence that myosin activity opposes microtubule-based axonal transport of mitochondria. *The Journal of Neuroscience, 30(26),* 8984-8992.

Pedersen, W. A., Fu, W., Keller, J. N., Markesbery, W. R., Appel, S., Smith, R. G., Kasarskis, E., & Mattson, M. P. (1998). Protein modification by the lipid peroxidation product 4-hydroxynonenal in the spinal cords of amyotrophic lateral sclerosis patients. *Annals of neurology*, *44*(5), 819-824.

Pesch, U. E., Leo-Kottler, B., Mayer, S., Jurklies, B., Kellner, U., Apfelstedt-Sylla, E., Zrenner, E., Alexander, C., & Wissinger, B. (2001). OPA1 mutations in patients with autosomal dominant optic atrophy and evidence for semi-dominant inheritance. *Human Molecular Genetics*, *10*(13), 1359-1368.

Peters, A., Palay, S., & Webster, H. (1991). The Fine Structure of the Nervous System: The Neurons and Supporting Cells. *New York: Oxford University Press.*

Pierce, G. B., Parchment, R. E., & Lewellyn, A. L. (1991). Hydrogen peroxide as a mediator of programmed cell death in the blastocyst. *Differentiation*, *46*(3), 181-186.

Pilling, A. D., Horiuchi, D., Lively, C. M., & Saxton, W. M. (2006). Kinesin-I and Dynein are the primary motors for fast transport of mitochondria in Drosophila motor axons. *Molecular Biology of the Cell. 17(4),* 2057-68.

Pitter, J. G., Maechler, P., Wollheim, C. B., & Spät, A. (2002). Mitochondria respond to Ca 2+ already in the submicromolar range: correlation with redox state. *Cell calcium*, *31*(2), 97-104.

Pletjushkina, O. Y., Lyamzaev, K. G., Popova, E. N., Nepryakhina, O. K., Ivanova, O. Y., Domnina, L. V., Chernyak, B. V., & Skulachev, V. P. (2006). Effect of oxidative stress on dynamics of mitochondrial reticulum. *Biochimica et Biophysica Acta (BBA)-Bioenergetics*, *1757*(5), 518-524.

Rankin, C. H., Beck, C., & Chiba, C. M. (1990). *Caenorhabditis elegans*: A new model system for the study of learning and memory. *Behavioral brain research*, *37*(1), 89-92.

Rappaport, L., Oliviero, P., & Samuel, J. L. (1998). Cytoskeleton and mitochondrial morphology and function. *Molecular and cellular biochemistry, 184*(1-2), 101-105.

Rayment, I. (1996). Kinesin and myosin: molecular motors with similar engines. *Structure, 4*(5), 501-504.

Robertson, S. J., & Martin, R. J. (1993). Levamisole activated single channel currents from muscle of the nematode parasite *Ascaris suum*. *British journal of pharmacology*, *108*(1), 170-178.

Rodgers, J. T., Lerin, C., Haas, W., Gygi, S.P., Spiegelman, B.M., & Puigserver, M. (2005). Nutrient control of glucose homeostasis through a complex of PGC-1alpha and SIRT1. *Nature 434*(7029), 113 – 118

Rogers, S. L., Rogers, G. C., Sharp, D. J., & Vale, R. D. (2002). Drosophila EB1 is important for proper assembly, dynamics, and positioning of the mitotic spindle. *The Journal of cell biology, 158*(5), 873-884.

Rojo, M., Legros, F., Chateau, D., & Lombès, A. (2002). Membrane topology and mitochondrial targeting of mitofusins, ubiquitous mammalian homologs of the transmembrane GTPase Fzo. *Journal of cell science*, *115*(8), 1663-1674.

Rolland, S. G., Lu, Y., David, C. N., & Conradt, B. (2009). The BCL-2–like protein CED-9 of *C. elegans* promotes FZO-1/Mfn1, 2–and EAT-3/Opa1–dependent mitochondrial fusion. *The Journal of cell biology*, *186*(4), 525-540.

Rostovtseva, T. K., Sheldon, K. L., Hassanzadeh, E., Monge, C., Saks, V., Bezrukov, S. M., & Sackett, D. L. (2008). Tubulin binding blocks mitochondrial voltage-dependent anion channel and regulates respiration. *Proceedings of the National Academy of Sciences, 105*(48), 18746-18751.

Rottenberg, H (1983). Uncoupling of oxidative phosphorylation in rat liver mitochondria by general anesthetics. *Proceedings of the National Academy of Sciences*. *80*(11), 3313-7.

Ruthel, G., & Hollenbeck, P. J. (2003). Response of mitochondrial traffic to axon determination and differential branch growth. *The Journal of neuroscience*, *23*(24), 8618-8624.

Saher, G., Brügger, B., Lappe-Siefke, C., Möbius, W., Tozawa, R. I., Wehr, M. C., Wieland, F., Ishibashi, S., & Nave, K. A. (2005). High cholesterol level is essential for myelin membrane growth. *Nature neuroscience*, *8*(4), 468-475.

Salzer, J. L., Brophy, P. J., & Peles, E. (2008). Molecular domains of myelinated axons in the peripheral nervous system. *Glia*, *56*(14), 1532-1540.

Sampson, M. J., Lovell, R. S., & Craigen, W. J. (1997). The Murine Voltage-dependent Anion Channel Gene Family Conserved Structure and Function. *Journal of Biological Chemistry, 272*(30), 18966-18973.

Santel, A., & Fuller, M. T. (2001). Control of mitochondrial morphology by a human mitofusin. *Journal of cell science*, *114*(5), 867-874.

Saotome, M., Safiulina, D., Szabadkai, G., Das, S., Fransson, Å., Aspenstrom, P., Rizzuto, R., & Hajnóczky, G. (2008). Bidirectional Ca2+-dependent control of mitochondrial dynamics by the Miro GTPase. *Proceedings of the National Academy of Sciences, 105*(52), 20728-20733.

Savage, C., Hamelin, M., Culotti, J. G., Coulson, A., Albertson, D. G., & Chalfie, M. (1989). mec-7 is a beta-tubulin gene required for the production of 15-protofilament microtubules in *Caenorhabditis elegans. Genes & development, 3*(6), 870-887

Scherz Shouval, R., Shvets, E., Fass, E., Shorer, H., Gil, L., & Elazar, Z. (2007). Reactive oxygen species are essential for autophagy and specifically regulate the activity of Atg4. *The EMBO journal*, *26*(7), 1749-1760.

Loop, T., Dovi-Akue, D., Frick, M., Roesslein, M., Egger, L., Humar, M., Hoetzel, A., Schmidt, R., Borner, C., Pahl, H. L., Geiger, K. K., & Pannen, B. H (2005). Volatile anesthetics induce caspase-dependent, mitochondria-mediated apoptosis in human T lymphocytes in vitro. *Anesthesiology*, *102*(6), 1147-1157.

Schuyler, S. C., & Pellman, D. (2001). Microtubule "plus-end-tracking proteins": the end is just the beginning. *Cell, 105*(4), 421-424.

Serasinghe, M. N., & Yoon, Y. (2008). The mitochondrial outer membrane protein hFis1 regulates mitochondrial morphology and fission through self-interaction. *Experimental cell research*, *314*(19), 3494-3507.

Sesaki, H., & Jensen, R. E. (2001). UGO1 encodes an outer membrane protein required for mitochondrial fusion. *The Journal of cell biology, 152*(6), 1123-1134.

Sesaki, H., Southard, S. M., Yaffe, M. P., & Jensen, R. E. (2003). Mgm1p, a dynamin-related GTPase, is essential for fusion of the mitochondrial outer membrane. *Molecular biology of the cell*, *14*(6), 2342-2356.

Shao, L., Martin, M. V., Watson, S. J., Schatzberg, A., Akil, H., Myers, R. M., Jones, E. G., Bunney, W. E., & Vawter, M. P. (2008). Mitochondrial involvement in psychiatric disorders. *Annals of medicine*, *40*(4), 281-295.

Simmer, F., Moorman, C., van der Linden, A. M., Kuijk, E., van den Berghe, P. V., Kamath, R. S., Fraser, A. G., Ahringer, J., & Plasterk, R. H. (2003). Genome-wide RNAi of *C. elegans* using the hypersensitive rrf-3 strain reveals novel gene functions. *PLoS biology*, *1*(1), e12.

Smirnova, E., Griparic, L., Shurland, D. L., & Van Der Bliek, A. M. (2001). Dynamin-related protein Drp1 is required for mitochondrial division in mammalian cells. *Molecular biology of the cell*, *12*(8), 2245-2256.

Smith, D. S., Järlfors, U., & Cameron, B. F. (1975). Morphological evidence for the participation of microtubules in axonal transport. *Annals of the New York Academy of Sciences*, *253*(1), 472-506.

Smith, D. S., Jarlfors, U., & Cayer, M. L. (1977). Structural cross-bridges between microtubules and mitochondria in central axons of an insect (*Periplaneta americana*). *Journal of cell science*, *27*(1), 255-272.

Song, Z., Ghochani, M., McCaffery, J. M., Frey, T. G., & Chan, D. C. (2009). Mitofusins and OPA1 mediate sequential steps in mitochondrial membrane fusion. *Molecular biology of the cell*, *20*(15), 3525-3532.

Spiegelman, B. M., Penningroth, S. M., & Kirschner, M. W. (1977). Turnover of tubulin and the N site GTP in Chinese hamster ovary cells. *Cell, 12*(3), 587-600.

Sturtz, L. A., Diekert, K., Jensen, L. T., Lill, R., & Culotta, V. C. (2001). A fraction of yeast cu, zn-superoxide dismutase and its metallochaperone, ccs, localize to the intermembrane space of mitochondria a physiological role for sod1 in guarding against mitochondrial oxidative damage. *Journal of Biological Chemistry*, *276*(41), 38084-38089.

Sulston, J. E., & Horvitz, H. R. (1977). Post-embryonic cell lineages of the nematode, *Caenorhabditis elegans*. *Developmental biology, 56*(1), 110-156.

Sulston, J. E., & Horvitz, H. R. (1981). Abnormal cell lineages in mutants of the nematode *Caenorhabditis elegans Developmental biology, 82*(1), 41-55.

Sulston, J. E. & Hodgkin, J. (1988). The Nematode *Caenorhabditis elegans*. The Community of *C. elegans* Researchers, Wood W B. Plainview, NY: *Cold Spring Harbor Lab Press 1988.*

Sulston, J. E., Schierenberg, E., White, J. G., & Thomson, J. N. (1983). The embryonic cell lineage of the nematode *Caenorhabditis elegans Developmental biology, 100*(1), 64-119.

Summerhayes, I. C., Wong, D. A., & Chen, L. B. (1983). Effect of microtubules and intermediate filaments on mitochondrial distribution. *Journal of cell science, 61*(1), 87-105.

Sun, F., Zhu, C., Dixit, R., & Cavalli, V. (2011). Sunday Driver/JIP3 binds kinesin heavy chain directly and enhances its motility. *The EMBO journal*, *30*(16), 3416-3429.

Suomalainen, A., Majander, A., Haltia, M., Somer, H., Lönnqvist, J., Savontaus, M. L., & Peltonen, L. (1992). Multiple deletions of mitochondrial DNA in several tissues of a patient with severe retarded depression and familial progressive external ophthalmoplegia. *Journal of Clinical Investigation*, *90*(1), 61.

Susalka, S. J., Hancock, W. O., & Pfister, K. K. (2000). Distinct cytoplasmic dynein complexes are transported by different mechanisms in axons. *Biochimica et Biophysica Acta (BBA)-Molecular Cell Research, 1496*(1), 76-88.

Suski, J. M., Lebiedzinska, M., Bonora, M., Pinton, P., Duszynski, J., & Wieckowski, M. R. (2012). Relation between mitochondrial membrane potential and ROS formation. In *Mitochondrial Bioenergetics*, Humana Press.183-205.

Suzuki, H., Kerr, R., Bianchi, L., Frøkjær-Jensen, C., Slone, D., Xue, J., Gerstbrein, B., Driscoll M, & Schafer, W. R. (2003). In Vivo Imaging of *C. elegans* Mechanosensory Neurons Demonstrates a Specific Role for the MEC-4 Channel in the Process of Gentle Touch Sensation. *Neuron, 39*(6), 1005-1017.

Suzuki, H., Kerr, R., Bianchi, L., Frøkjær-Jensen, C., Slone, D., Xue, J., Gerstbrein, B., Driscoll, M., & Schafer, W. R. (2003). In Vivo Imaging of *C. elegans* Mechanosensory Neurons Demonstrates a Specific Role for the MEC-4 Channel in the Process of Gentle Touch Sensation. *Neuron*, *39*(6), 1005-1017.

Suzuki, M., Jeong, S. Y., Karbowski, M., Youle, R. J., & Tjandra, N. (2003). The solution structure of human mitochondria fission protein Fis1 reveals a novel TPR-like helix bundle. *Journal of molecular biology*, *334*(3), 445-458.

Swerdlow, R. H., Parks, J. K., Miller, S. W., Davis, R. E., Tuttle, J. B., Trimmer, P. A., Sheehan, J. P., Bennett, J. P. Jr., Davis, R. E, & Parker, W. D. (1996). Origin and functional consequences of the complex I defect in Parkinson's disease. *Annals of neurology*, *40*(4), 663-671.

Tanaka, Y., Kanai, Y., Okada, Y., Nonaka, S., Takeda, S., Harada, A., & Hirokawa, N. (1998). Targeted Disruption of Mouse Conventional Kinesin Heavy Chain kif5B Results in Abnormal Perinuclear Clustering of Mitochondria. *Cell, 93*(7), 1147-1158.

Tang, Y. G., & Zucker, R. S. (1997). Mitochondrial involvement in post-tetanic potentiation of synaptic transmission. *Neuron*, *18*(3), 483-491.

Tavernarakis, N., & Driscoll, M. (2000). *Caenorhabditis elegans* degenerins and vertebrate ENaC ion channels contain an extracellular domain related to venom neurotoxins. *Journal of neurogenetics*, *13*(4), 257-264.

Tavernarakis, N., Everett, J. K., Kyrpides, N. C., & Driscoll, M. (2001). Structural and functional features of the intracellular amino terminus of DEG/ENaC ion channels. *Current Biology*, *11*(6), R205-R208.

Terasaki, M., & Reese, T. S. (1994). Interactions among endoplasmic reticulum, microtubules, and retrograde movements of the cell surface. *Cell motility and the cytoskeleton*, *29*(4), 291-300.

The *C. elegans* Sequencing Consortium. Science. (1998). Genome sequence of the nematode *C. elegans:* a platform for investigating biology. *Science, 282*(5396), 2012-8.

Thomas, J. H., Stern, M. J., & Horvitz, H. R. (1990). Cell interactions coordinate the development of *the C. elegans* egg-laying system. *Cell*, *62*(6), 1041-1052.

Thompson, R. F., & Spencer, W. A. (1966). Habituation: a model phenomenon for the study of neuronal substrates of behavior. *Psychological review*, *73*(1), 16.

Thyberg, J., & Moskalewski, S. (1985). Microtubules and the organization of the Golgi complex. *Experimental cell research, 159(1),* 1-16.

Tieu, Q., Okreglak, V., Naylor, K., & Nunnari, J. (2002). The WD repeat protein, Mdv1p, functions as a molecular adaptor by interacting with Dnm1p and Fis1p during mitochondrial fission. *The Journal of cell biology*, *158*(3), 445-452.

Tsujimoto, Y., & Shimizu, S. (2007). Role of the mitochondrial membrane permeability transition in cell death. *Apoptosis*, *12*(5), 835-840.

Tsyganiĭ, A. A., & Medvinskaia, N. A. (1983). Characteristics of the change in oxidative phosphorylation in the mitochondria of various organs under nitrous oxide anesthesia. *Farmakologiia i toksikologiia, 47(4),* 30-33.

Twig, G., Hyde, B., & Shirihai, O. S. (2008). Mitochondrial fusion, fission and autophagy as a quality control axis: the bioenergetic view. *Biochimica et Biophysica Acta (BBA)-Bioenergetics*, *1777*(9), 1092-1097.

Tyynismaa, H., Carroll, C. J., Raimundo, N., Ahola-Erkkilä, S., Wenz, T., Ruhanen, H., Guse, K., Hemminki, A., Peltola-Mjøsund, K. E., Tulkki, V., Oresic, M., Moraes, C. T., Pietiläinen, K., Hovatta, I., & Suomalainen, A. (2010). Mitochondrial myopathy induces a starvation-like response. *Human molecular genetics*, *19*(20), 3948-3958.

Vale, R. D. (2003). The molecular motor toolbox for intracellular transport. *Cell, 112*(4), 467-480.

Valko, M., Izakovic, M., Mazur, M., Rhodes, C. J., & Telser, J. (2004). Role of oxygen radicals in DNA damage and cancer incidence. *Molecular and cellular biochemistry*, *266*(1-2), 37-56.

Van der Bend, R. L., Duetz, W., Colen, A. M., Van Dam, K., & Berden, J. A. (1985). Differential effects of triphenyltin and 8-azido-ATP on the ATP synthesis, ATP-Pi exchange, and ATP hydrolysis in liposomes containing ATP synthase and bacteriorhodopsin. *Archives of biochemistry and biophysics*, *241*(2), 461-471.

van der Bliek, A. M. (1999). Functional diversity in the dynamin family. *Trends in cell biology*, *9*(3), 96-102.

Varadi, A., Johnson-Cadwell, L. I., Cirulli, V., Yoon, Y., Allan, V. J., & Rutter, G. A. (2004). Cytoplasmic dynein regulates the subcellular distribution of mitochondria by controlling the recruitment of the fission factor dynamin-related protein-1. *Journal of cell science, 117*(19), 4389-4400.

Varshney, L. R., Chen, B. L., Paniagua, E., Hall, D. H., & Chklovskii, D. B. (2011). Structural properties of the *Caenorhabditis elegans* neuronal network. *PLoS computational biology, 7*(2), e1001066.

Vayssière, J. L., Cordeau-Lossouarn, L., Larcher, J. C., Basseville, M., Gros, F., & Croizat, B. (1992). Participation of the mitochondrial genome in the differentiation of neuroblastoma cells. *In Vitro Cellular & Developmental Biology-Animal*, *28*(11-12), 763-772.

Verhey, K. J., Meyer, D., Deehan, R., Blenis, J., Schnapp, B. J., Rapoport, T. A., & Margolis, B. (2001). Cargo of kinesin identified as JIP scaffolding proteins and associated signaling molecules. *The Journal of cell biology*, *152*(5), 959-970.

Verstreken, P., Ly, C. V., Venken, K. J., Koh, T. W., Zhou, Y., & Bellen, H. J. (2005). Synaptic Mitochondria Are Critical for Mobilization of Reserve Pool Vesicles at Drosophila Neuromuscular Junctions. *Neuron*, *47*(3), 365-378.

Vitre, B., Coquelle, F. M., Heichette, C., Garnier, C., Chrétien, D., & Arnal, I. (2008). EB1 regulates microtubule dynamics and tubulin sheet closure in vitro. *Nature cell biology, 10*(4), 415-421.

Vyssokikh, M., Katz, A., Rueck, A., Wuensch, C., Dorner, A., Zorov, D., & Brdiczka, D. (2001). Adenine nucleotide translocator isoforms 1 and 2 are differently distributed in the mitochondrial inner membrane and have distinct affinities to cyclophilin D. *Biochem. J, 358*(2), 349-358.

Wallace, D. C. (2005). A mitochondrial paradigm of metabolic and degenerative diseases, aging, and cancer: a dawn for evolutionary medicine. *Annual review of genetics*, *39*, 359.

Wang, X., & Schwarz, T. L. (2009). The Mechanism of Ca2+Dependent Regulation of Kinesin-Mediated Mitochondrial Motility. *Cell*, *136*(1), 163-174.

Wang, X., Winter, D., Ashrafi, G., Schlehe, J., Wong, Y. L., Selkoe, D., Rice, S., Steen, J.,. LaVoie, M. J & Schwarz, T. L. (2011). PINK1 and Parkin target Miro for phosphorylation and degradation to arrest mitochondrial motility. *Cell*, *147*(4), 893-906.

Wappler, E. A., Institoris, A., Dutta, S., Katakam, P. V., & Busija, D. W. (2013). Mitochondrial dynamics associated with oxygen-glucose deprivation in rat primary neuronal cultures. *PloS one*, *8*(5), e63206.

Wei, H., Liang, G., Yang, H., Wang, Q., Hawkins, B., Madesh, M., Wang, S., & Eckenhoff, R. G. (2008). The common inhalational anesthetic isoflurane induces apoptosis via activation of inositol 1, 4, 5-trisphosphate receptors. *Anesthesiology*, *108*(2), 251-260.

Weir, B. A., & Yaffe, M. P. (2004). Mmd1p, a novel, conserved protein essential for normal mitochondrial morphology and distribution in the fission yeast *Schizosaccharomyces pombe. Molecular biology of the cell*, *15*(4), 1656-1665.

Westermann, B. (2002). Merging mitochondria matters. *EMBO reports*, *3*(6), 527-531.

White, J. G., Southgate, E., Thomson, J. N., & Brenner, S. (1986). The structure of the nervous system of the nematode *Caenorhabditis elegans*. *Philosophical Transactions of the Royal Society of London. B, Biological Sciences, 314*(1165), 1-340.

Witte, M. E., Bø, L., Rodenburg, R. J., Belien, J. A., Musters, R., Hazes, T., Hazes, T., Wintjes, L. T., Smeitink, J. A., Geurts, J. J., De Vries, H. E., van der Valk, P., & van Horssen, J. (2009). Enhanced number and activity of mitochondria in multiple sclerosis lesions. *The Journal of pathology*, *219*(2), 193-204.

Wong, E. D., Wagner, J. A., Scott, S. V., Okreglak, V., Holewinske, T. J., Cassidy-Stone, A., & Nunnari, J. (2003). The intramitochondrial dynamin-related GTPase, Mgm1p, is a component of a protein complex that mediates mitochondrial fusion. *The Journal of cell biology*, *160*(3), 303-311

Yaffe, M. P., Harata, D., Verde, F., Eddison, M., Toda, T., & Nurse, P. (1996). Microtubules mediate mitochondrial distribution in fission yeast. *Proceedings of the National Academy of Sciences*, *93*(21), 11664-11668.

Yan, J., Chao, D. L., Toba, S., Koyasako, K., Yasunaga, T., Hirotsune, S., & Shen, K. (2013). Kinesin-1 regulates dendrite microtubule polarity in *Caenorhabditis elegans*. *Elife, 2.*

Yang, D., Oyaizu, Y., Oyaizu, H., Olsen, G. J., & Woese, C. R. (1985). Mitochondrial origins. *Proceedings of the National Academy of Sciences, 82*(13), 4443-4447.

Yang, H., Liang, G., Hawkins, B., Madesh, M., Pierwola, A., & Wei, H. (2008). Inhalational anesthetics induce cell damage by disruption of intracellular calcium homeostasis with different potencies. *Anesthesiology*, *109*(2), 243.

Yang, Y., Gehrke, S., Imai, Y., Huang, Z., Ouyang, Y., Wang, J. W., Yang, L., Beal, M. F., Vogel, H & Lu, B. (2006). Mitochondrial pathology and muscle and dopaminergic neuron degeneration caused by inactivation of Drosophila Pink1 is rescued by Parkin. *Proceedings of the National Academy of Sciences*, *103*(28), 10793-10798.

Yarosh, W., Monserrate, J., Tong, J. J., Tse, S., Le, P. K., Nguyen, K., Brachmann, C. B., Wallace, D. C., & Huang, T. (2008). The molecular mechanisms of OPA1-mediated optic atrophy in Drosophila model and prospects for antioxidant treatment. *PLoS genetics*, *4*(1), e6.

Yi, M., Weaver, D., & Hajnóczky, G. (2004). Control of mitochondrial motility and distribution by the calcium signal a homeostatic circuit. *The Journal of cell biology*, *167*(4), 661-672.

Yoo, B. K., Choi, J. W., Yoon, S. Y., & Ko, K. H. (2005). Protective effect of adenosine and purine nucleos (t) ides against the death by hydrogen peroxide and glucose deprivation in rat primary astrocytes. *Neuroscience research*, *51*(1), 39-44.

Yoon, Y., Krueger, E. W., Oswald, B. J., & McNiven, M. A. (2003). The mitochondrial protein hFis1 regulates mitochondrial fission in mammalian cells through an interaction with the dynamin-like protein DLP1. *Molecular and cellular biology*, *23*(15), 5409-5420.

Youle, R. J., & Van Der Bliek, A. M. (2012). Mitochondrial fission, fusion, and stress. *Science*, *337*(6098), 1062-1065.

Young, M. J., Bay, D. C., & Hausner, G. (2007). The evolutionary history of mitochondrial porins. *BMC evolutionary biology*, *7*(1), 31.

Yu, T., Fox, R. J., Burwell, L. S., & Yoon, Y. (2005). Regulation of mitochondrial fission and apoptosis by the mitochondrial outer membrane protein hFis1. *Journal of cell science*, *118*(18), 4141-4151.

Zar, J. H. (1999). Biostatistical Analysis. *Upper Saddler River,* NJ: Prentice Hall.

Zhang, C. L., Ho, P. L., Kintner, D. B., Sun, D., & Chiu, S. Y. (2010). Activity-dependent regulation of mitochondrial motility by calcium and Na/K-ATPase at nodes of Ranvier of myelinated nerves. *The Journal of Neuroscience*, *30*(10), 3555-3566.

Zhang, C. L., Verbny, Y., Malek, S. A., Stys, P. K., & Chiu, S. Y. (2004). Nicotinic acetylcholine receptors in mouse and rat optic nerves. *Journal of neurophysiology*, *91*(2), 1025-1035.

Zhang, C. L., Wilson, J. A., Williams, J., & Chiu, S. Y. (2006). Action potentials induce uniform calcium influx in mammalian myelinated optic nerves. *Journal of neurophysiology*, *96*(2), 695-709.

Zhang, H., Kong, X., Kang, J., Su, J., Li, Y., Zhong, J., & Sun, L. (2009). Oxidative stress induces parallel autophagy and mitochondria dysfunction in human glioma U251 cells. *Toxicological Sciences*, *110*(2), 376-388.

Zhang, L., Shimoji, M., Thomas, B., Moore, D. J., Yu, S. W., Marupudi, N. I., Torp, R., Torgner, I. A., Ottersen, O. P., Dawson, T. M., & Dawson, V. L. (2005). Mitochondrial localization of the Parkinson's disease related protein DJ-1: implications for pathogenesis. *Human molecular genetics*, *14*(14), 2063-2073.

Zhang, S., Arnadottir, J., Keller, C., Caldwell, G. A., Yao, C. A., & Chalfie, M. (2004). MEC-2 Is Recruited to the Putative Mechanosensory Complex in *C. elegans* Touch Receptor Neurons through Its Stomatin-like Domain. *Current biology, 14*(21), 1888-1896.

Züchner, S., Mersiyanova, I. V., Muglia, M., Bissar-Tadmouri, N., Rochelle, J., Dadali, E. L., Zappia, M., Nelis, E., Patitucci, A., Senderek, J., Parman, Y., Evgrafov, O., Jonghe, P. D., Takahashi, Y., Tsuji, S., Pericak-Vance, M. A., Quattrone, A., Battaloglu, E., Polyakov, A. V., Timmerman, V., Schröder, J. M., & Vance, J. M. (2004). Mutations in the mitochondrial GTPase mitofusin 2 cause Charcot-Marie-Tooth neuropathy type 2A. *Nature genetics*, *36*(5), 449-451.

# Appendix

## A. Composition of NGM (Nematode Growth Media) Agar per Litre

| Chemicals | Quantity |
|---|---|
| NaCl | 3 g |
| Peptone | 2.5 g |
| Agar | 17 g |
| $H_2O$ | 975 ml |
| Autoclave the above mix and cool to 55$^oC$ and add chemicals listed below. | |
| 1M $CaCl_2$ | 1 ml |
| 1M $MgSO_4$ | 1 ml |
| 1M Potassium Phosphate pH 6.0 | 25 ml |
| Cholesterol (5mg/ml in EtOH) | 1 ml |

## B. Preparation of *E.coli* OP50 Growth Media per Litre

| Chemicals | Quantity |
|---|---|
| Bacto-tryptone | 10g |
| Bacto-yeast | 5g |
| NaCl | 5g |
| $H_2O$ | make-up vol to 1L |
| Set pH to 7.0. Autoclave and than inoculate with *E. coli OP50* single colony and incubate at 37$^oC$. Allow to grow overnight. Spot liquid culture on NGM plates and allow the culture to grow overnight at room temperature. | |

## C. Composition of M9 Buffer per Litre

| Chemicals | Quantity |
|---|---|
| $KH_2PO_4$ | 3 g |
| $Na_2HPO_4$ | 6 g |
| NaCl | 5 g |
| 1M $MgSO_4$ | 1 ml |
| $H_2O$ | make-up vol to 1L |

**D. Composition of Freezing Solution per Litre**

| **Chemicals** | **Quantity** |
|---|---|
| NaCl | 5.85 g |
| $KH_2PO_4$ | 6.8 g |
| Glycerol | 300 g |
| 1M NaOH | 5.6 ml |
| $H_2O$ | make-up vol to 1L |
| Autoclave above mix than add | |
| 0.1 M $MgSO_4$ | 3 ml |

**E. Composition of 1Litre 10X TE (Tris-EDTA) Buffer**

| **Chemicals** | **Quantity** |
|---|---|
| 1 M Tris-HCl pH 7.5 | 100 ml |
| 500 mM EDTA pH 8.0 | 20 ml |
| $H_2O$ (ultrapure) | 880ml |

# List of Publications and Presentations

**List of Papers Published by the Candidate**

1. Bholanath Paul, Vani Mishra, Bhushan Chaudhury, **Anjali Awasthi**, Asim Bikas Das, Urmila Saxena, Ashok Saxena, Lalit K. Chauhan, Pradeep Kumar, Sheikh Raisuddin. **Status of Stat3 in an Ovalbumin-Induced Mouse Model of Asthma: Analysis of the Role of Socs3 and IL-6.** Int Arch Allergy Immunol 2009; 148:99-108.
2. Jitendra Kumar, Kyung-Chae Park and **Anjali Awasthi**. **An approach to examine the effect of pharmacological drugs on insulin signaling in *C.elegans***. The Worm Breeders Gazette 2014; Volume 20, Number 1.
3. Jitendra Kumar*, Kyung-Chae Park*, **Anjali Awasthi*,** Birendra Prasad. **Silymarin extends lifespan and reduces proteotoxicity in *C.elegans* Alzheimers model** In review in CNS & Neurological Disorders-DrugTargets. (* Shared first co-author).
4. Ravi Raghav Sonani, Niraj Kumar Singh, **Anjali Awasthi** , Birendra Prasad, Jitendra Kumar, Datta Madamwar. **Phycoerythrin extends lifespan and healthspan in *Caenorhabditis elegans.*** In review in AGE Journal (The Official Journal of the American Aging Association)
5. **Anjali Awasthi,** Guruprasad Reddy Sure, Eva Romero, Sudip Mondal and Sandhya P. Koushika. **Mitochondria number and distribution correlates to neuronal behavior in *C.elegans*** (Manuscript in preparation).
6. Bikash C. Choudhary, **Anjali Awasthi**, Jitendra Kumar, Takashi Fukuzono, Kunihiro Matsumoto, Naoki Hisamoto, Sandhya P. Koushika. **A Novel Role for UNC-16 (JIP-3) with LRK-1 and UNC-101 in Trafficking of SV Precursors from Neuronal Cell Bodies of *C.elegans.*** (Manuscript in preparation).
7. Siddharth Khare, **Anjali Awasthi**, Sandhya P. Koushika, V. Venkataraman. **Coloured PDMS force sensing micro-pillar arrays for high throughput measurements of forces applied by genetic model organisms**. (Manuscript in preparation).
8. Guruprasada Reddy Sure, Nikhil Mishra, **Anjali Awasthi,** Swathi Devireddy, Swetha Mohan, Sandhya P. Koushika. **Vesicular cargo adaptor UNC-16/JIP3 inhibits anterograde mitochondrial transport in neurons.** (Manuscript in prepration).

**List of Presentations**

1. Poster entitled "Study of factors affecting mitochondria number and distribution and its correlation with neuronal behavior" presented at INCF/INNNI workshop held in IMSc Chennai from Nov 5$^{th}$ -7$^{th}$Nov 2012.
2. Poster entitled "Mitochondria number and distribution correlates with neuronal behavior" presented at 19$^{th}$ Biennial meeting of the International Society for Development Neuroscience (ISDN 2012) held in TIFR Mumbai from 11$^{th}$ -14$^{th}$ Jan 2012.
3. Poster entitled "Mitochondria number and distribution correlates with neuronal behavior" presented in 1$^{st}$ Annual Conference of Society for Mitochondrial Research and Medicine held in Centre for Cellular and Molecular Biology, Hyderabad from 9$^{th}$ -10$^{th}$ Dec 2011. Poster was awarded best poster prize.

## Biography of the Candidate

Anjali Awasthi did her schooling from Jawaharlal Nehru School, Bhopal. After completing her schooling she did B. Sc. (Biology) from Sarojini Naidu Govt Girls College Bhopal. She pursued M. Sc. in Microbiolgy from Barkatullah University Bhopal. After a short stint in academics she joined M. E. (Biotechnolgy) at BITS-Pilani. After completing M. E., she joined BITS-Pilani as an Off-campus faculty in Bangalore. She got registered for Ph.D. with BITS-Pilani and carried out her doctoral research work at National Centre for Biological Sciences, TIFR, Bangalore under the guidance of Dr Sandhya P Koushika. She is currently also associated with BITS-Pilani as an Off-Campus Faculty in Bangalore.

## Biography of the Supervisor

Dr Sandhya P Koushika did her B. Sc. (Chemistry) and M. Sc. (Biochemistry) from Maharaja Sayajirao University, Baroda. She did her Ph. D. in Molecular and Cell Biology from Brandeis University USA under the guidance of Dr Kalpana White. She did her Post-doctoral training at Washington University School of Medicine, USA under the guidance of Dr Michael L Nonet. She joined National Centre for Biological Sciences-TIFR, Bangalore as a Reader in 2005. She is currently working as Associate Professor in Department of Biological Sciences, TIFR-Mumbai. She is recipient of many academic honours and awards including HHMI international early career scientist in 2012. She has given many scientific talks and has published many reputed papers in the international forum.